Developing robust DEM models to simulate element tests

Catherine O'Sullivan

Imperial College London

Talk overview

- DEM in geomechanics
- Choice of DEM code
- Code validation
- Time step
- Boundary conditions
- Specimen generation + sample size
- Input parameters
- Contact model
- Running the simulation
- Post processing – data interpretation
- Conclusions

DEM in geomechanics

Use of DEM – No of Publications per Year

c

F

e

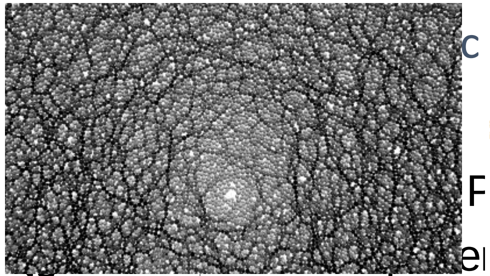

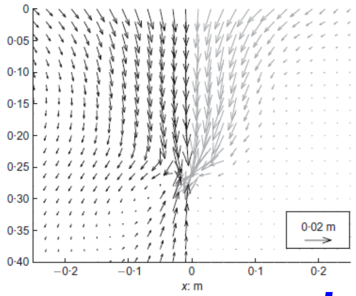

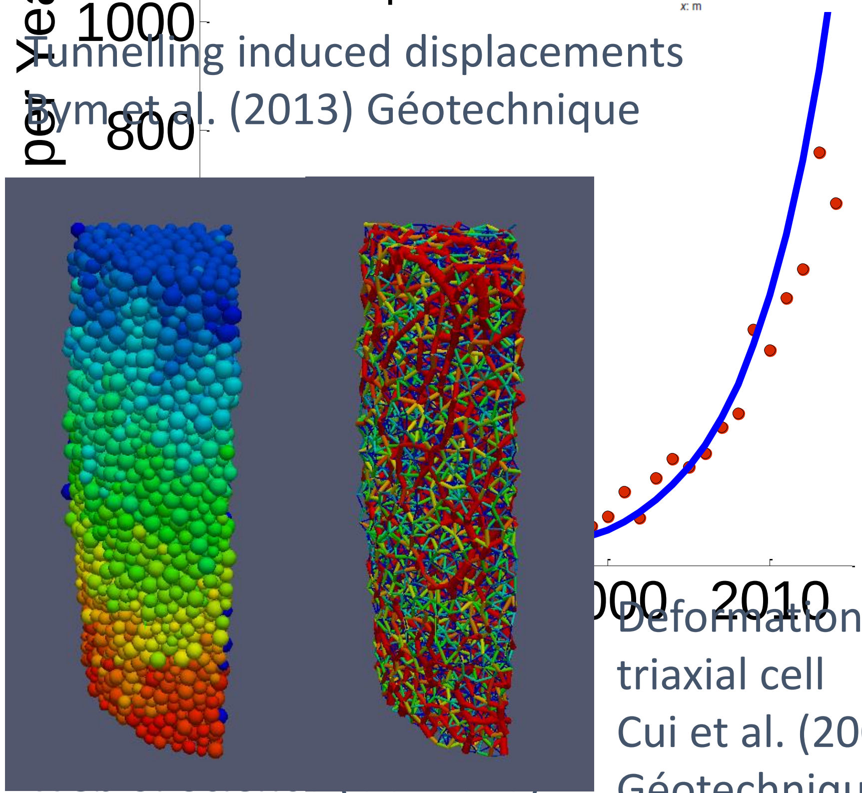

Tunnelling induced displacements
Jacobsz et al. (2013) Géotechnique

Deformation in triaxial cell
Cui et al. (2007) Géotechnique

nnical journals

of

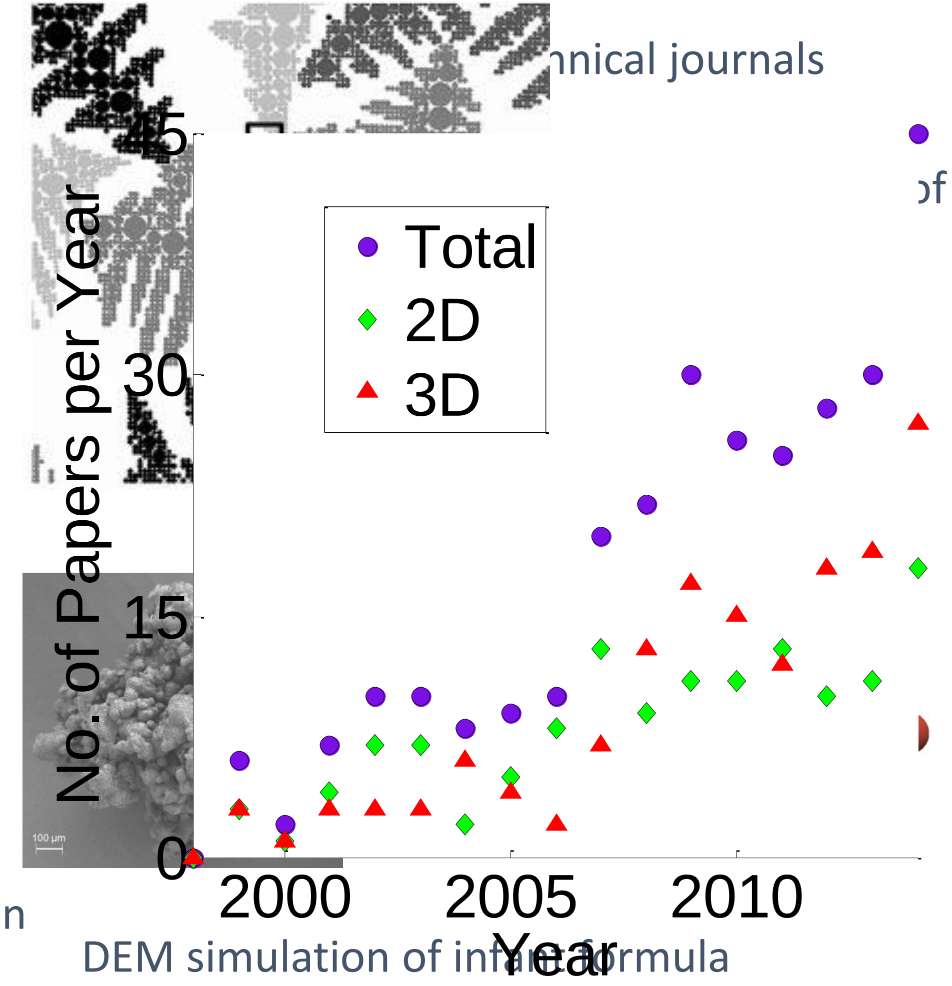

DEM simulation of infant formula
Hanley et al (2012)

Choice of DEM code

TRUBAL

- Original DEM code developed by Cundall and Strack – code listing + validation given in 1979 report to the US National Science Foundation

- Written in Fortran to run in serial mode

- Derivatives of this code:
  - Aston DEM code used by Colin Thornton (e.g. Thornton (2000) *Géotechnique*)
  - ELLIPSE3D (Ng, e.g. Ng (2006) *Géotechnique*)
  - Modified Trubal code used by O'Sullivan/Barreto/Cui

LAMMPS

- LAMMPS (http://lammps.sandia.gov/)
- Classical molecular dynamics code that can be used for DEM
- Uses spatial decomposition and MPI (message passage interface)
- Can run large high performance computers (hpc) with distributed memory
- Researchers at IC (Marketos, Hanley, Shire, Huang, Otsubo) have been working to modify the granular LAMMPS package

LIGGHTS

- Derivative of LAMMPS – developed by Christof Kloss
- No longer compatible with main LAMMPS codebase
- Specifically developed for granular materials
- Commercial and public versions of code exist
- Limited experience at IC with this code

PFC

- Commercial software – developed by Itasca.
- Peter Cundall close connection to Itasca.
- Flexible
- Used by O’Sullivan / Cheung / Ciantia
- Coupled version used by Kawano

Other codes

- Oval
- YADE
- EDEM

Conclusions

- PFC is the most popular DEM code based on review of DEM studies published in geomechanics / geotechnical /soil mechanics journals
- Now a good few DEM codes available open source
- Tendency to exploit parallelism.
- YADE / PFC Version 5 – shared memory
- LIGGGHTS / LAMMPS – distributed memory

Code validation

Code validation

Calibration → tuning code to match experimental data – optimization problem

Validation → verification / confirmation that code correctly and accurately captures the intended physics / mechanics

2D DEM validation with glass rods

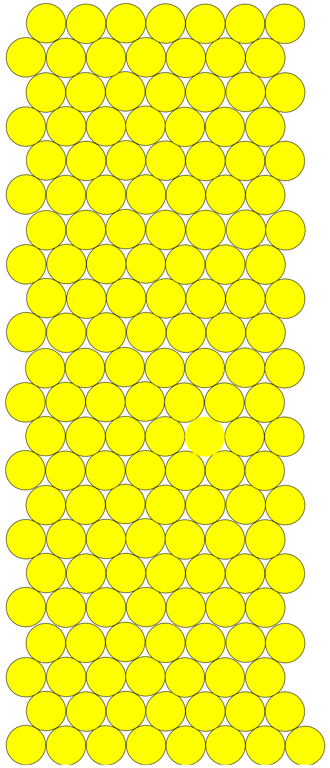

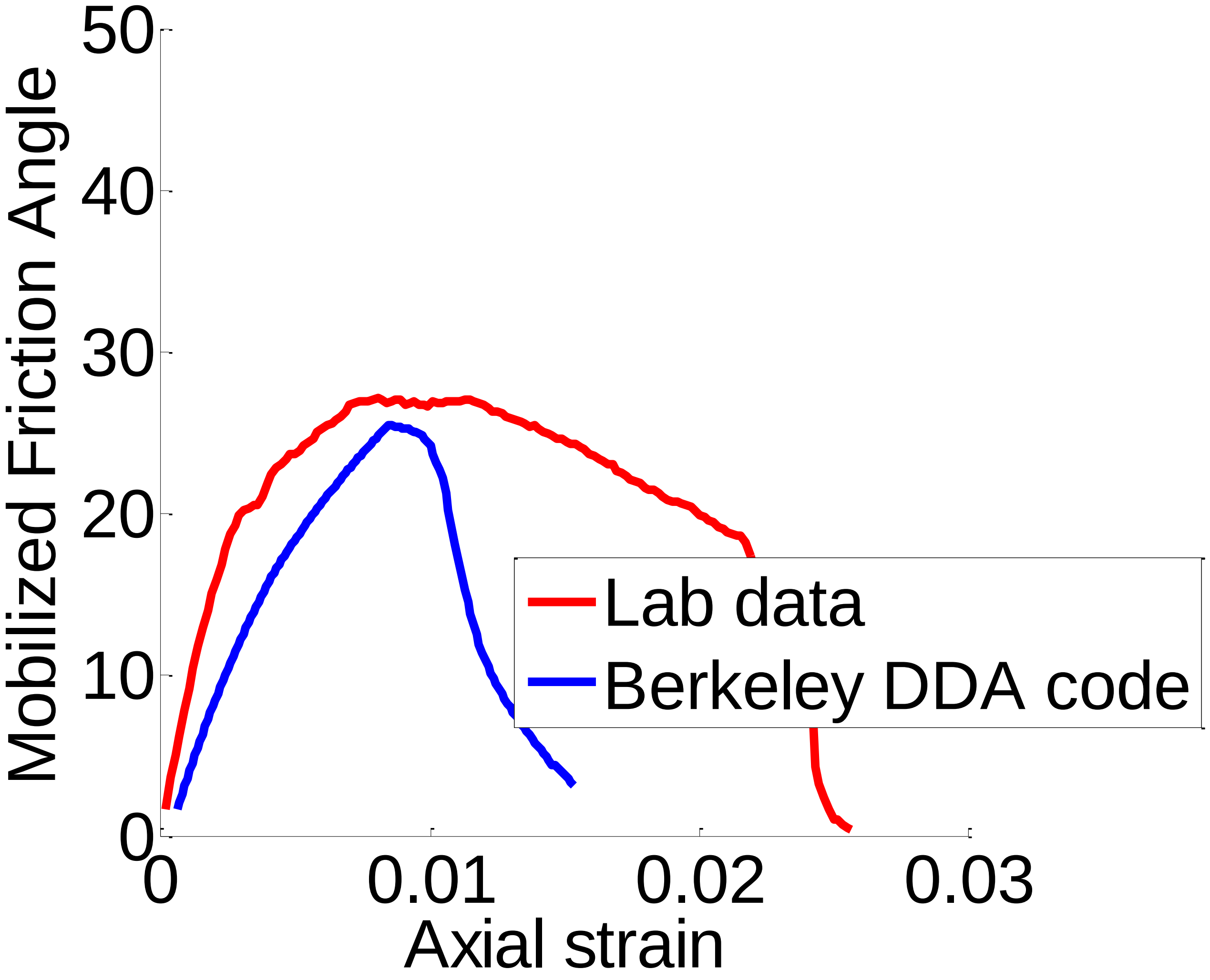

O'Sullivan and Bray (2003)

2D DEM validation with glass rods

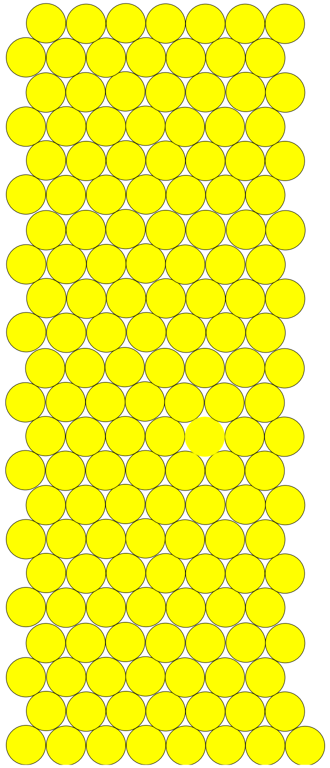

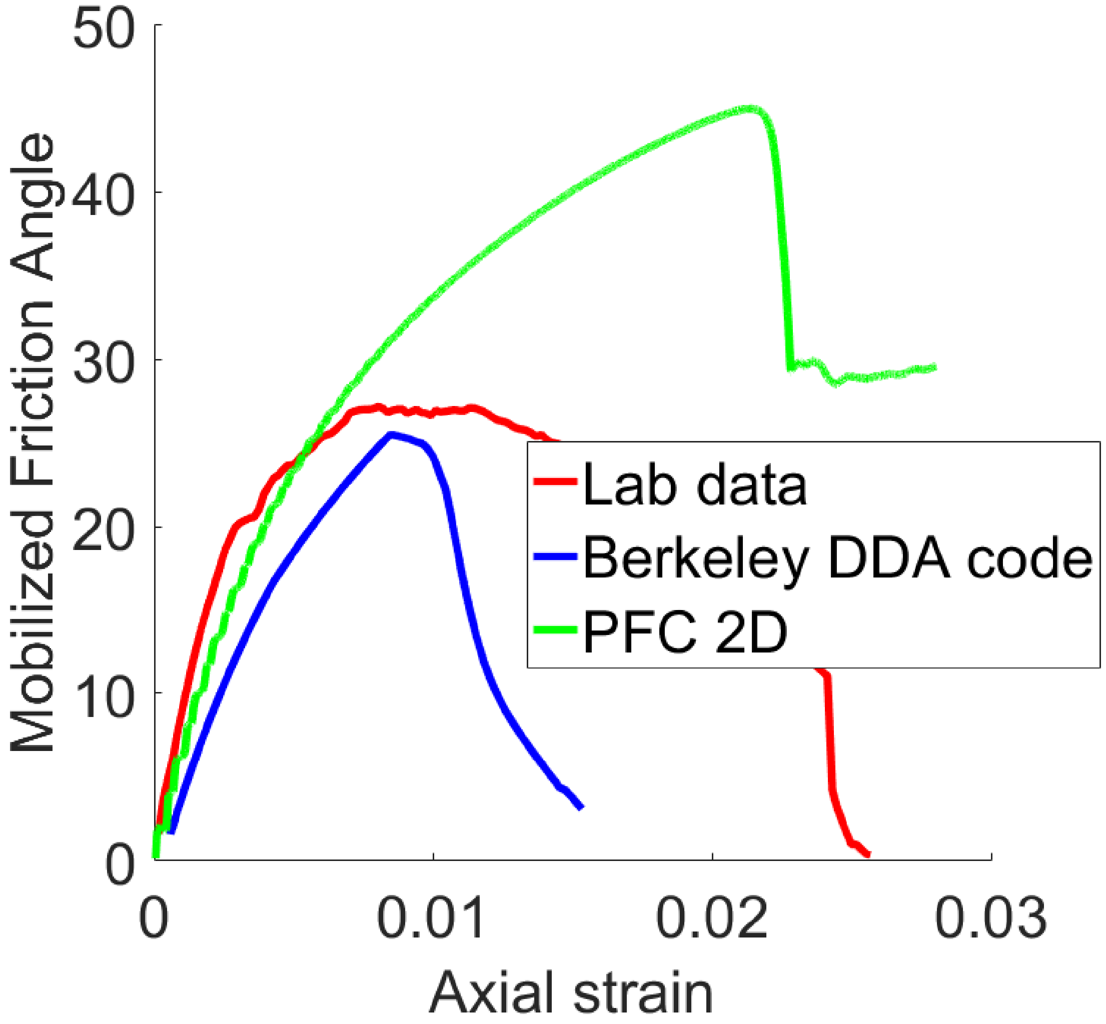

O'Sullivan and Bray (2003)

2D DEM validation with glass rods

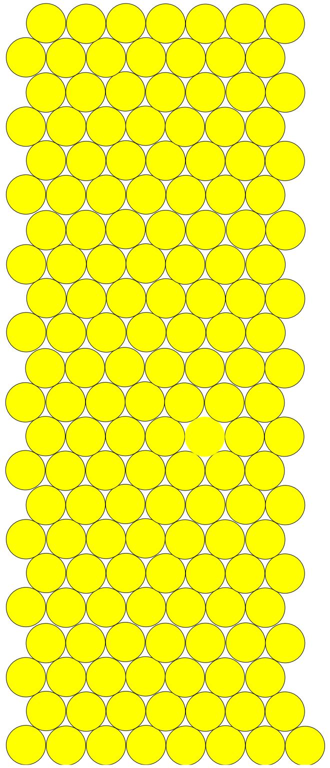

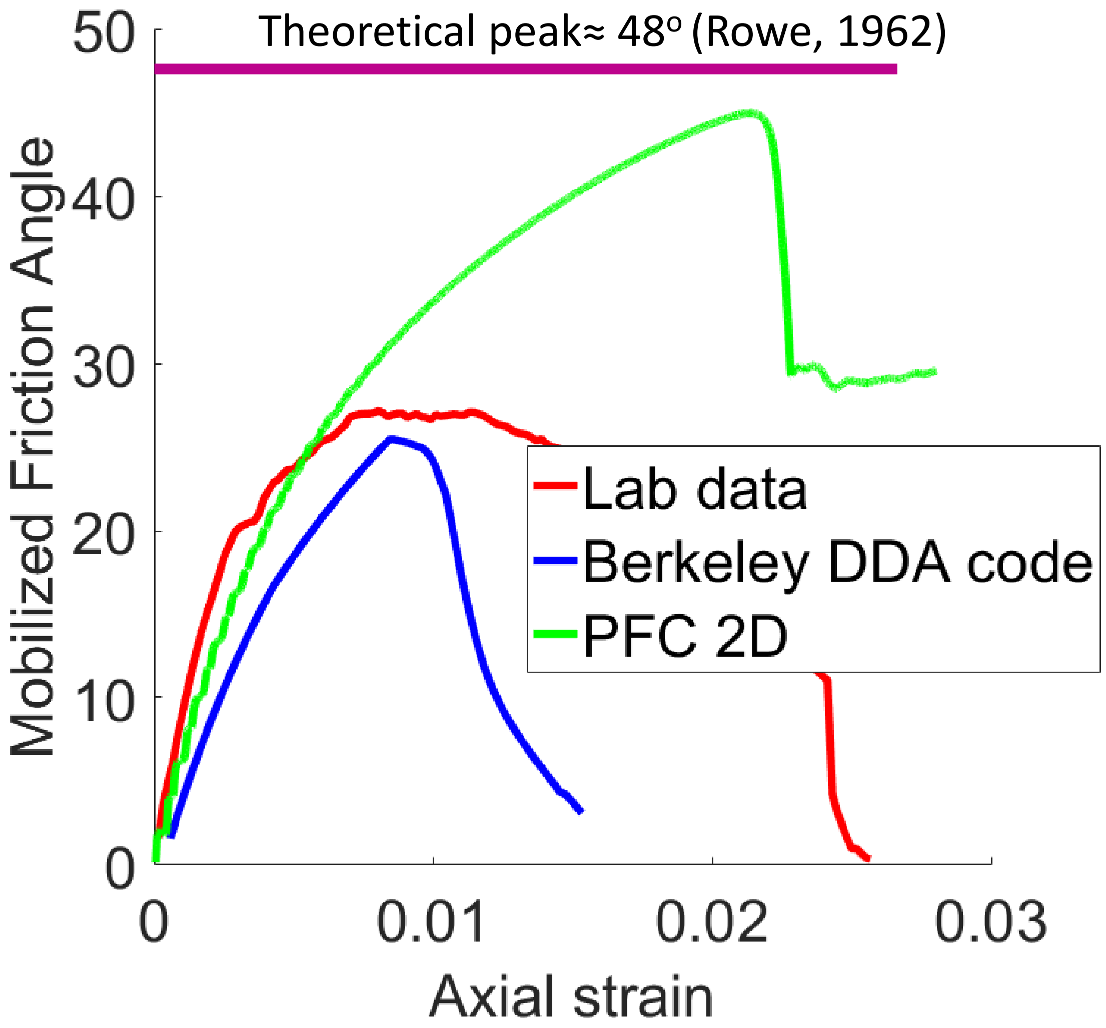

O'Sullivan and Bray (2003)

2D DEM validation with glass rods

- Original DDAD formulation: incremental shear spring

$$F_s = k_s \Delta u_s$$

- DEM formulation in PFC: cumulative shear spring

$$F_s = \sum k_s \Delta u_s$$

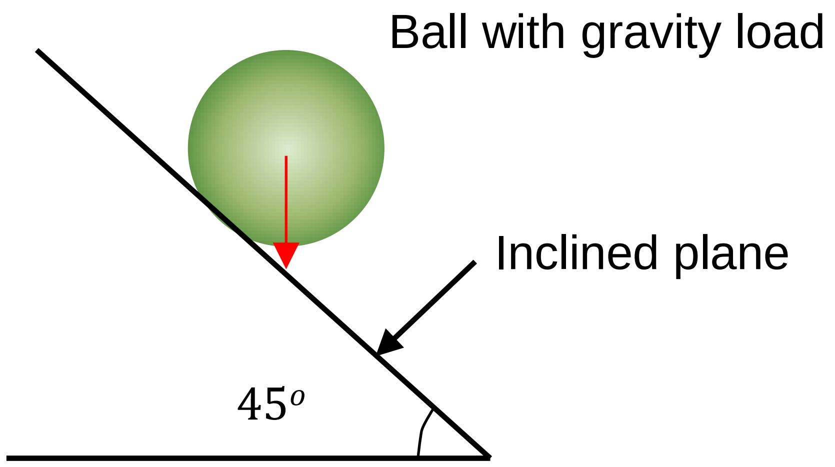

O'Sullivan and Bray (2003)

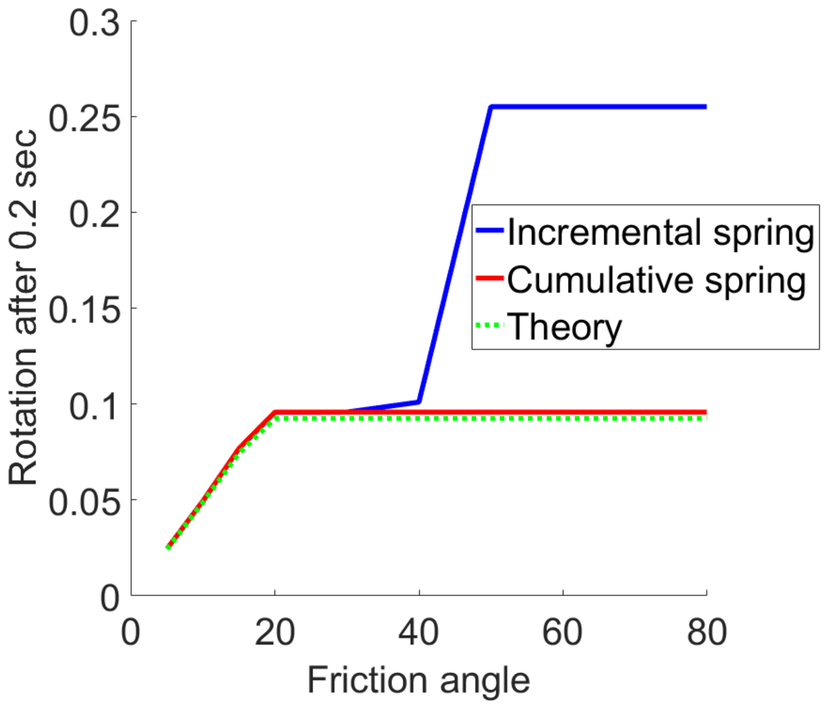

Repeat tests and simulations

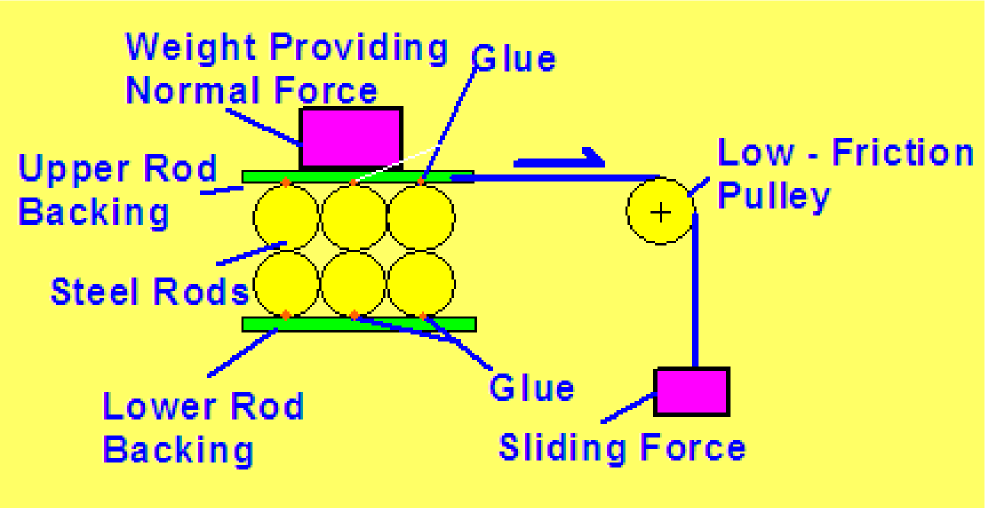

Steel Rods:

Size: 5.3 - 6.3 mm Diameter

Tolerance 1/400 mm

Friction Mean 12.1 º,

Std. Dev. 3.0 º

New tests + simulations

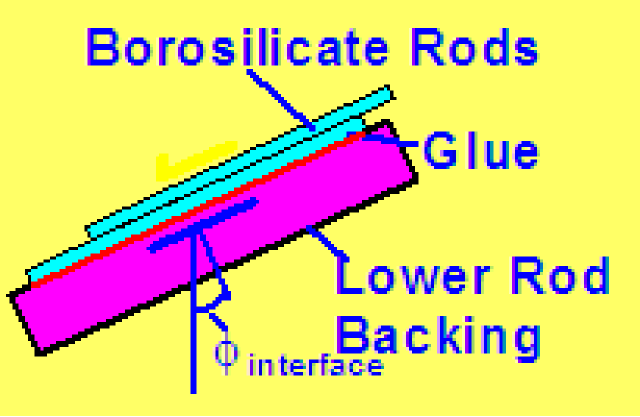

Borosilicate Rods

Size: 4,5 and 6 mm Diameter

Standard Deviation 0.5% - 1.5%

Aspect ratio 1.002-1.016

Friction Mean 18º,

Std. Dev. 2.15º

New simulations

O'Sullivan et al. (2002)

Repeat tests and simulations: steel rods

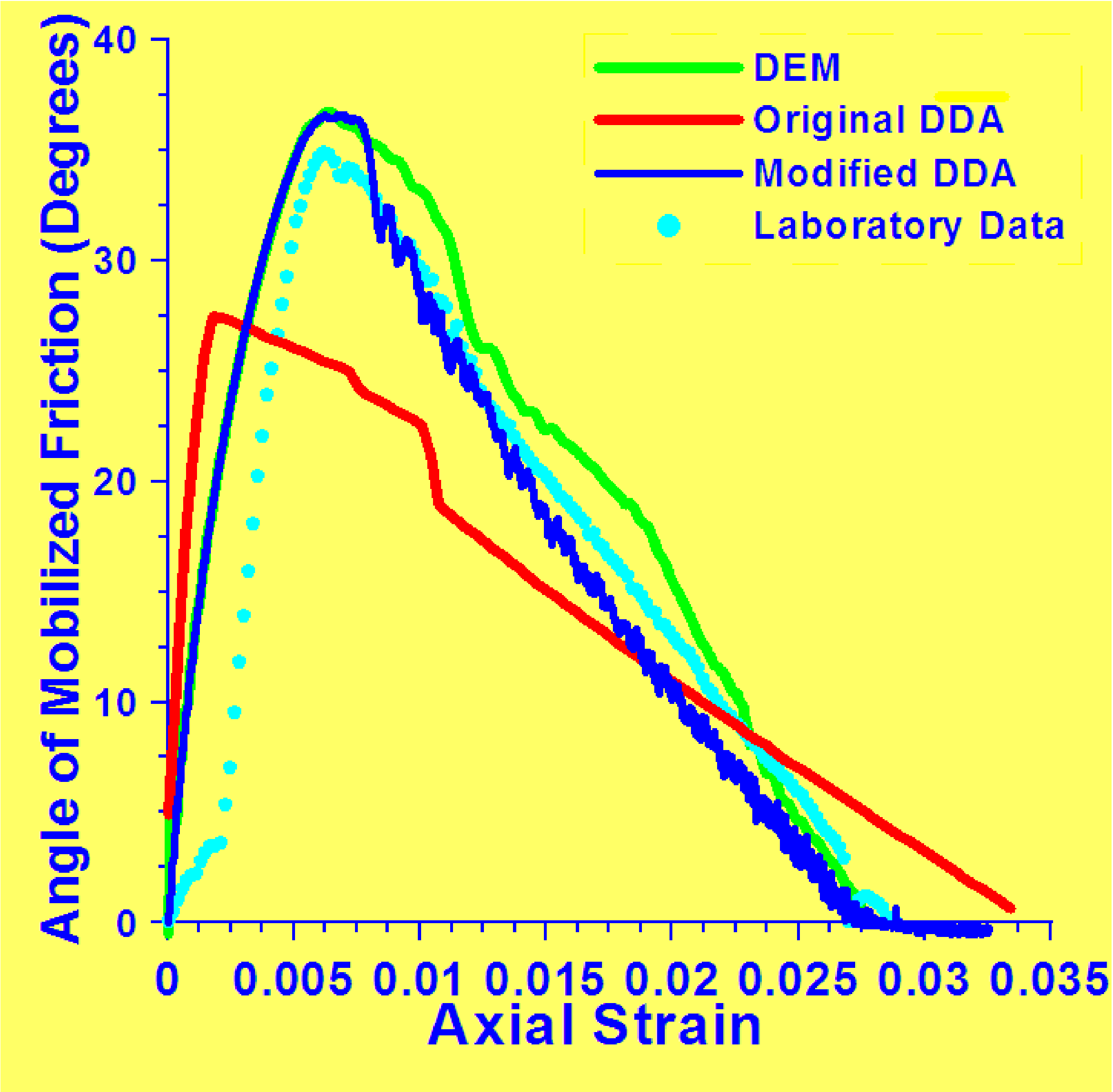

Repeat tests and simulations: steel rods

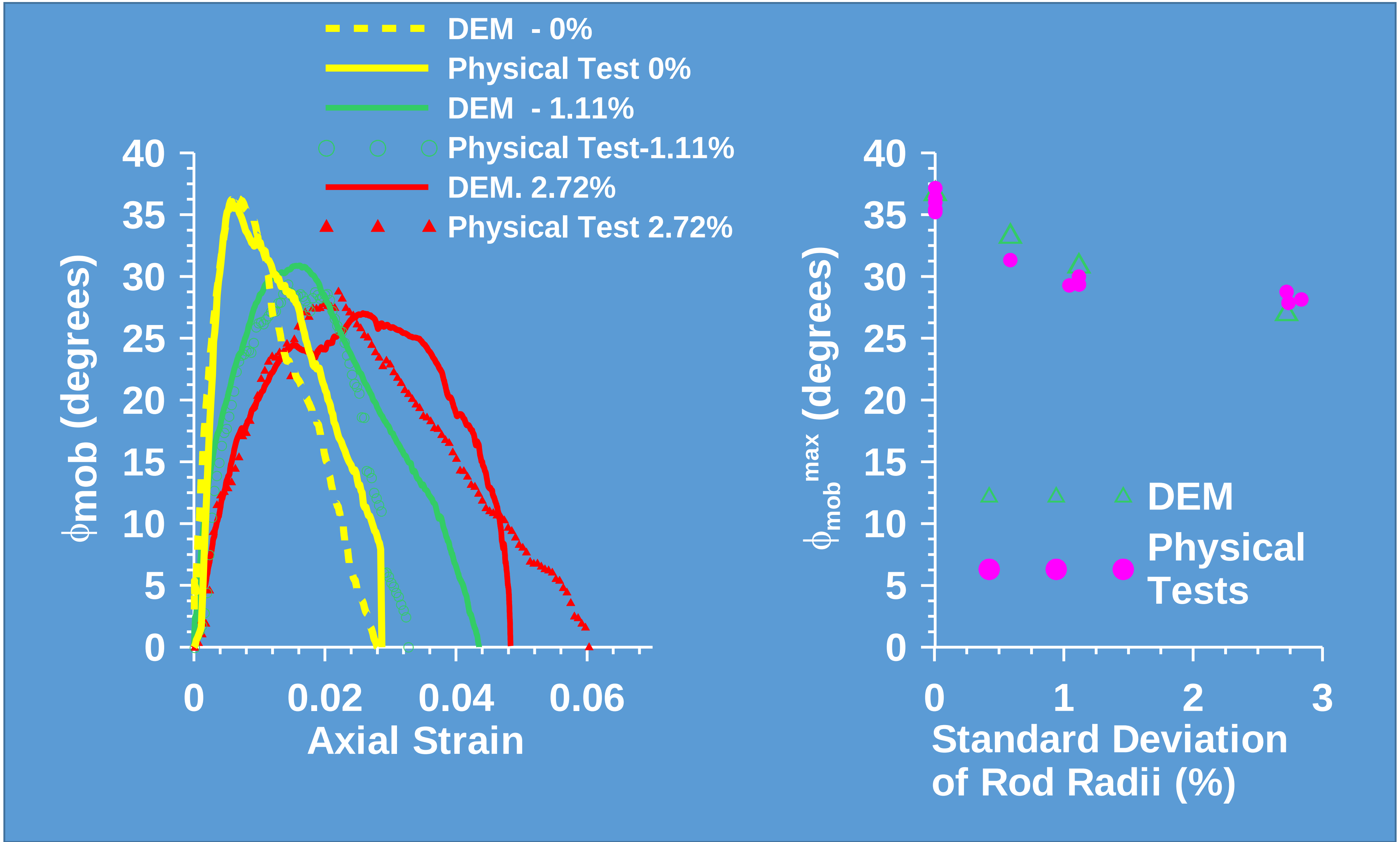

O'Sullivan et al. (2002)

Repeat tests and simulations: steel rods

Uniform Specimen

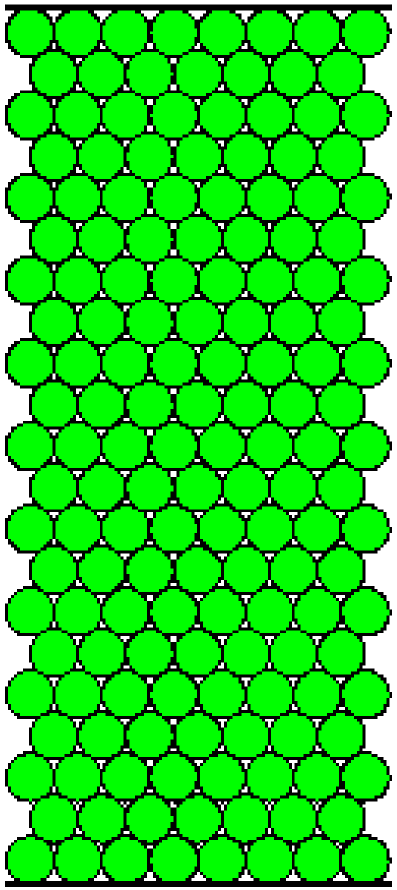

Std. Dev. 2.7%

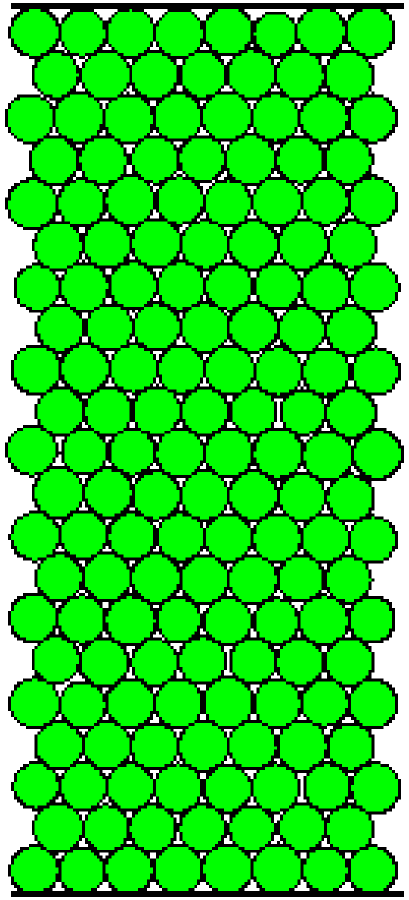

Repeat tests and simulations: steel rods

Uniform Specimen

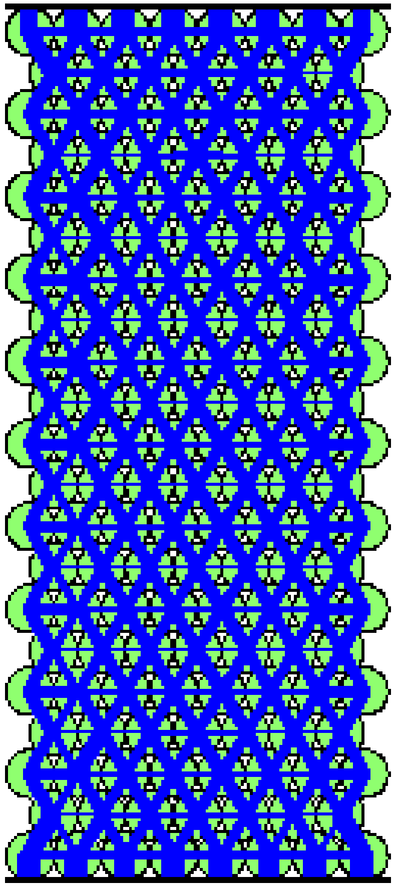

Std. Dev. 2.7%

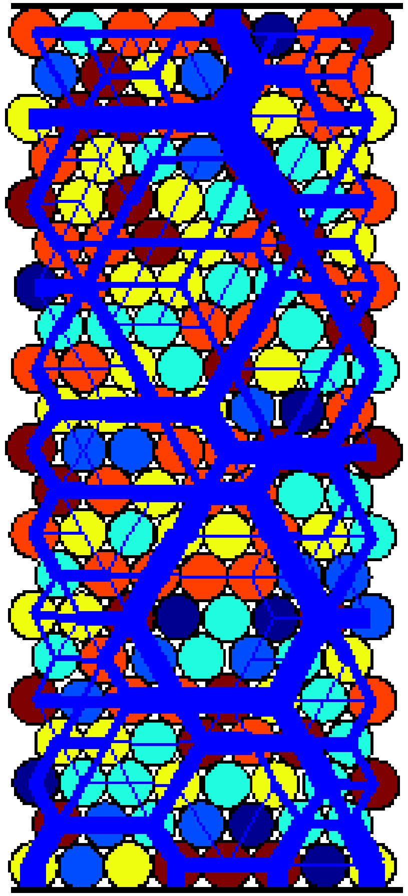

Repeat simulations: glass rods

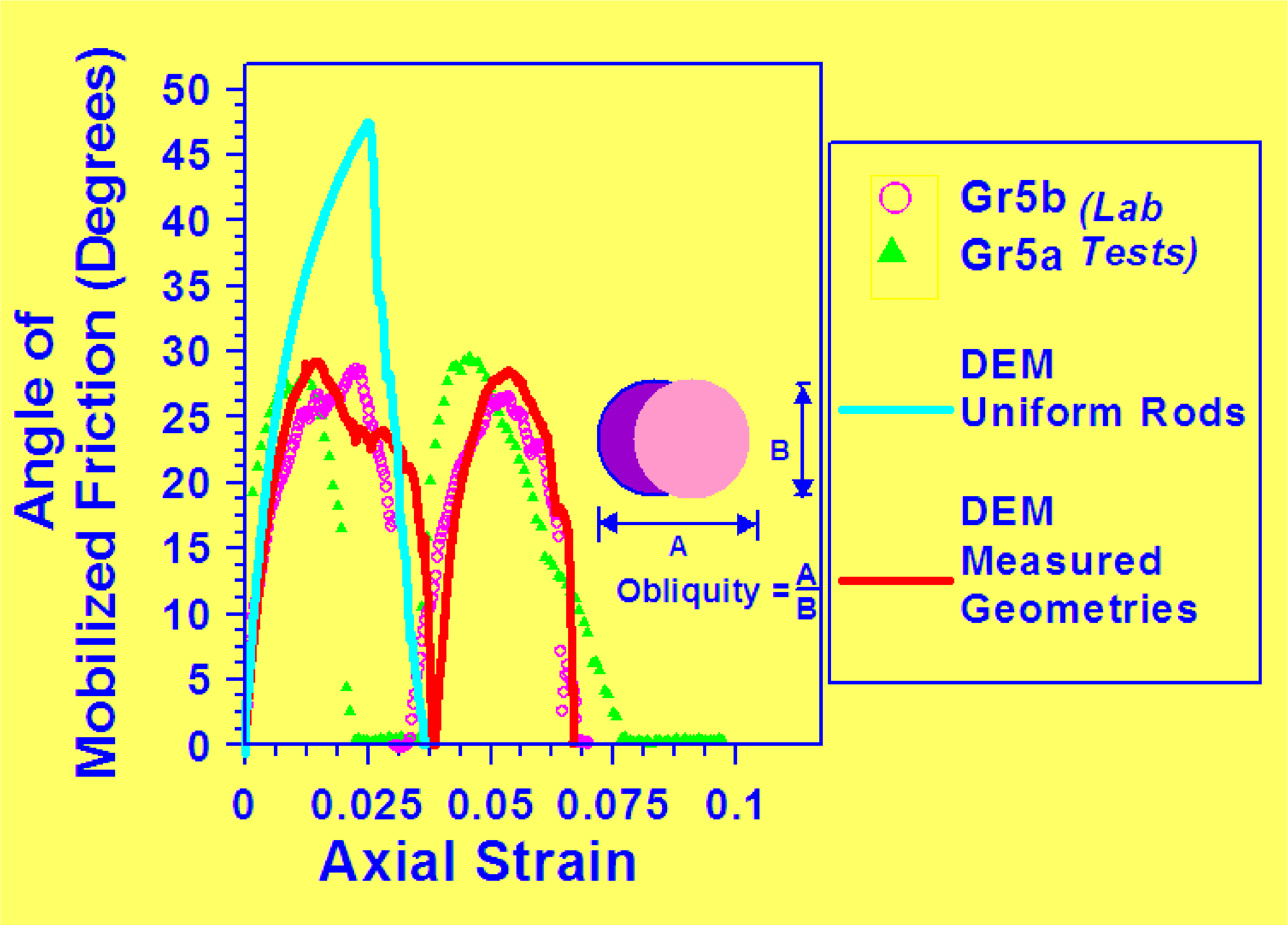

O'Sullivan et al. (2002)

Validation of simulation approach

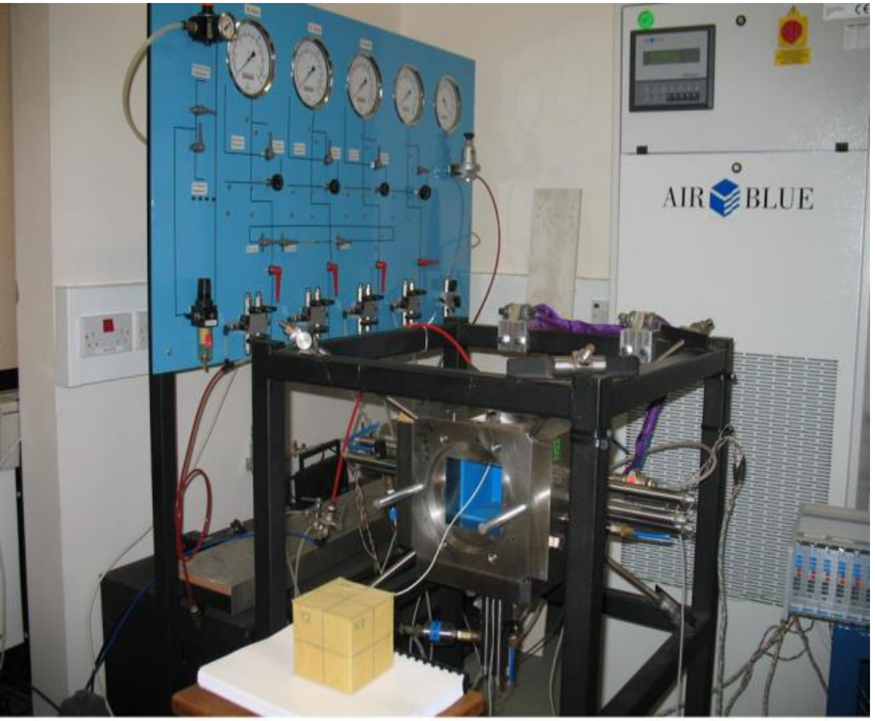

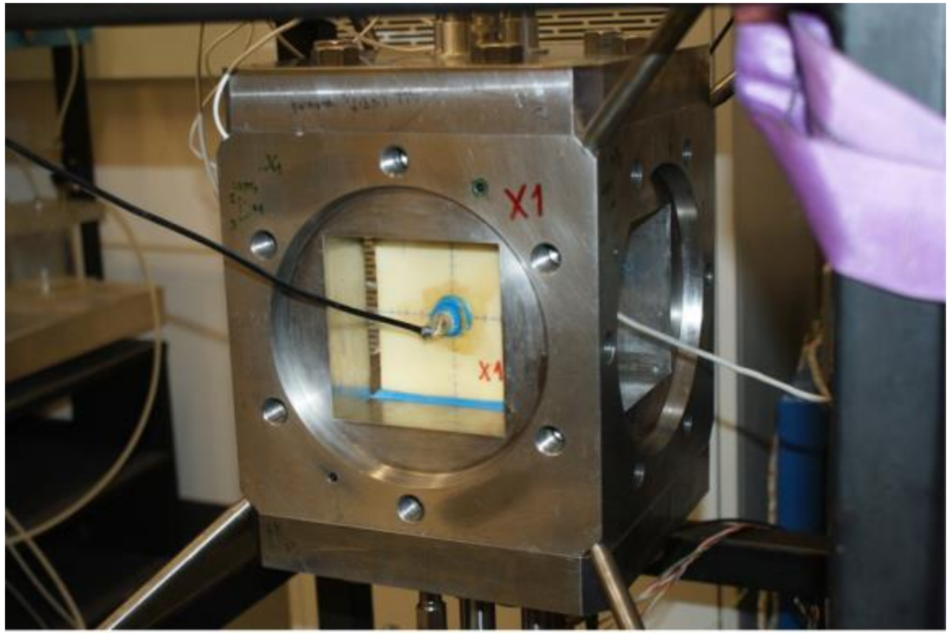

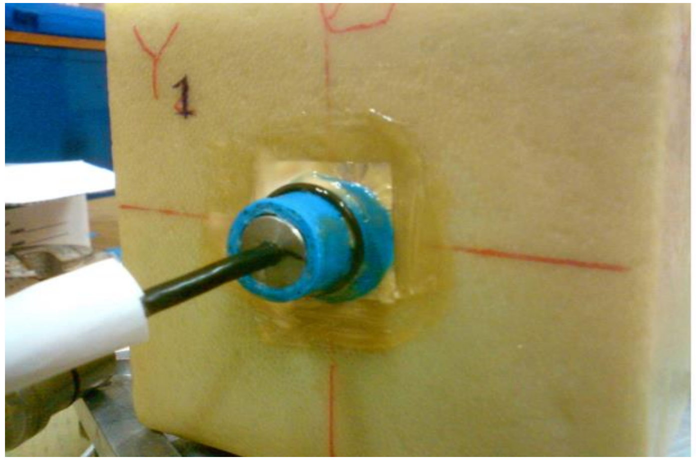

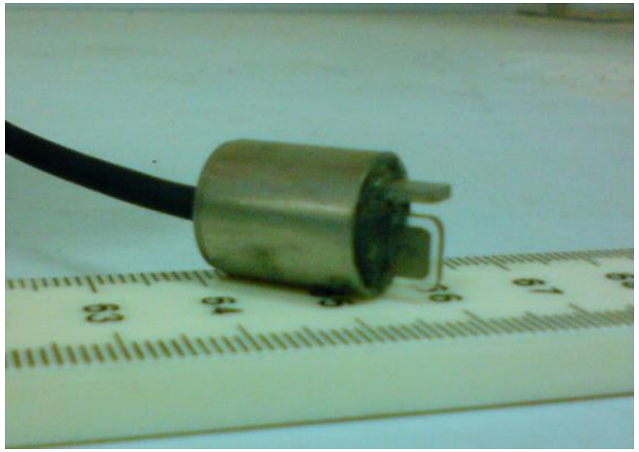

University of Bristol Cubical Cell

O’Donovan et
al. (2016)

Validation of simulation approach

Borosilicate glass ballotini
Diameter 2.4 mm – 2.7 mm
Cavarretta et al. (2012)

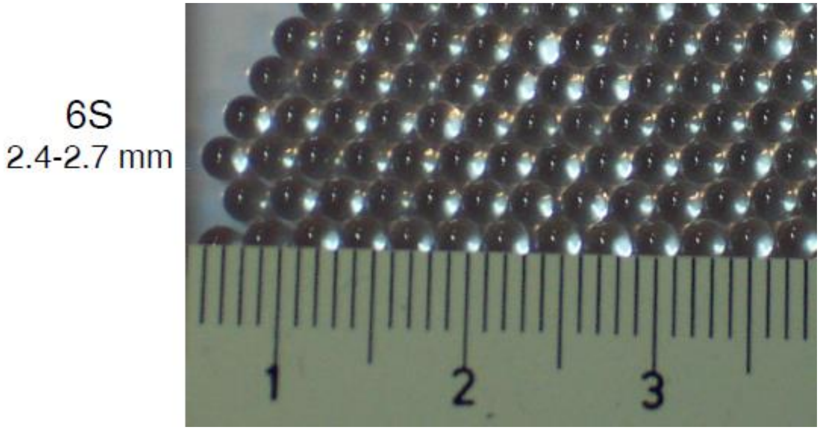

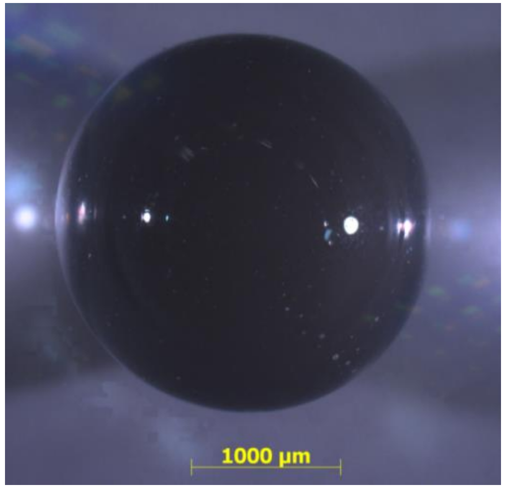

Controlled pluviation into membrane lined mould

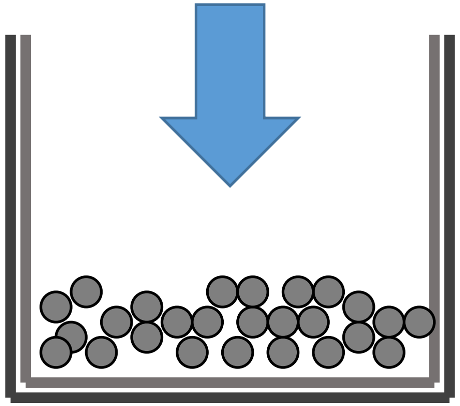

50 kPa vacuum applied to place sample in apparatus

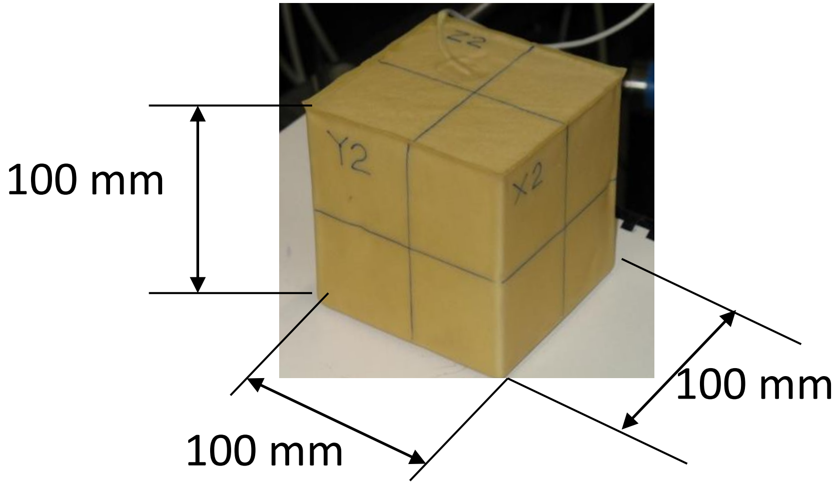

Void ratio: e_{lab}=0.60

O'Donovan et al. (2016)

Validation of simulation approach

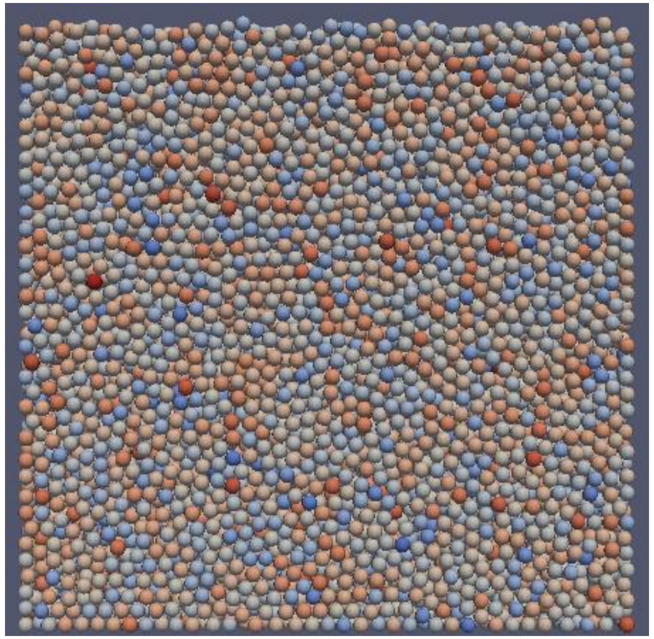

62,445 particles
Pluviated using Granular Lammps
Ave. coord. number: 5.185
Cross-anisotropic fabric

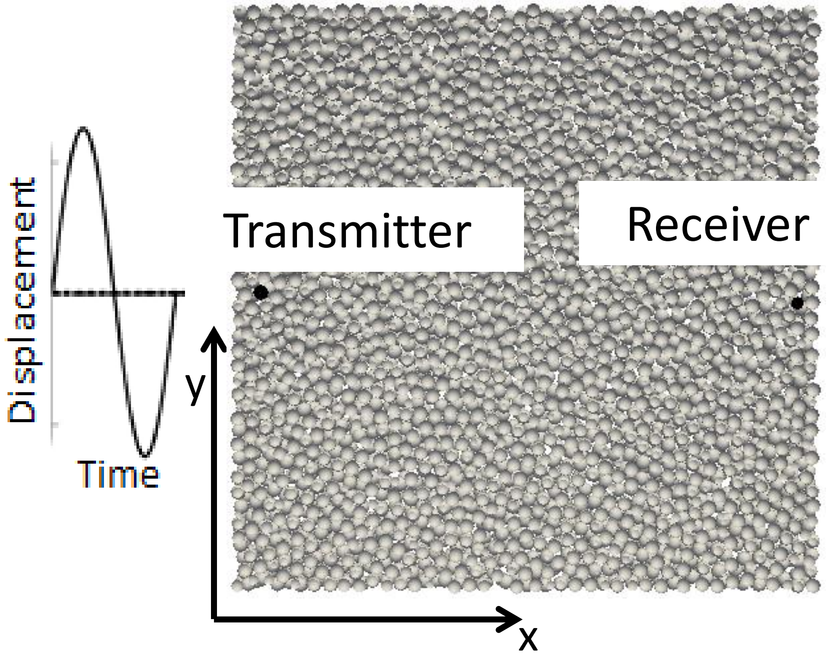

Simulated using PFC 3D
Flexible membrane boundaries
Simplified Hertz-Mindlin contact model
Bender/extender elements modelled as point sources

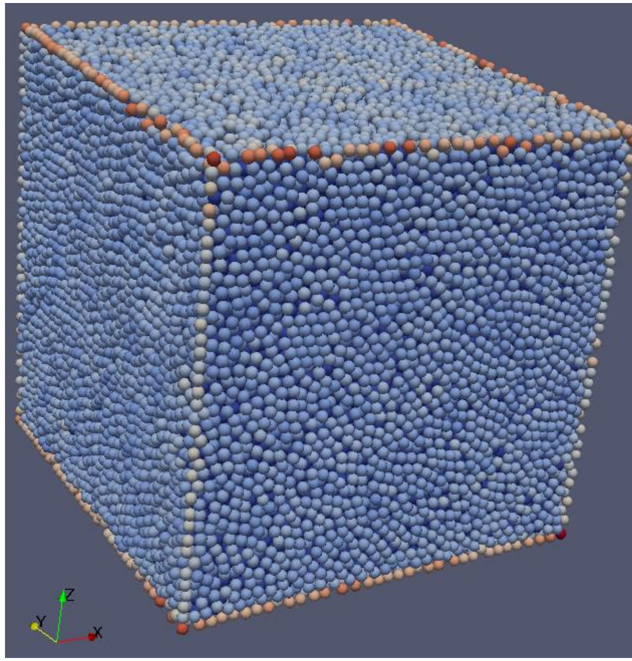

Void ratio: e_{DEM}=0.67

O'Donovan et al. (2016)

Validation of simulation approach

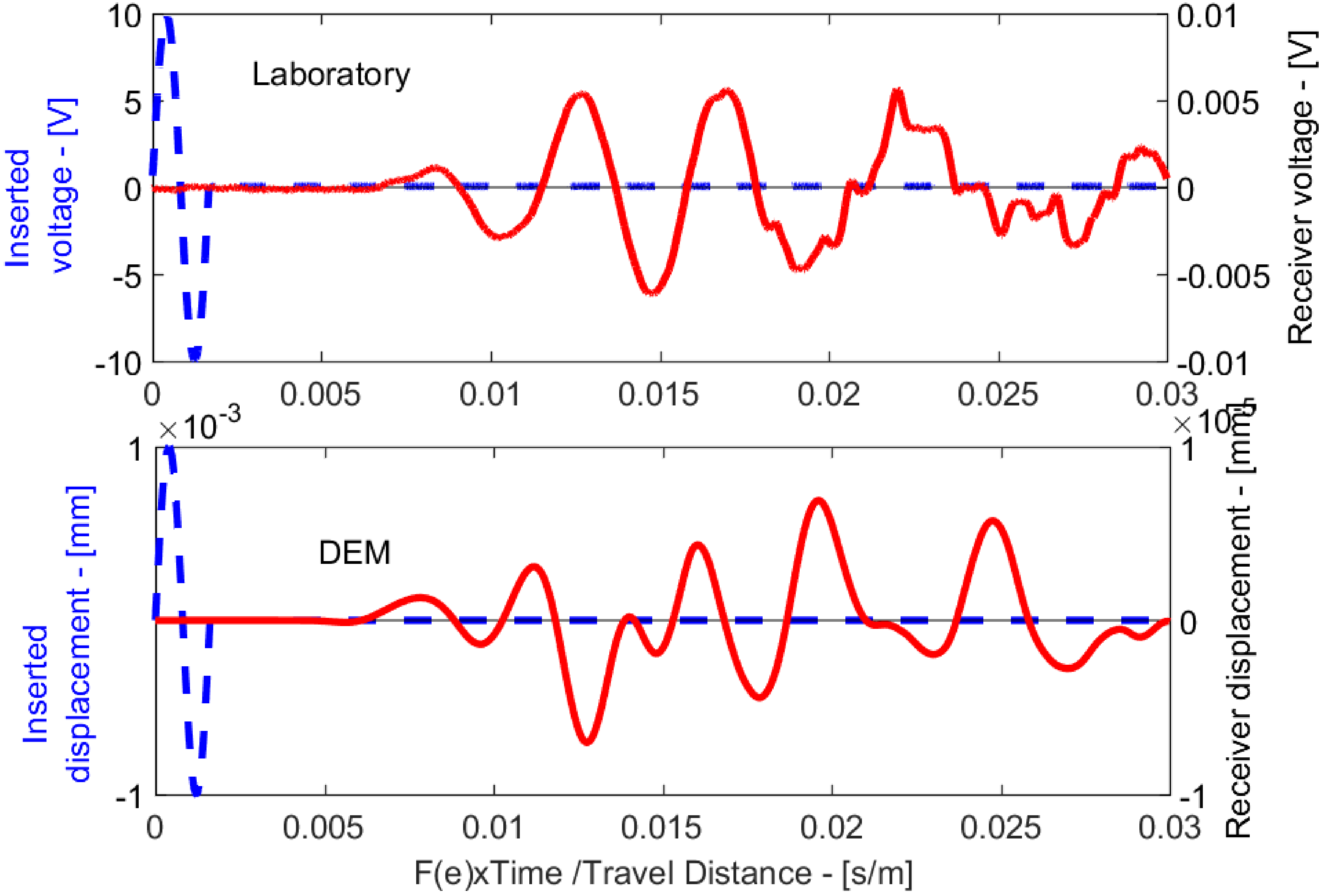

Time domain comparison

- Void ratio correction:
  F(e) = 2.9-e
- Adjusted for differences in travel distance

O'Donovan et al. (2016)

Validation of simulation approach

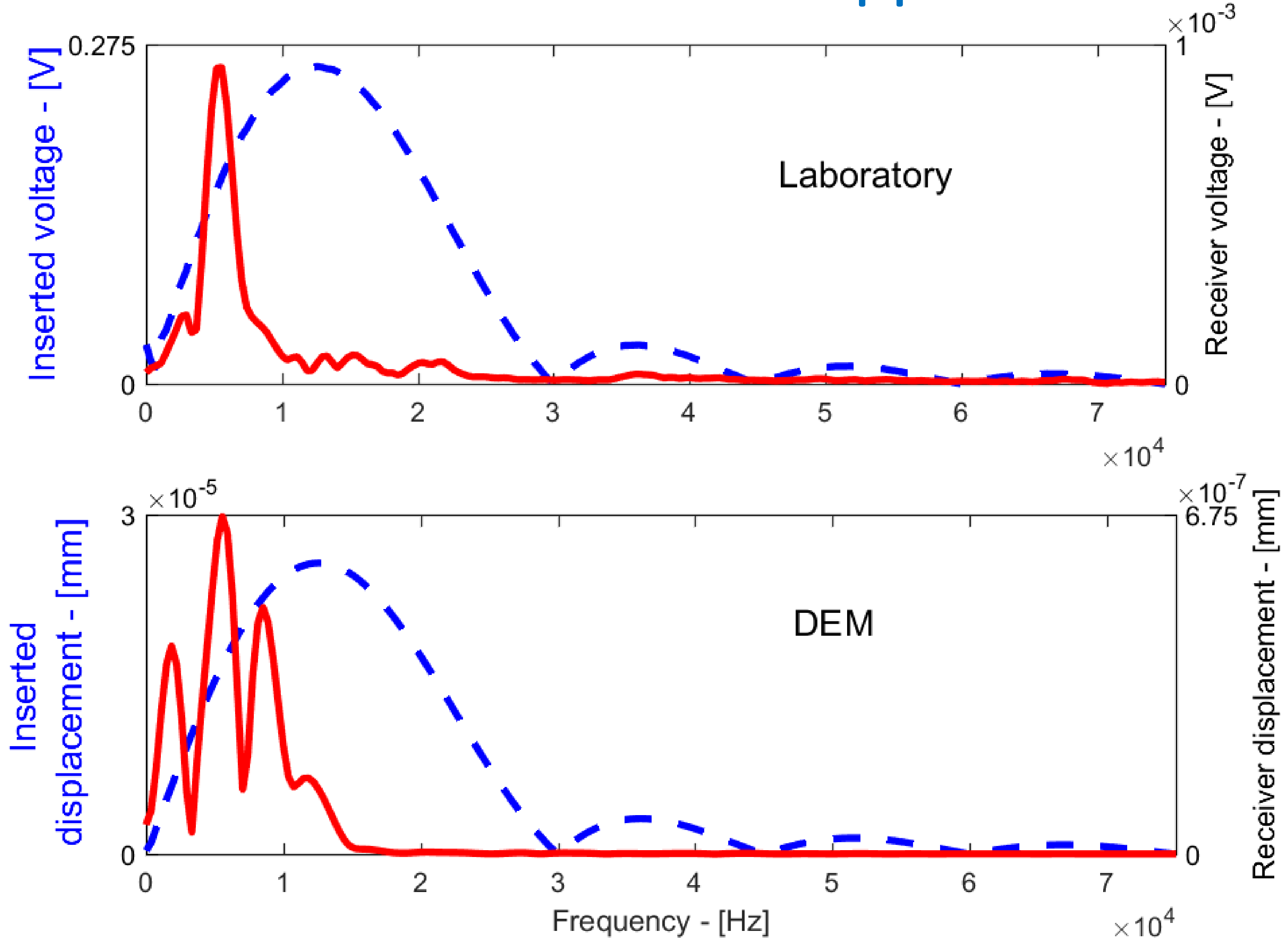

Frequency domain comparison

O'Donovan et al. (2016)

Analytical validation

- Response of single ball systems worth checking
- Assemblies of contacting grains form statically indeterminate systems
- Lattice packings - can exploit symmetric to get analytical expressions for strength
- Thornton (1979) Géotechnique contribution – cited in PFC manual – very useful

Validation of granular LAMMPS

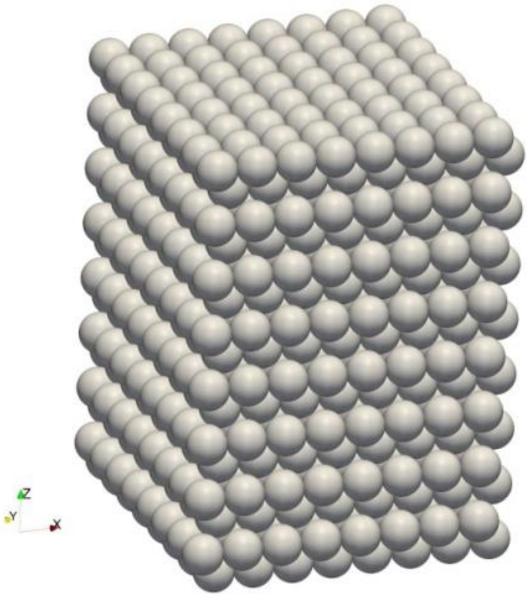

Compression of face-centred-cubic array of spheres.

Analytical solution documented in Thornton (1979) Géotechnique

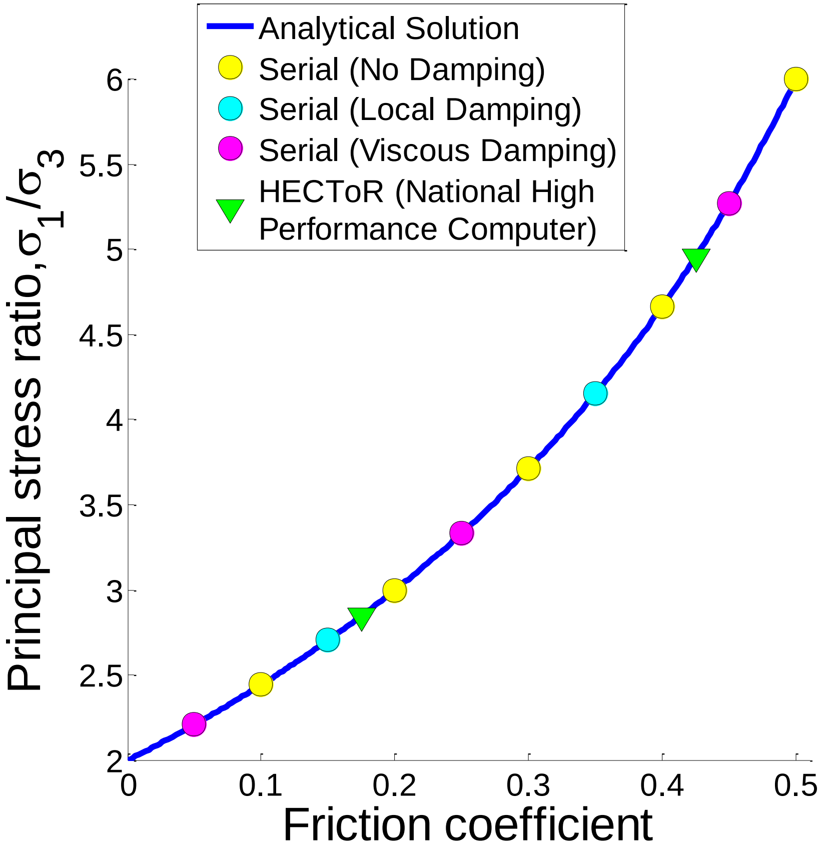

Validations by
K. Hanley and X. Huang

O'Sullivan (2014)

Validation - granular LAMMPS – small strain / dynamic response

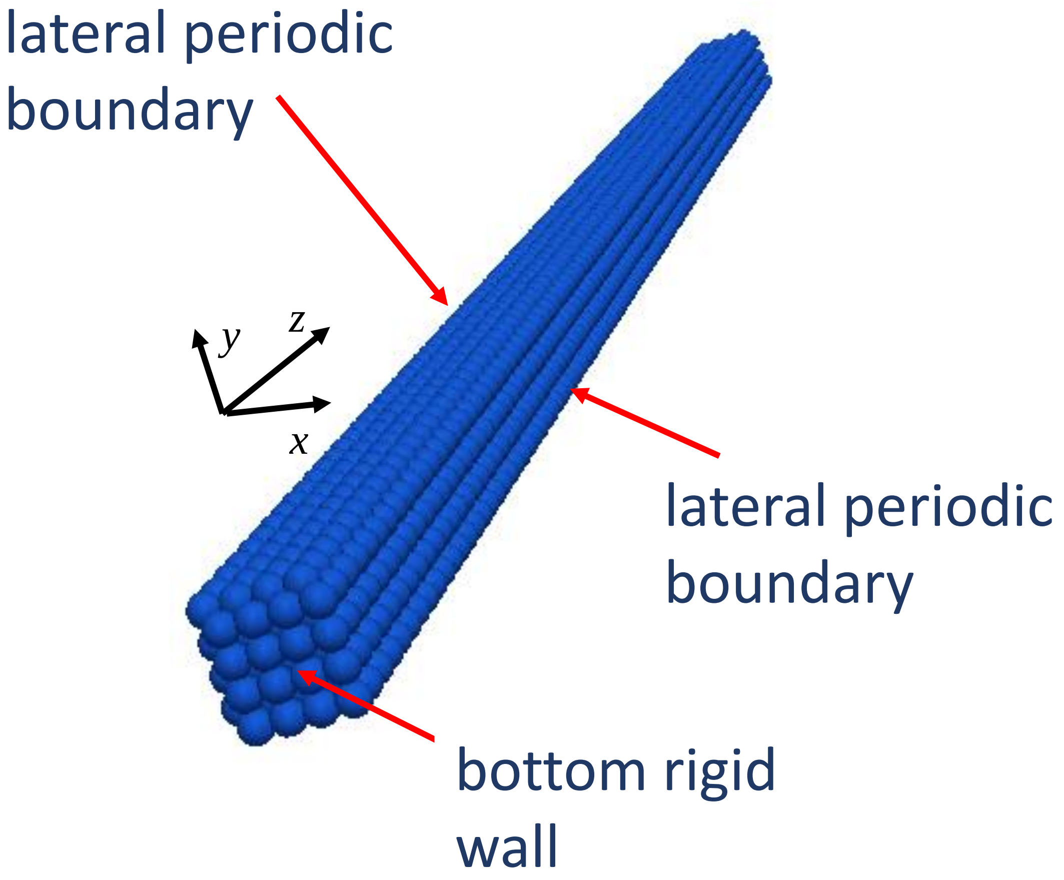

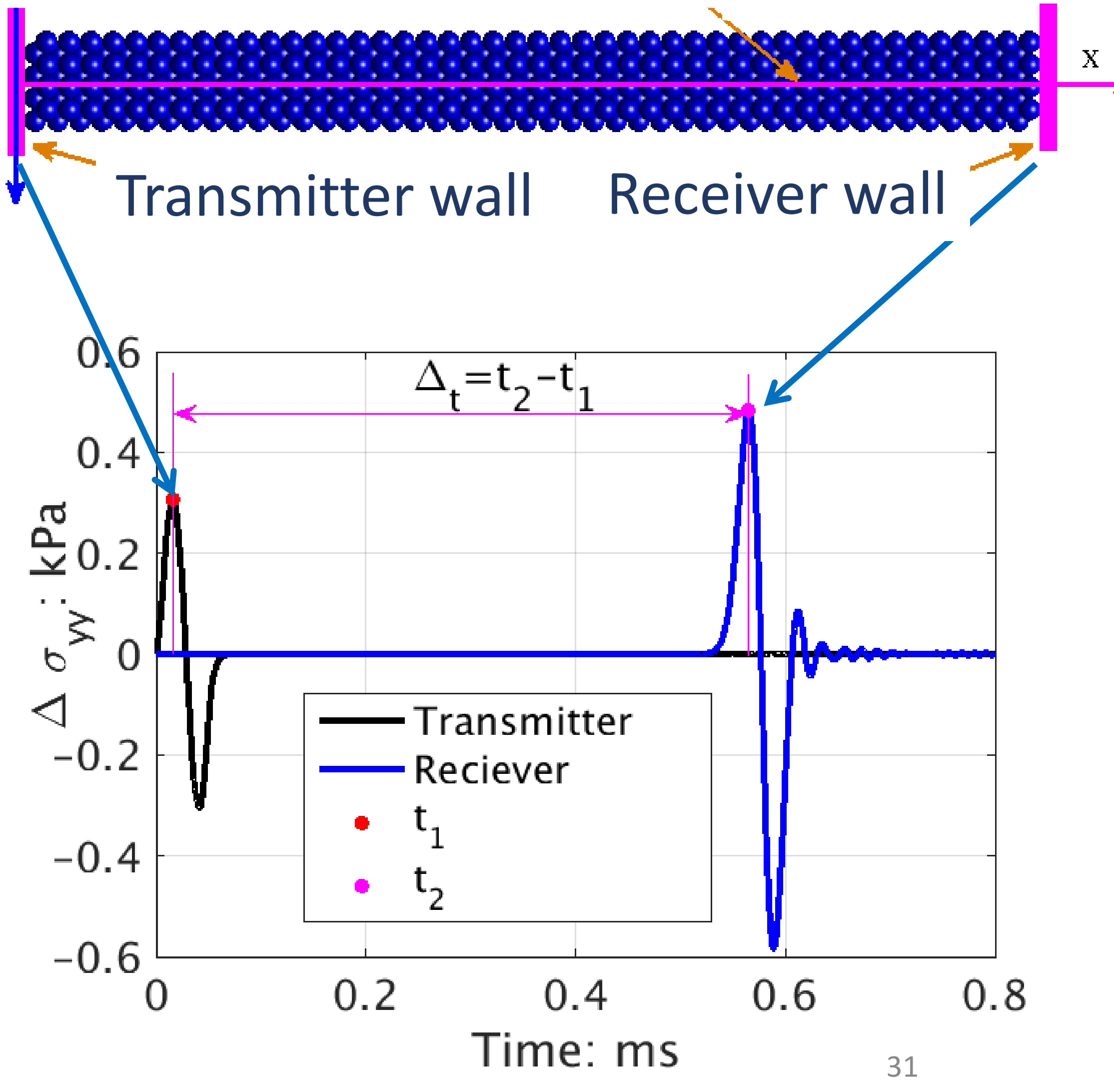

Nguyen et al. (2017)

Validation - granular LAMMPS – small strain / dynamic response

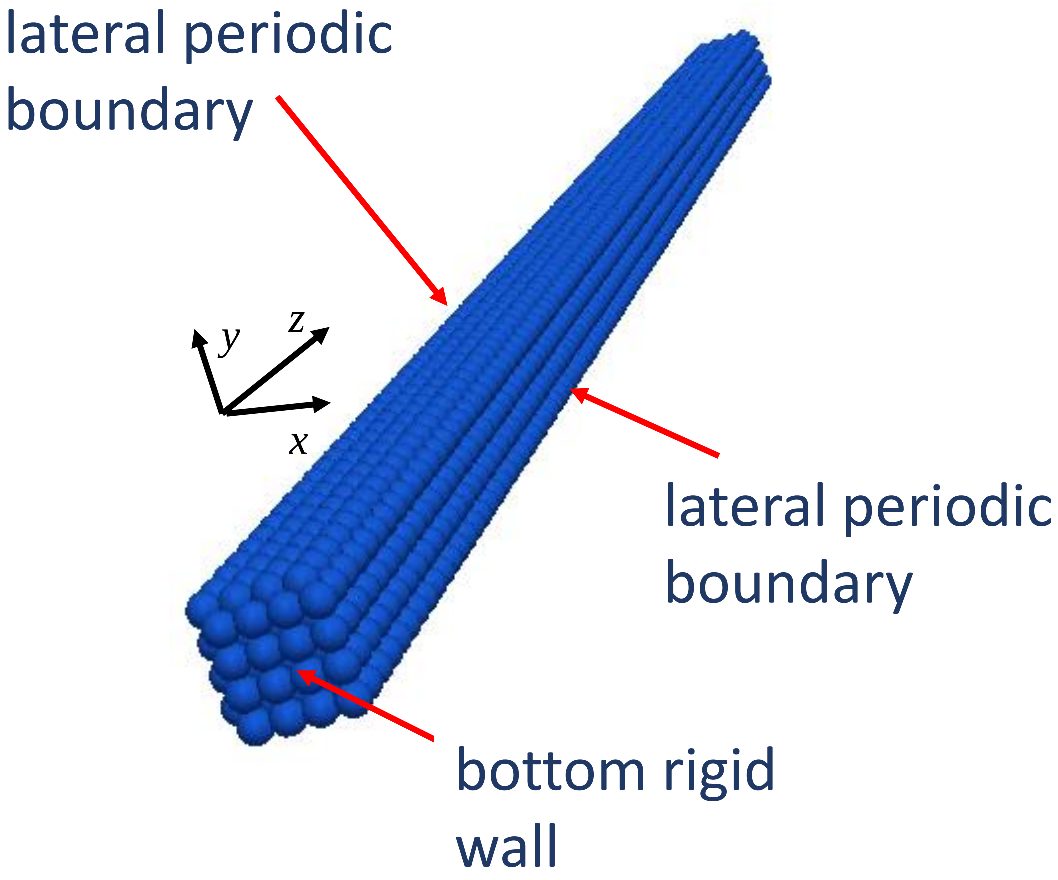

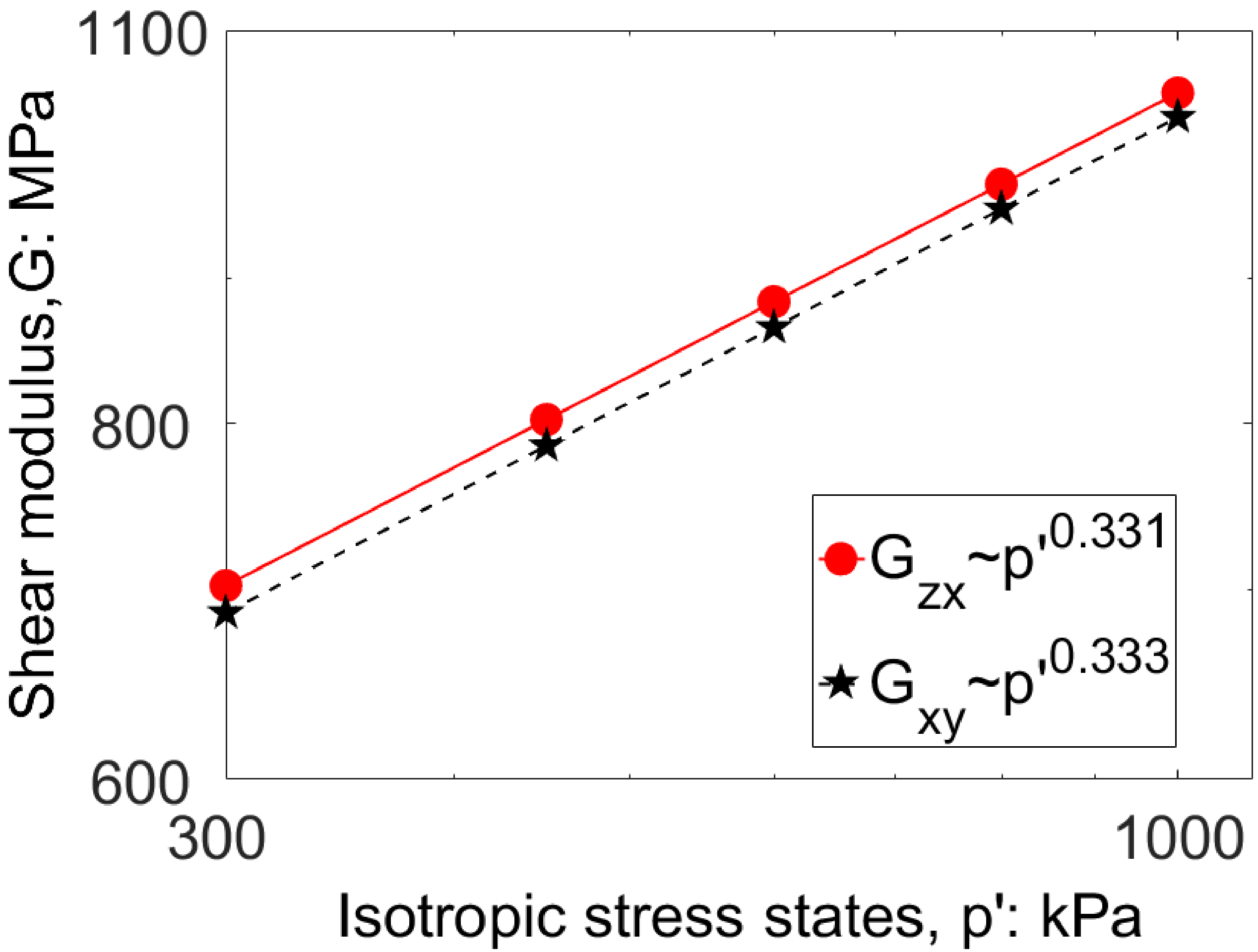

Nguyen et al. (2017)

Conclusions

- Experimental validation is useful/essential, but not straightforward
- Analytical approaches using regular packing v important
- Benchmarking on random systems is helpful – cross comparison of codes (more later)

Time step

Time integration in DEM

- The displacement of each particle is calculated using the explicit, conditionally stable, Verlet time integration approach.

  $$\Delta u_i^t = (v_i^{t-\Delta t/2} + (F_i^t / M_i) \times (\Delta t)) \times \Delta t$$

  - Δu_i^t = incremental displacement from time t to time $t+\Delta t$ for particle i
  - $v_i^{t-\Delta t/2}$ = velocity at time $t-\Delta t/2$ for particle i
  - F_i^t = total force acting on particle i at time t
  - M_i = mass of particle i

- Very similar to finite difference method

Calculating critical time increment

Single ball on a boundary

Single degree of freedom system

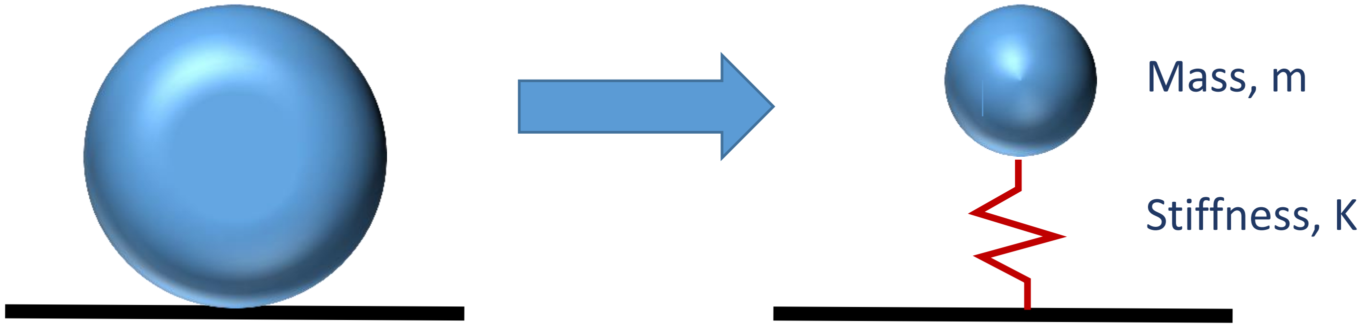

$$\Delta t_{crit,SDOF} = 2\sqrt{m/K}$$

Calculating critical time increment

Single ball on a boundary

Single degree of freedom system

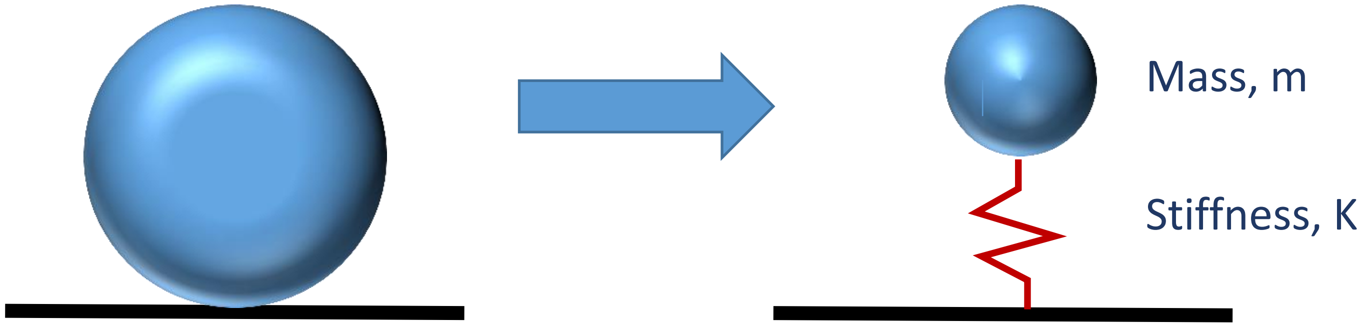

Hart et al. (1988):

$$\Delta t_{crit,DEM} = 2\alpha \sqrt{m_{min} / 2K_{max}}$$

If α =0.1:

$$\Delta t_{crit,DEM} = 0.14 \sqrt{m_{min} / K_{max}}$$

Calculating critical time increment

Single ball on a boundary

Single degree of freedom system

Tsuji et al. (1993):

Parametric study

Monodisperse spheres

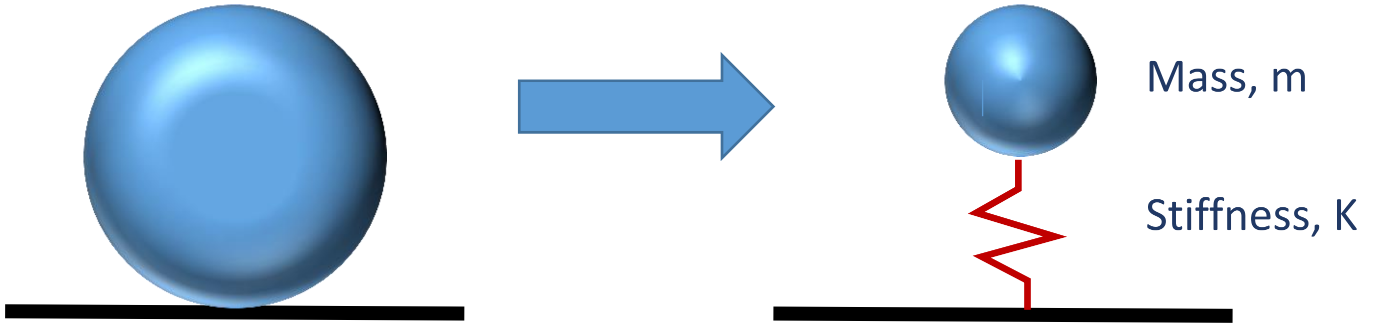

$$\Delta t_{crit,DEM} = \frac{\pi}{5}\sqrt{m/K}$$

$$\Delta t_{crit,DEM} = 0.63\sqrt{m/K}$$

Calculating critical time increment

Single ball on a boundary

Single degree of freedom system

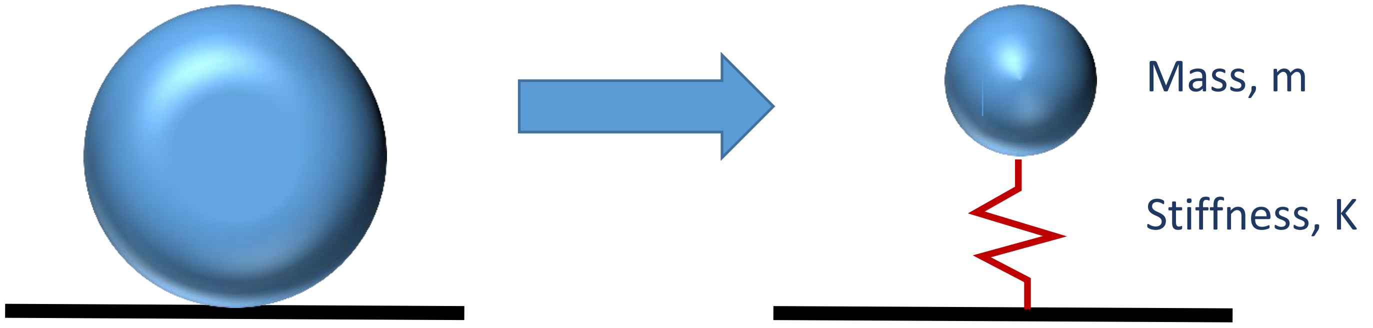

Tu and Andrade (2008)

Rotation critical

$$\Delta t_{crit,DEM} = 1.2\sqrt{m_{min}/K_T}$$

K_T is the tangential spring stiffness

Calculating critical time increment: Itasca Approach

- Based on estimating eigenvalues of system
- For each particle assume rotational and translational degrees of freedom are uncoupled
- Sum contributions from all contacts to get translational and rotational stiffnesses (k_{trans}, k_{rotate})
- Look at minimum of ratios $\sqrt{m/_{k_{trans}}}$, $\sqrt{I/_{k_{rot}}}$, I moment of inertia

Calculating critical time increment: Rayleigh wave speed approach

- Considers time for a Rayleigh wave to pass a sphere in a single time step

$$T_R = \frac{\pi R \sqrt{\frac{\rho}{G}}}{0.1631\nu + 0.8766}$$

- ρ is the particle density, ν is the particle Poisson's ratio, G is the particle shear modulus, R is the particle radius

- Expression given in Kremmer and Favier (2001), Li et al. (2005) amongst others

- Some authors focus on minimum particle radius (R_{min}) others on average radius (R_{ave})

Calculating critical time increment: eigenvalue approach

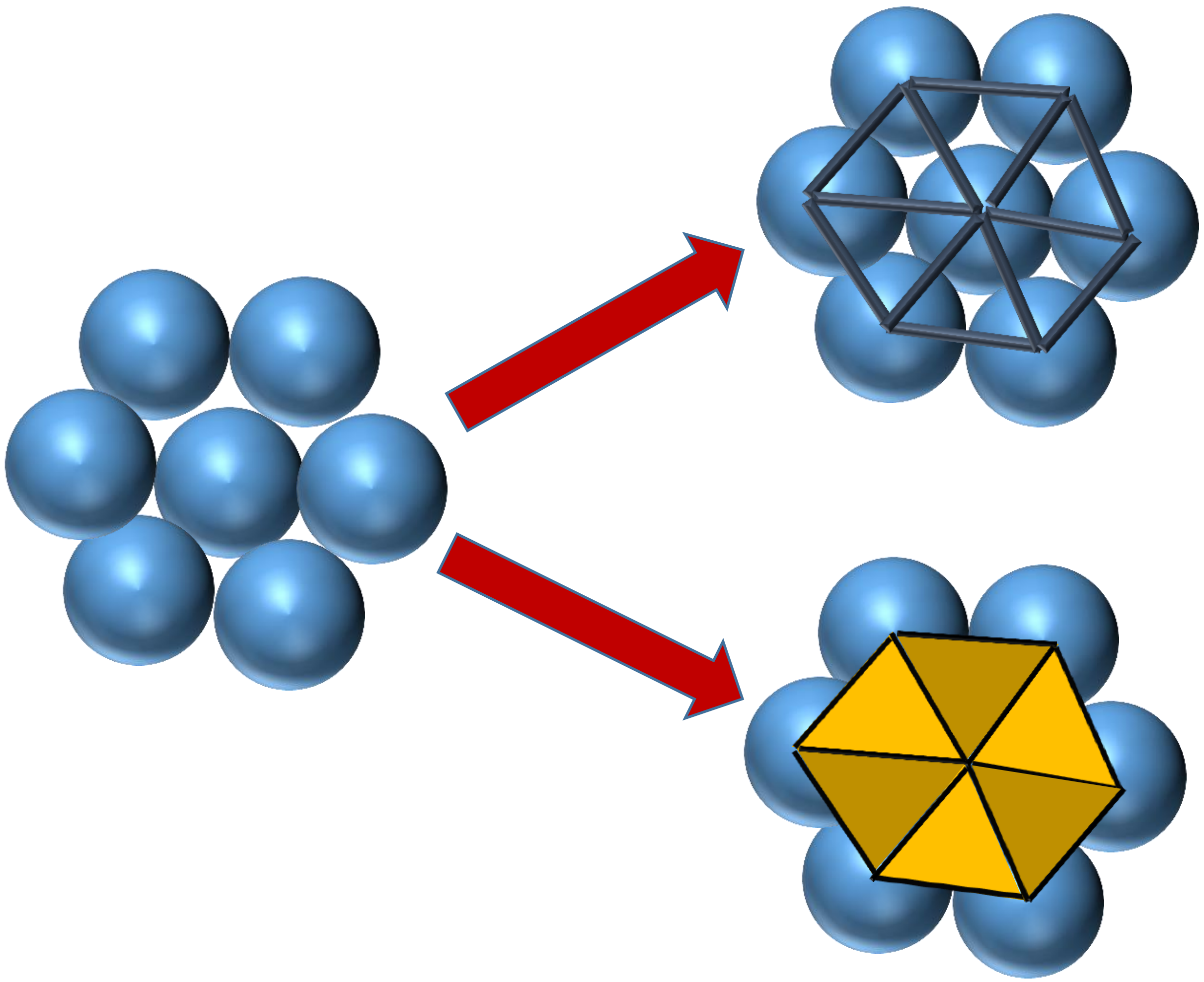

Structural truss / system

Finite element mesh

$$\Delta t_{crit} = \frac{2}{\omega_{max}} \leq \min_{ele} \frac{2}{\omega_{ele}}$$

ω_{max}=max frequency of linearized system

ω_{ele}= frequency of element *ele*

Calculating critical time increment: eigenvalue approach

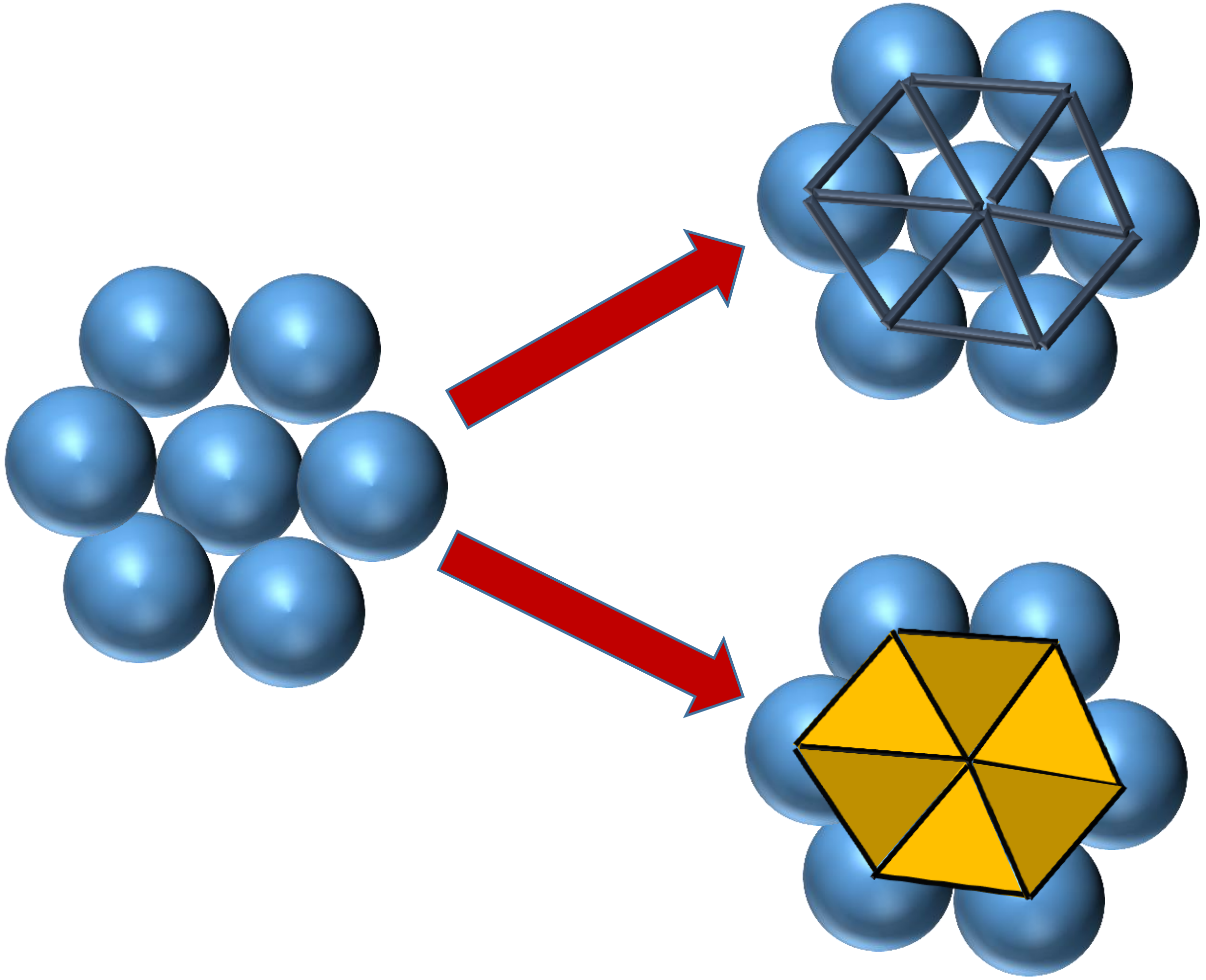

Structural truss / system

Finite element mesh

$$\Delta t_{crit} = \frac{2}{\omega_{max}} \leq \min_{ele} \frac{2}{\omega_{ele}}$$

- $\omega_{max} = \sqrt{\lambda_{max}}$
- λ_{max} = max eigenvalue of $\mathbf{M}^{-1}\mathbf{K}$
- $\mathbf{M}$ global mass matrix
- $\mathbf{K}$ global stiffnes matrix

Calculating critical time increment: eigenvalue approach

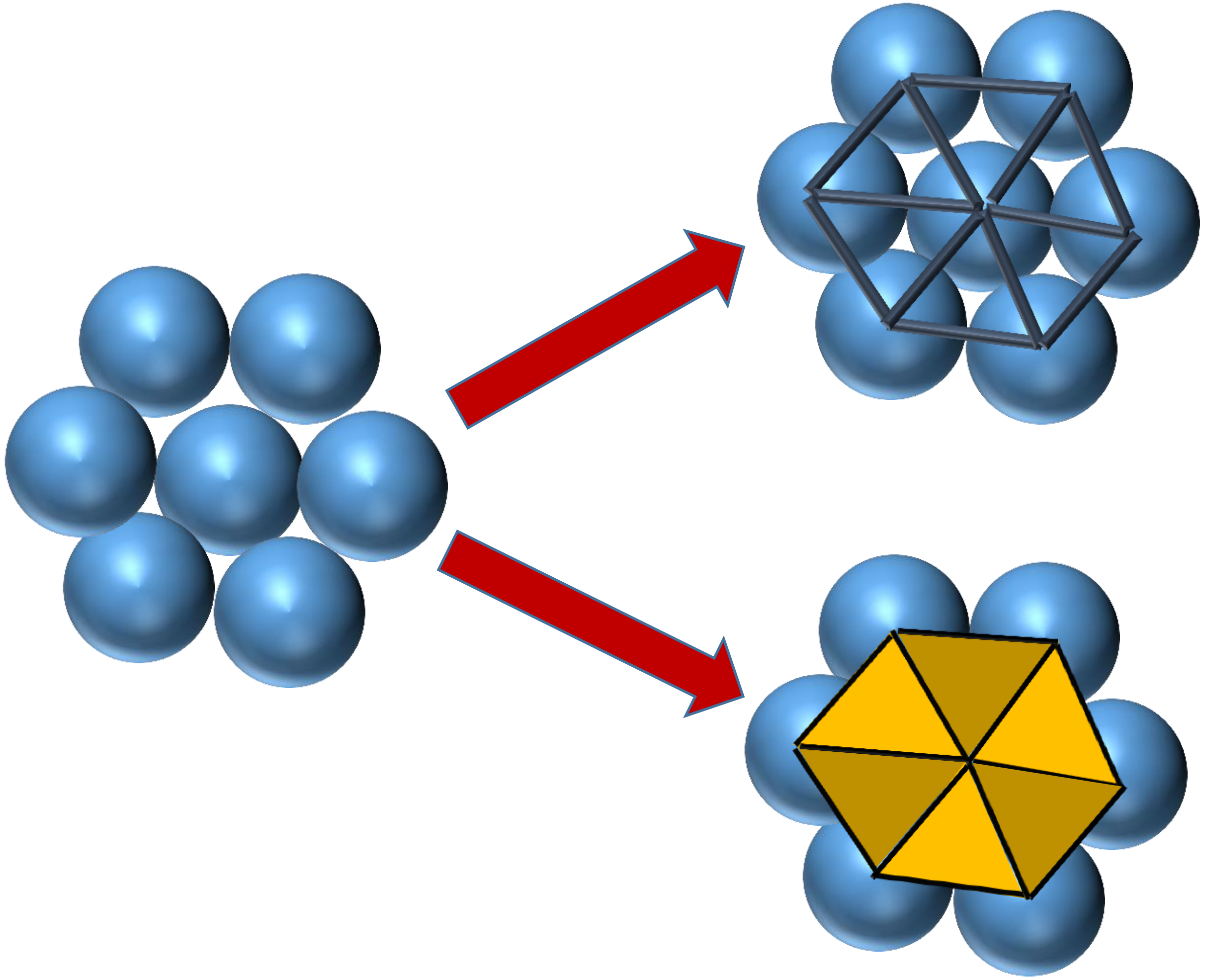

Structural truss / system

$$\Delta t_{crit} = \frac{2}{\omega_{max}} \leq \min_{ele} \frac{2}{\omega_{ele}}$$

- $\omega_{max} = \sqrt{\lambda_{max}}$
- λ_{max} = max eigenvalue of $\mathbf{M}^{-1}\mathbf{K}$
- $\lambda_{max} \leq \lambda_{max}^{ele}$
- λ_{max}^{ele} max eigenvalue of $\mathbf{M}^{ele\text{-}1}\mathbf{K}^{ele}$

Finite element mesh

Calculating critical time increment: eigenvalue approach

O'Sullivan and Bray (2004): Analytical study

Regular (lattice packings) – linear spring, stiffness k

2D and 3D

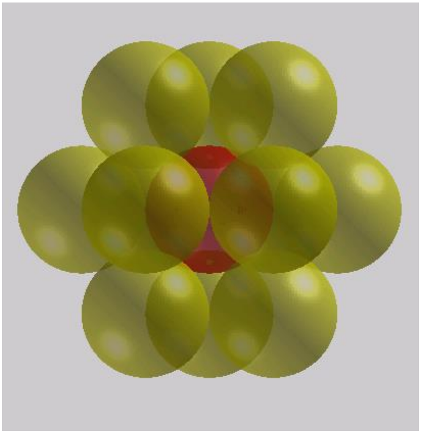

$$\Delta t_{crit} = 0.22\sqrt{m/k}$$

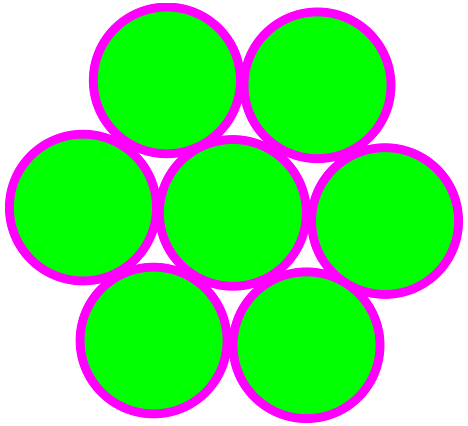

$$\Delta t_{crit} = 0.41\sqrt{m/k}$$

Calculating critical time increment: eigenvalue approach

O'Sullivan and Bray (2004): Analytical study

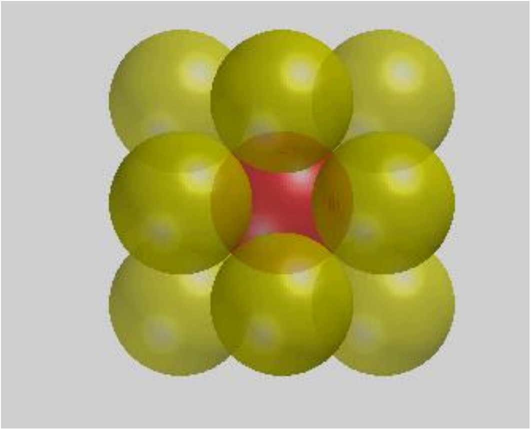

Face-Centered-Cubic

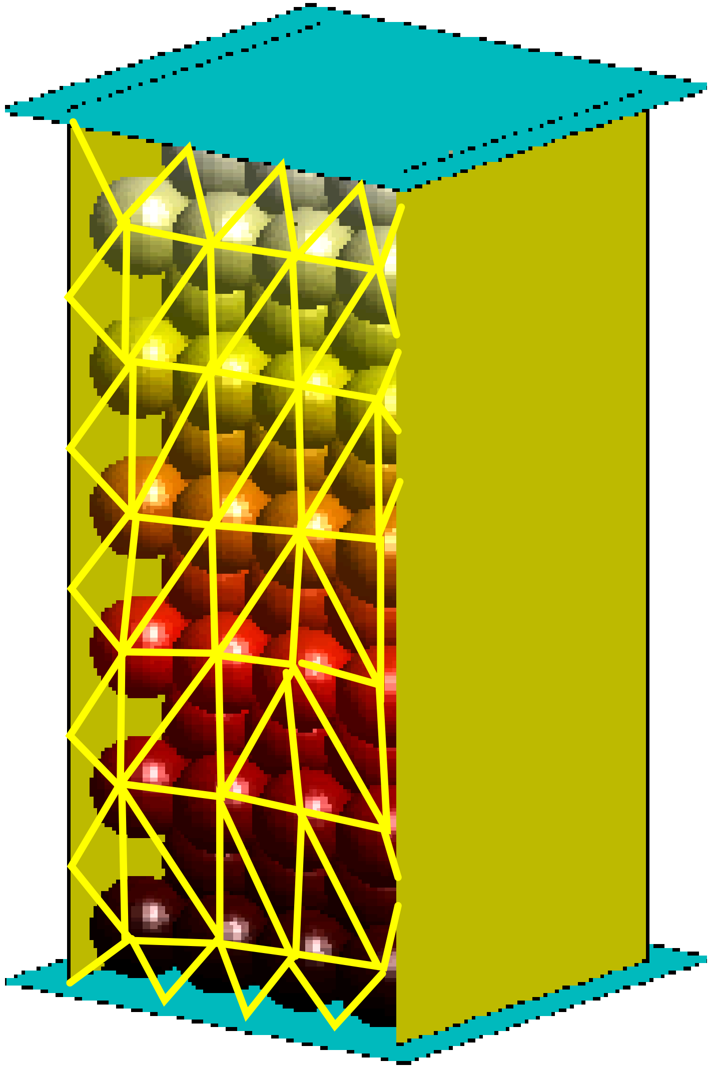

3-D Plane Strain

Compression of 150 spheres

Calculating critical time increment: eigenvalue approach

O'Sullivan and Bray (2004): Analytical study

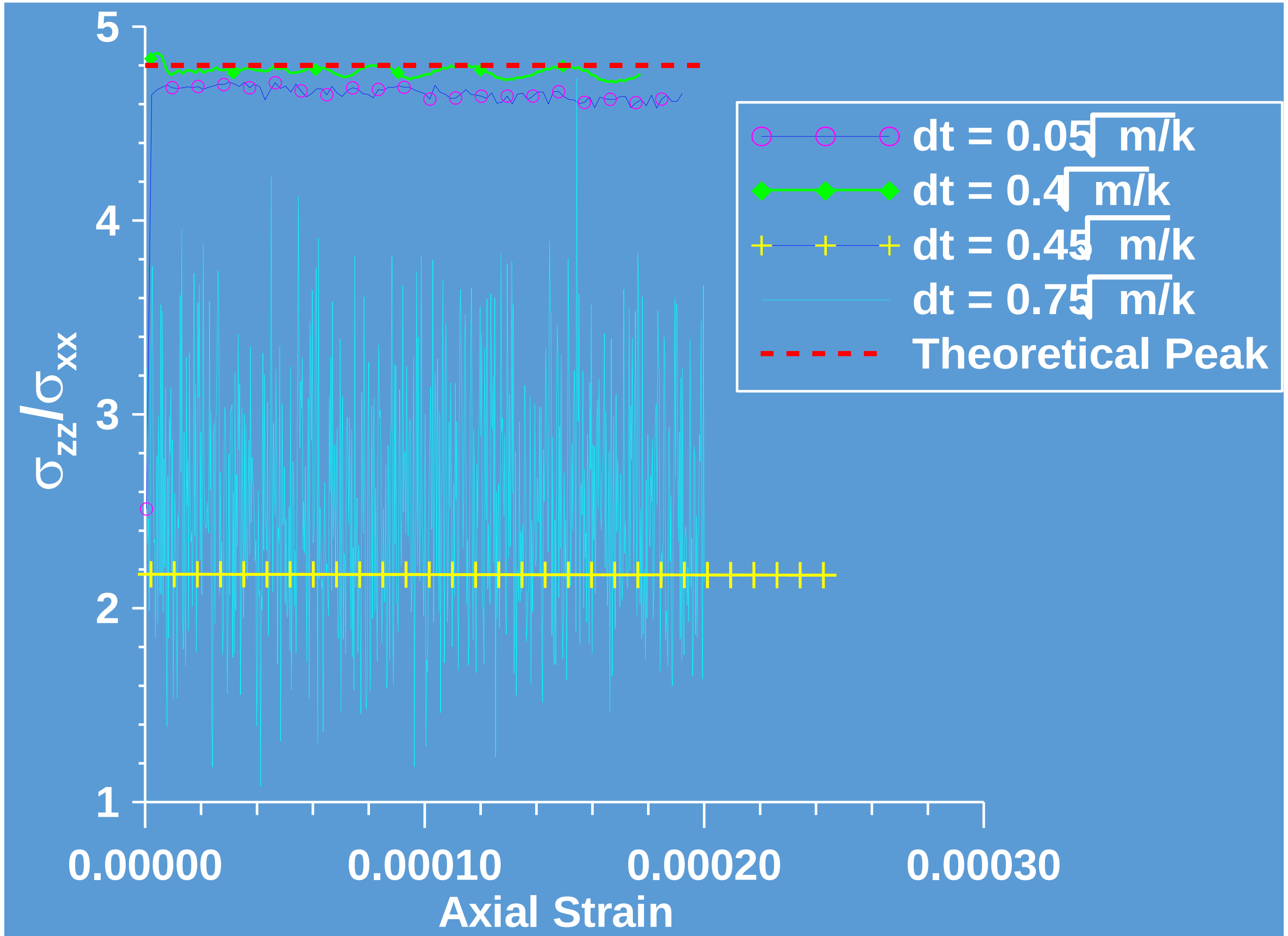

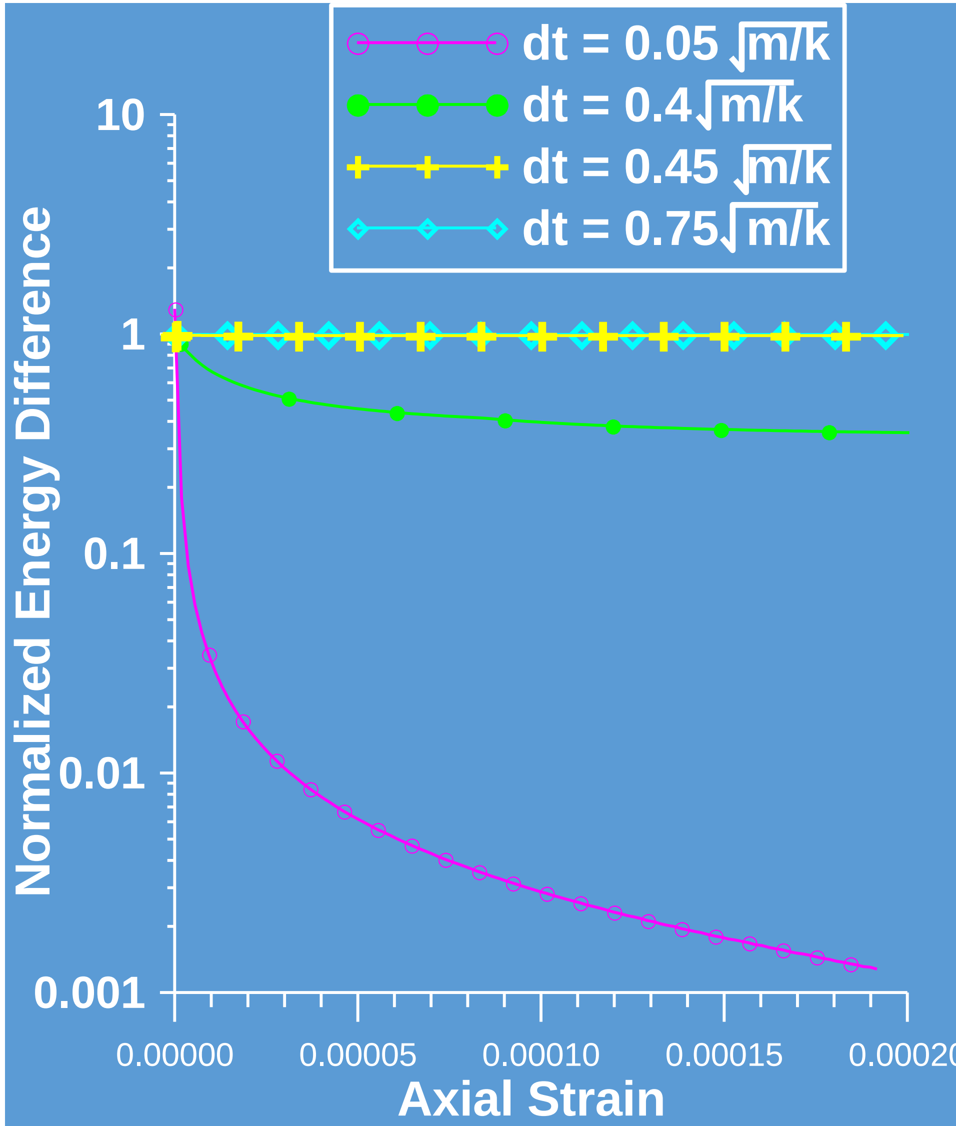

Calculating critical time increment: eigenvalue approach

O'Sullivan and Bray (2004): Analytical study

- Highlighted dependency of critical time increment on no of contacts per particle
- Consideration of rotation reduced critical time increment
- Study limited to lattice packings of uniform spheres
- Contact model linear springs

Conclusions

- Conditionally stable method

- Essential to be within stability limit, but should not be over conservative

From eigenvalue approach:

- Critical time step depends on contact stiffness (which depends on confining pressure for Hertz-Mindlin model), particle mass and packing density (coordination number)

- Method based on Rayleigh wave speed not always conservative

Boundary conditions

Rigid wall boundaries

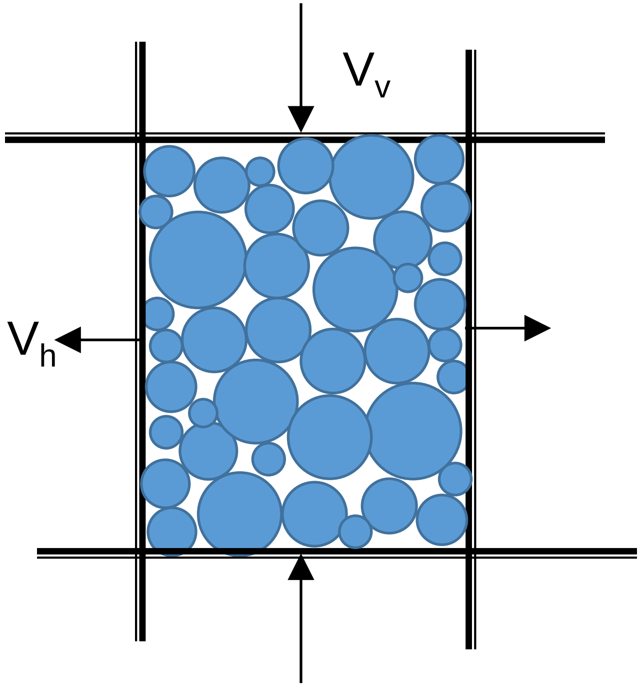

- Planar / cylindrical / mesh of triangles
- Can move to control stress - servo control
- Can control stress on boundary or in specified internal region

Rigid wall boundaries – simulation of direct shear test

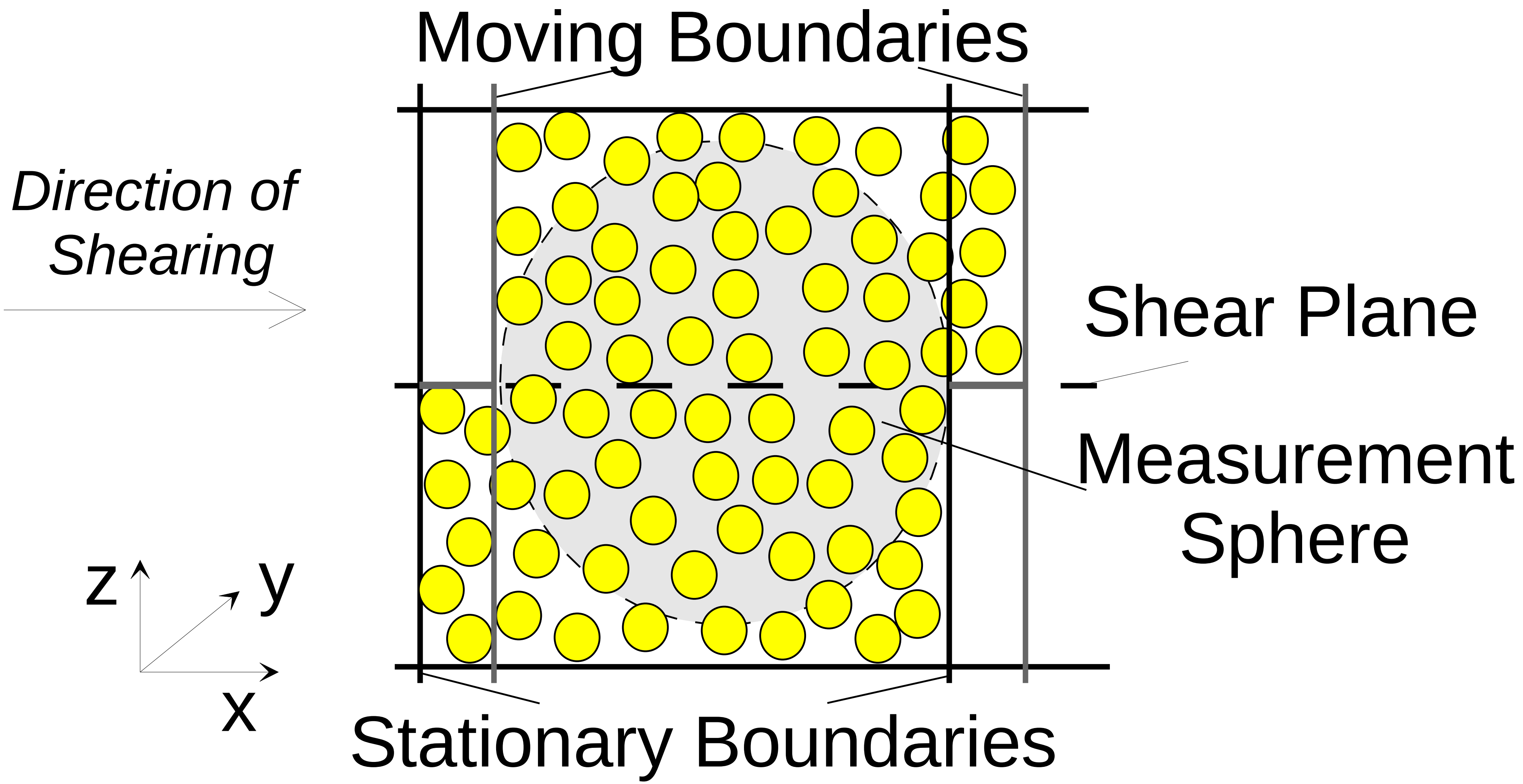

Rigid wall boundaries – simulation of direct shear test

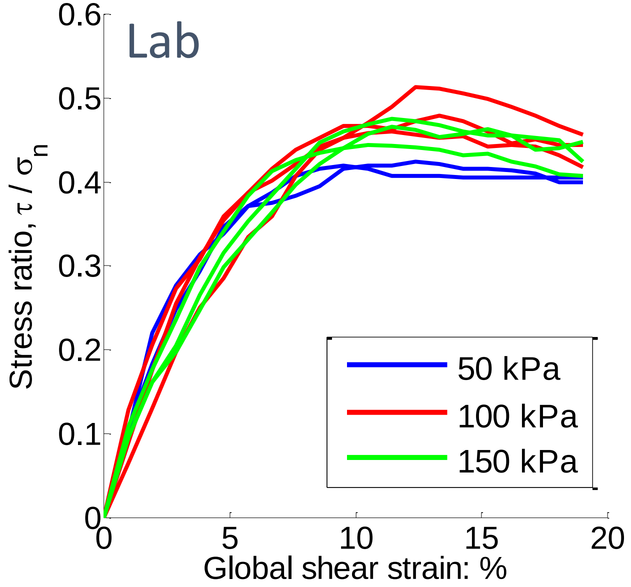

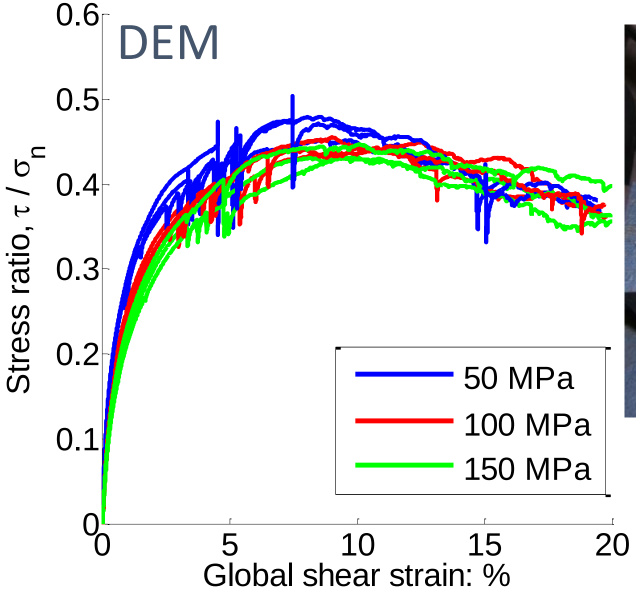

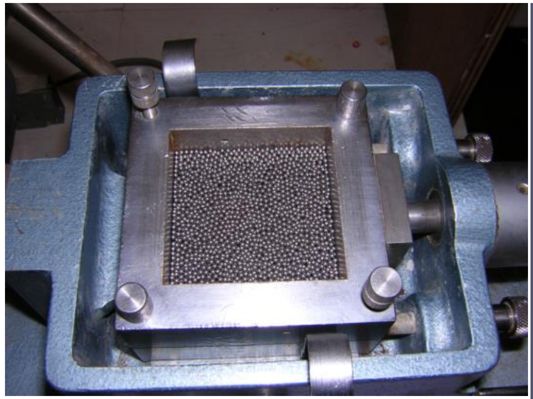

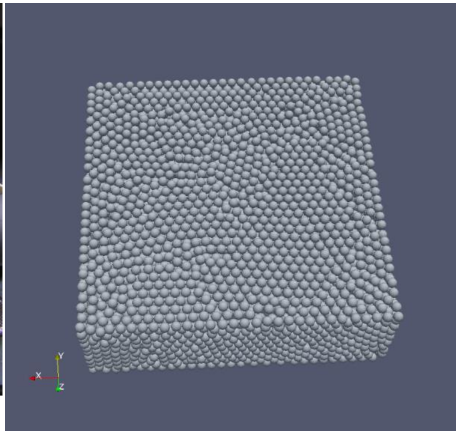

Grade 25 steel precision balls

Diameter 0.992 mm

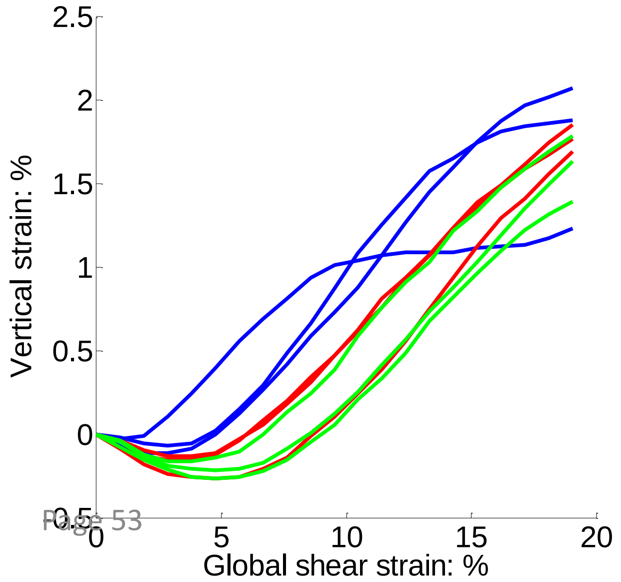

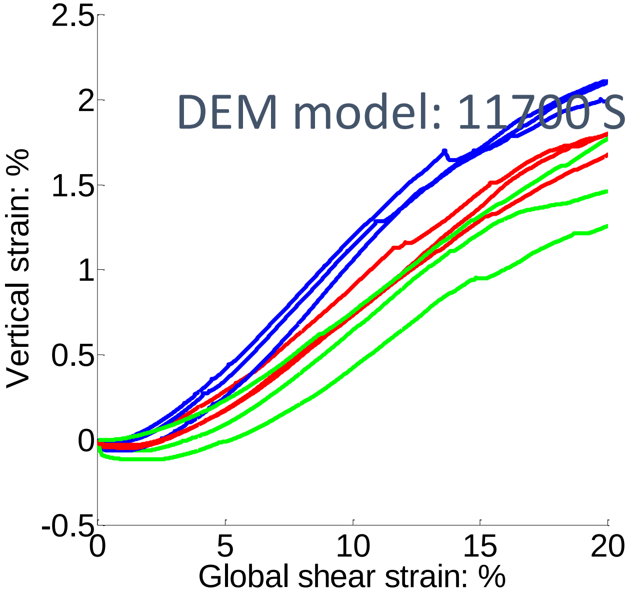

DEM model: 11700 Spheres

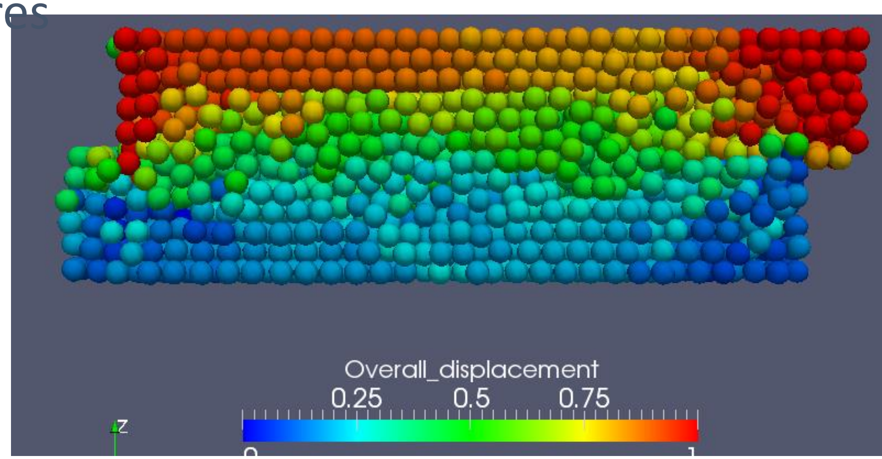

Simple shear simulations – Laminar (NGI) Device

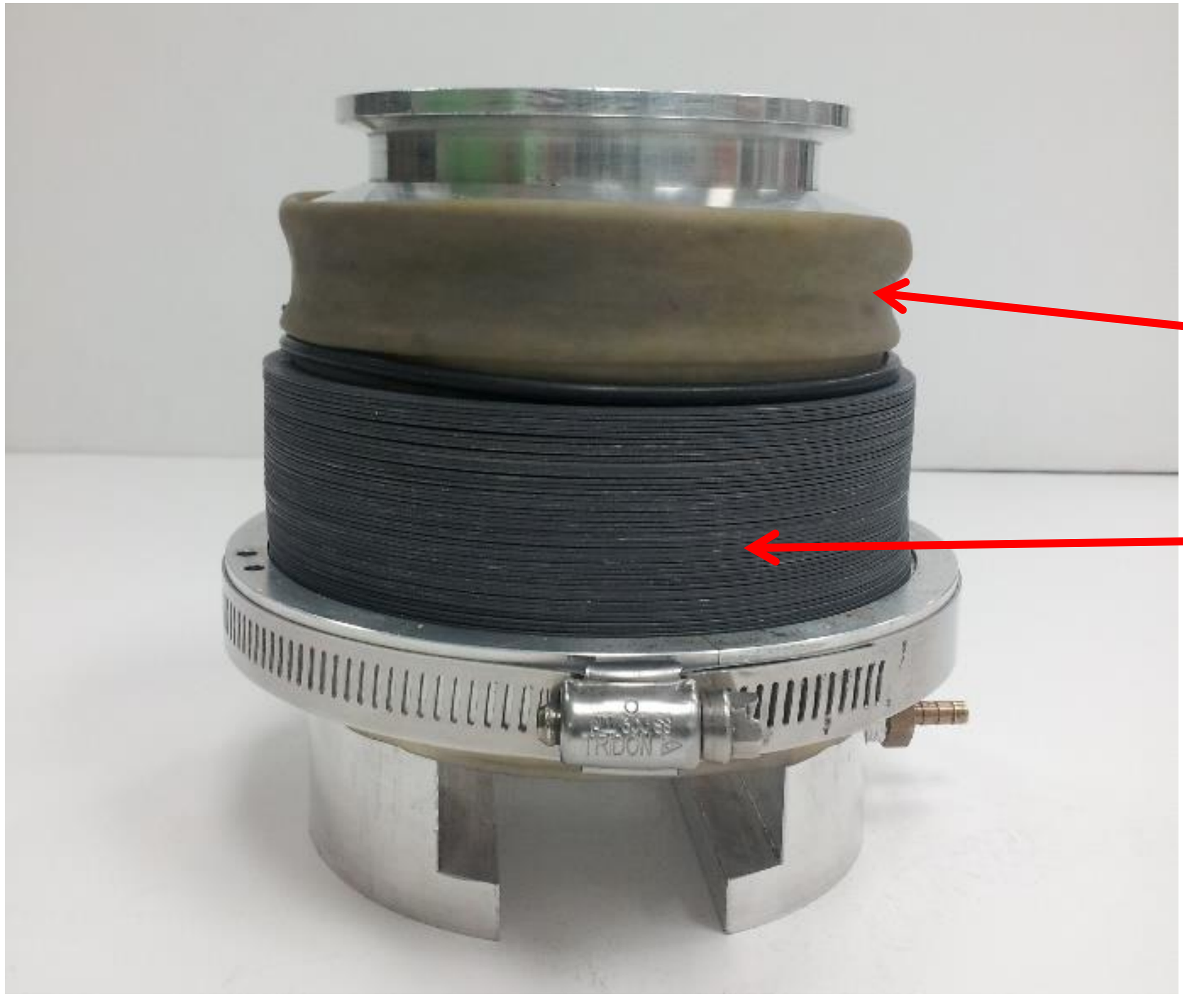

Membrane

Stacked ring configuration

Bernhardt et al. (2016)

Simple shear simulations – Laminar (NGI) Device

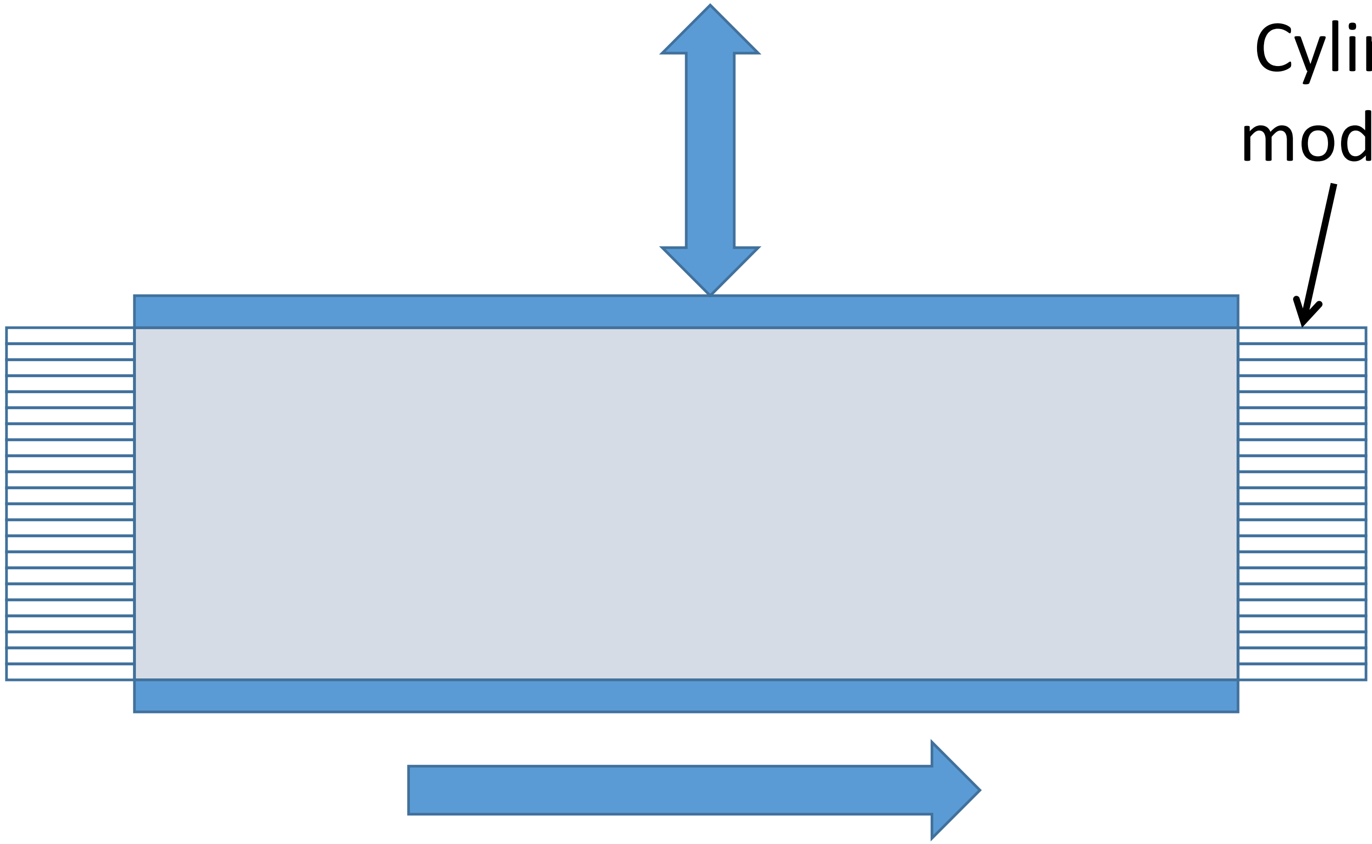

Bernhardt et al. (2016)

Simple shear simulations – Laminar (NGI) Device

Normal force
(stress servo controlled wall)

Challenge is that wall entities do not have inertia

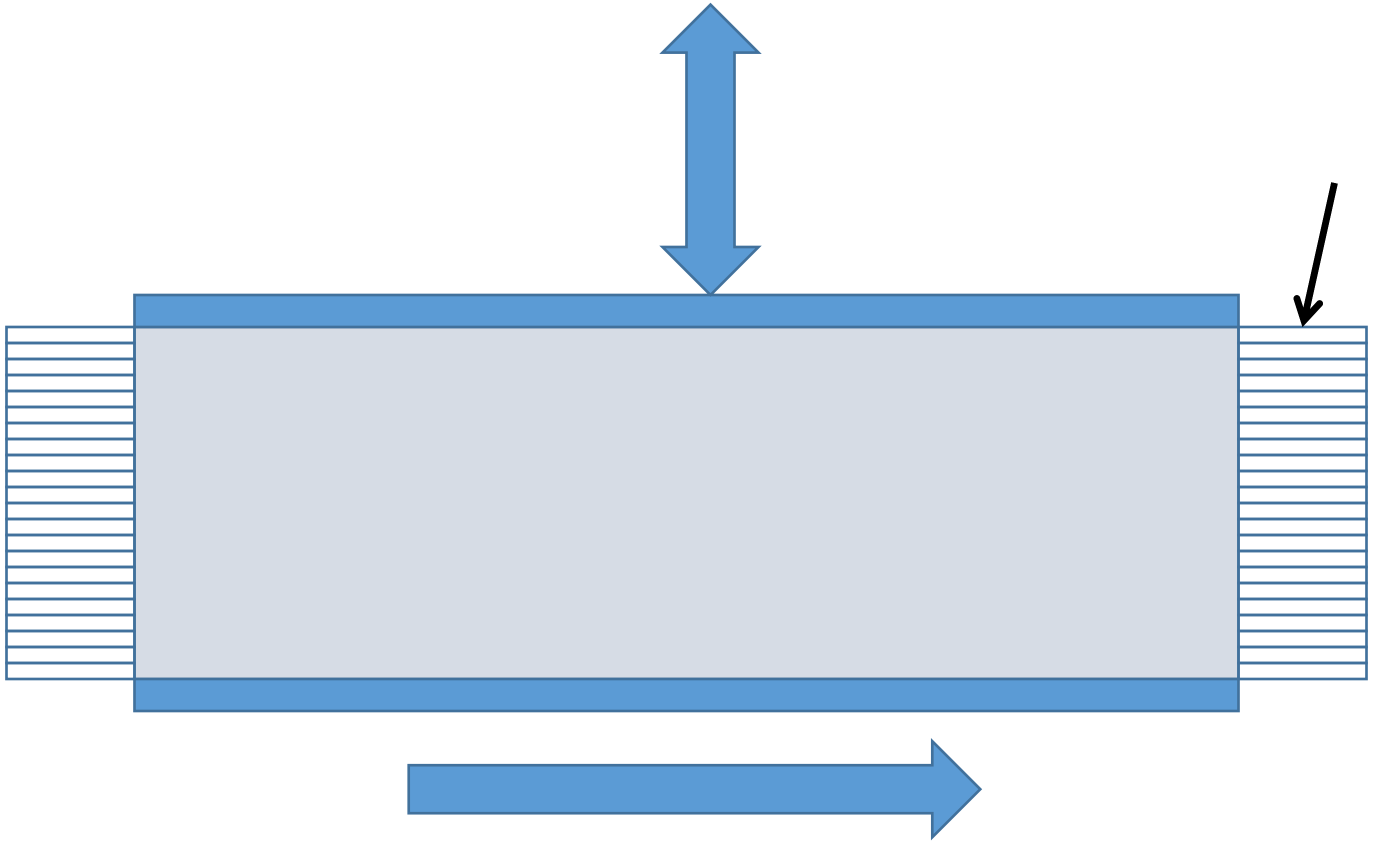

Need a special algorithm to control wall position

Lateral movement – velocity specified

Bernhardt et al. (2016)

Simple shear simulations – Laminar (NGI) Device

- Used cylindrical wall boundaries
- Controlled wall motion by using forces acting on wall – aim to have resultant force is 0.0

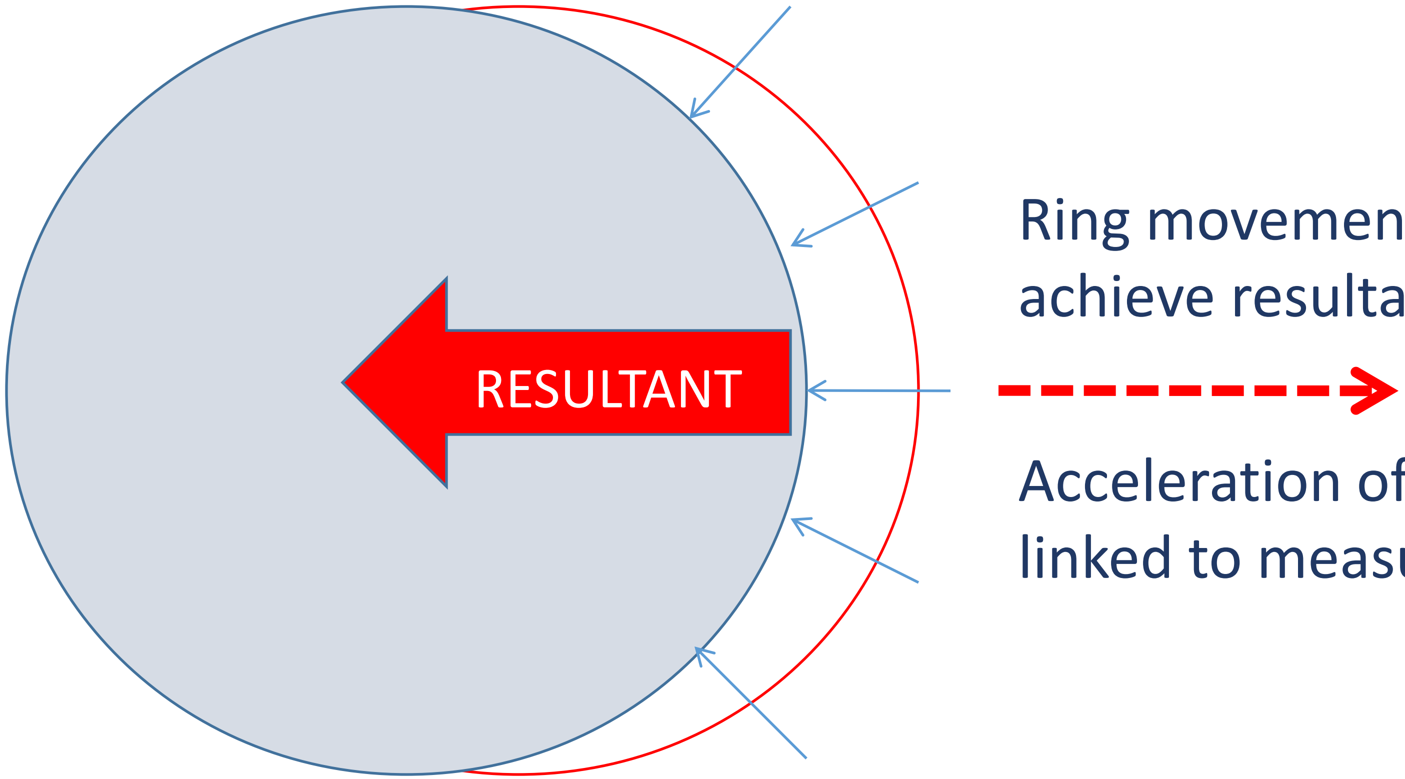

Ring movement controlled to achieve resultant force of 0

Acceleration of movement linked to measured force

Bernhardt et al. (2016)

Simple shear simulations – Laminar (NGI) Device

10 confining rings

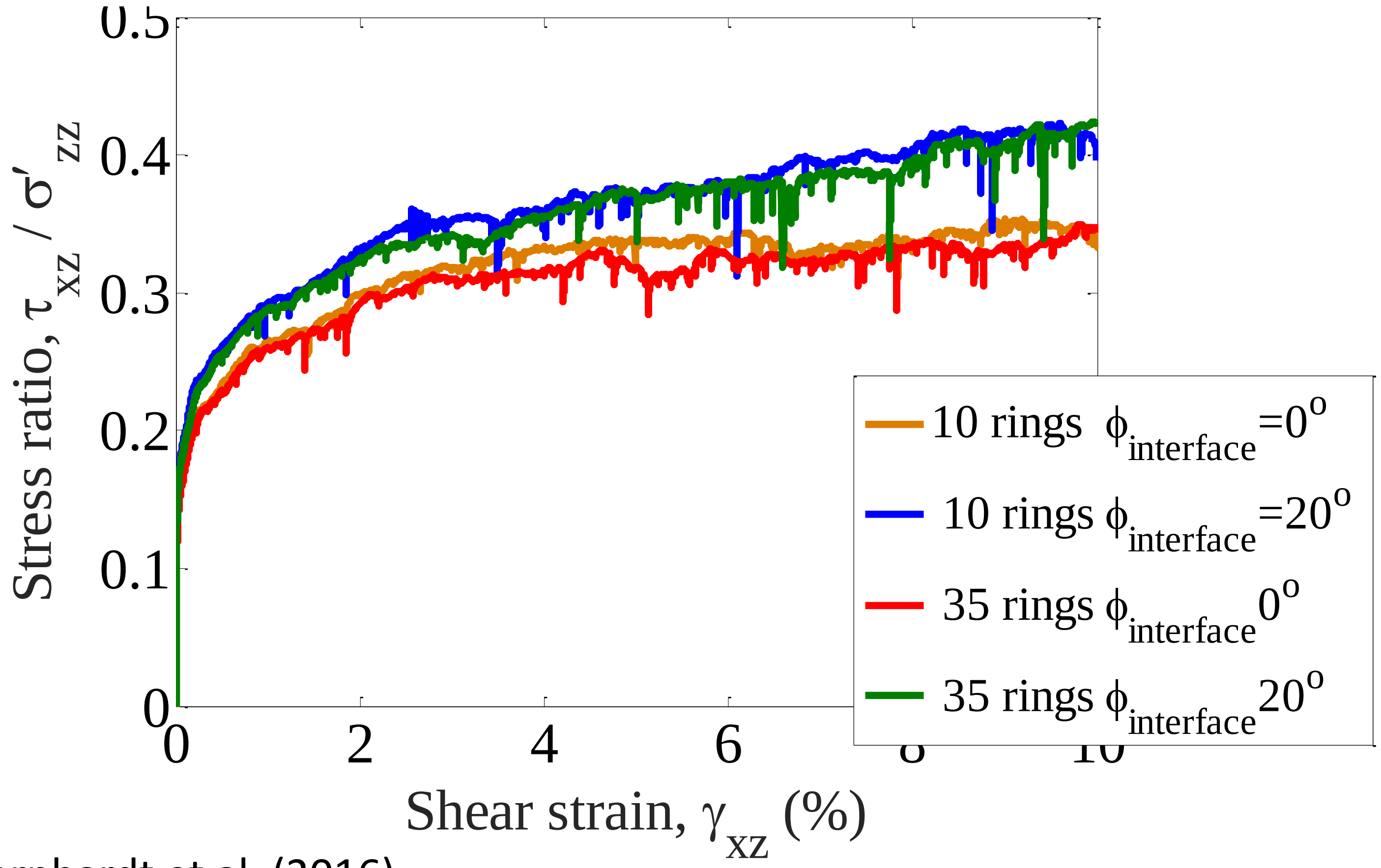

Bernhardt et al. (2016)

- Load-deformation responses equivalent for 10 and 35 rings
- Considered assumption of smooth interface
- 20o is friction measured between membrane and rings

Simple shear simulations – Laminar (NGI) Device

Horizontal boundaries

Option 1 – Flat friction → localization close to boundaries)

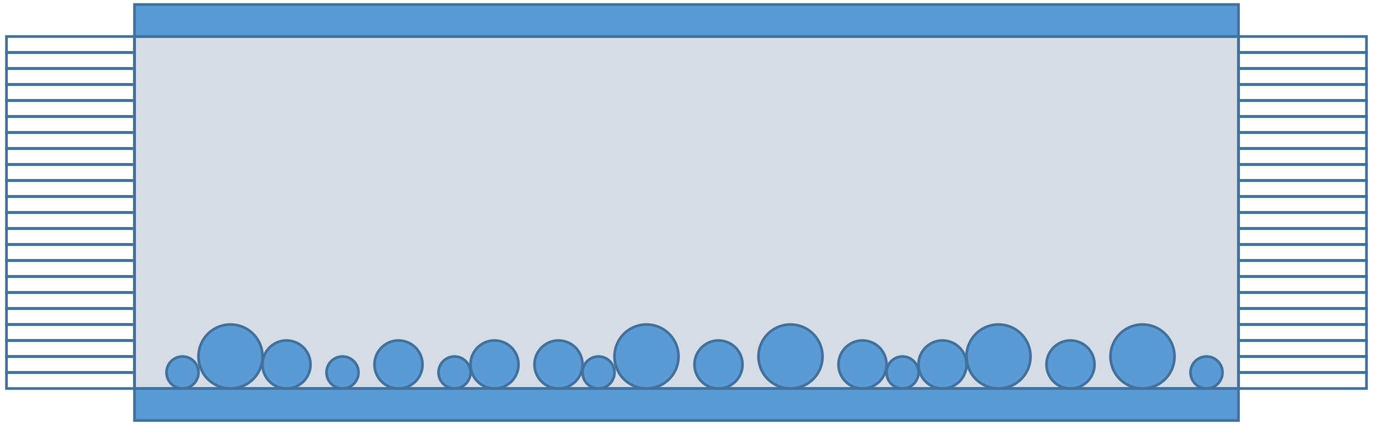

Option 2 – Rough surface achieved by gluing particles to boundary walls

Simple shear simulations – Laminar (NGI) Device

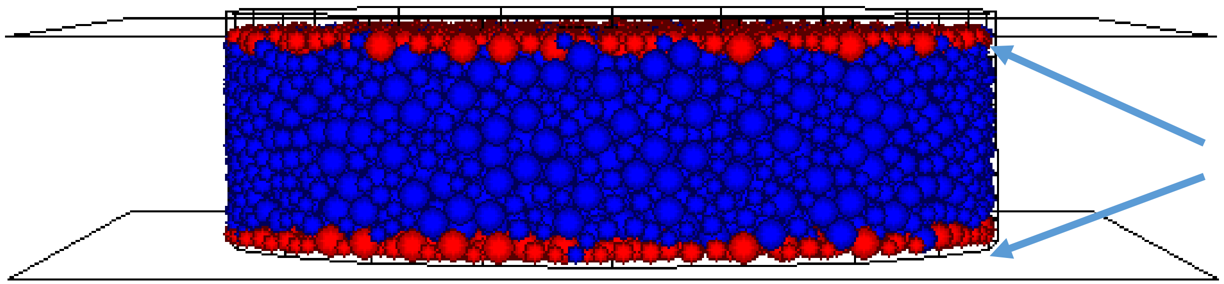

Spheres fixed to boundary

- Vertical stress applied by considering the sum of the out of balance forces on the group of "glued" particles and the force on the wall coming from contact with these particles.
- Contact forces with the wall remain constant once the particles are glued.
- Additional forces are given by out of balance forces on the individual particles.

Bernhardt et al. (2016)

Stress controlled boundaries / membranes

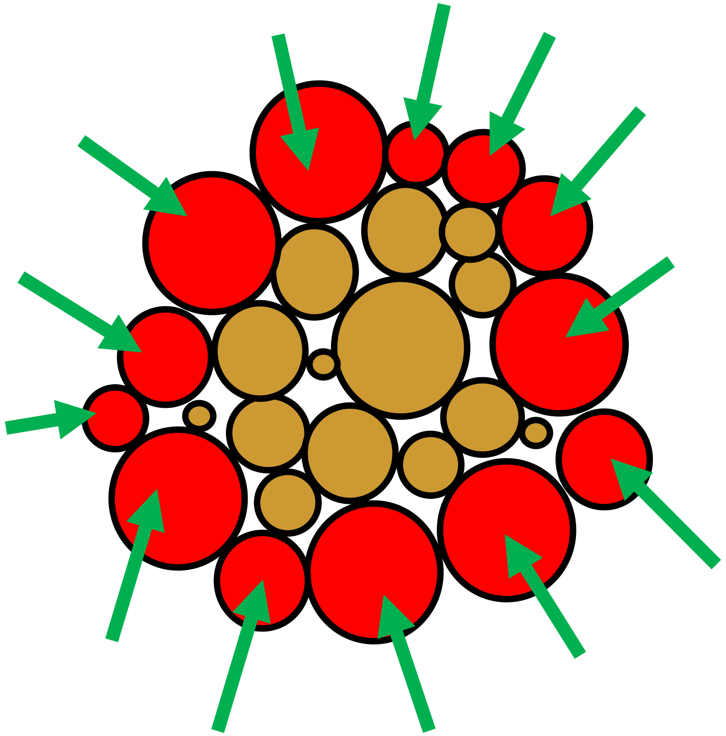

Discrete forces applied to boundary particles

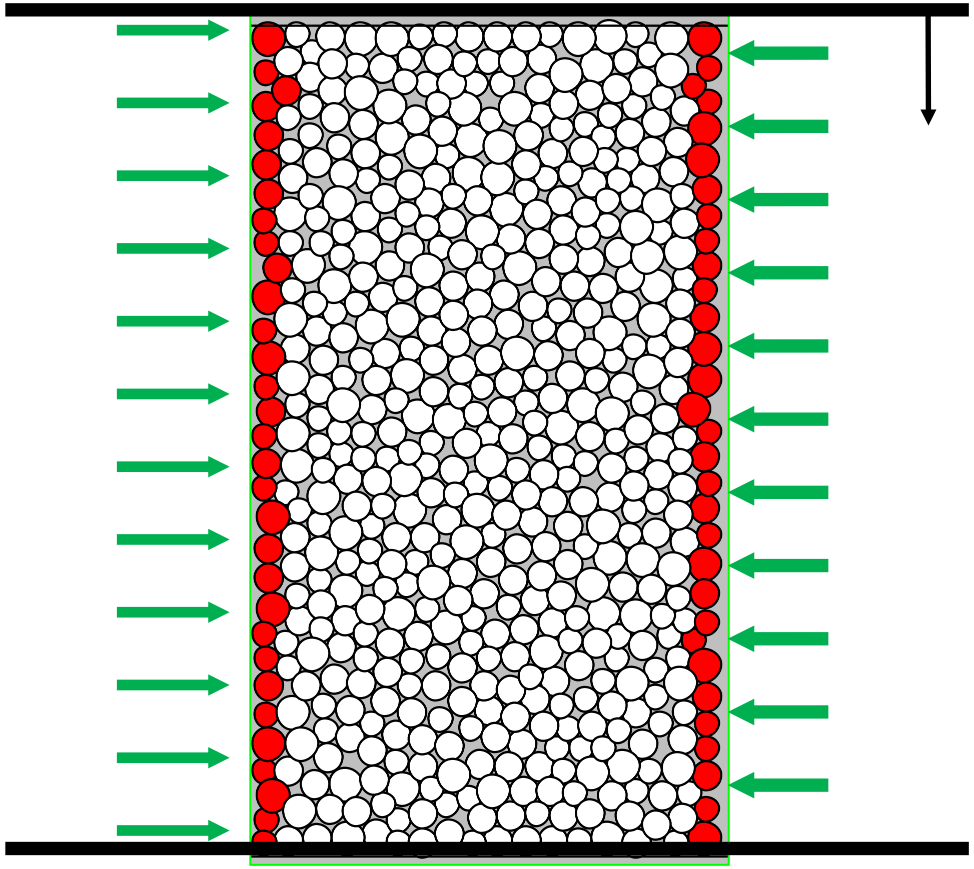

Cheung and O'Sullivan (2014)

2D Membrane

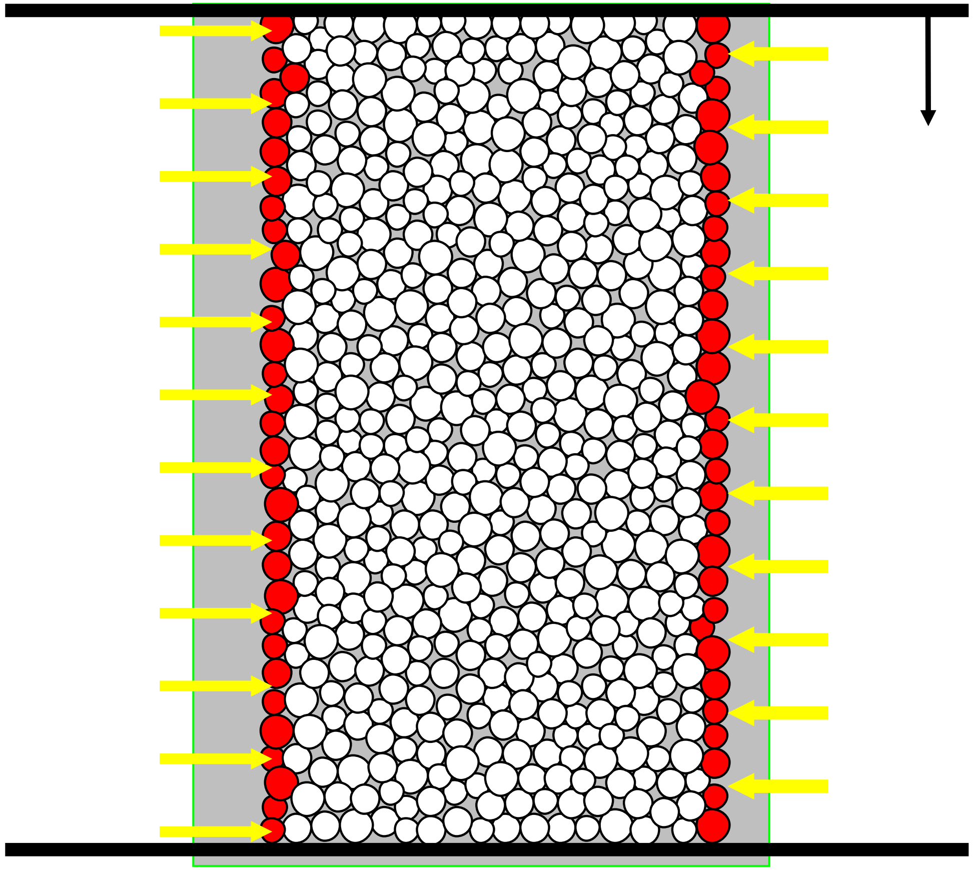

Contact based identification most effective

Cheung and O'Sullivan (2014)

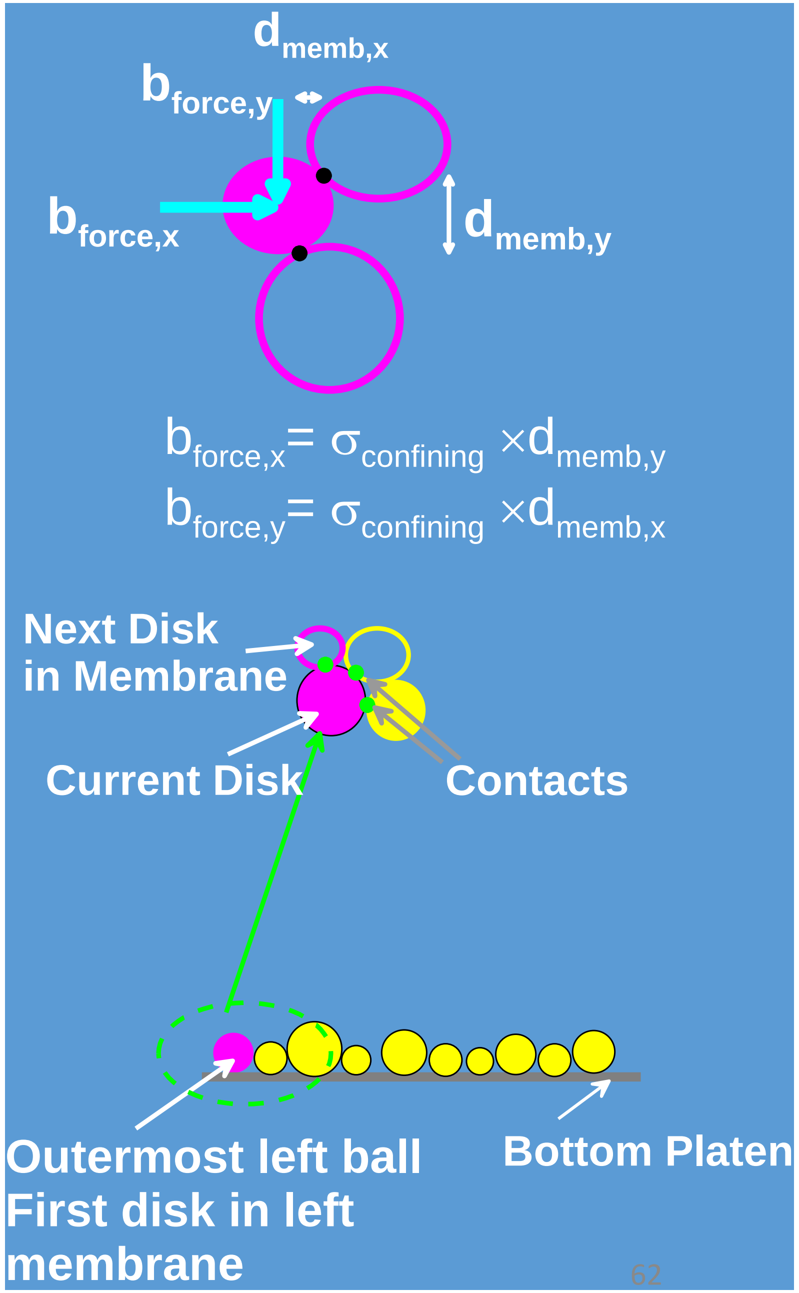

3D Membrane

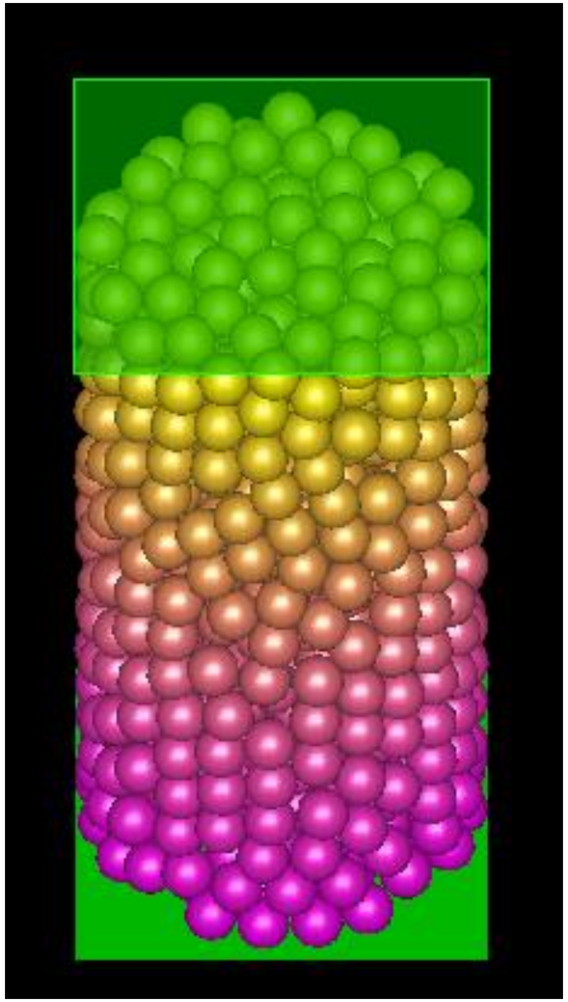

Cheung and
O'Sullivan (2014)

Identification of "membrane" balls

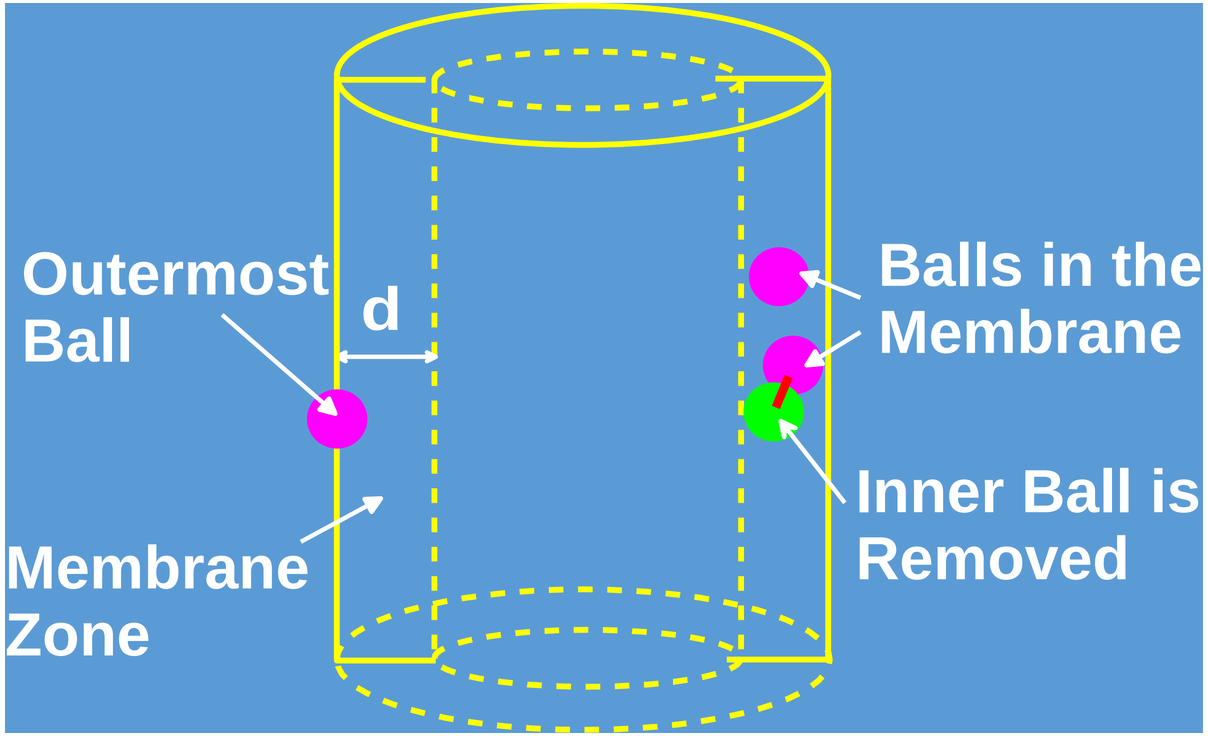

3D Membrane

Force Boundary – Voronoi Diagram

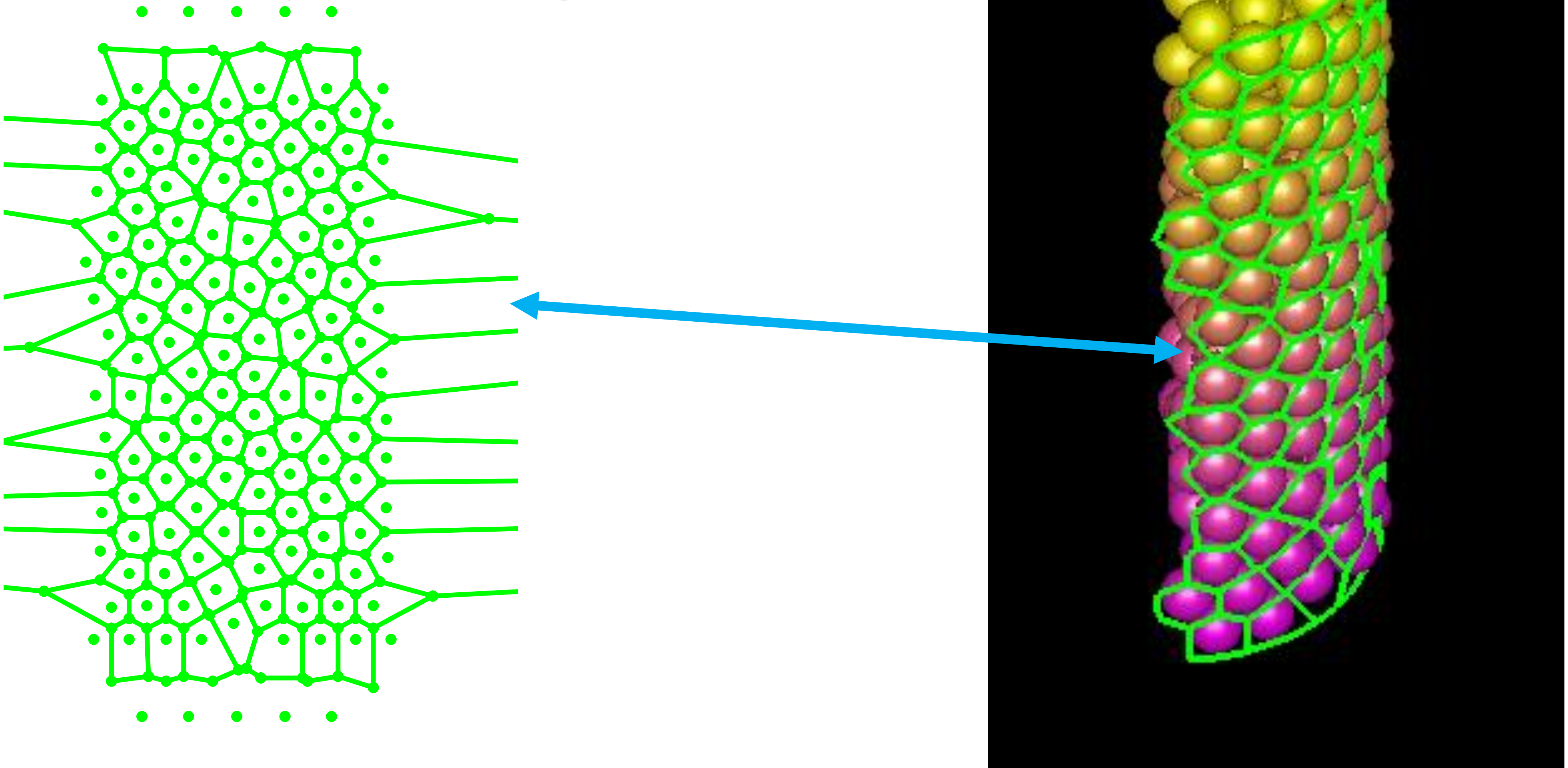

Influence of boundaries on response: 2D

- Specimen size:

  40 mm x 80 mm
- 2377 disks
- Radii uniformly distributed between 0.48 mm and 0.72 mm
- m= 0.5
- No bonding

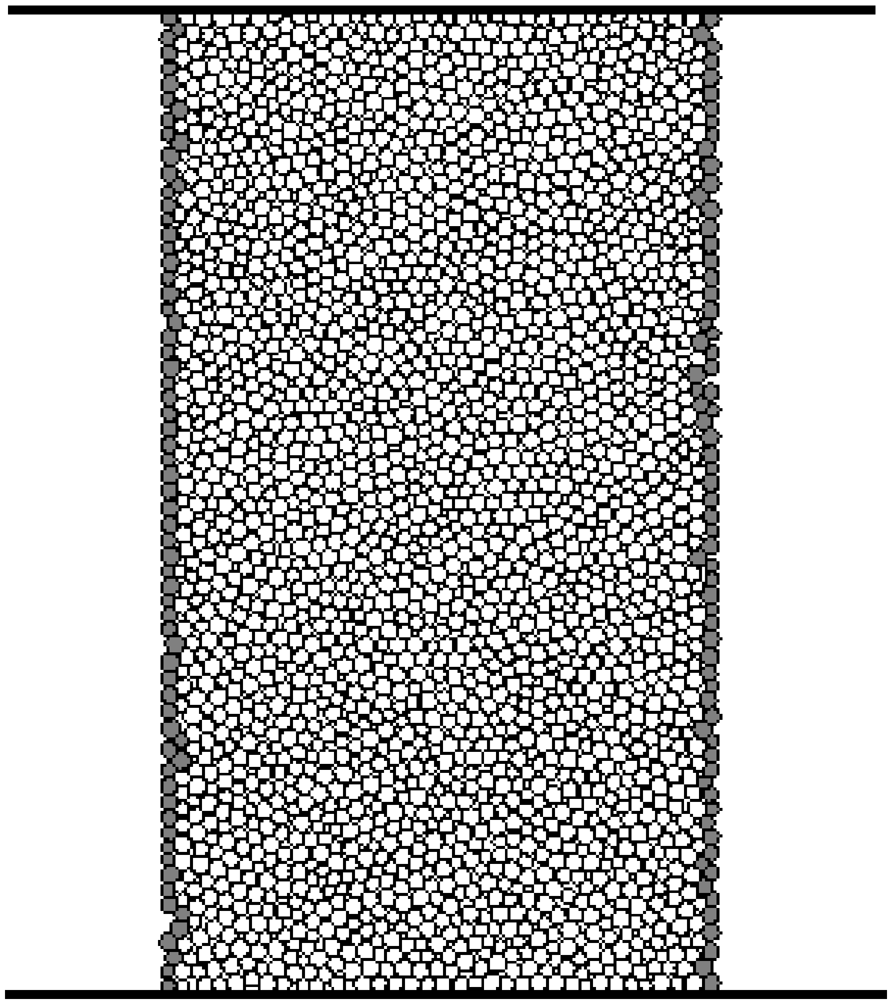

Cheung and O'Sullivan (2014)

Influence of boundaries on response: 2D

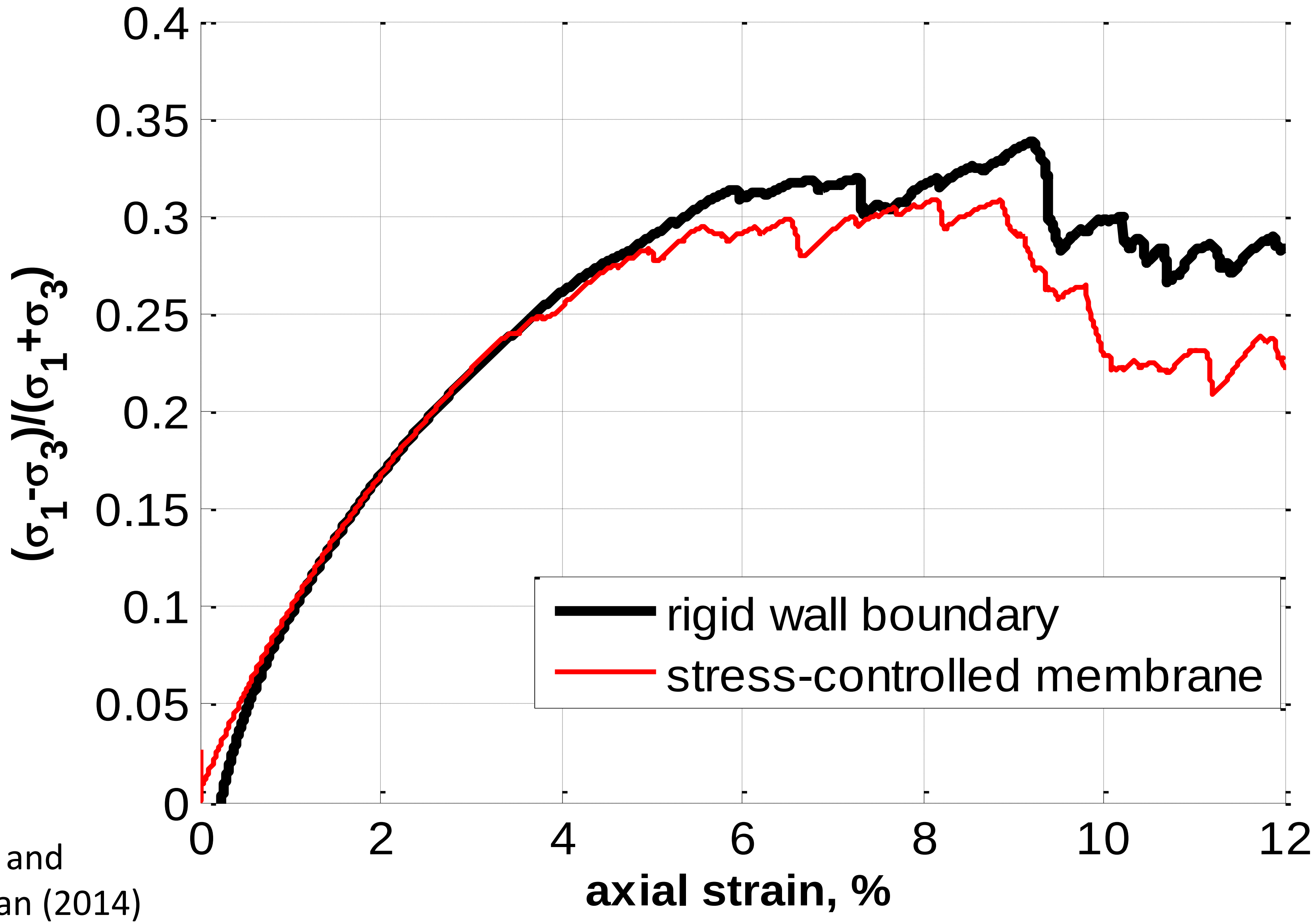

Cheung and O'Sullivan (2014)

Influence of boundaries on response: 2D

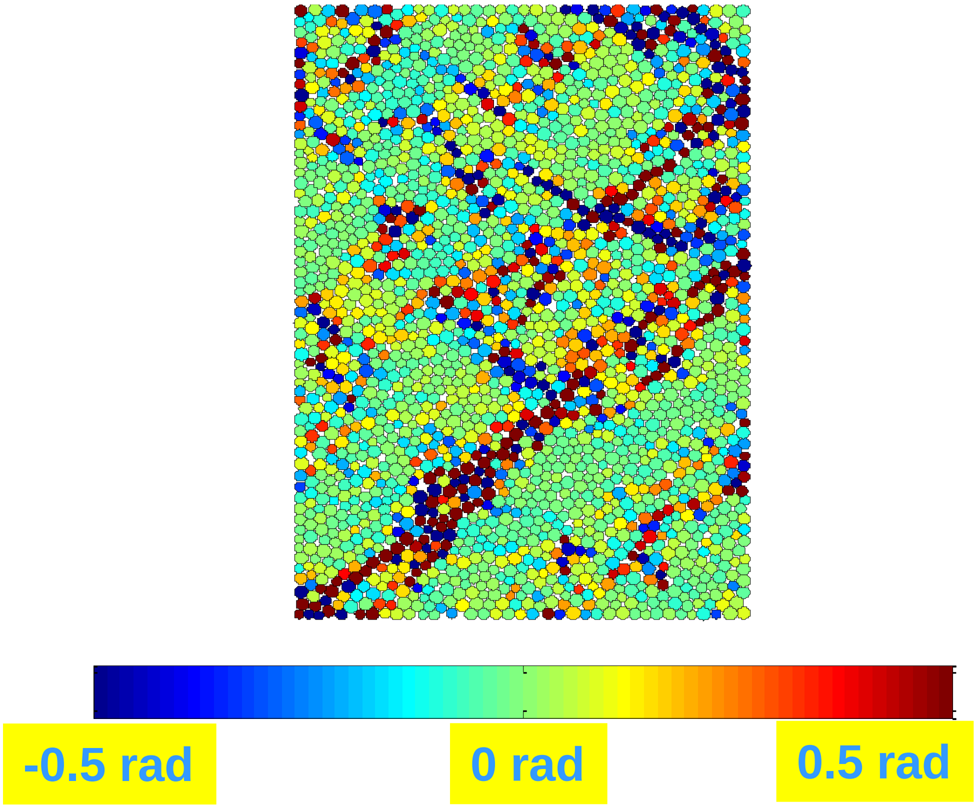

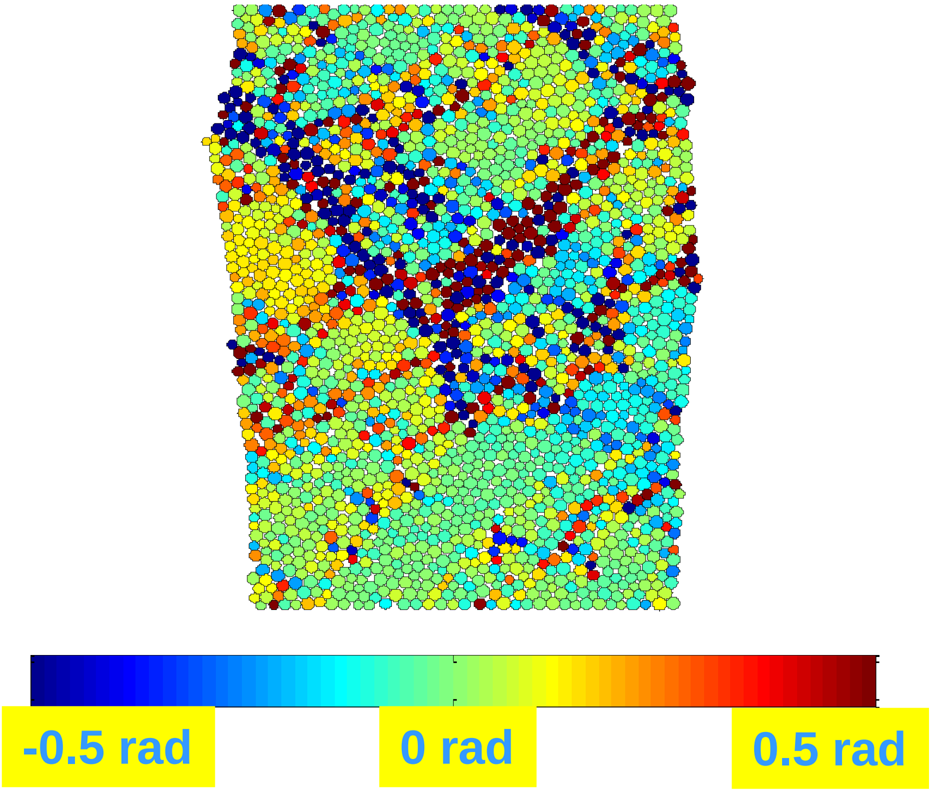

Cheung and O'Sullivan (2014)

Influence of boundaries on response: 2D

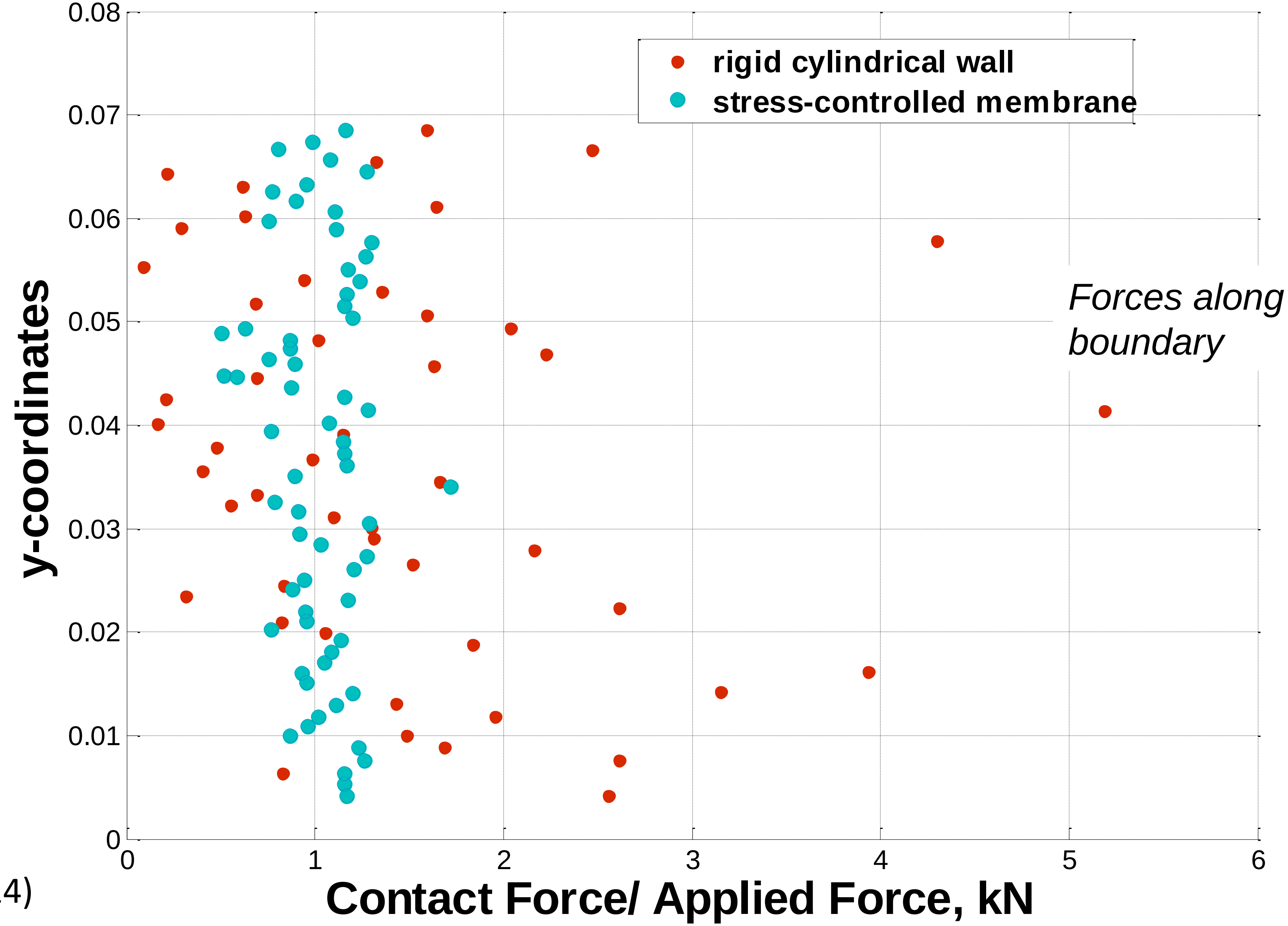

Forces along right boundary

Cheung and O'Sullivan (2014)

Influence of boundaries on response: 3D

- Specimen Size:
  40 mm (diameter) x 80 mm

- 12,622 spheres

- Sphere radii uniformly distributed between 0.88mm and 1.32mm

- A parallel bond used to model cementation

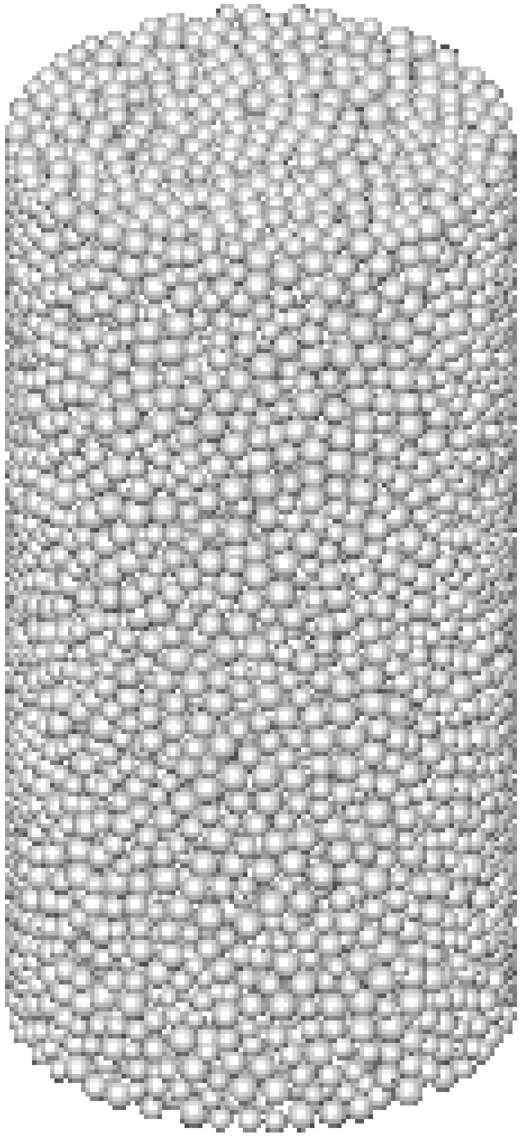

Cheung and O'Sullivan (2014)

Influence of boundaries on response: 2D

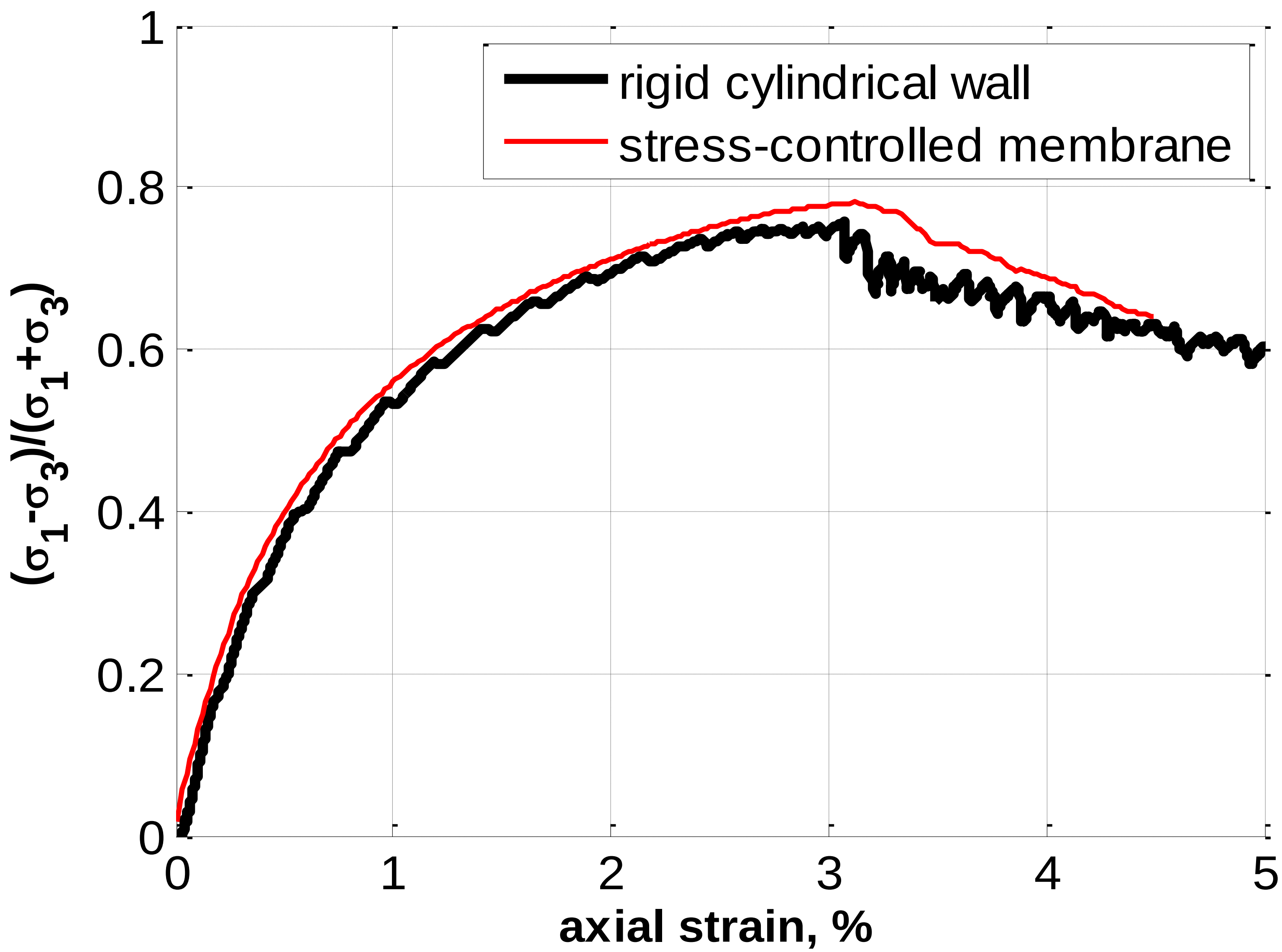

Cheung and O'Sullivan (2014)

Influence of boundaries on response: 3D

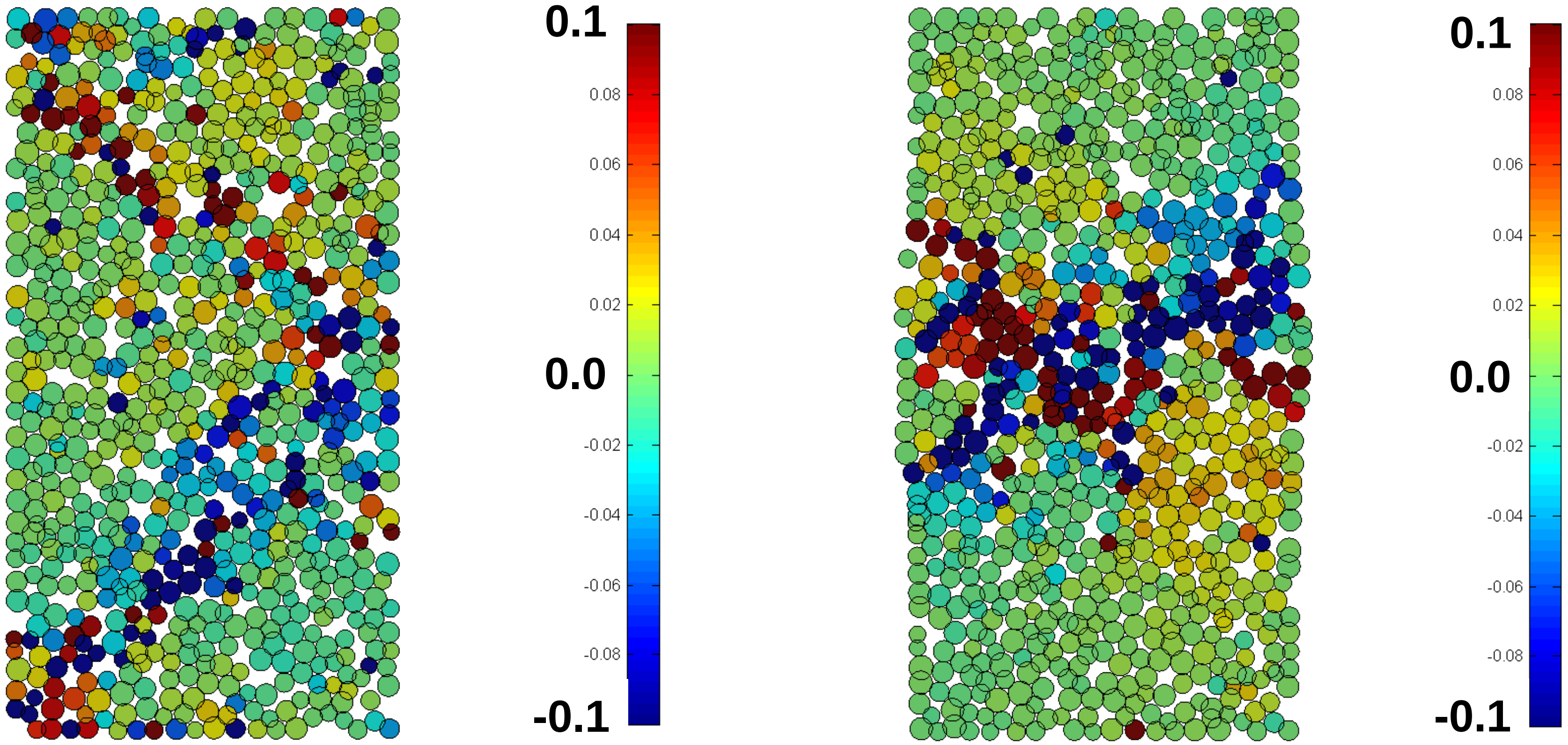

Cheung and
O'Sullivan (2014)

Periodic boundaries

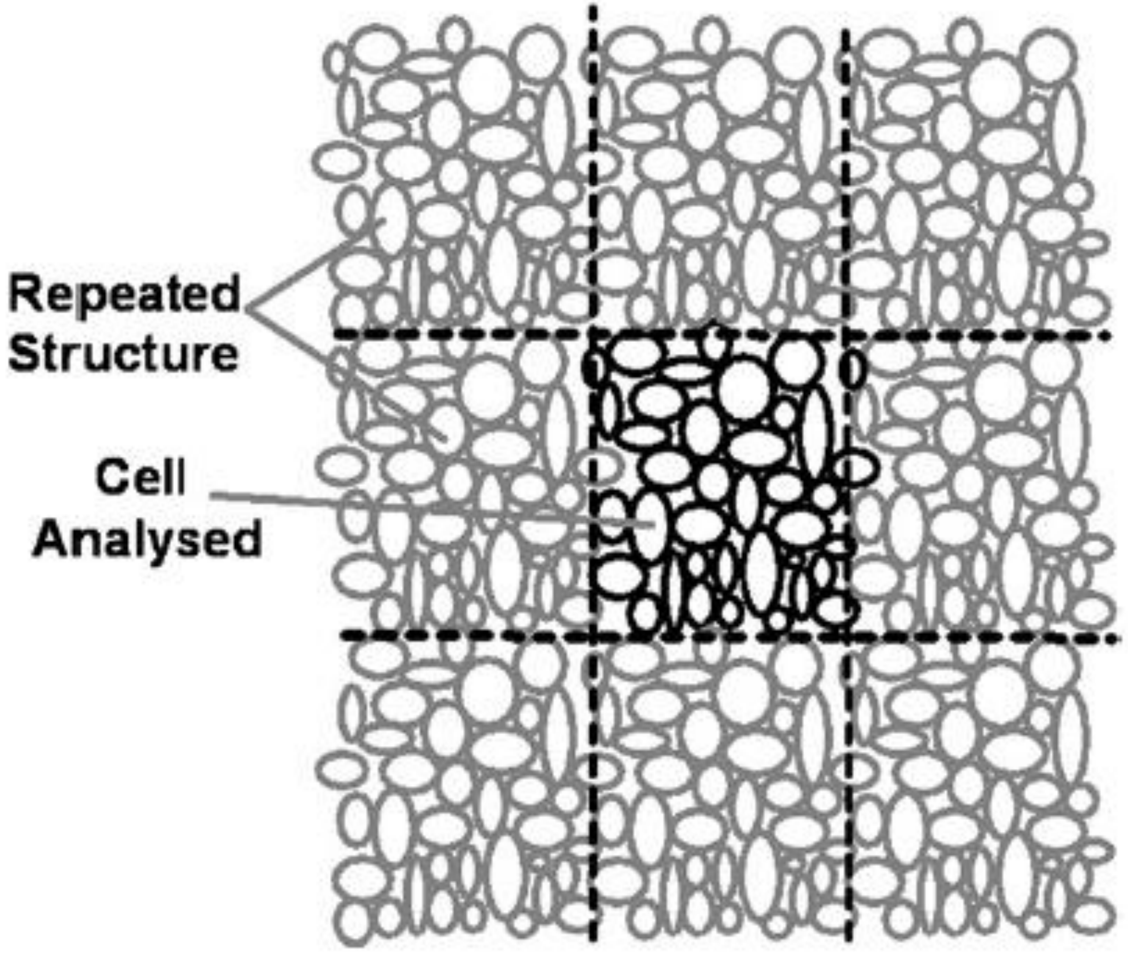

- Contacts are detected across periodic boundaries
- Less sensitive to sample size
- Homogeneous

Periodic boundaries

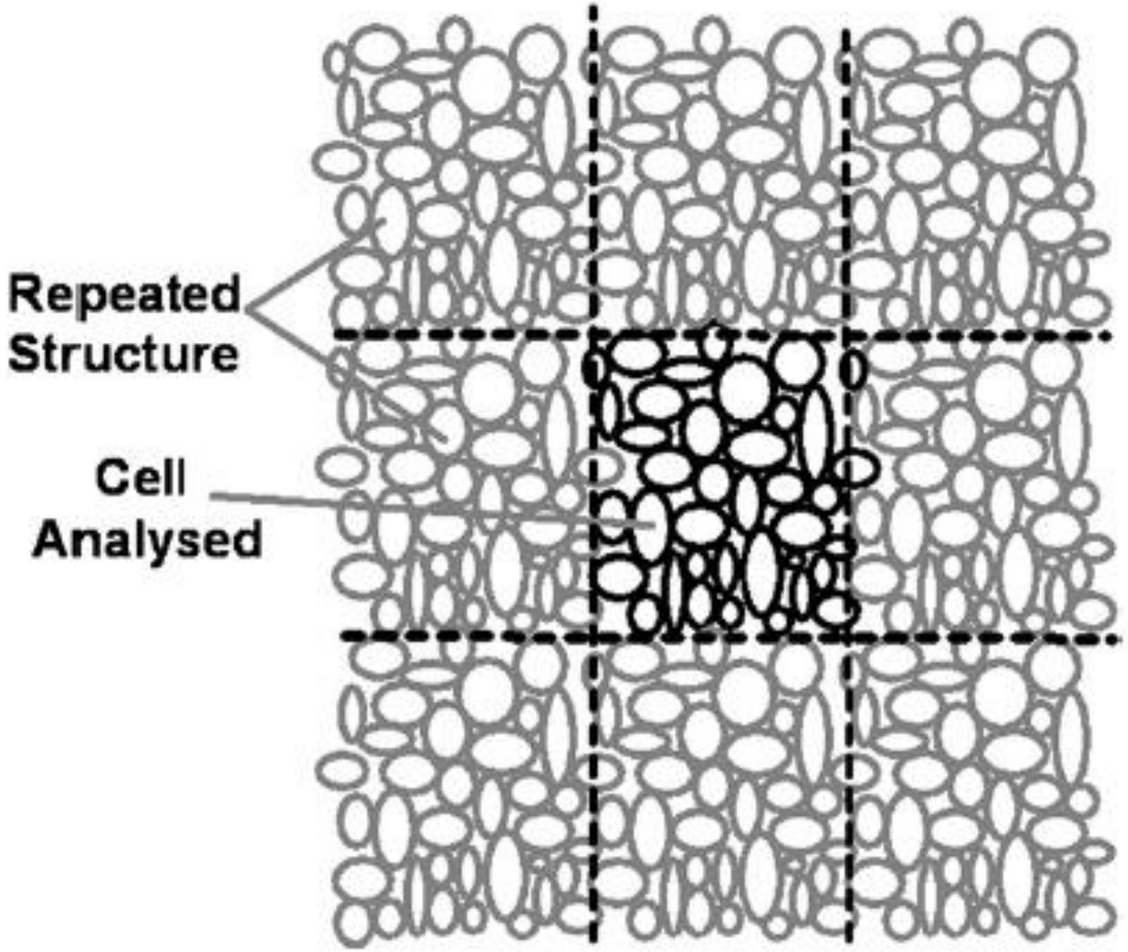

- Deformation achieved by moving both boundaries and particles according to global strain rate
- Need to account for movement of particles in shear component of contact model
- Good explanation given in Thornton (2000)

$$\Delta x_i = \dot{\varepsilon}_{ij} x_j \Delta t$$

Δx_i	Increment in displacement
$\dot{\varepsilon}_{ij}$	Strain rate
x_j	Position

Periodic boundaries

Effective to achieve a REV

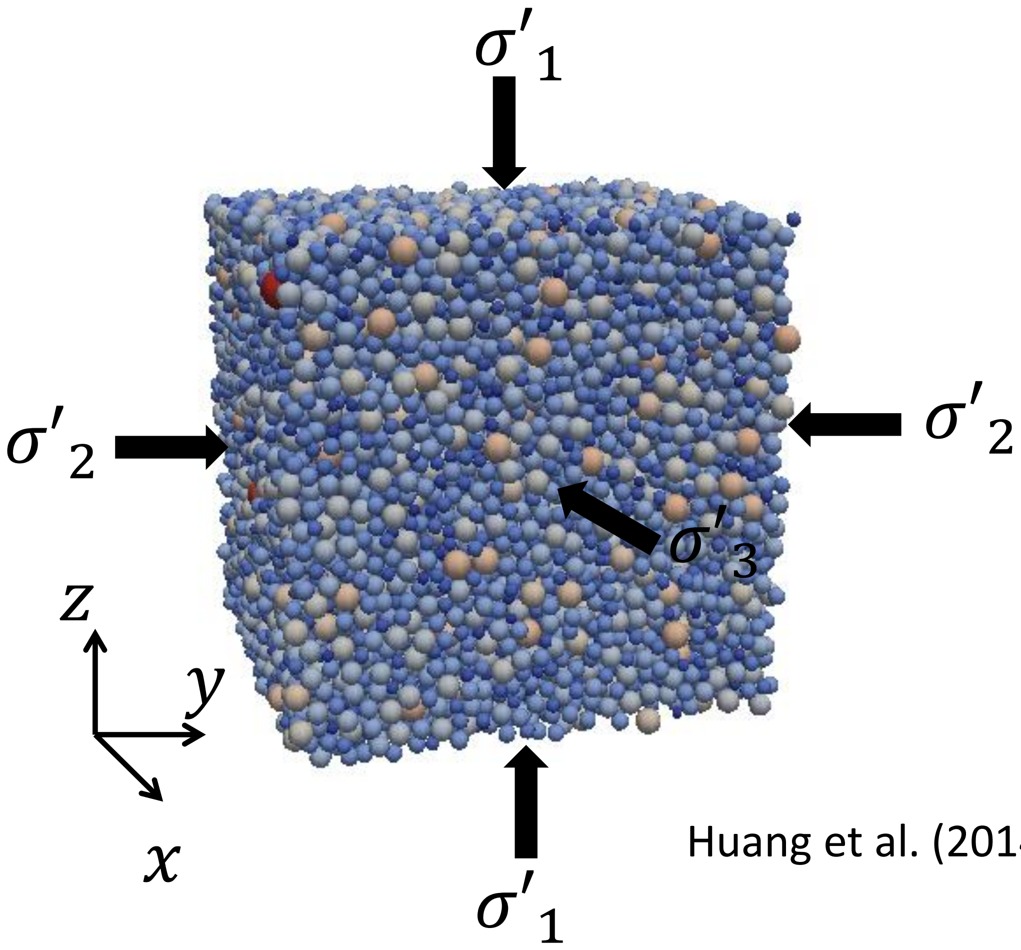

Huang et al. (2014)

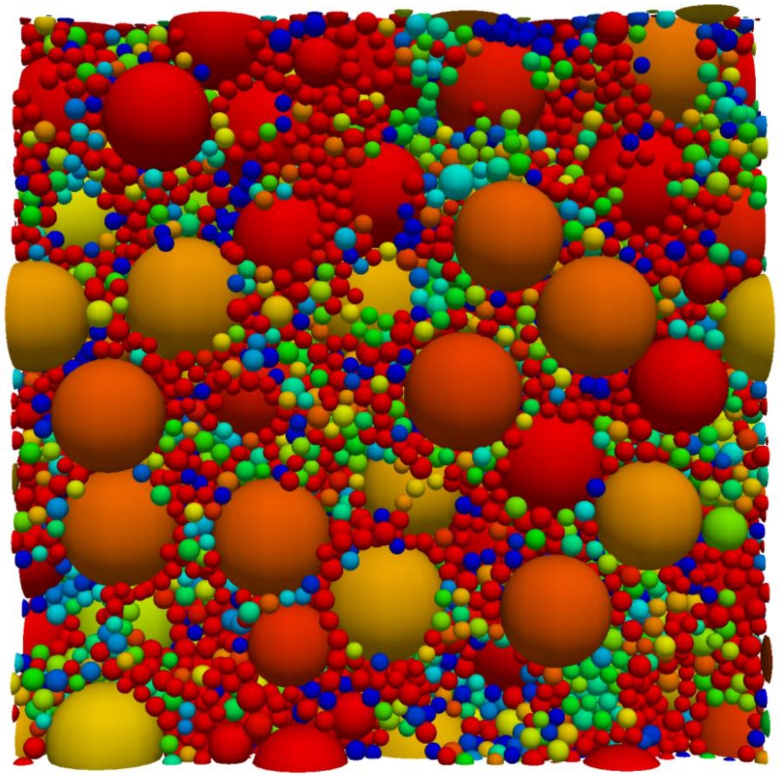

Shire et al. (2014)

20,164 particles

Up to 300,000 particles

Influence of boundaries on response: Wave propagation

Face-centred cubic (FCC) packing
Ave. coord. no. = 11.54

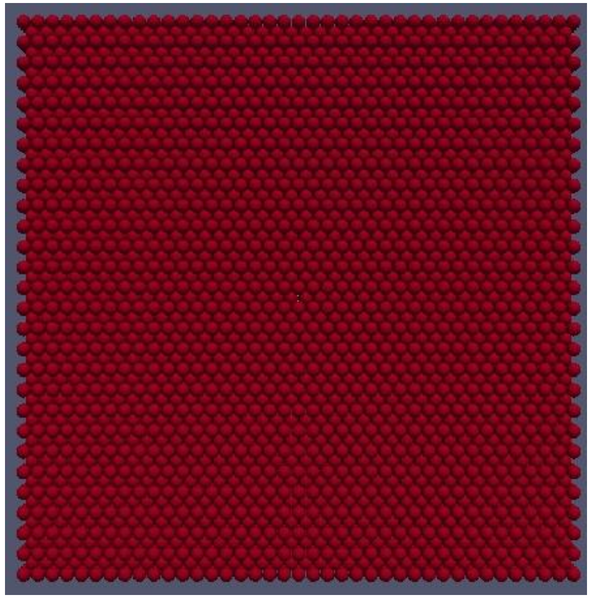

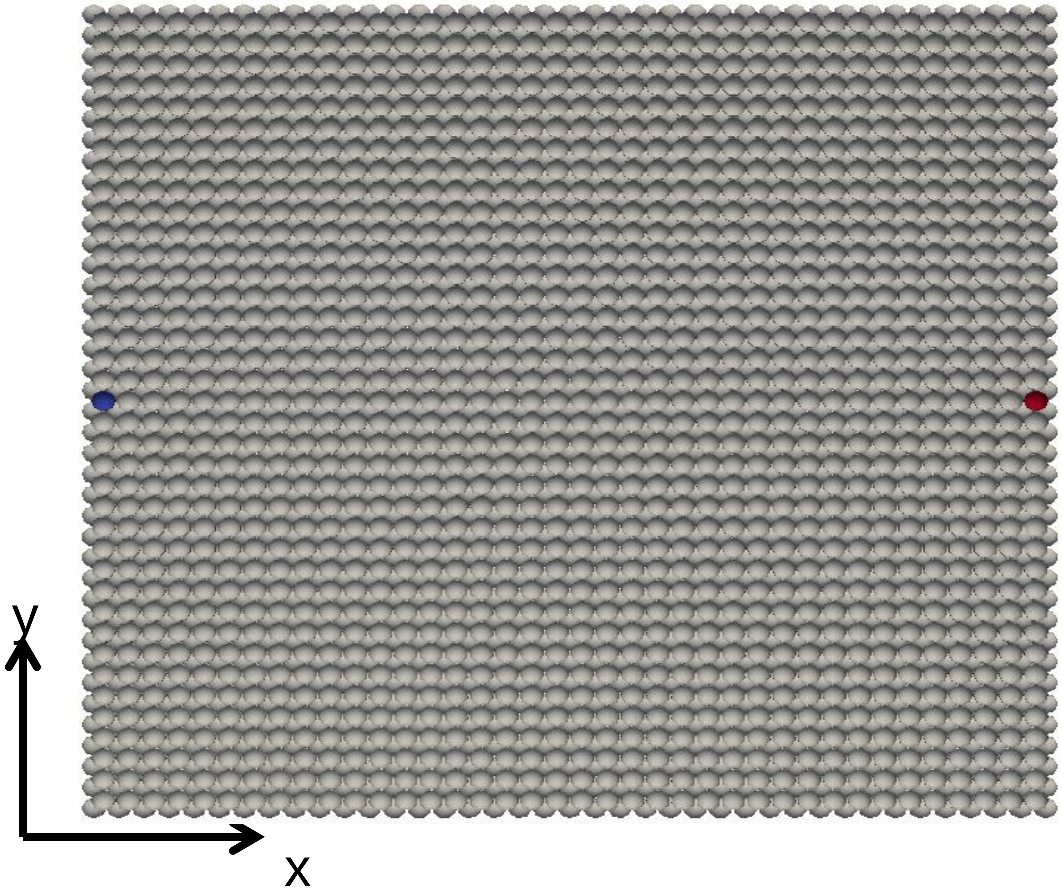

81, 576 particles

f_{trans} = *30 kHz*
R_d = 5.63 and λ/d_{50} = 6.40

Conclusions

- Largely three types of boundaries: rigid wall, force, periodic
- Servo control can be used to capture complex conditions
- Use of computationally expensive force / membrane boundaries may not always be justifiable (small strain)
- Post-peak deformation patterns may be more sensitive

Sample size

No of particles in DEM related publications

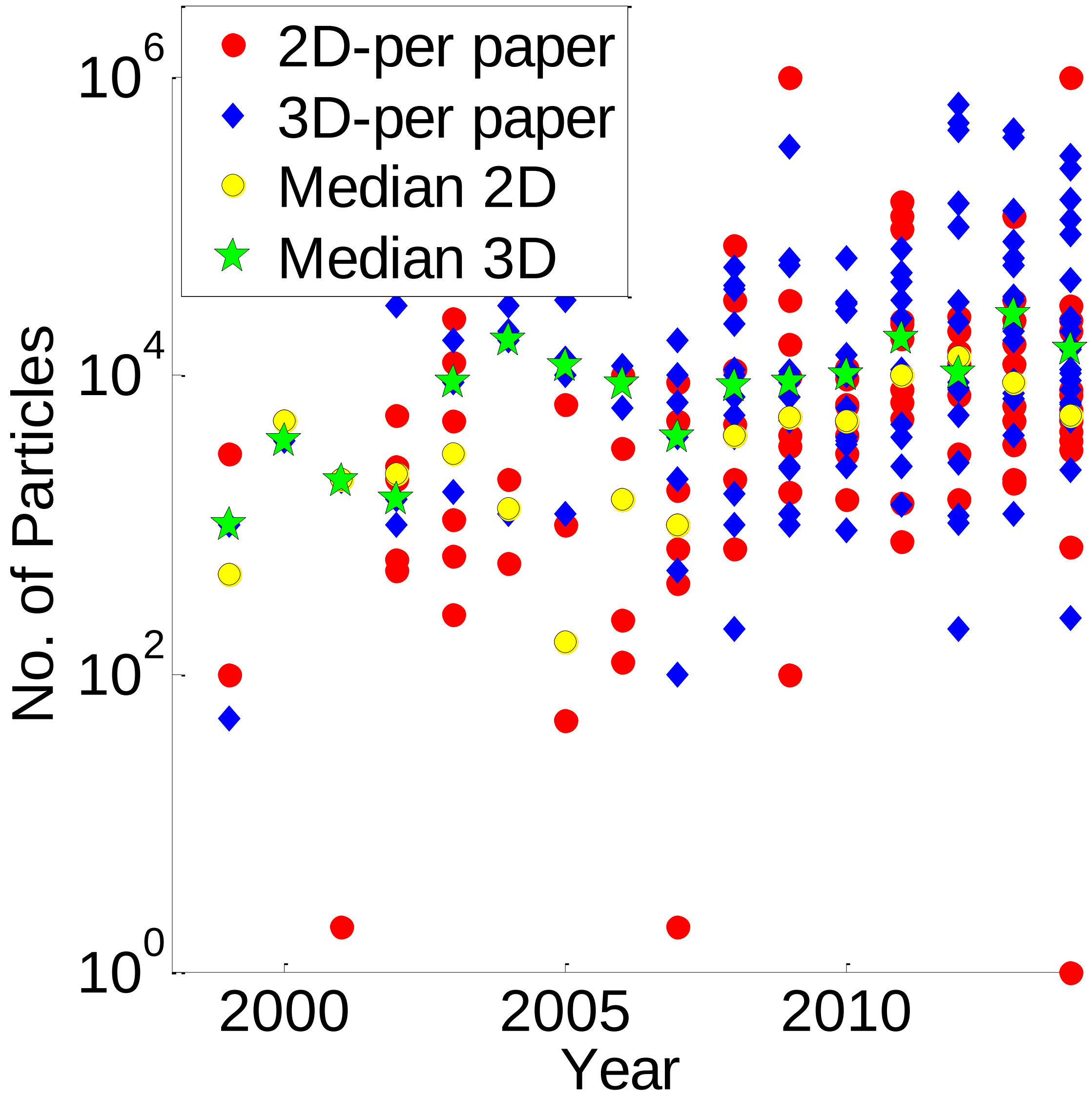

D_{50}=200 micron
>150,000 particles

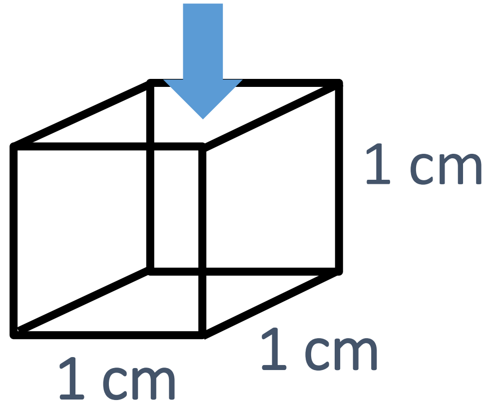

Very small samples – erratic load:deformation response

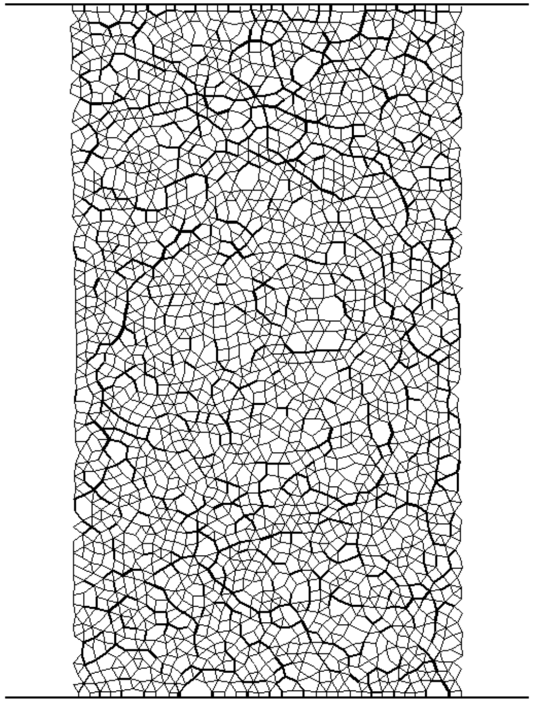

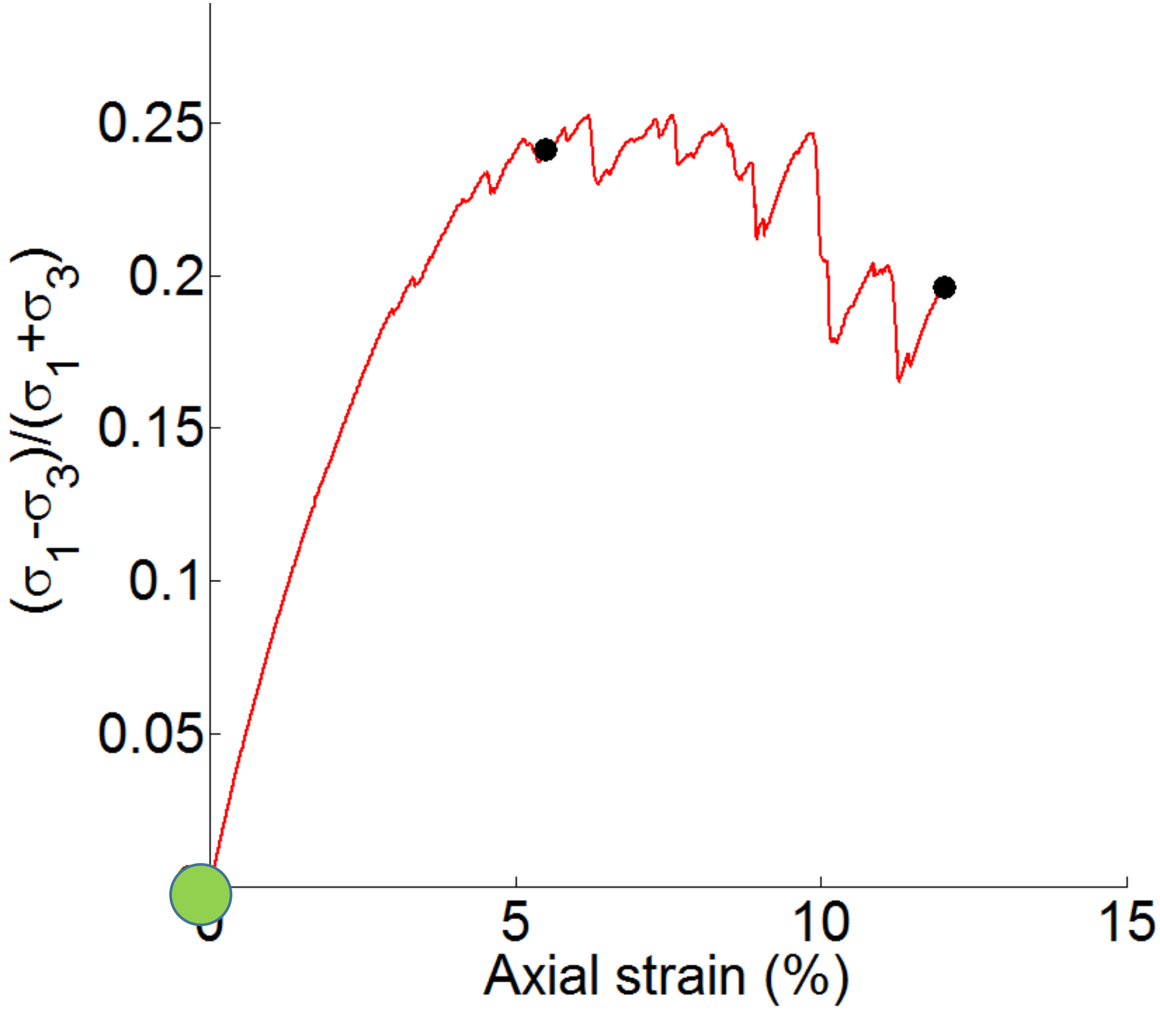

Sensitivity of CSL to sample size

Simplified Hertz-Mindlin Contact Model

5×11.0 mm

4×8.8 mm

3×6.6 mm

5.25×5.25×5.25 mm

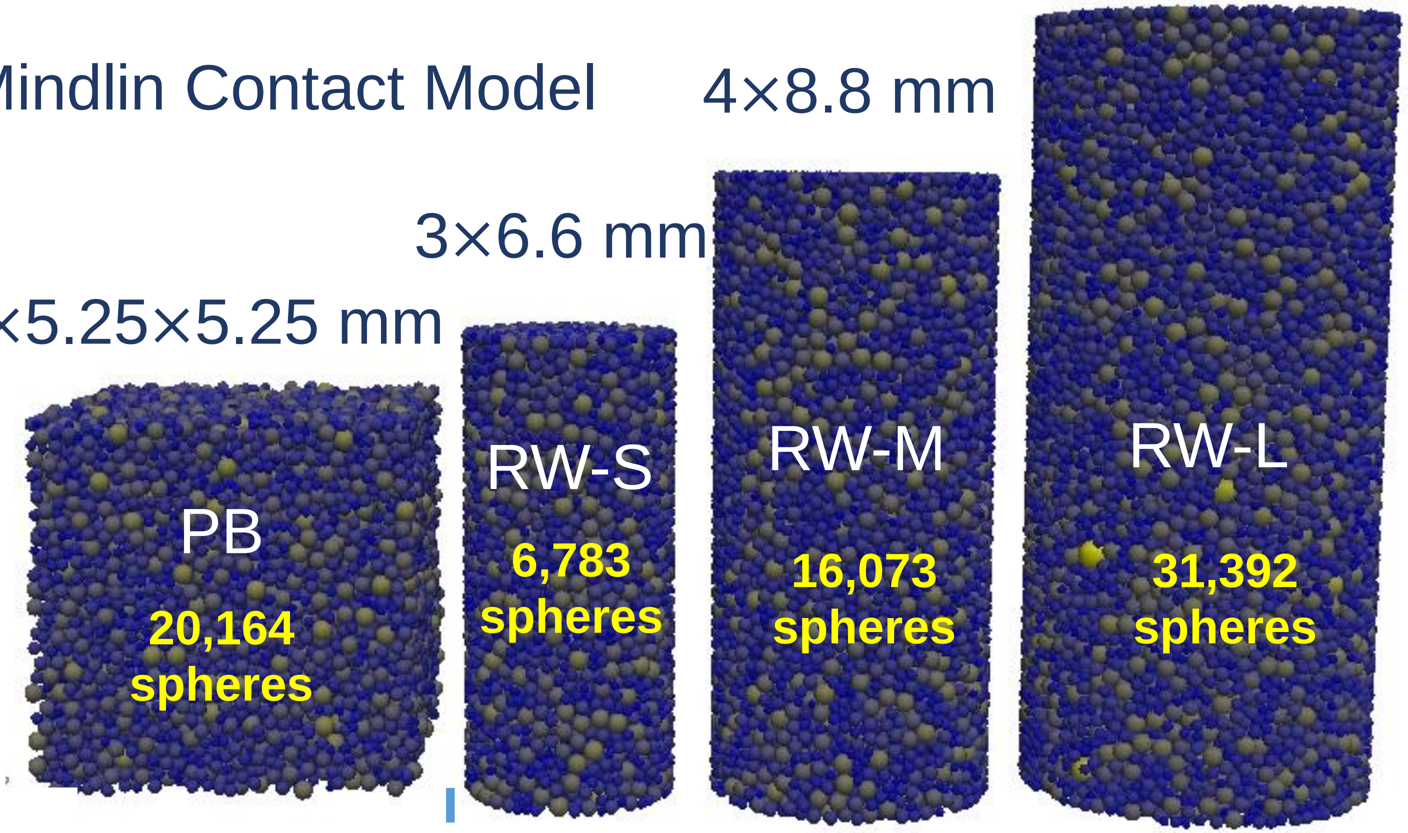

$(\text{Dimension})_{min}/D_{50}$ =	25	14	19	24

LAMMPS

PFC

Huang et al. (2014)

Sensitivity of CSL to sample size

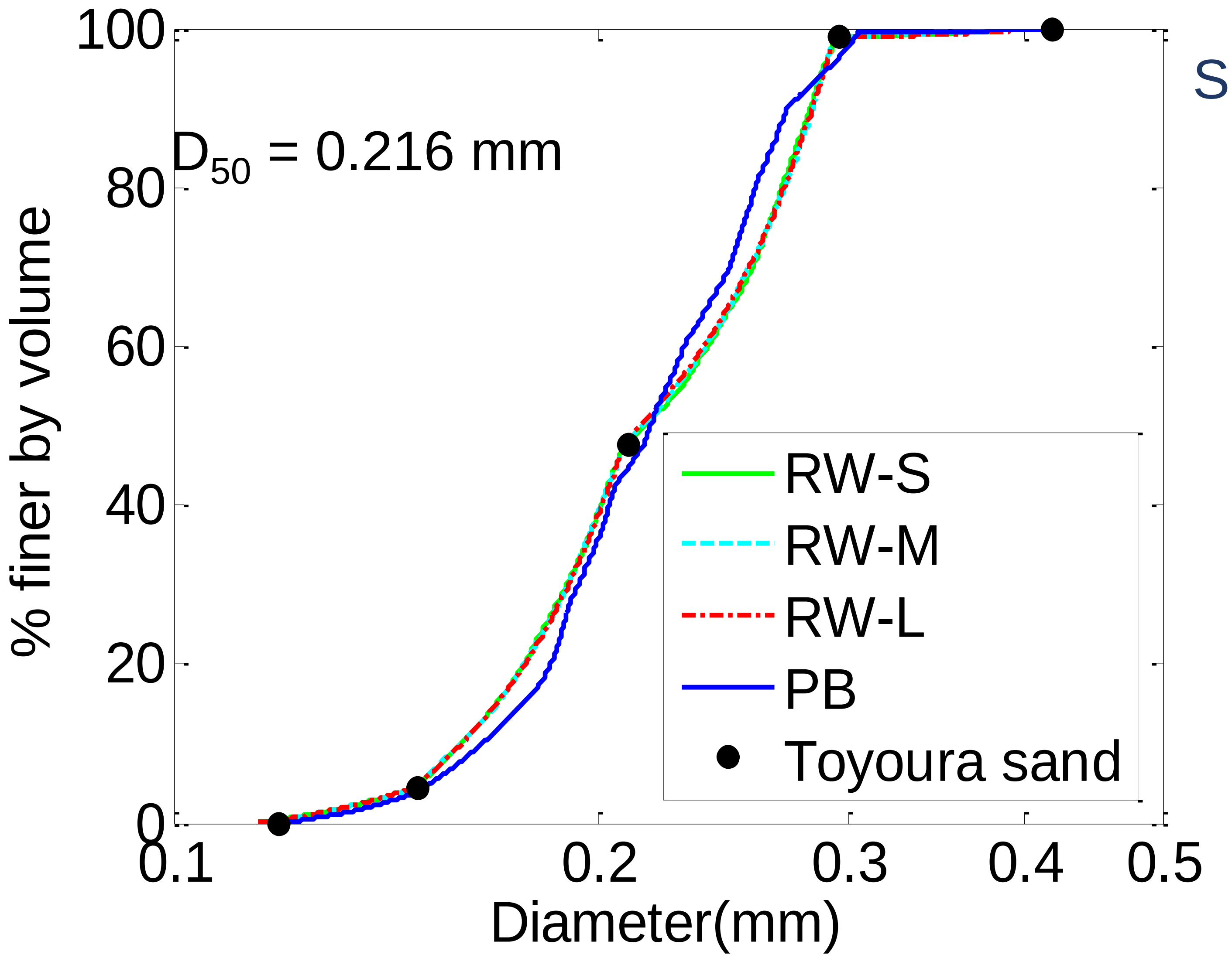

Simplified Hertz-Mindlin Contact Model

G	Shear modulus	29 GPa
ν	Poisson's ratio	0.12
μ	Inter-particle friction	0.25

Huang et al. (2014)

Sensitivity of CSL to sample size

$e_0 = 0.646$, $\sigma'_3 = 500$ kPa ; $q=\sigma'_1-\sigma'_3$

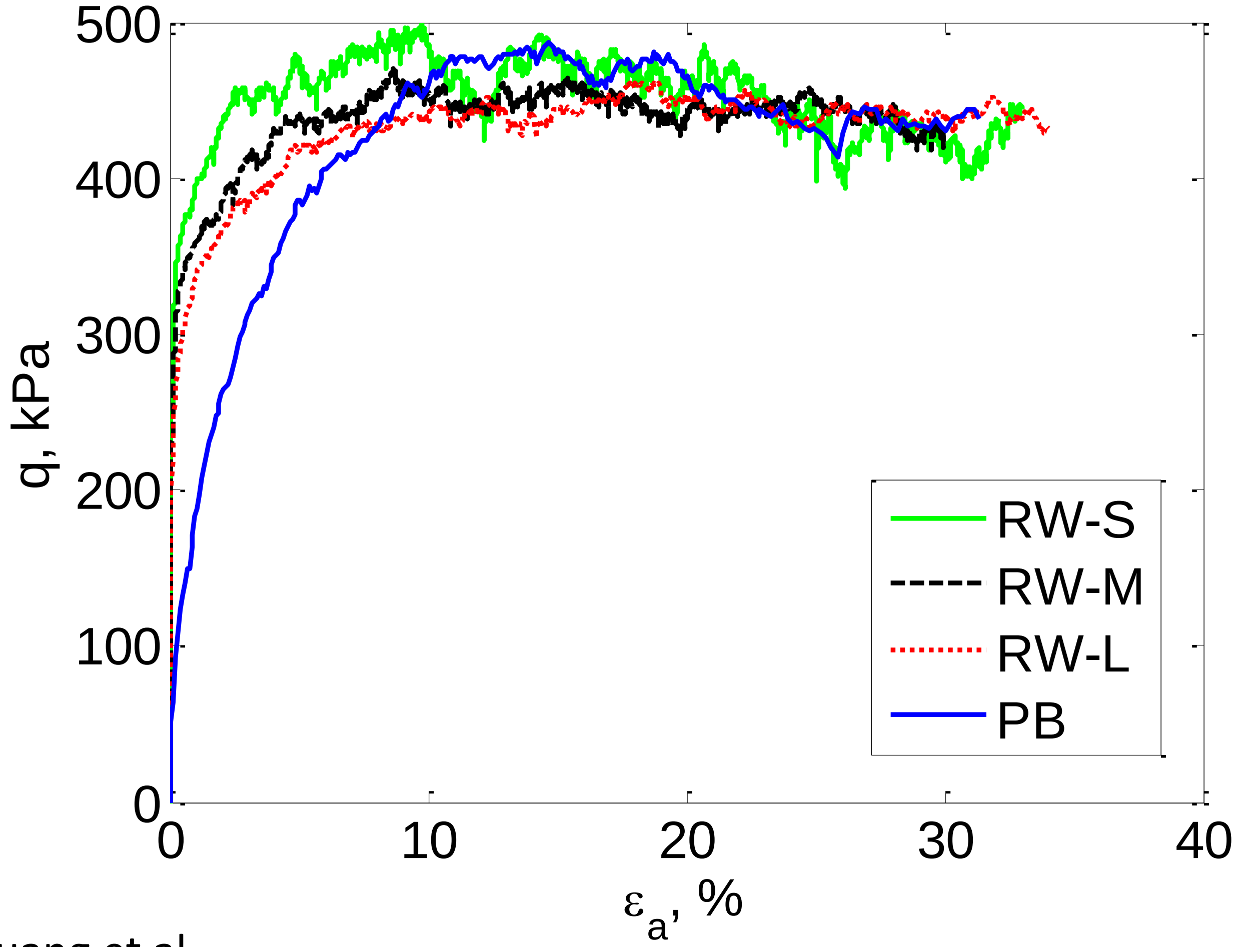

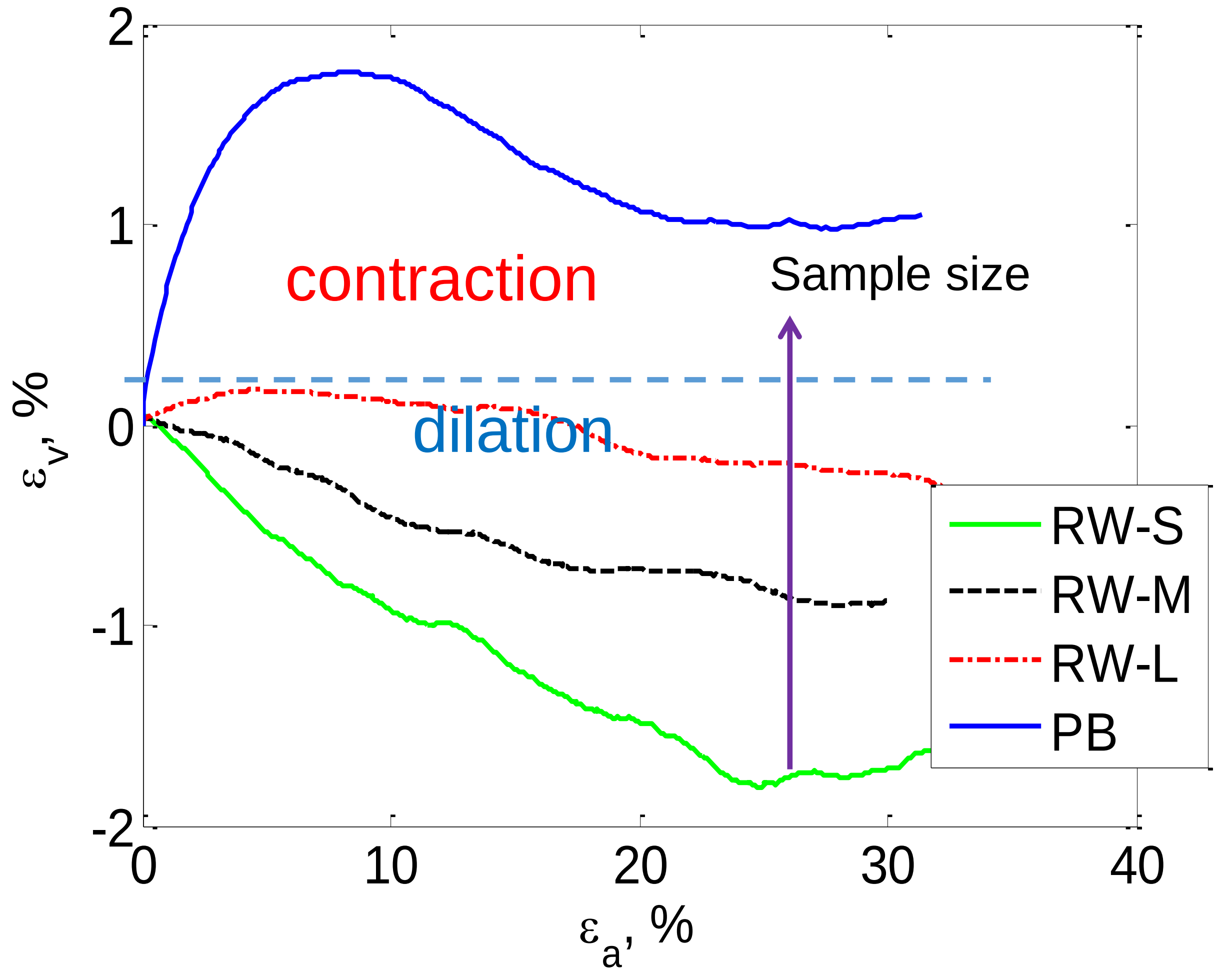

Huang et al. (2014)

Sensitivity of CSL to sample size

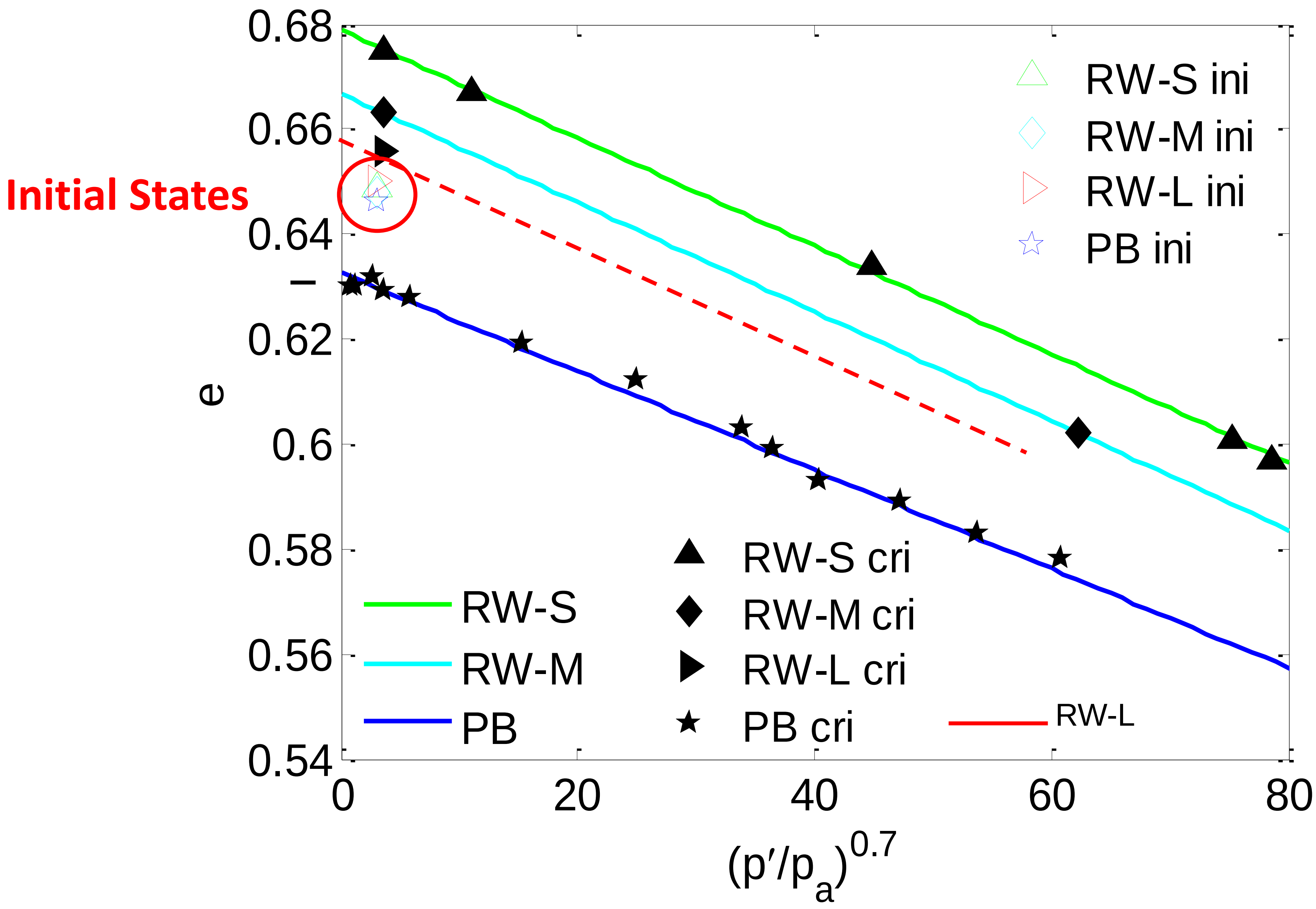

Initial States

Huang et al. (2014)

Sensitivity of CSL to sample size

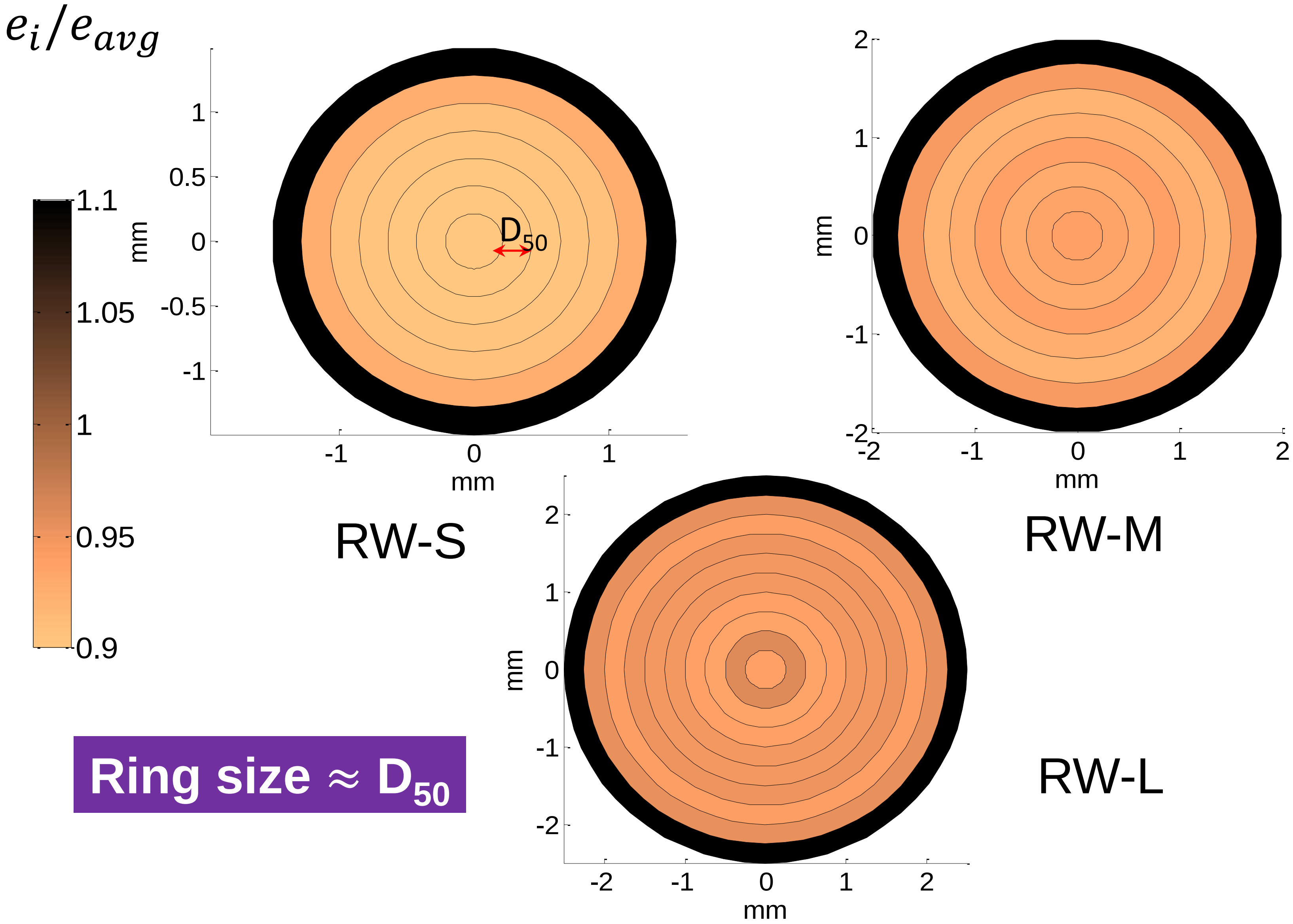

Ring size ≈ D_{50}

Huang et al. (2014)

Sensitivity of CSL to sample size

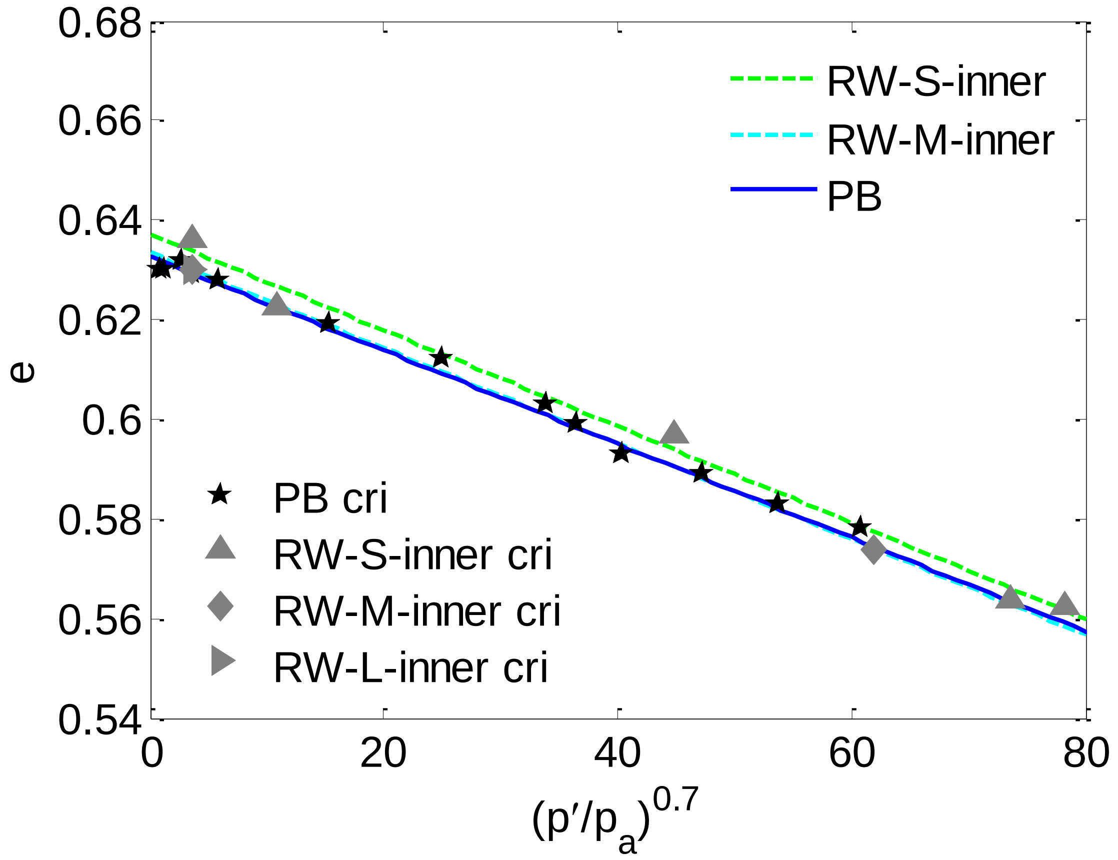

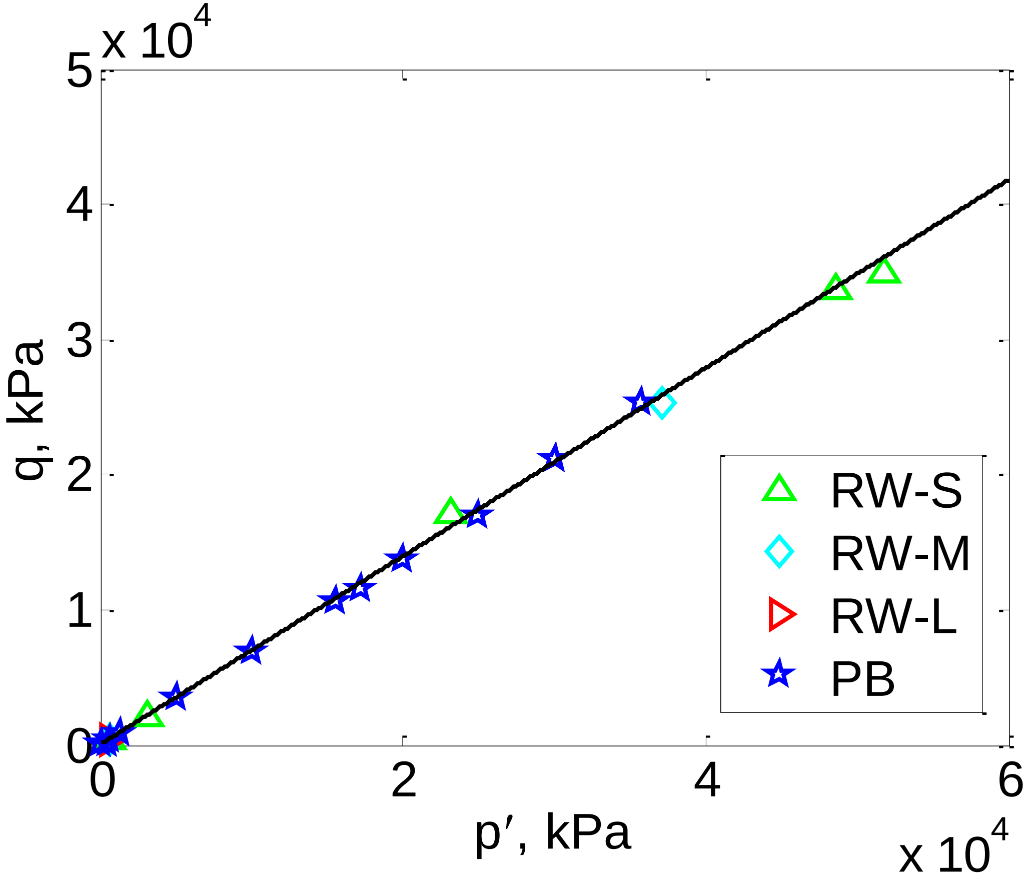

Critical state: Interior region

Huang et al.
(2014)

Periodic cell simulations – sample size considerations

Daniel Barreto PhD Research– Simulations using Trubal

Spheres with Dmin / Dmax up to 1.4

Simulations considered 2000, 4000, 8000 samples

Macroscale load:deformation responses similar

Fabric different for 2000 – considered 2nd order fabric tensor

Simulations for main body of research – 4000 particles

Barreto and O'Sullivan (2012)

Periodic cell simulations – sample size considerations

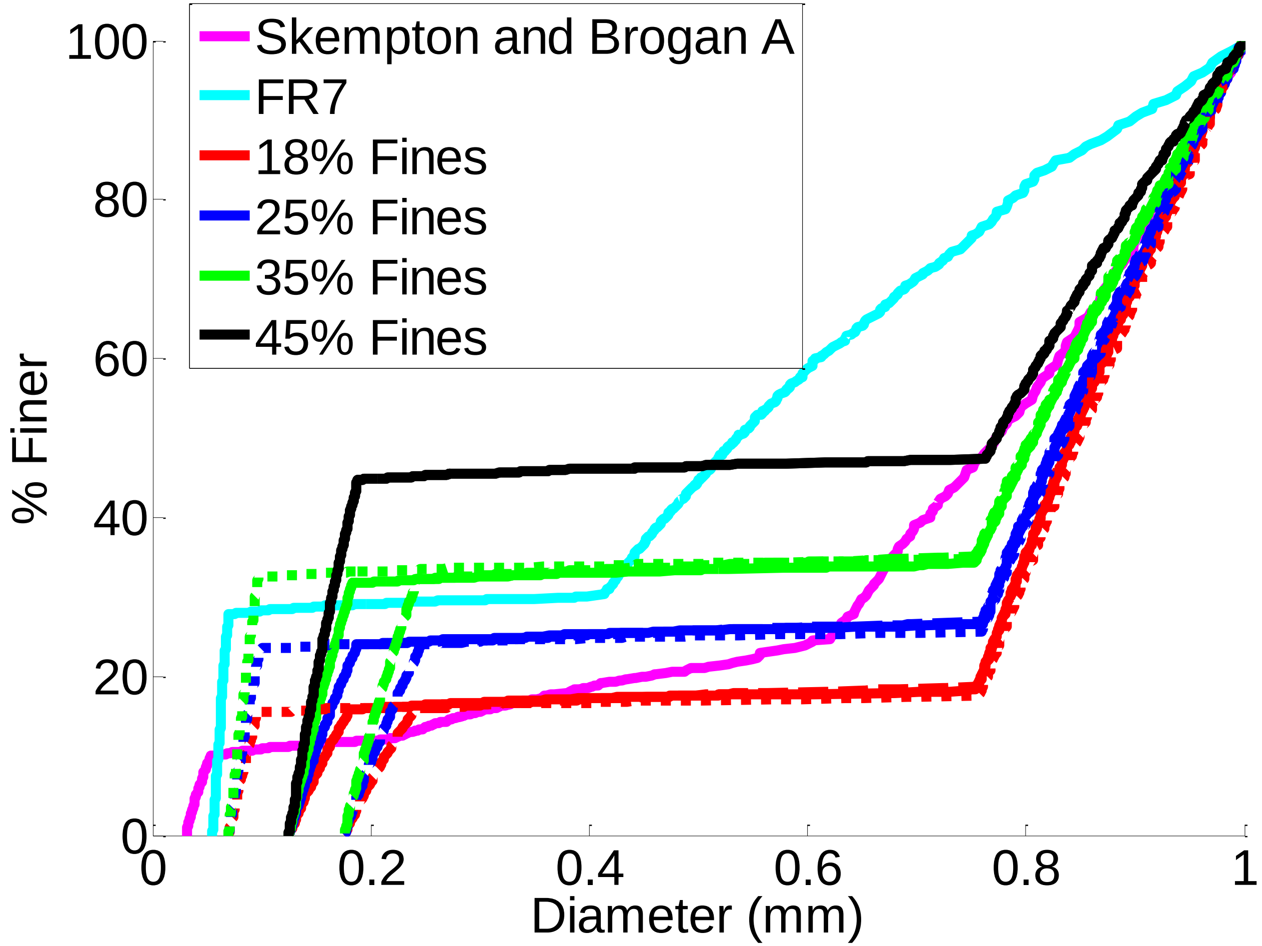

Shire et al. (2014)

- Parametric study to assess the effect of gap ratio and fines content on fabric of gap graded soils
- If 500 coarse particles used – up to 300,000 particles per simulation
- Is this adequate?

Periodic cell simulations – sample size considerations

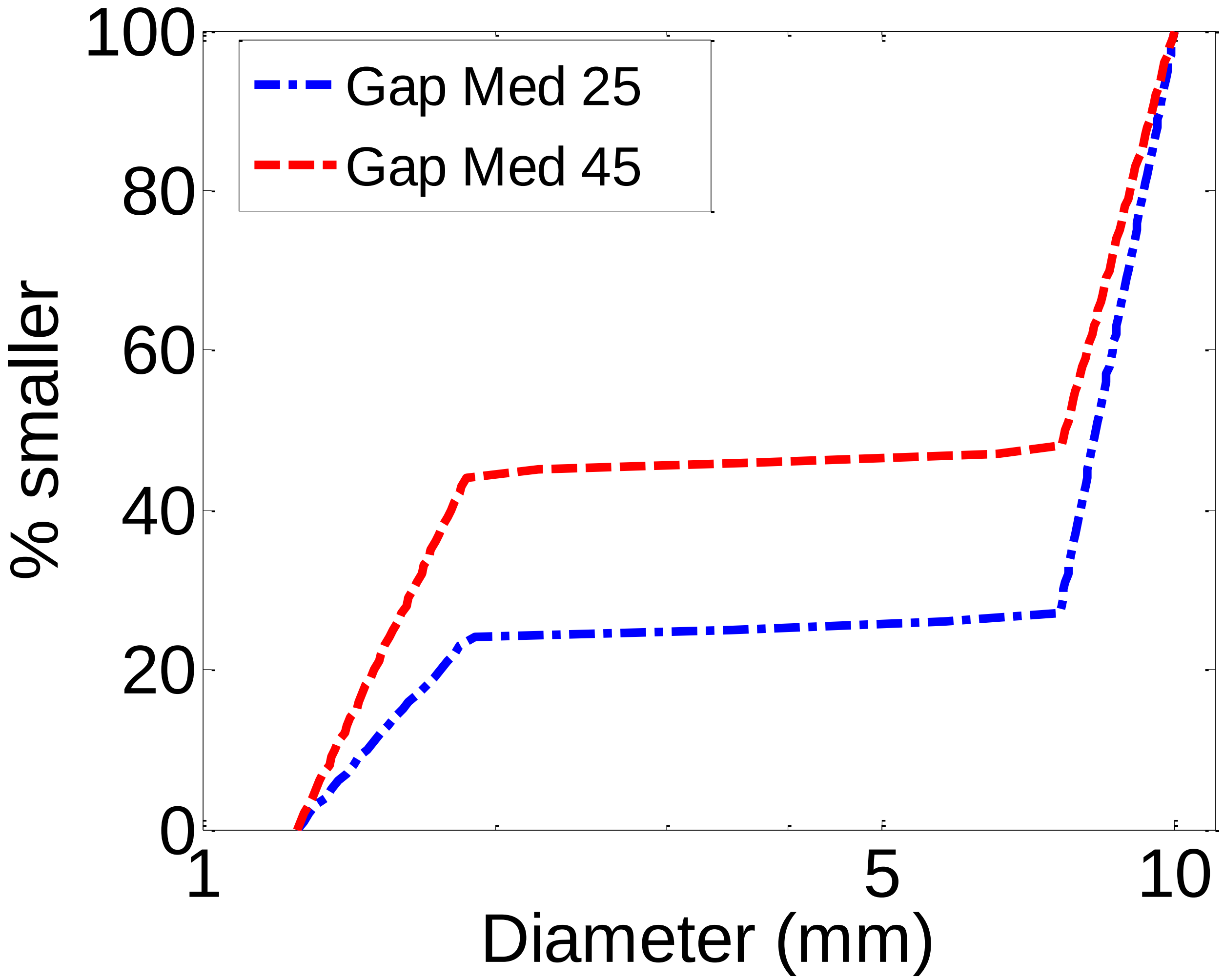

Shire (2014)

- Simulations on a gap-graded material
- Preliminary study to assess whether 500 coarse particles gave a satisfactory REV

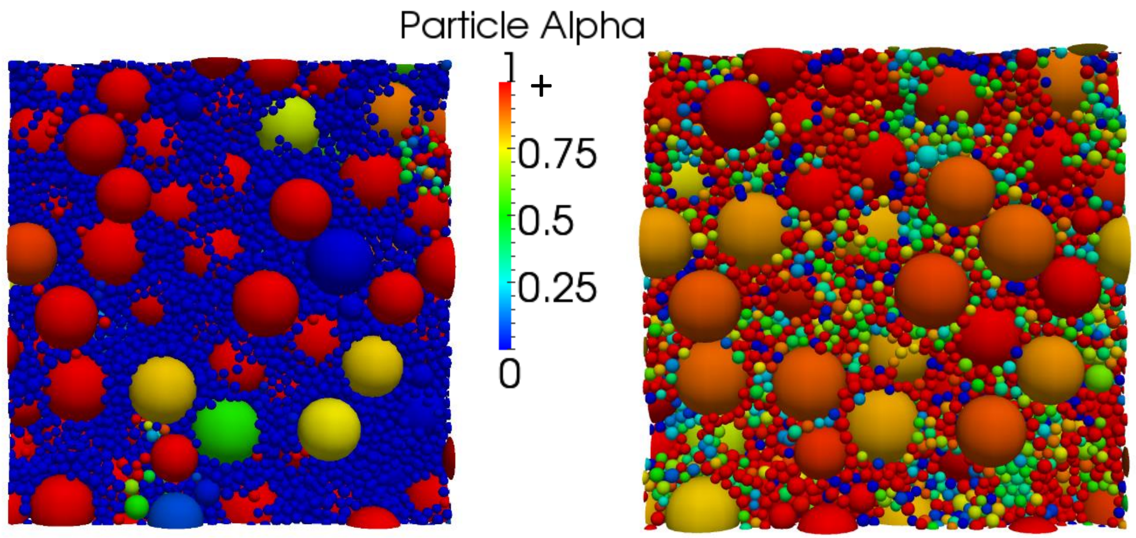

30% Fines - Loose

30% Fines - Dense

Periodic cell simulations – sample size considerations

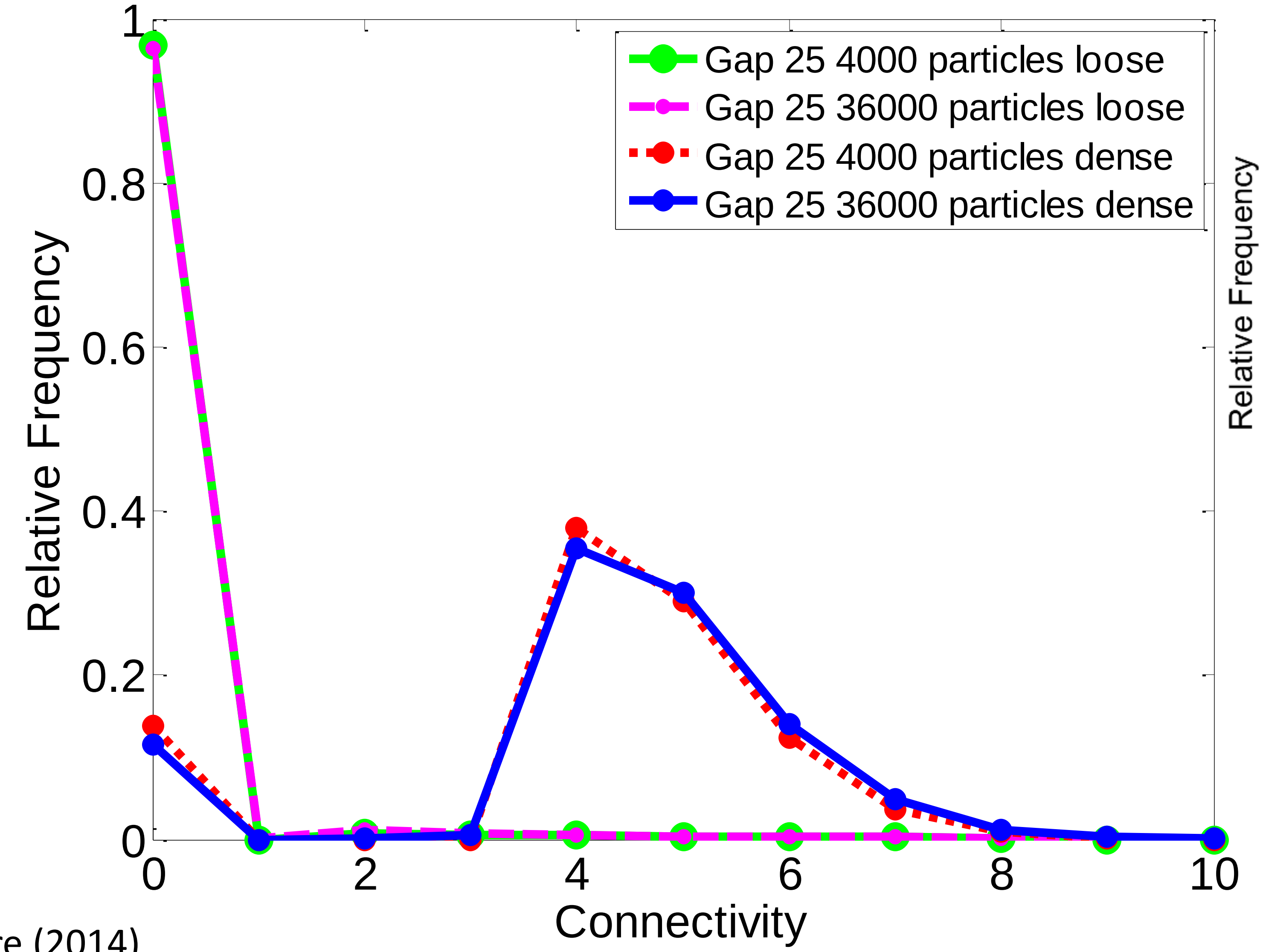

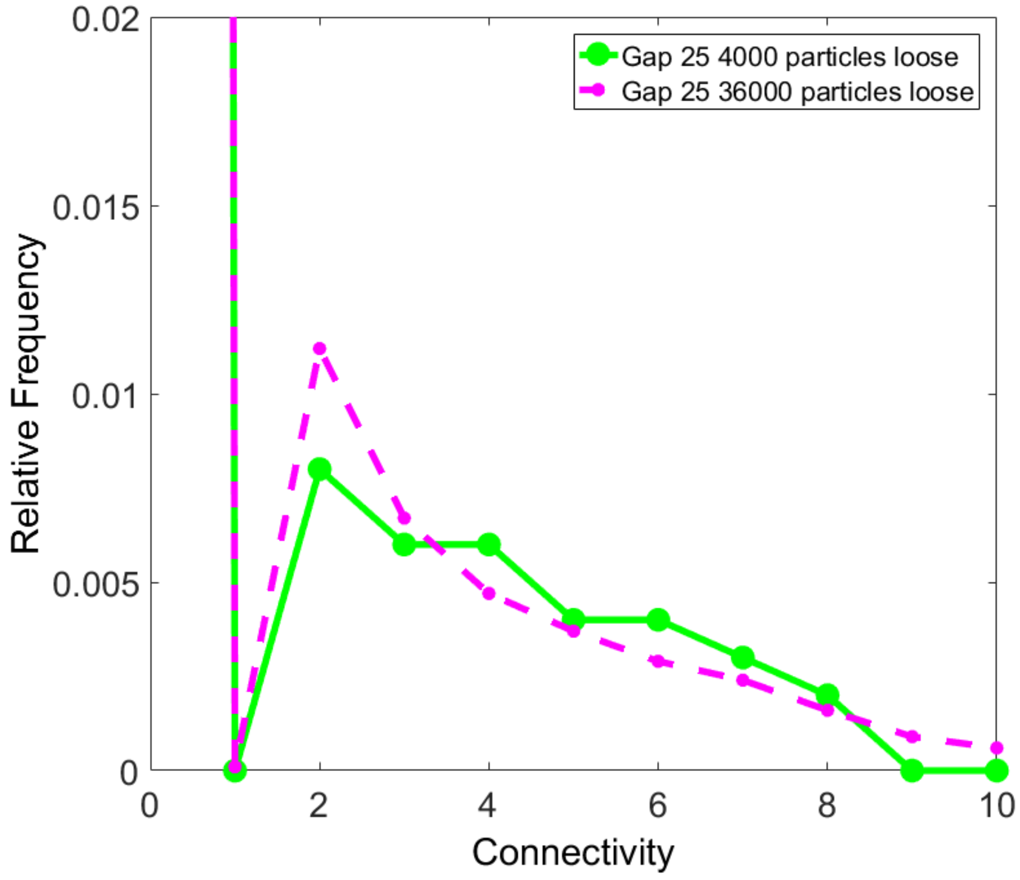

Shire (2014)

Periodic cell simulations – sample size considerations

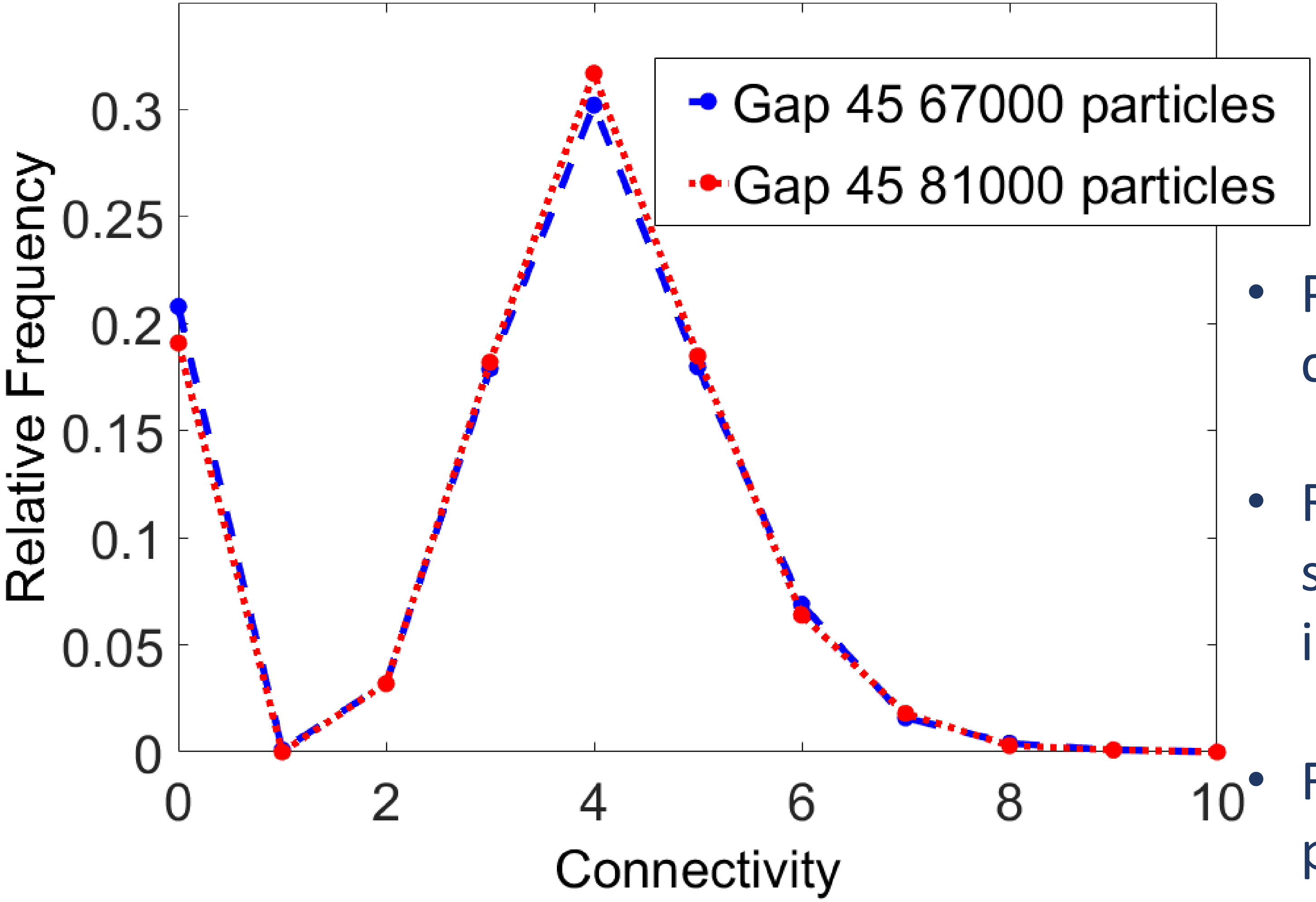

Shire (2014)

- Preliminary study to assess whether 500 coarse particles gave a satisfactory REV
- Reducing number of particles no significant effect on fabric measure of interest
- Full parametric study used 500 coarse particles for each sample

Conclusions

- V important to establish you have an REV (representative element volume)
- Critical state line position can be affected by boundary conditions – v significant implications for understanding behaviour
- Plots of local void ratio helpful to understand extent of boundary effects
- Periodic cell very useful, but you still need to check an REV is achieved

Specimen generation

Response of samples consolidated with μ=0.1

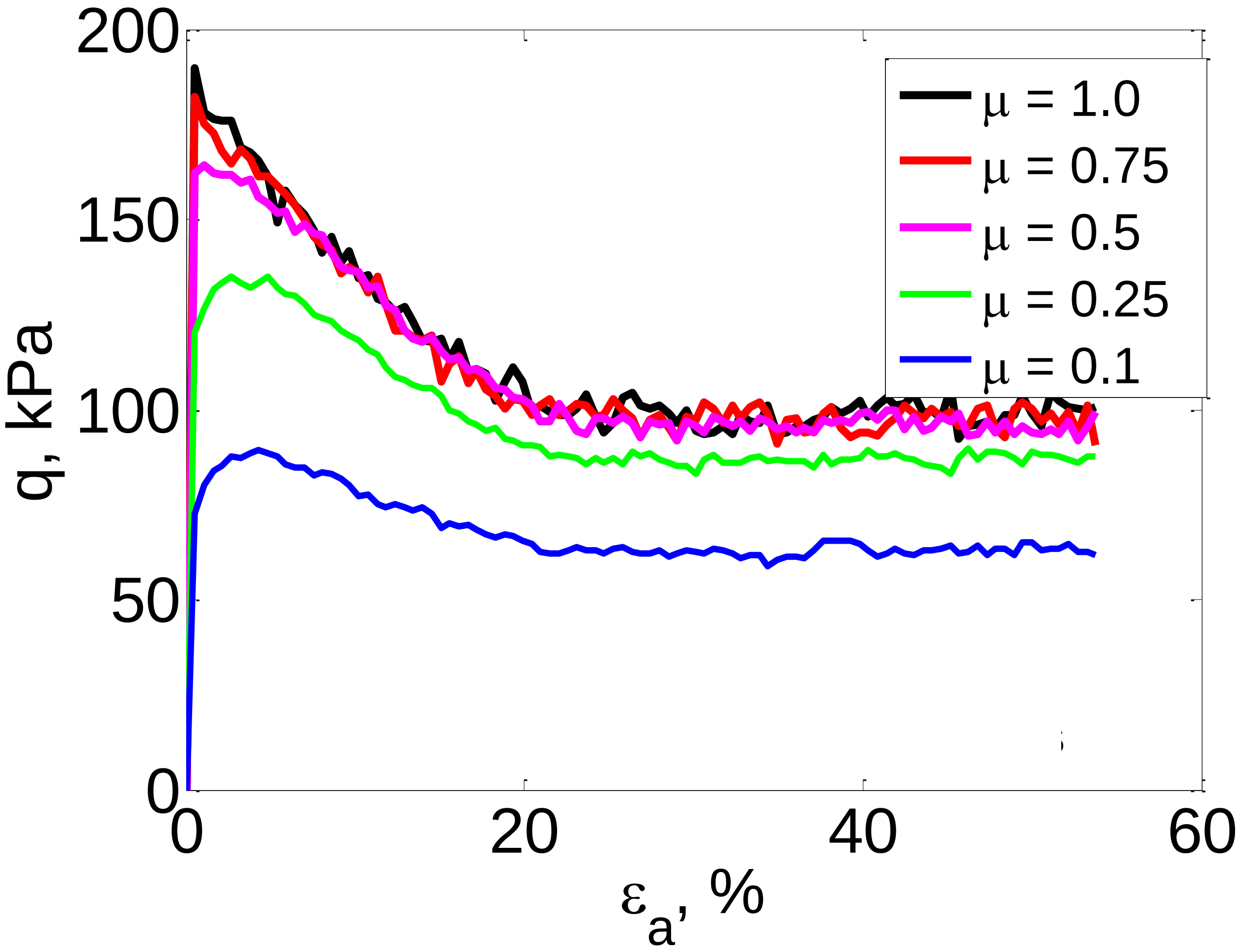

- Toyoura sand PSD
- Initial void ratio, $e_0 = 0.533$
- $\sigma'_3 = 100$ kPa
- Strain controlled triaxial compression

Huang et al. (2014)

Simple shear experiments

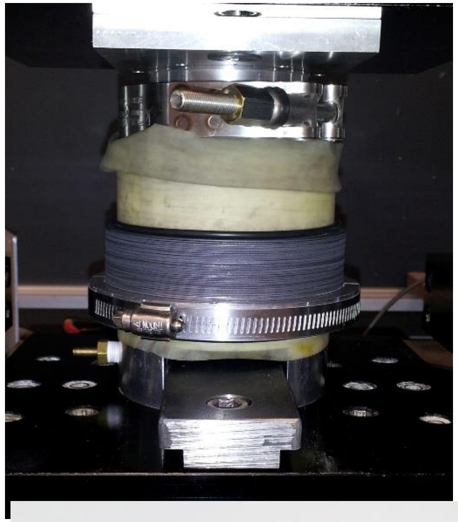

Experimental set up -
Texas A+M University

- NGI type simple shear
- Stacked ring configuration

Loose and dense samples subjected to monotonic simple shear

Material:

- Grade 25 chrome steel balls
- 3 sizes
- Sample 1: 2.28, 3.18, 3.97 mm, 1:1:1
  Total: 7,500 spheres
- Sample 2: 1.19, 1.59, 1.98 mm, 1:1:1
  Total: 60,000 spheres

Bernhardt et al. (2016)

Simple shear simulations

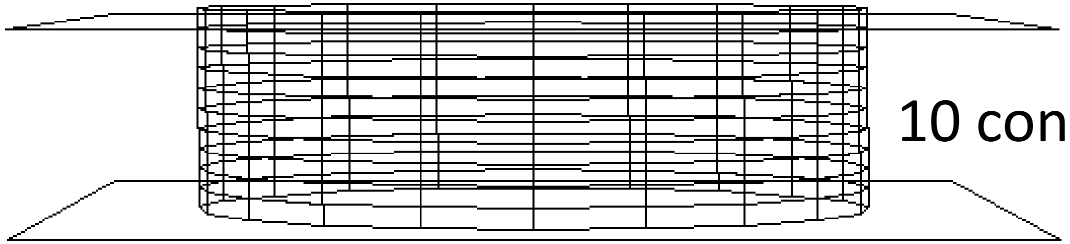

Simulation details:

- PFC3D
- Input parameters matched experiments
- G=80GPa, ν=0.3, ρ=7800 kg/m^3
- ϕ_μ=5.5^o

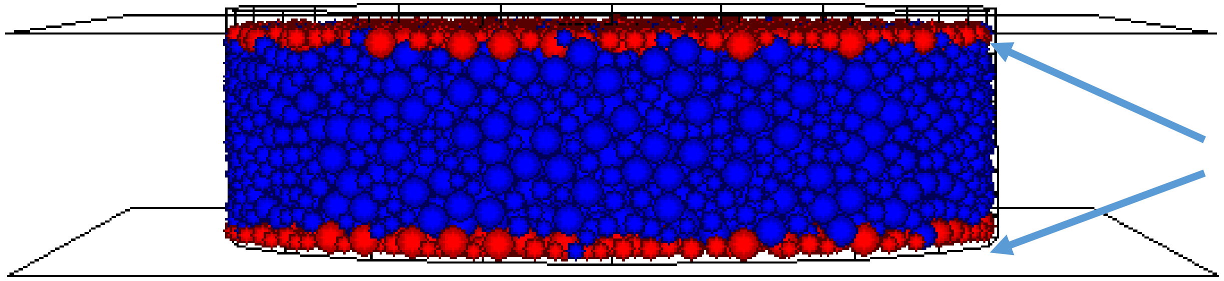

Bernhardt et al. (2016)

Simple shear simulations: specimen preparation

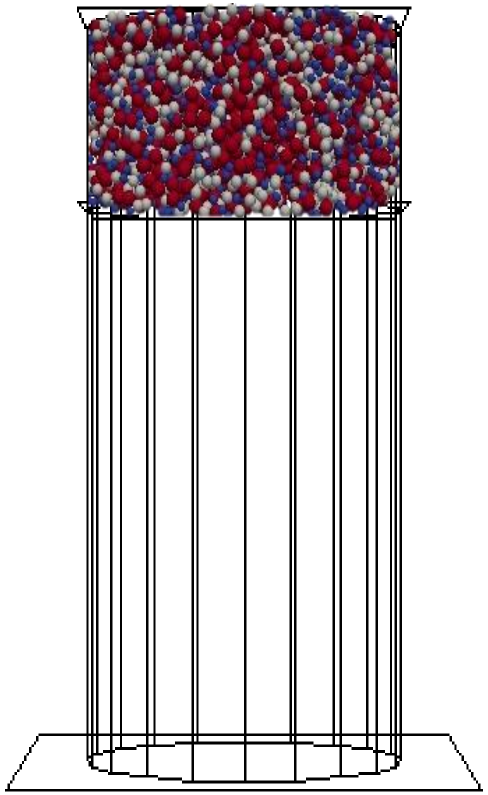

Cloud of non contacting spheres

Bernhardt et al. (2016)

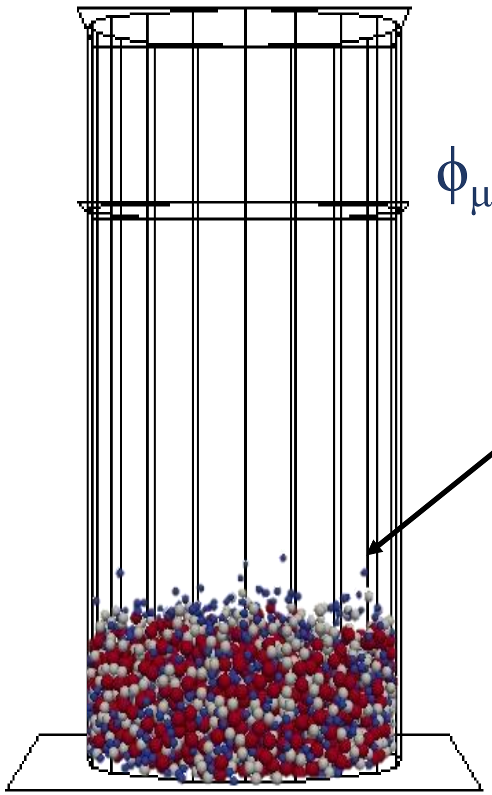

Gravity settling

To create dense

ϕ_{μ} reset to 5.5^{o} during shearing

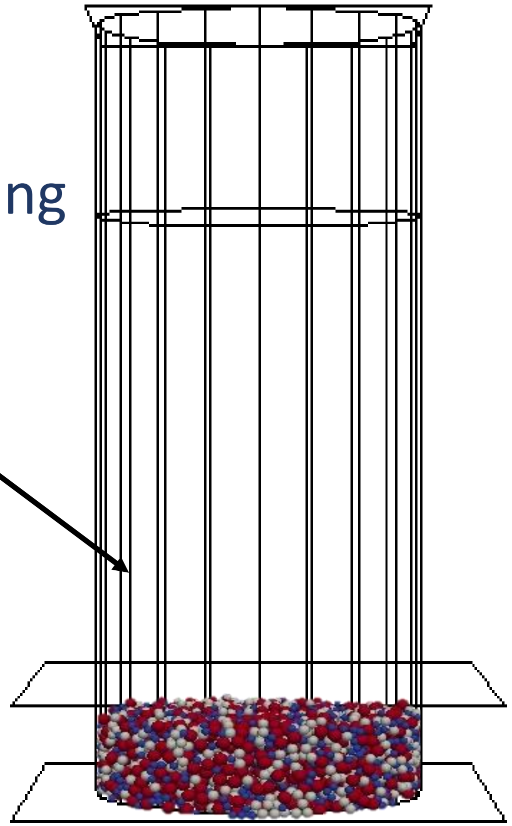

Servo-control walls to get target vertical stress

Simple shear simulations: specimen preparation

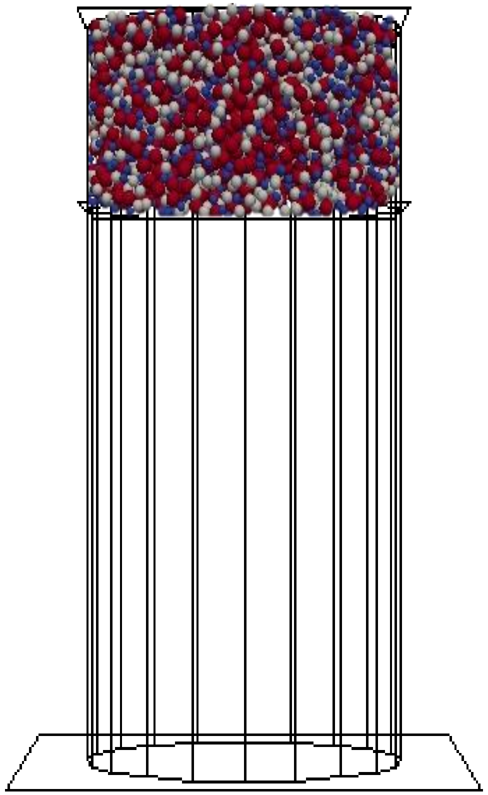

Cloud of non contacting spheres

Bernhardt et al. (2016)

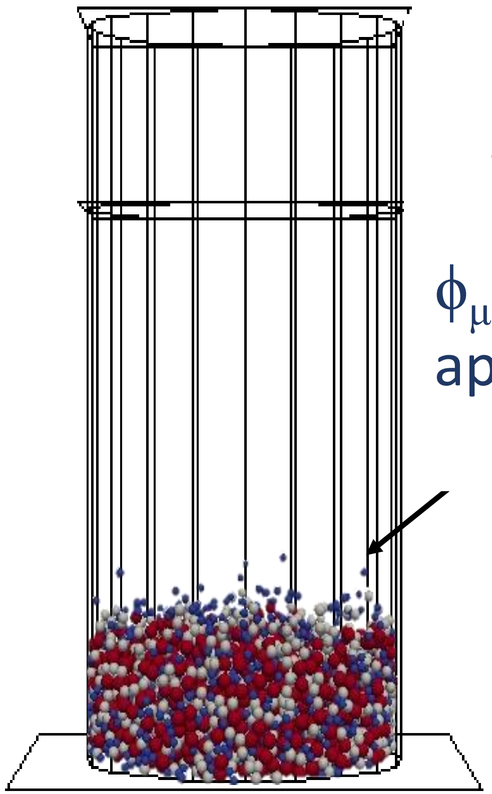

Gravity settling

To create loose samples samples
$\phi_{..}$set to 45^{o}
ϕ_{μ}reset to 5.5^{o} before application of vertical stress

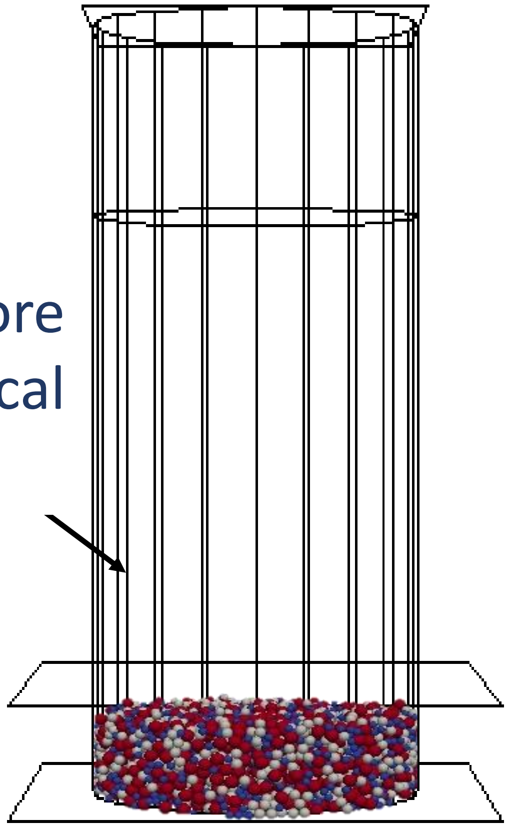

Servo-control walls to get target vertical stress

Simple shear simulations: Observed response sample 1

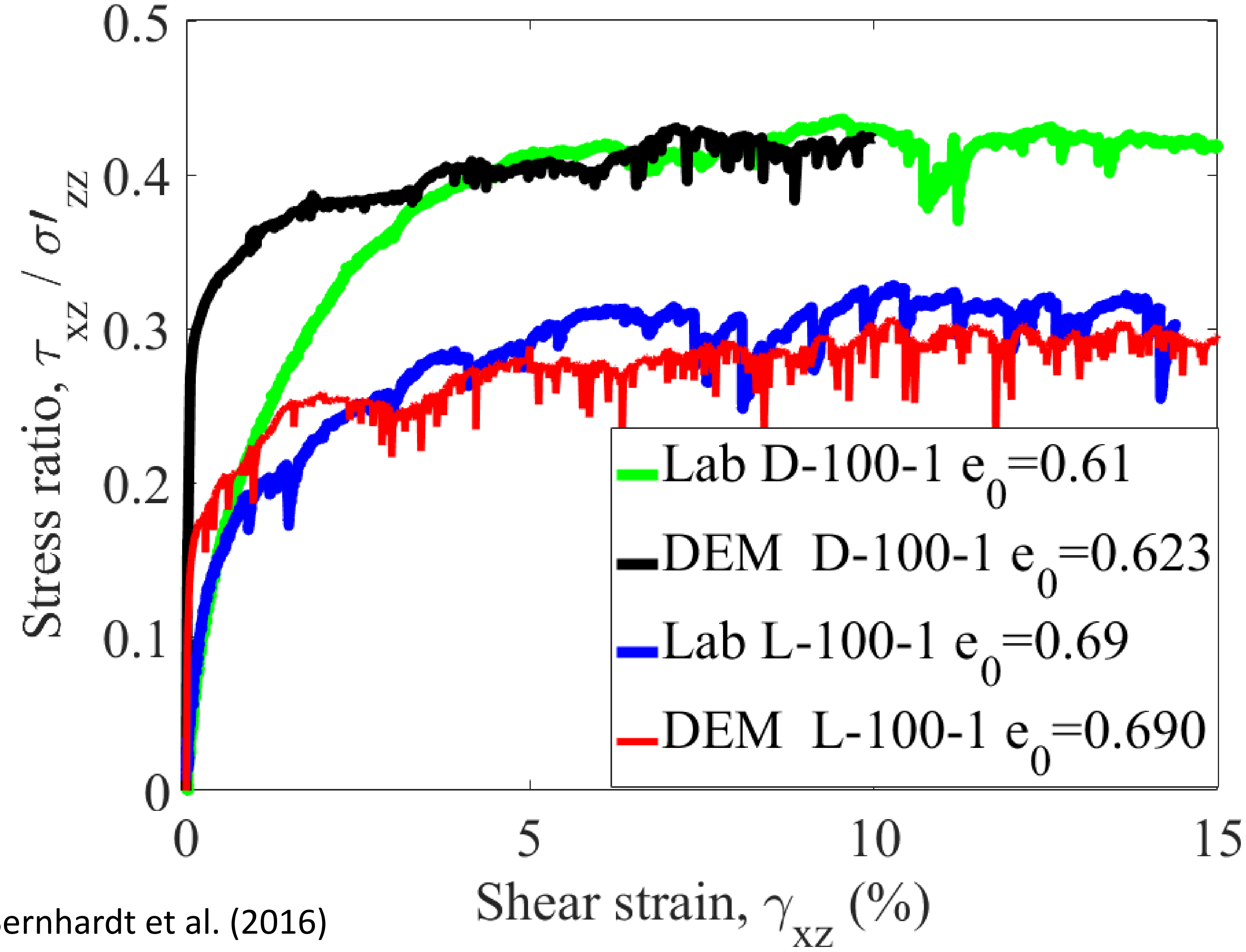

7,500 particles

Vertical stress = 100 kPa

Bernhardt et al. (2016)

Simple shear simulations: Observed response sample 1

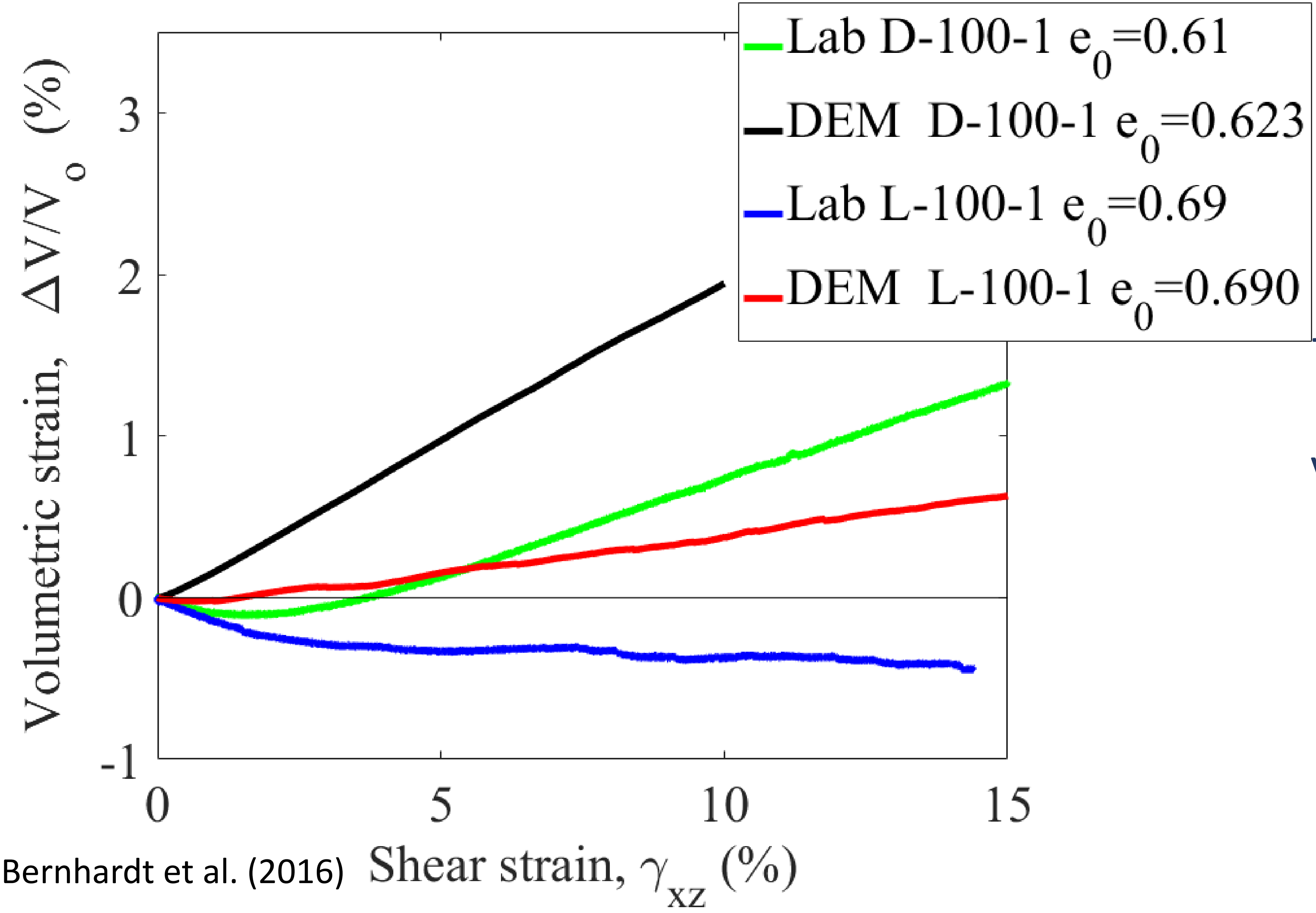

Bernhardt et al. (2016)

7,500 particles

Vertical stress = 100 kPa

Simple shear simulations: Observed response sample 2

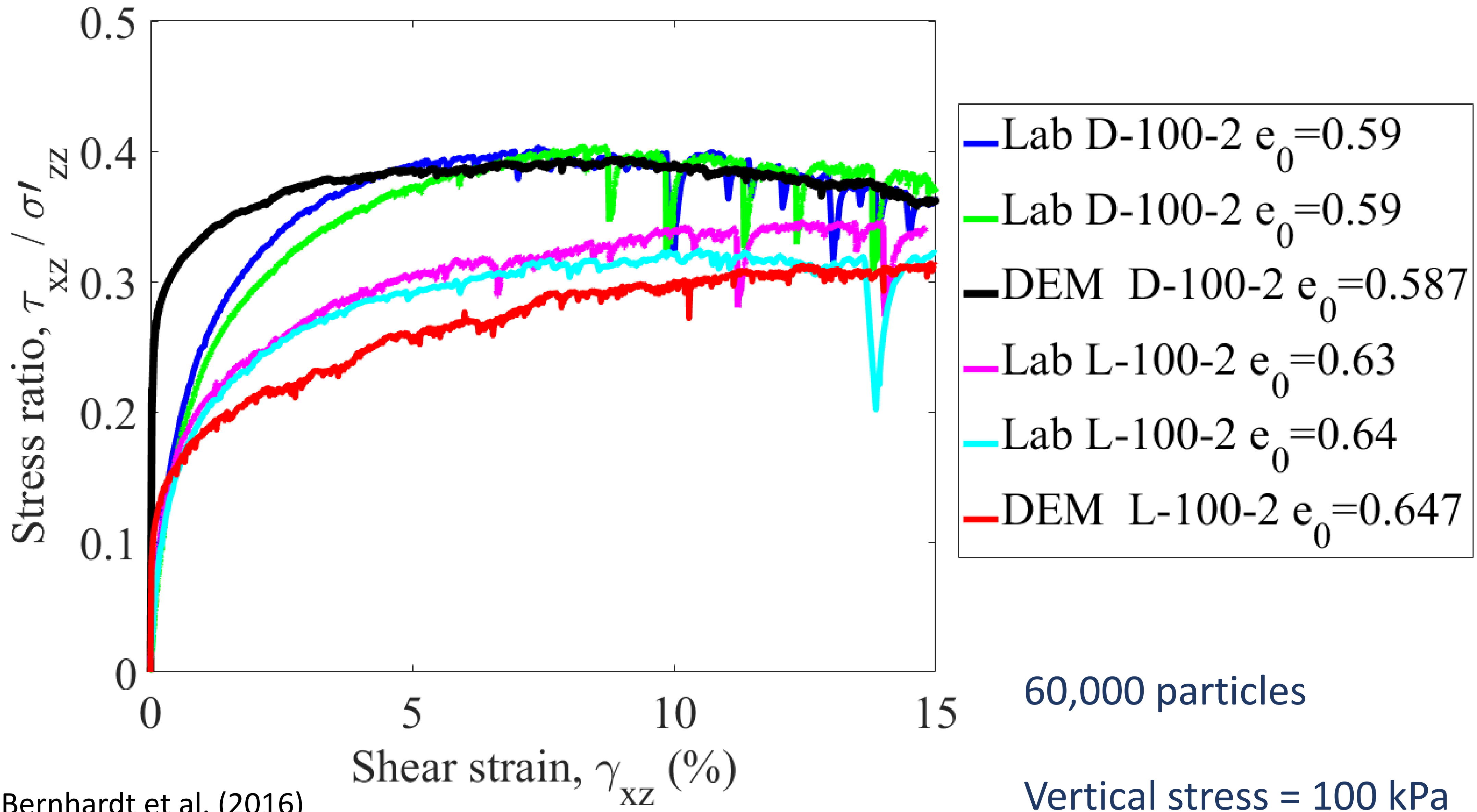

Bernhardt et al. (2016)

60,000 particles

Vertical stress = 100 kPa

Simple shear simulations: Observed response sample 2

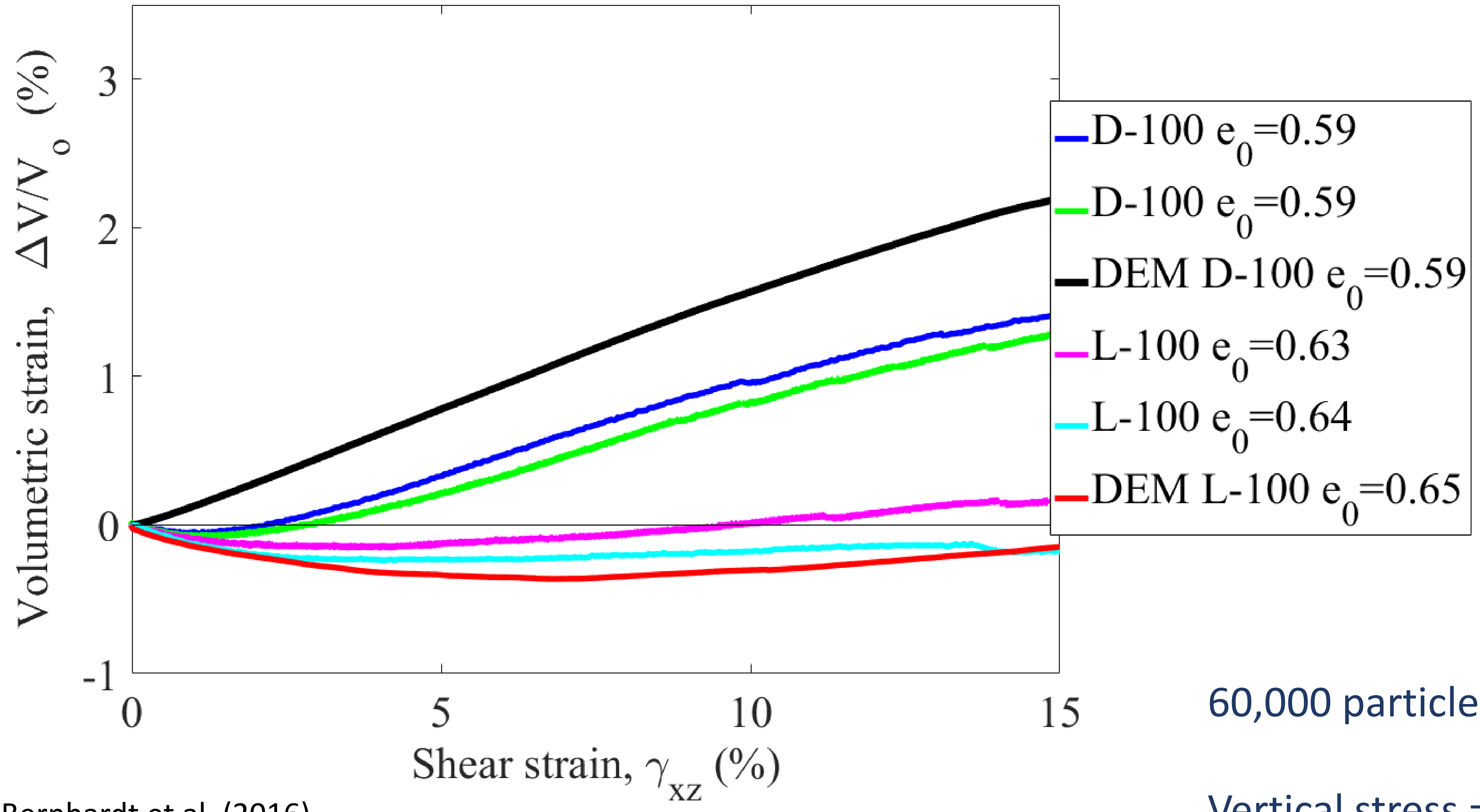

Bernhardt et al. (2016)

60,000 particles

Vertical stress = 100 kPa

Simple shear simulations: Observations

- For both sample types at large strains DEM simulation and lab data agree
- Agreement is more effective for loose samples in both cases
- Very stiff response, dilatant response observed for dense DEM samples

Bernhardt et al. (2016)

Simple shear simulations: Reduction of ϕ_μ during preparation

- ϕ_μ was reduced only for dense samples where simulation / lab agreement is poor
- For dense samples at start of shearing shear forces far from yield

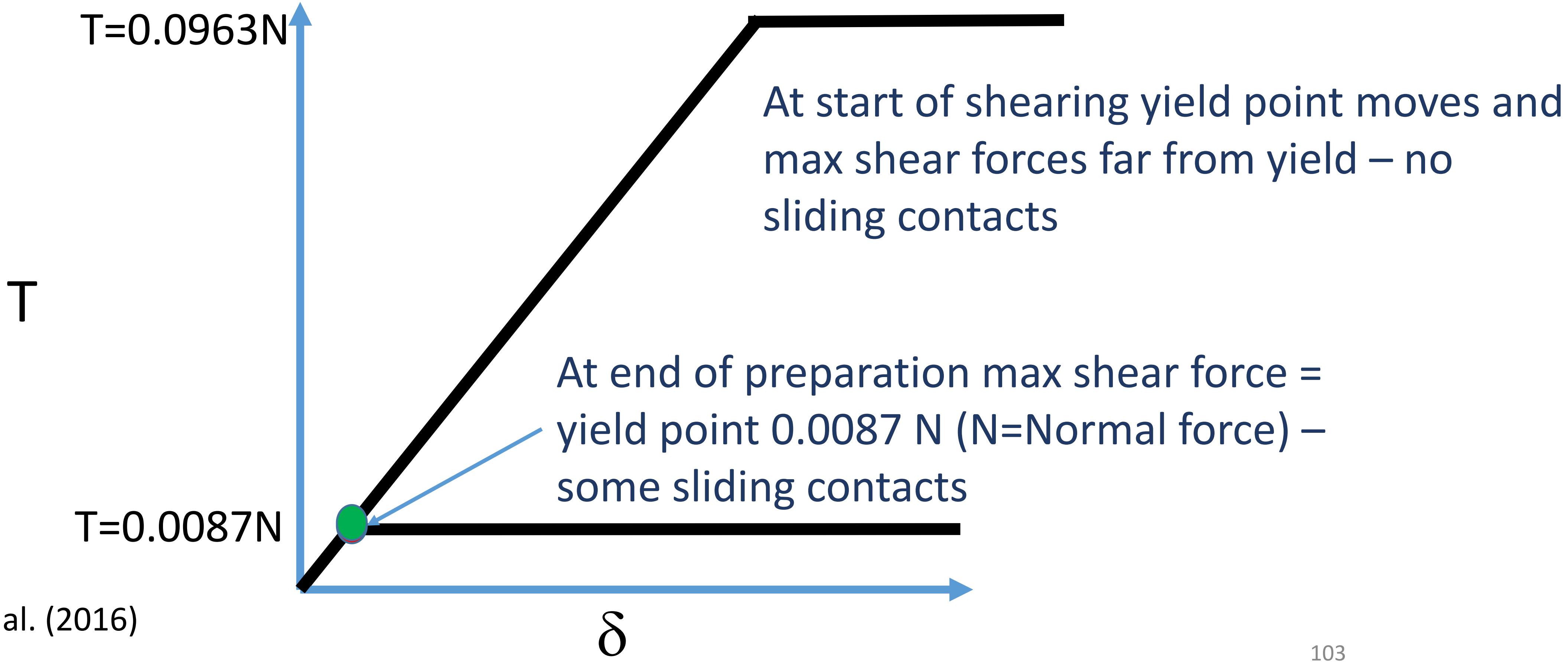

Bernhardt et al. (2016)

Conclusions

- You can achieve a range of densities by varying particle friction during preparation

- May detrimentally effect pre-peak response

Input parameters

Influence of friction on critical state line

Critical state is a state where the soil deforms at constant stress and constant void ratio

Been and Jefferies (1985) Géotechnique

Critical state locus (CSL) for Toyoura sand
Verdugo (1992) Géotechnique

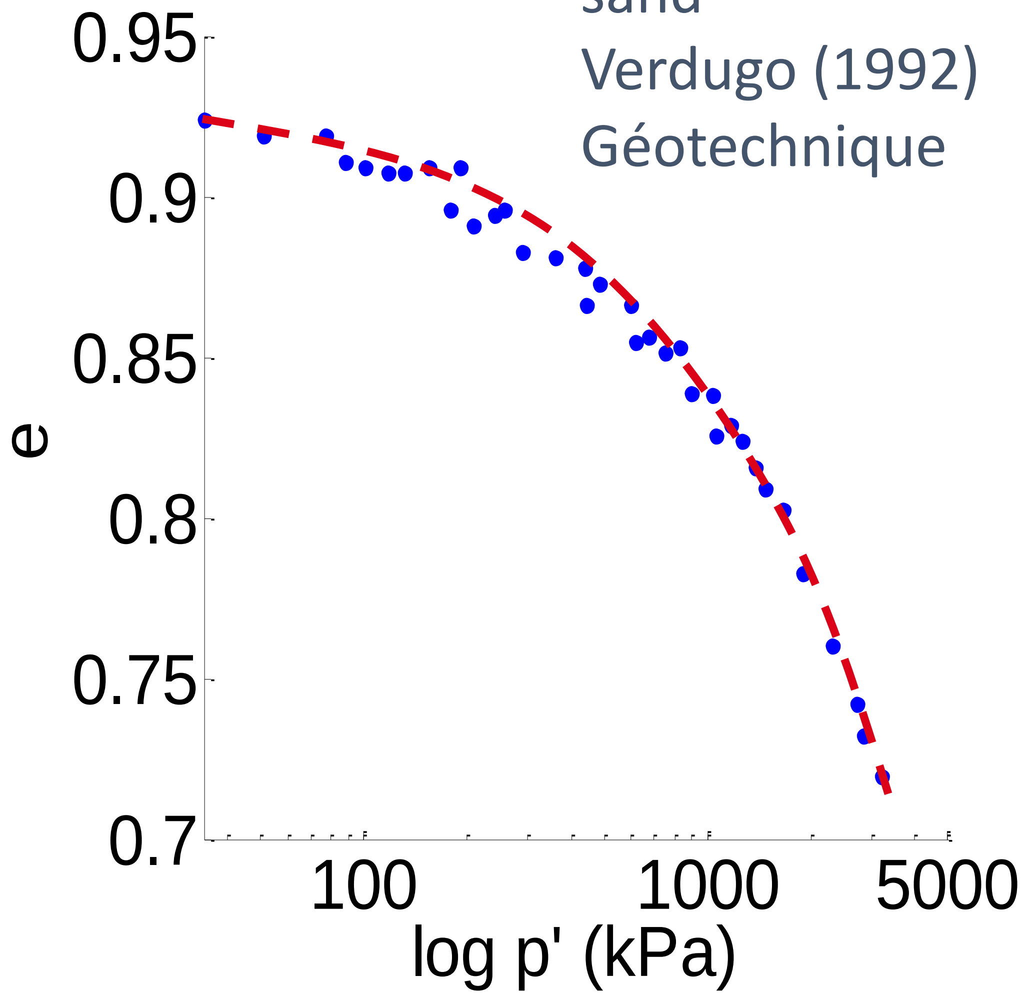

Huang et al. (2014)

Influence of friction on critical state line

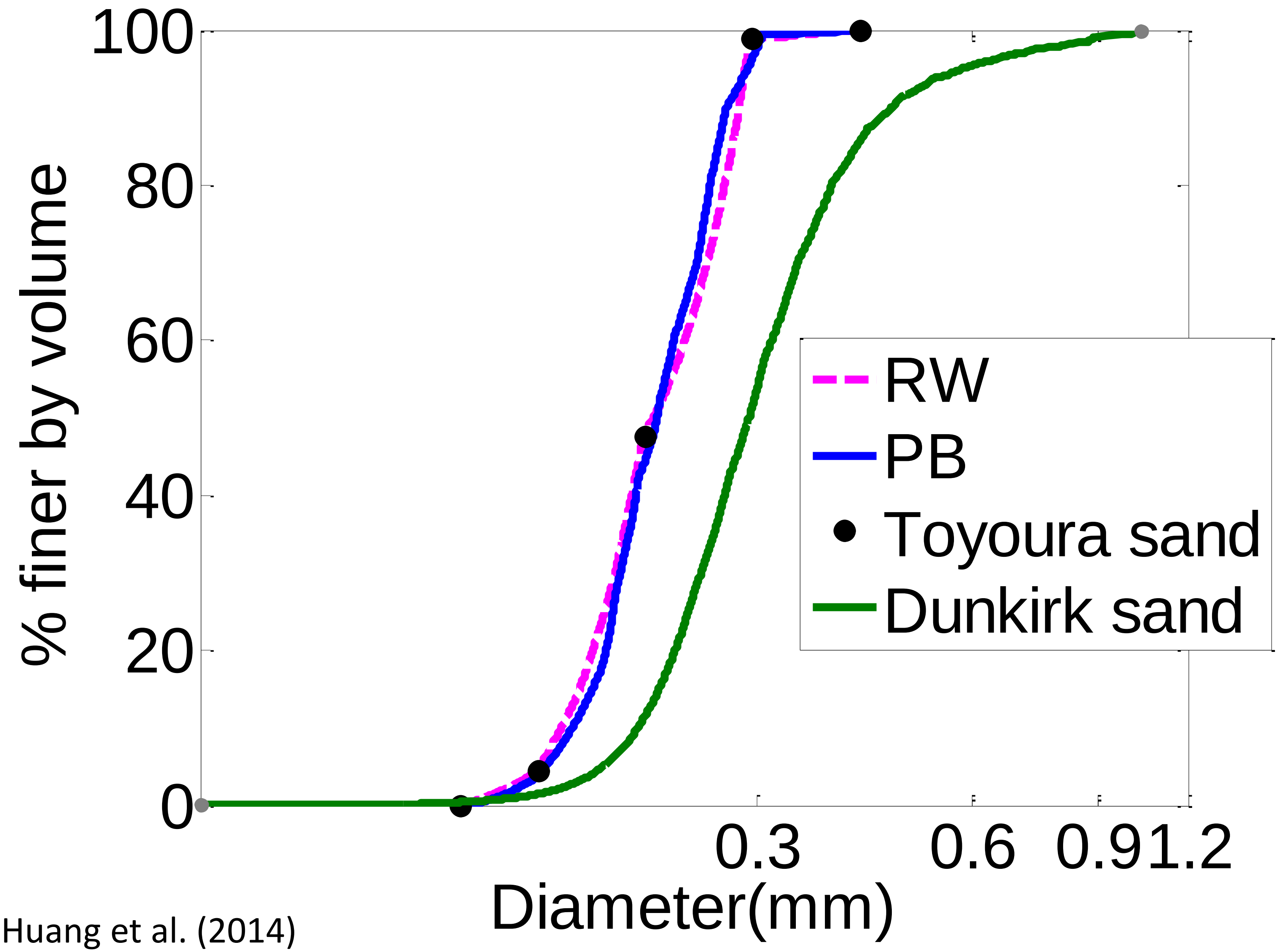

Huang et al. (2014)

Critical state line e-log p' - Toyoura grading

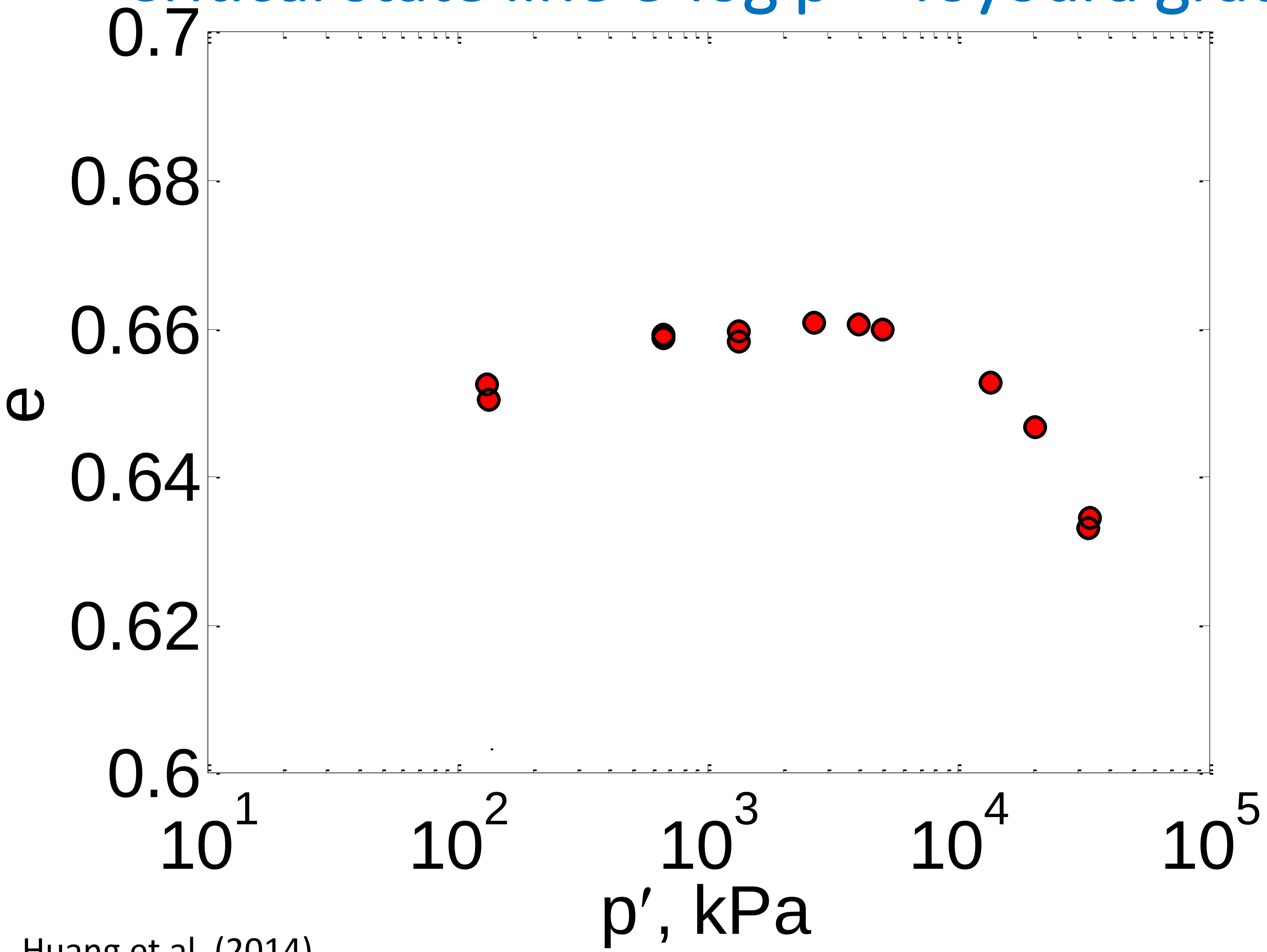

- Hertz-Mindlin contact model
- μ=0.5
- DEM Code LAMMPS

Huang et al. (2014)

Critical state line e-log p' - Toyoura grading

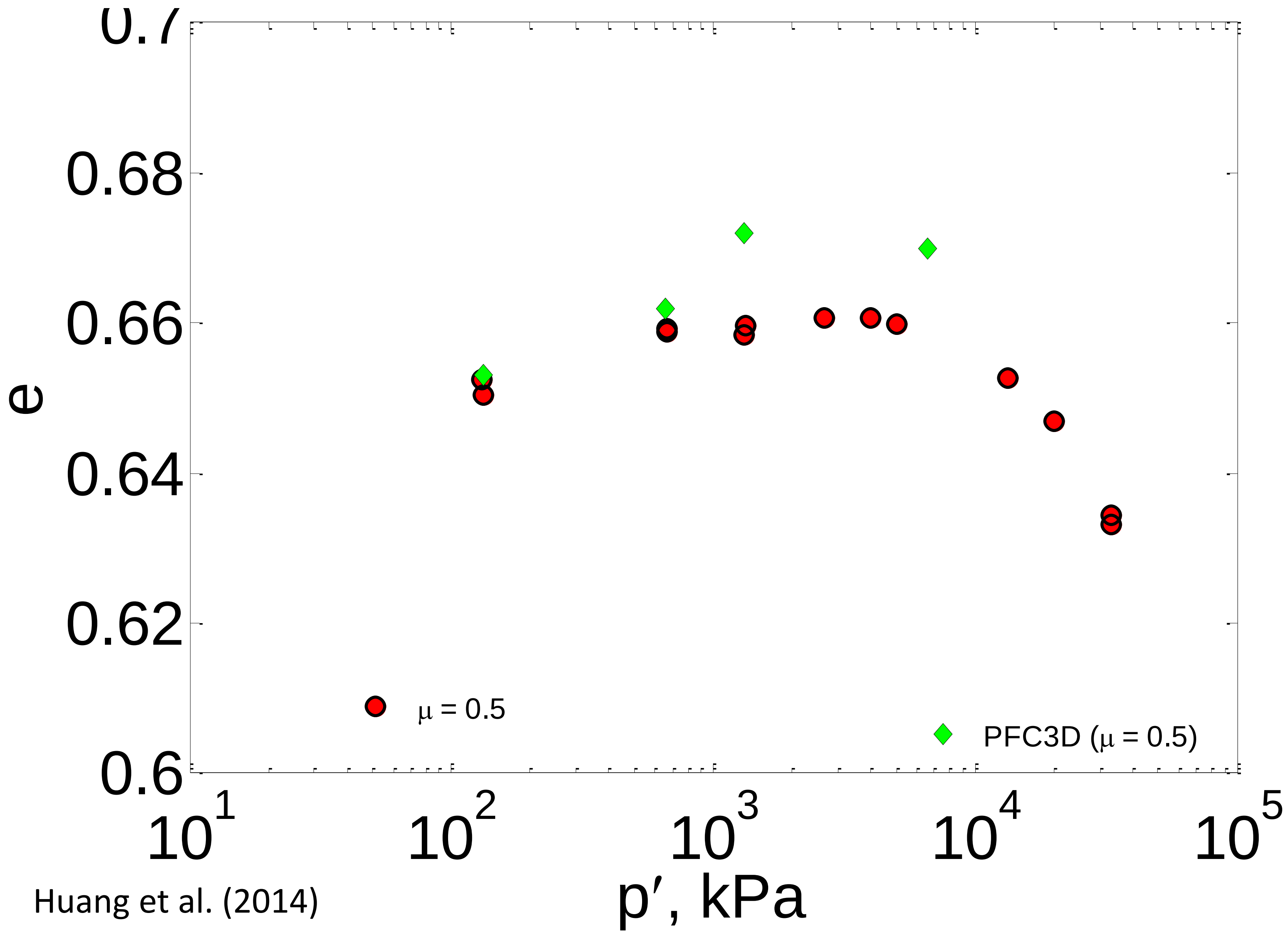

Huang et al. (2014)

- Hertz-Mindlin contact model
- μ=0.5
- DEM Codes LAMMPS + PFC 3D

Critical state line e-log p' - Toyoura grading

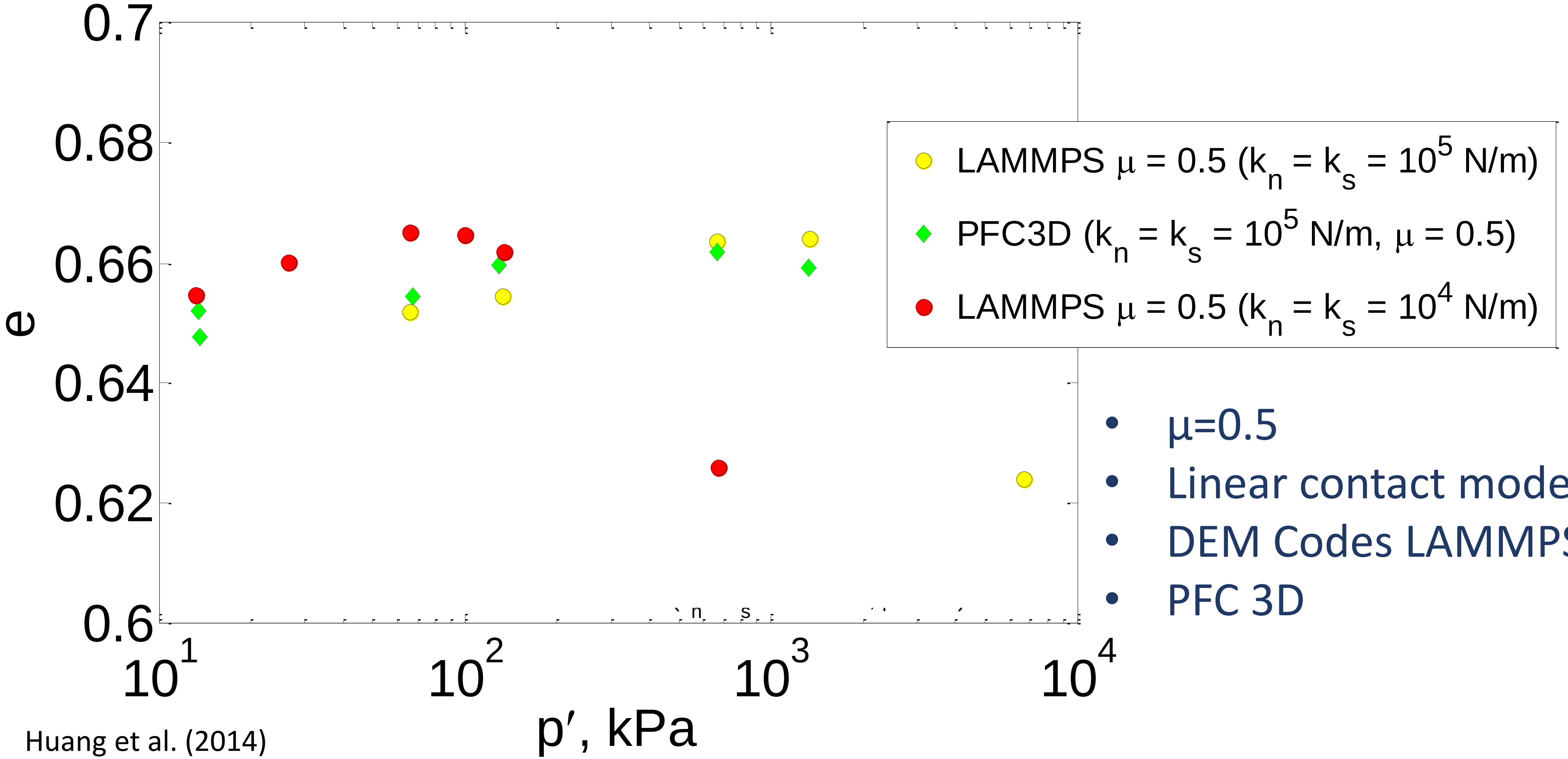

Huang et al. (2014)

- μ=0.5
- Linear contact model
- DEM Codes LAMMPS +
- PFC 3D

Critical state line e-log p' - Toyoura grading

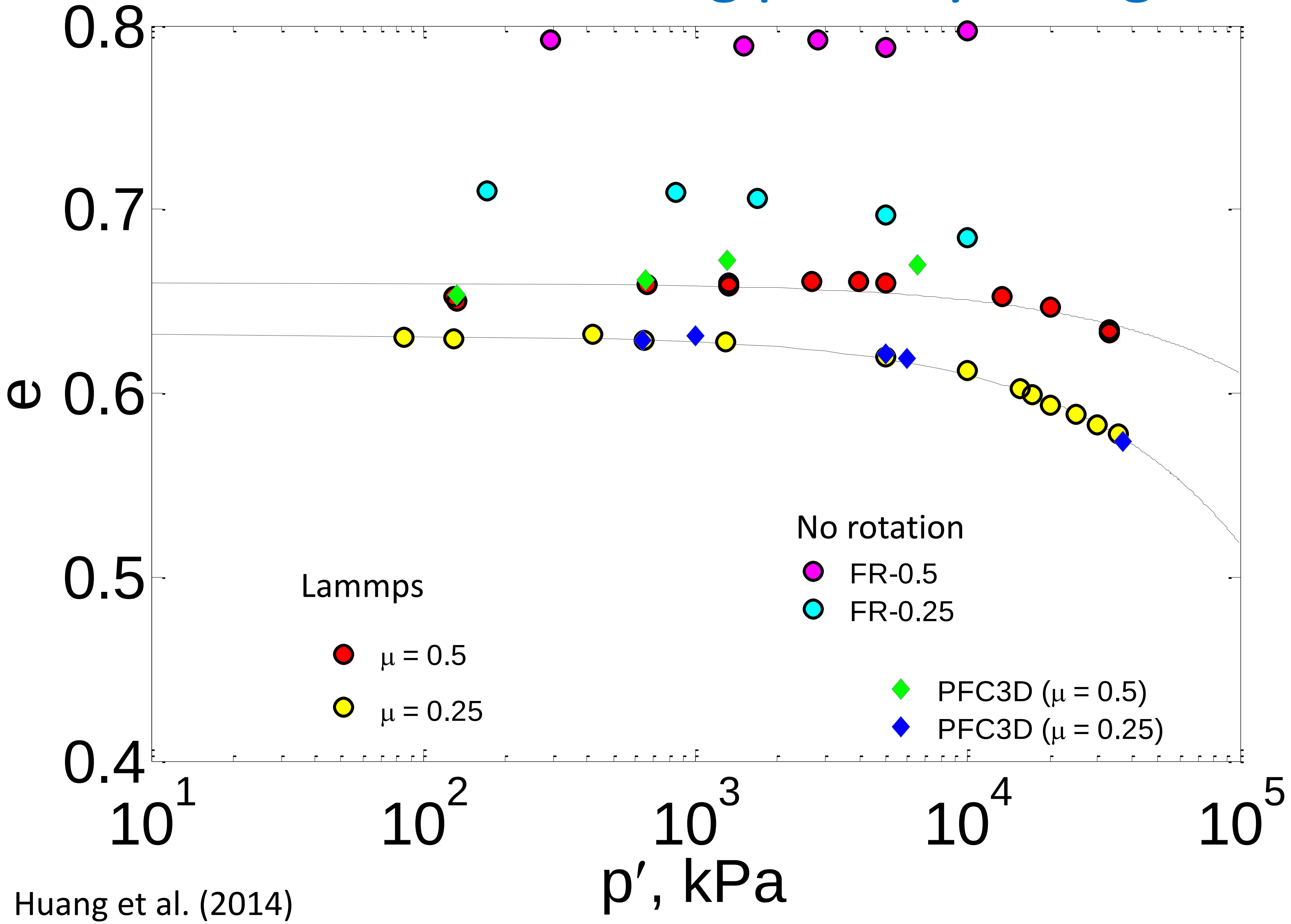

- Hertz-Mindlin contact model
- μ=0.5 + μ=0.25
- DEM Codes LAMMPS + PFC 3D

Huang et al. (2014)

Critical state line e-log p‘ - Toyoura grading

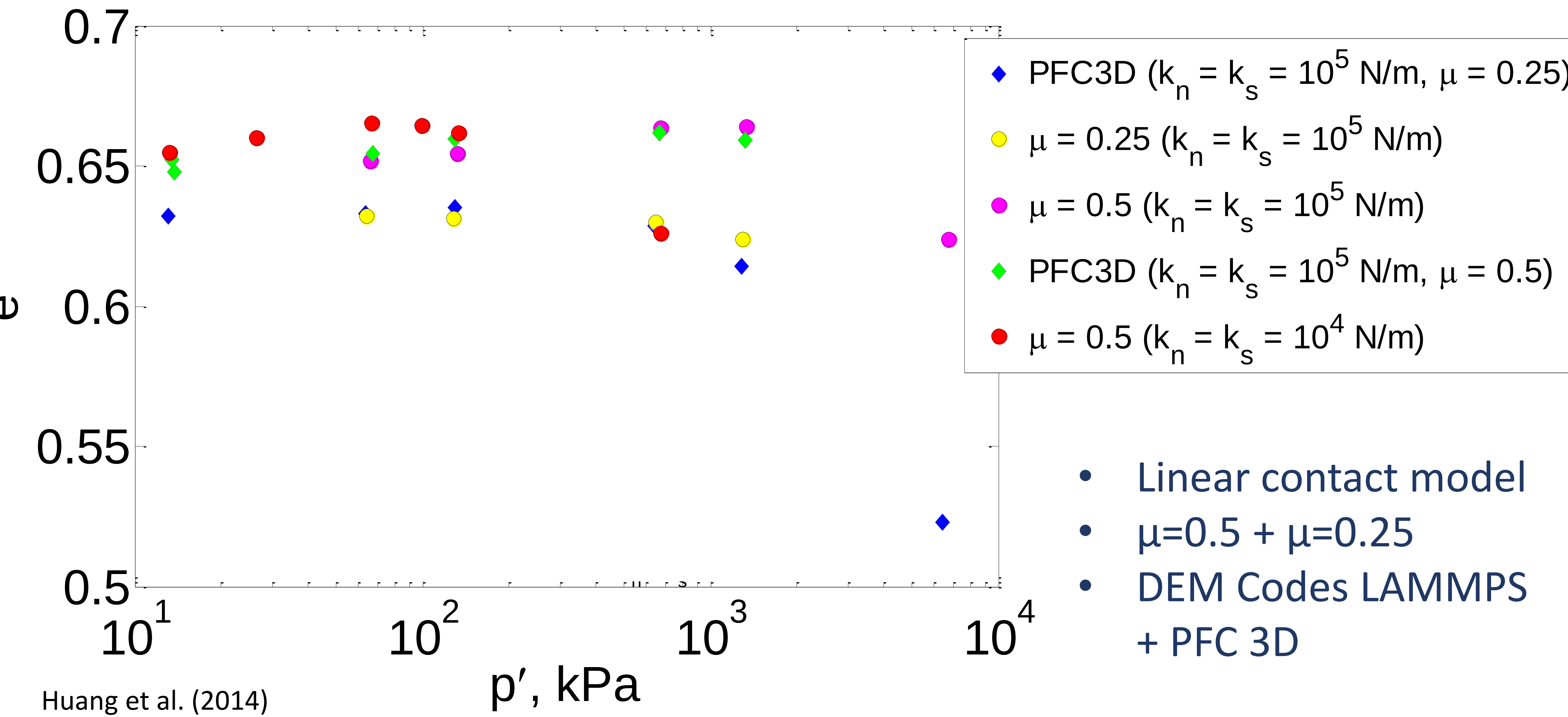

Huang et al. (2014)

- Linear contact model
- μ=0.5 + μ=0.25
- DEM Codes LAMMPS + PFC 3D

Critical state angle of shearing resistance (ϕ_{cv})

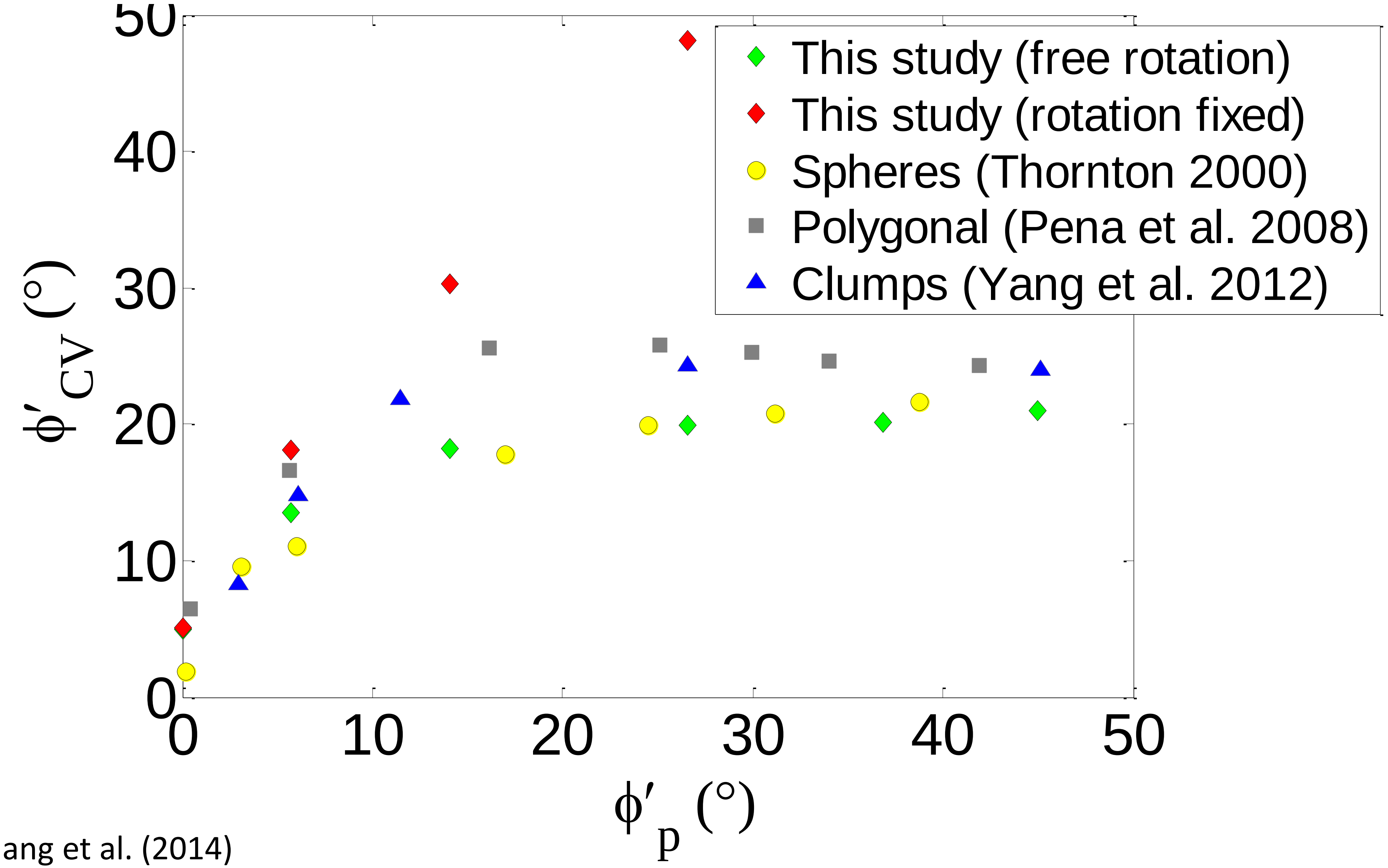

Huang et al. (2014)

Response of samples consolidated with μ=0.1

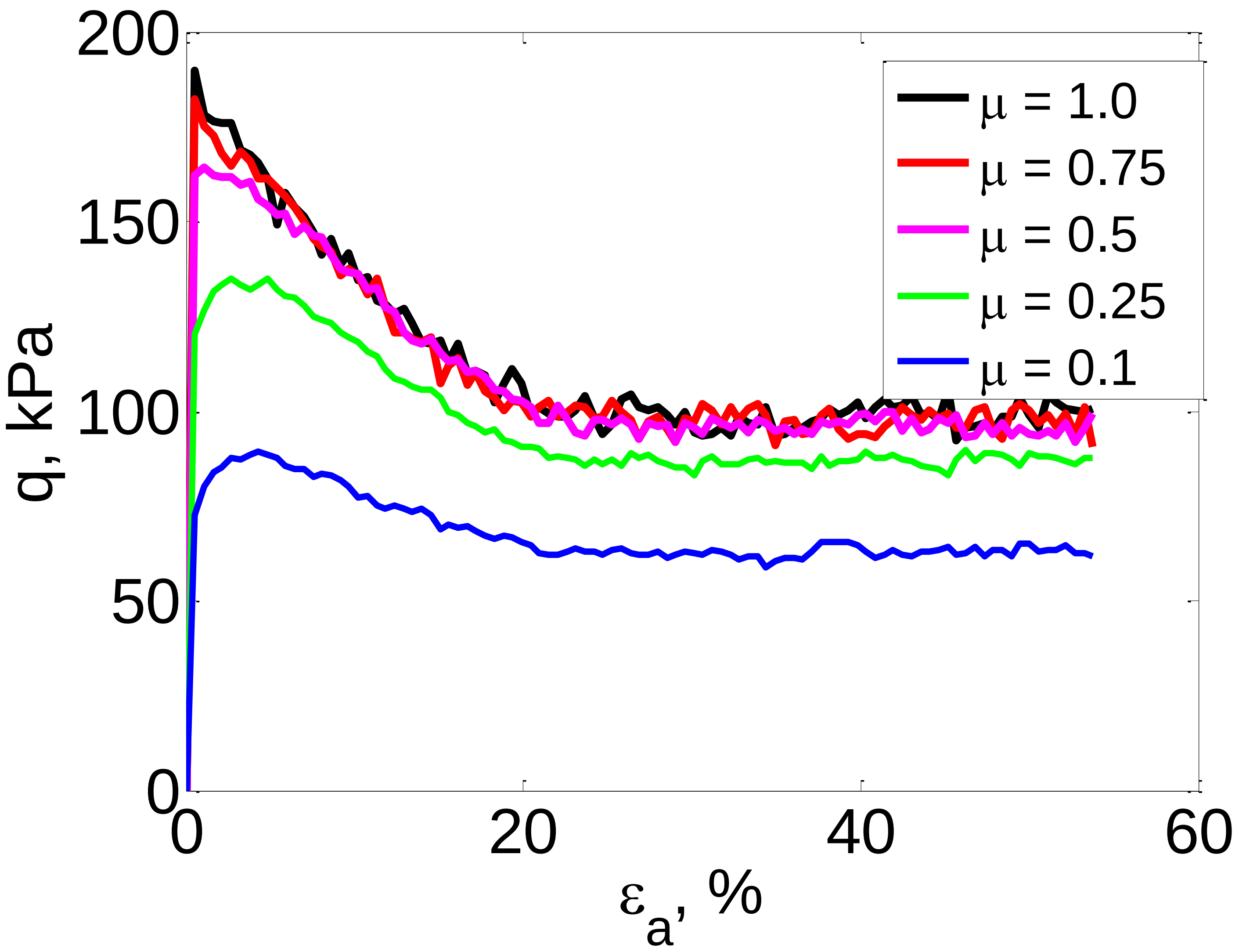

- Initial void ratio, e_0 = 0.533
- σ'_3 = 100 kPa

Huang et al. (2014)

Response of samples consolidated with μ=0.1

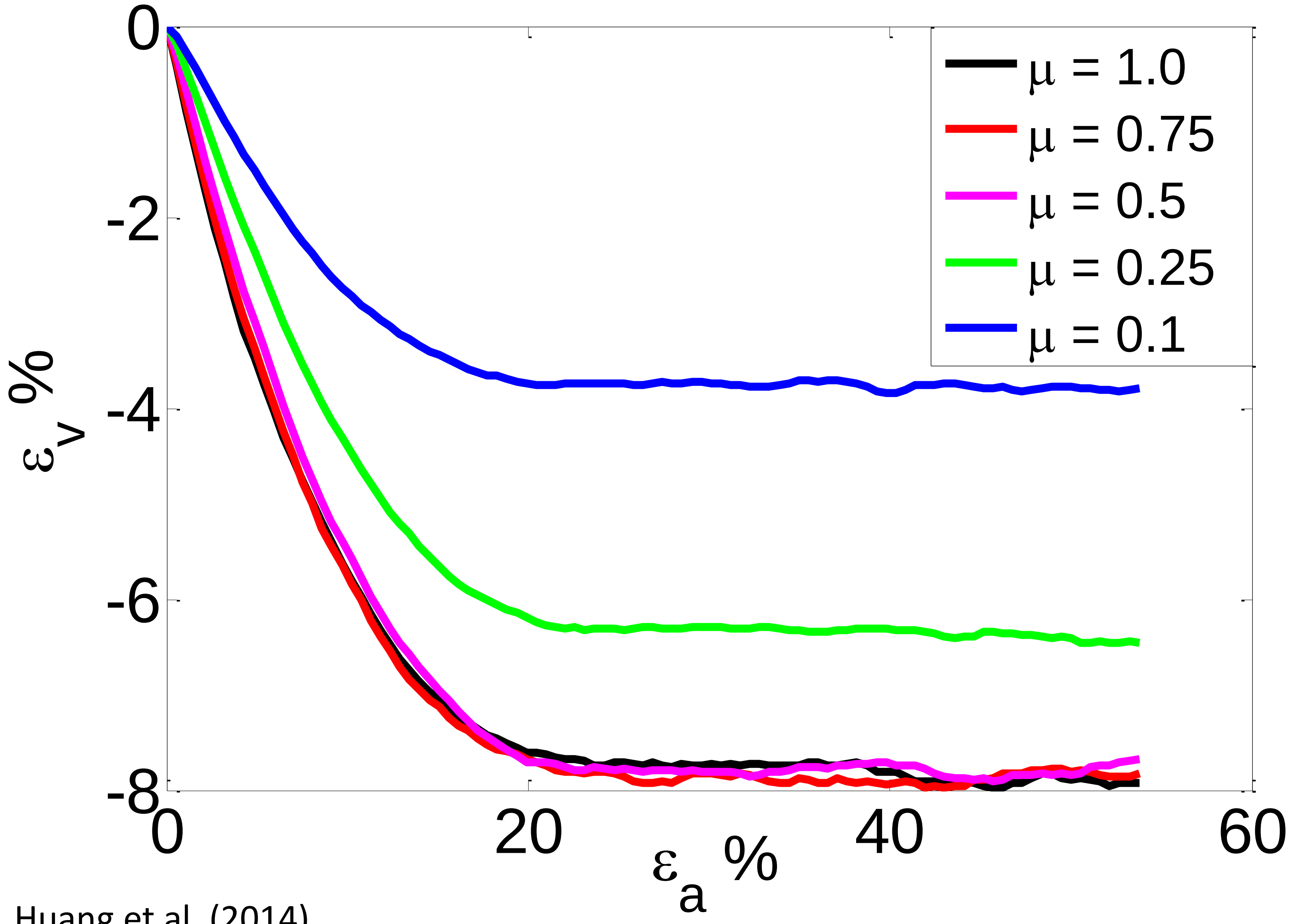

- Initial void ratio, e_0 = 0.533
- σ'_3 = 100 kPa

Huang et al. (2014)

Critical state line in e-log p' space

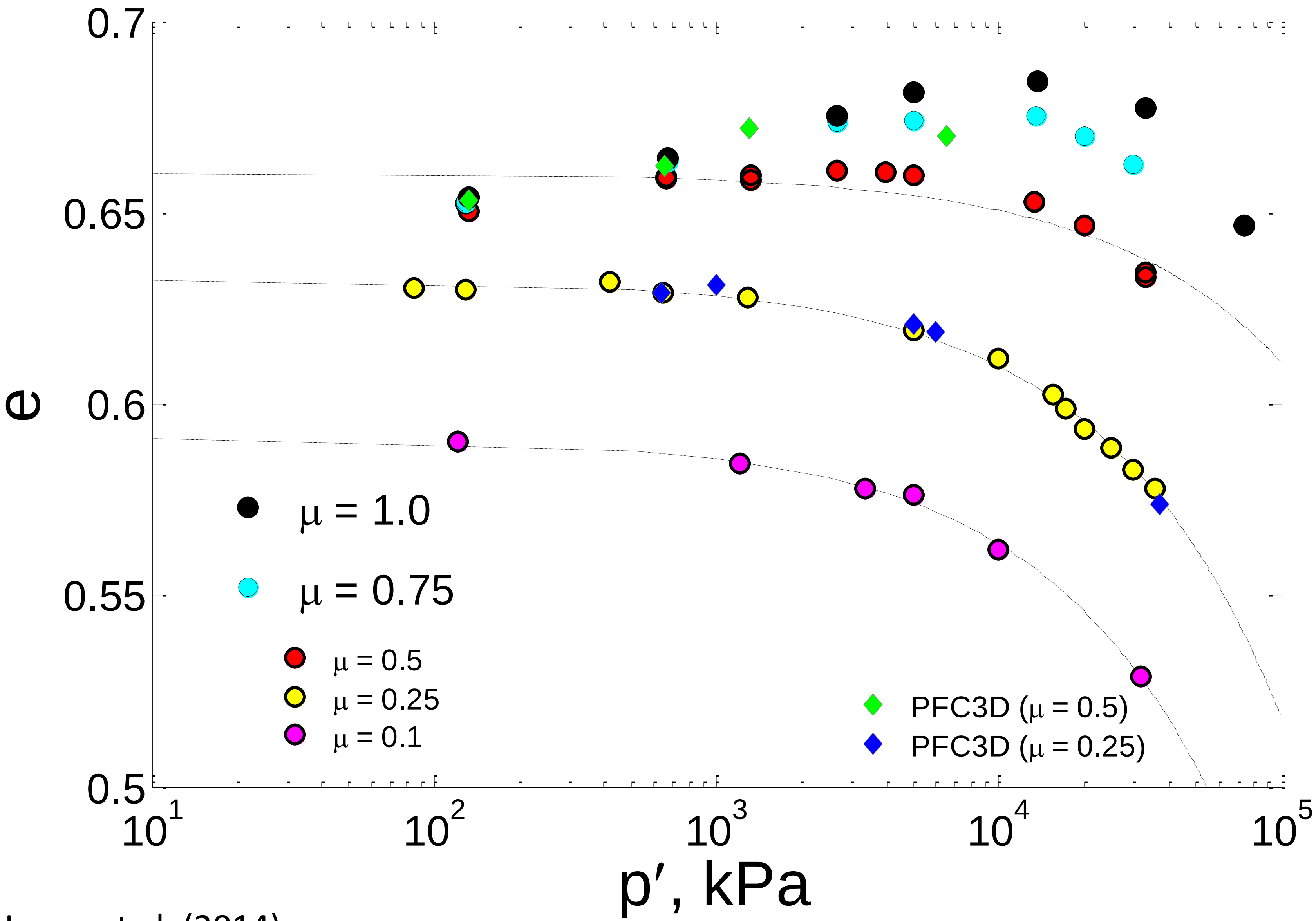

- Hertz-Mindlin contact model
- DEM Codes LAMMPS + PFC 3D

Huang et al. (2014)

Single force chain stability

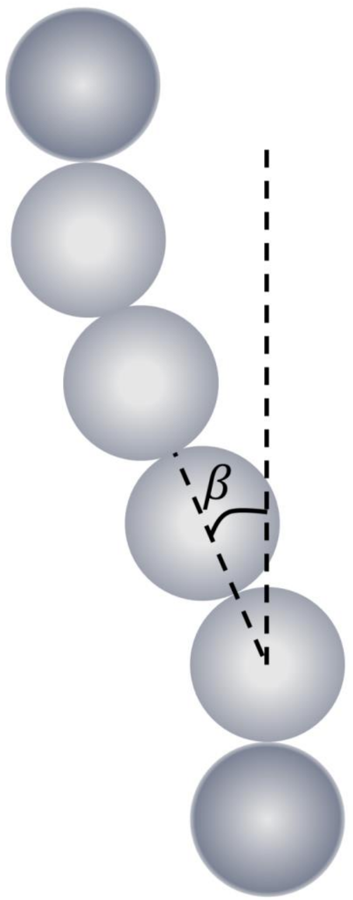

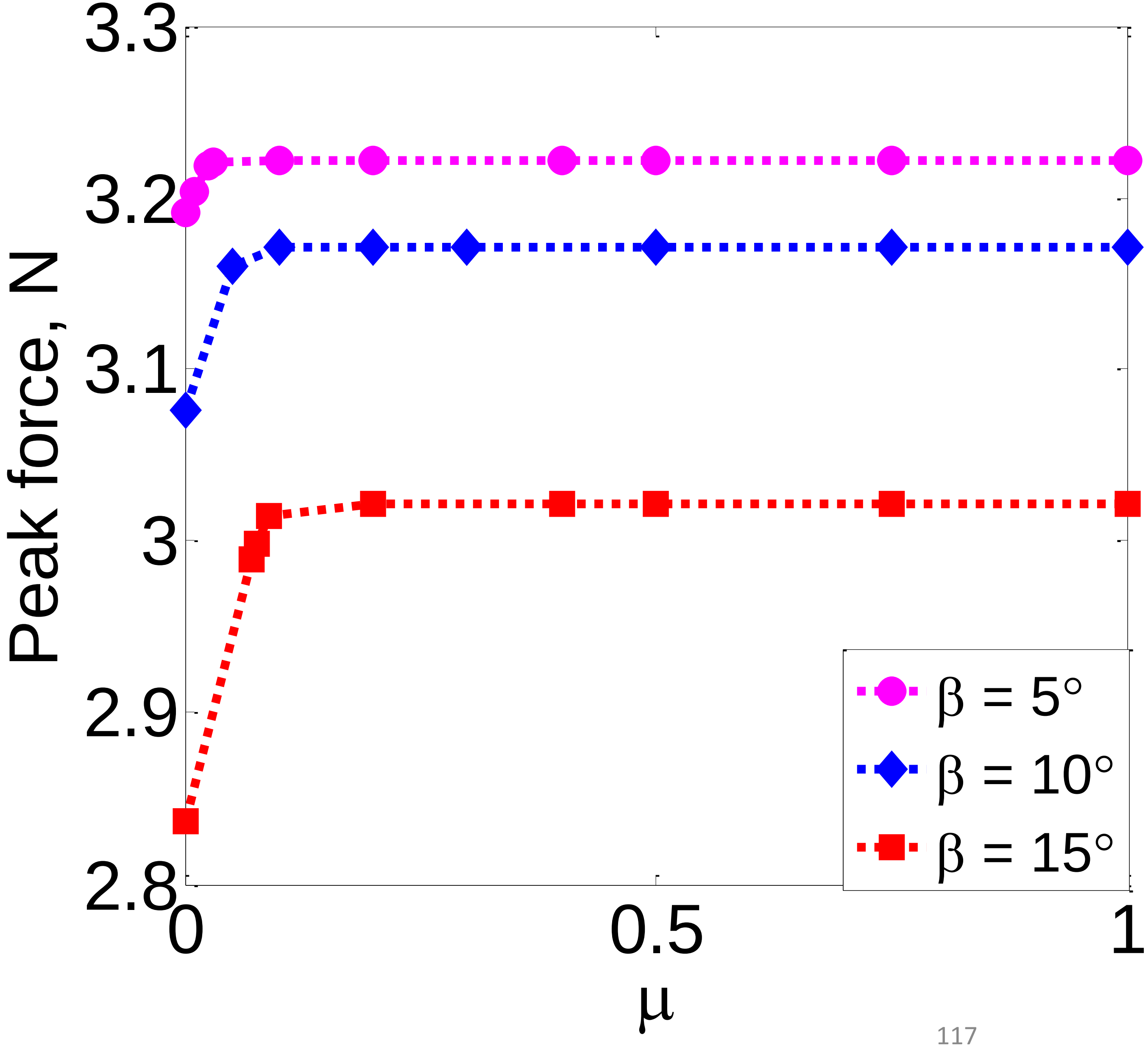

Transition from sliding to rolling

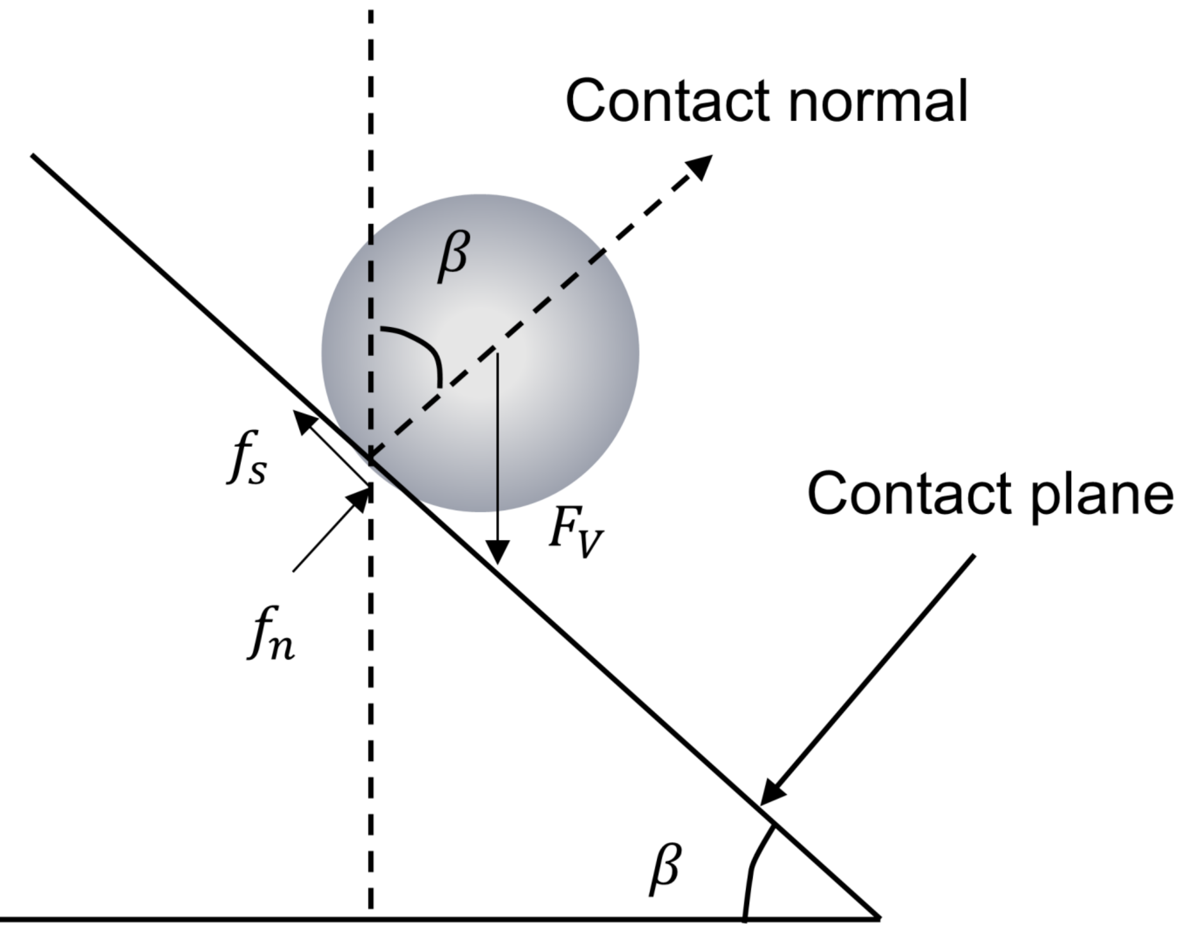

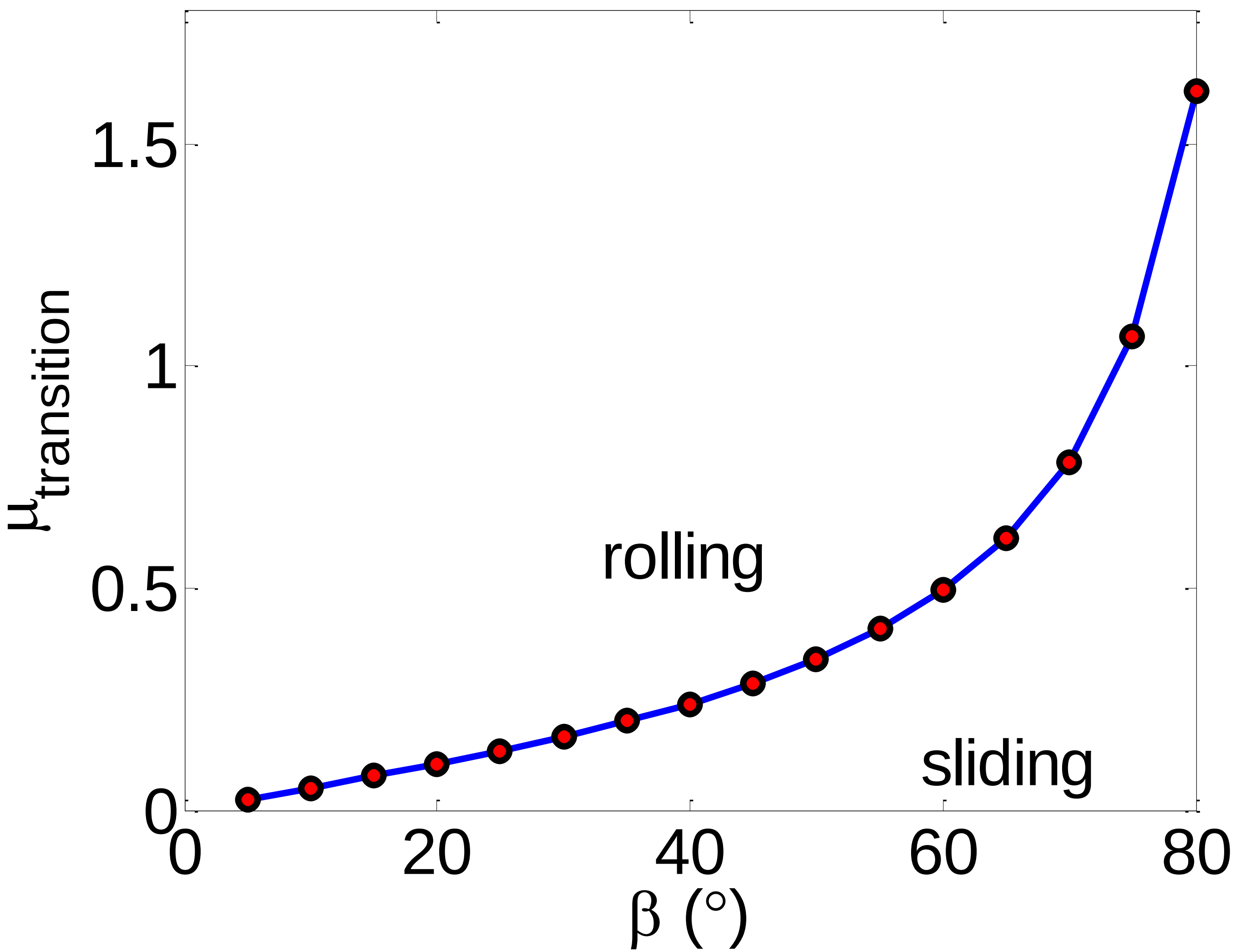

Transition from sliding to rolling

Effect of μ on the angular velocity

LAMMPS simulations
e_0 = 0.533, σ'_3 = 100 kPa

Cumulative distribution
of resultant angular velocities at ε_a = 50%.

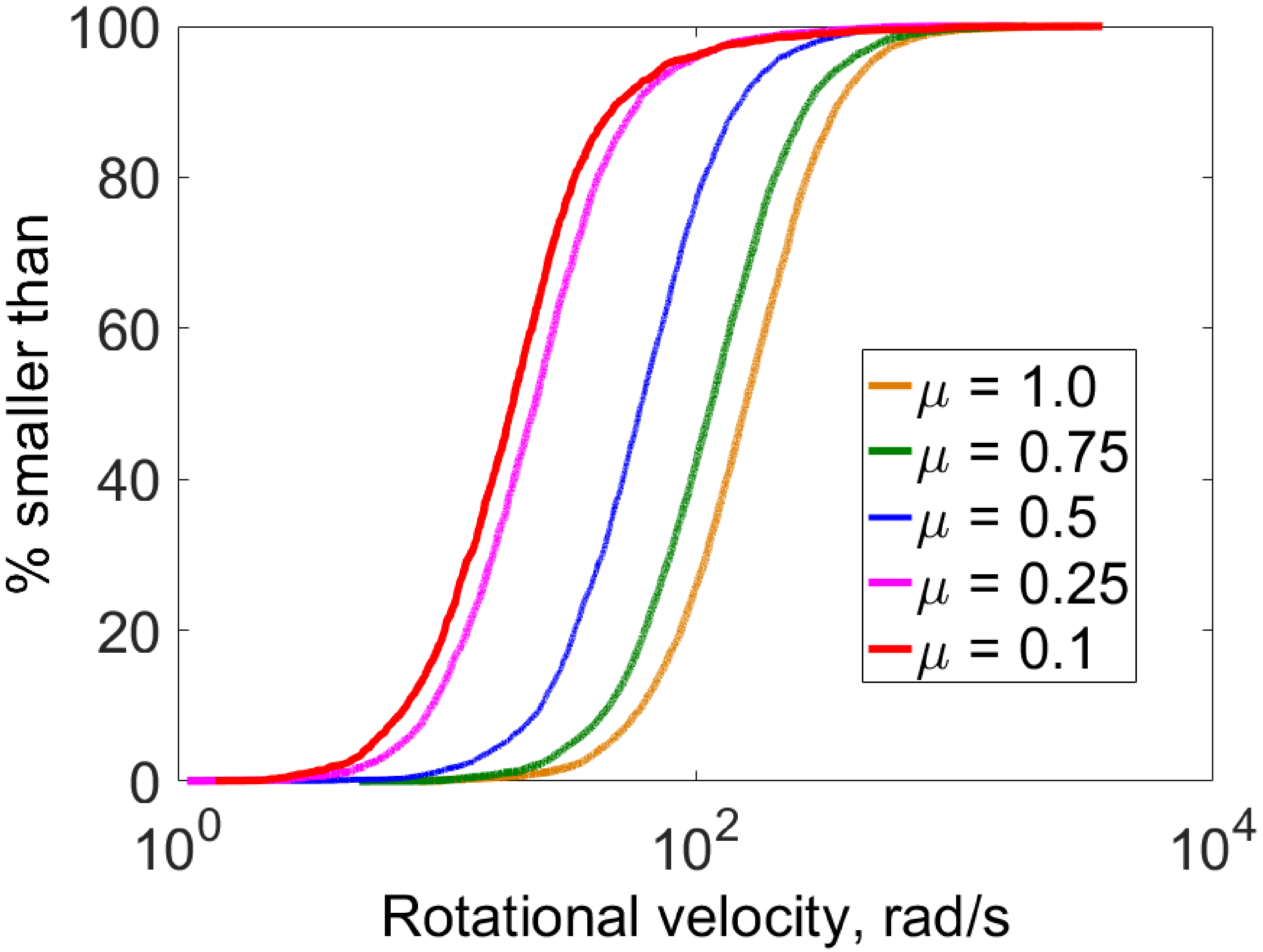

Huang et al. (2014)

Conclusions

- Using a high coefficient of friction (>0.5) with freely rotating spheres gives a response that is not representative of soil
- Explanation seems to be a transition from sliding to rolling at the contact points
- Use of two codes enhanced our confidence in observations
- Supplemental abstract analyses of small elements of the system were very useful

Contact Model

Deviations from Hertzian contact mechanics

- Rough surface effects
- Partial slip effect

Deviations from Hertzian contact mechanics

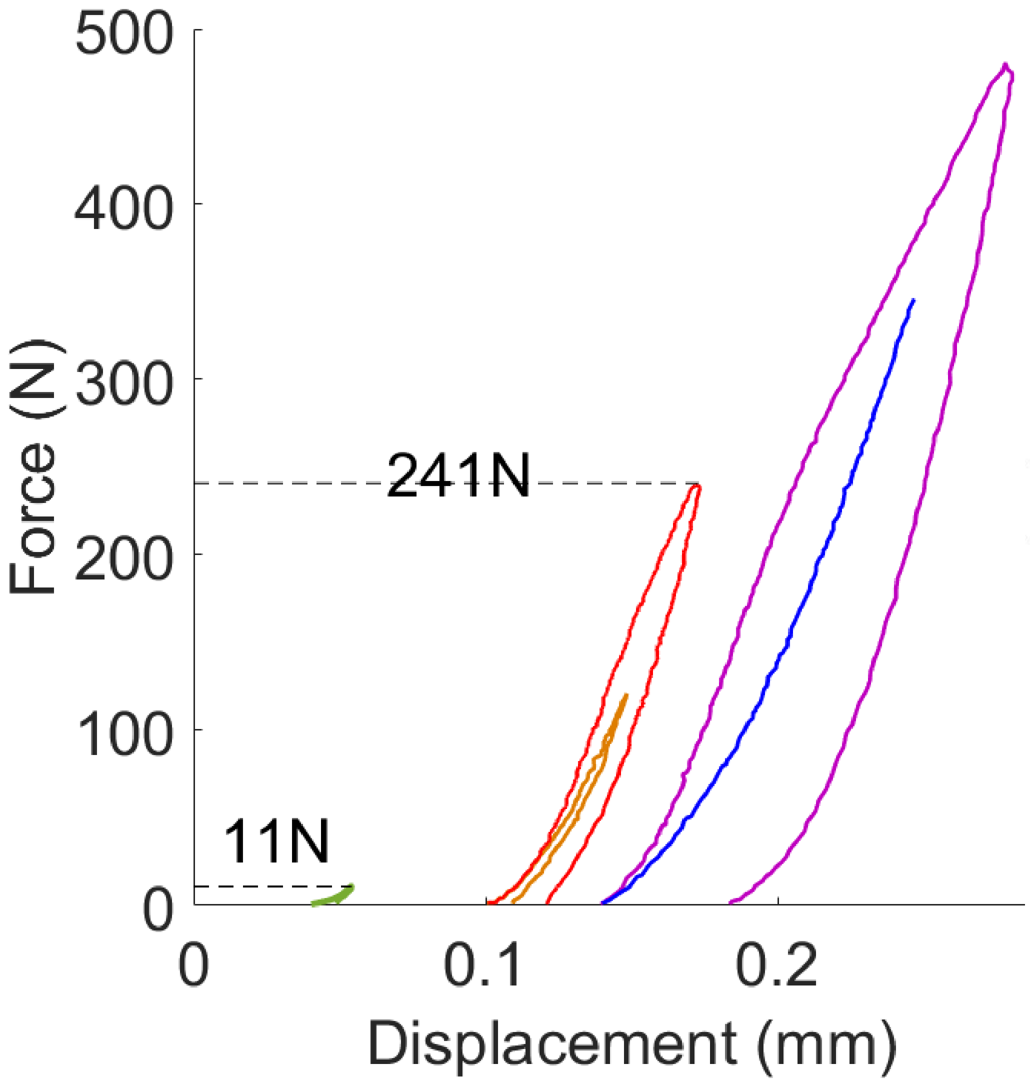

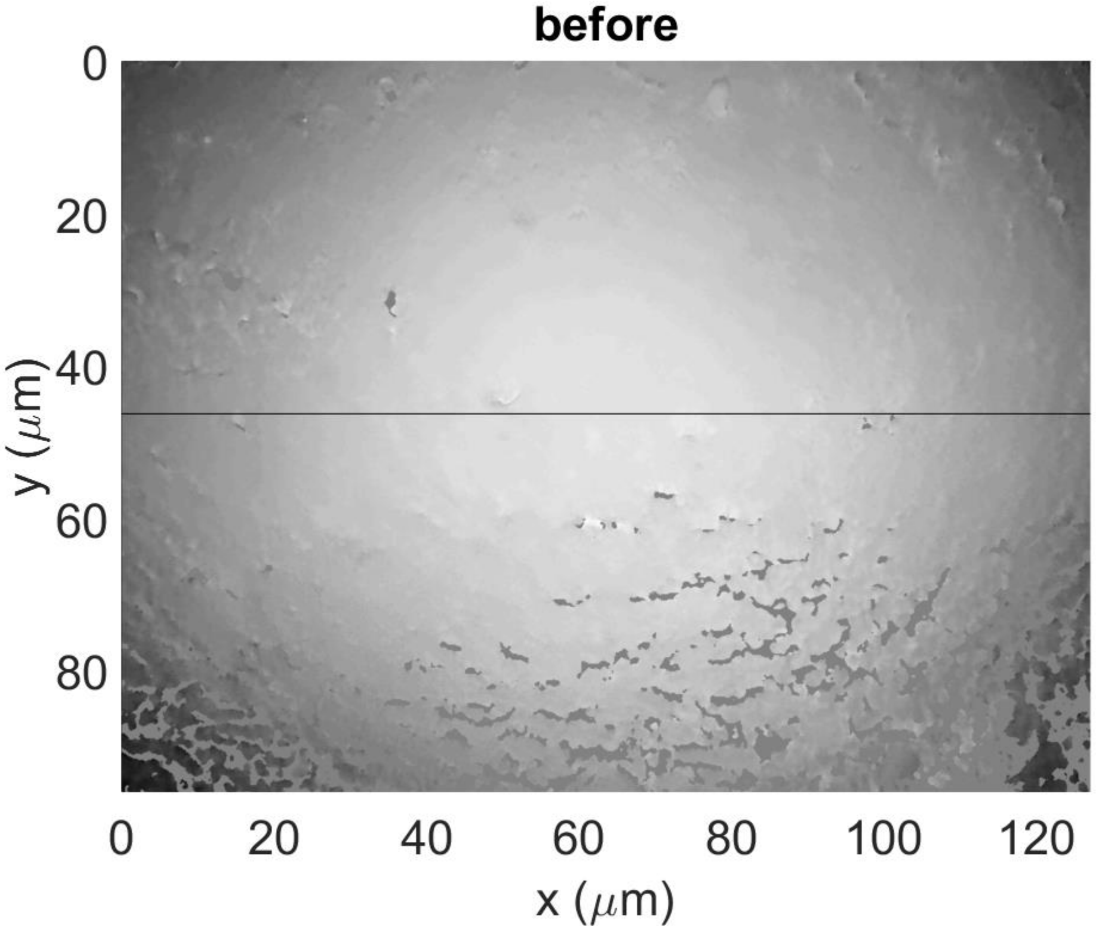

Cavarretta et al. (2016)

Rough surface effects

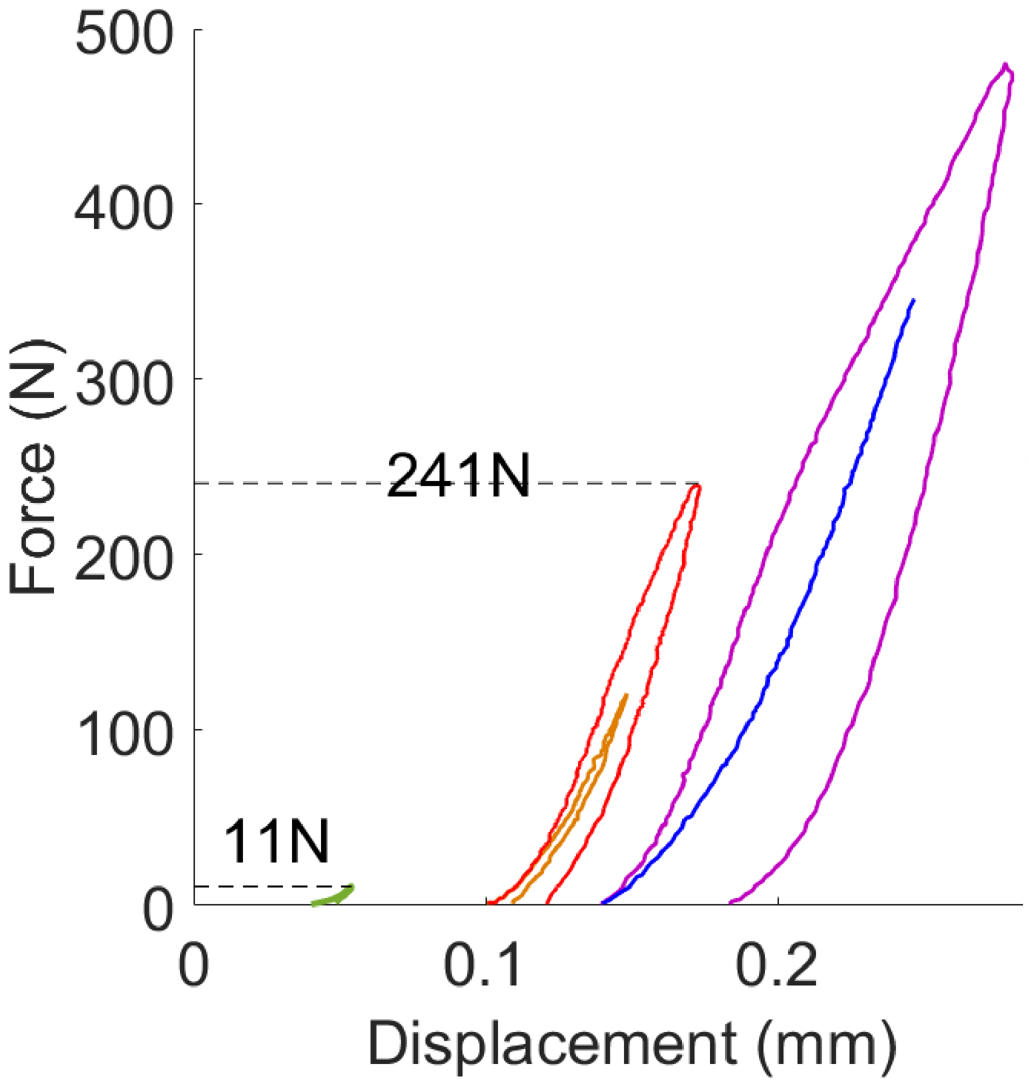

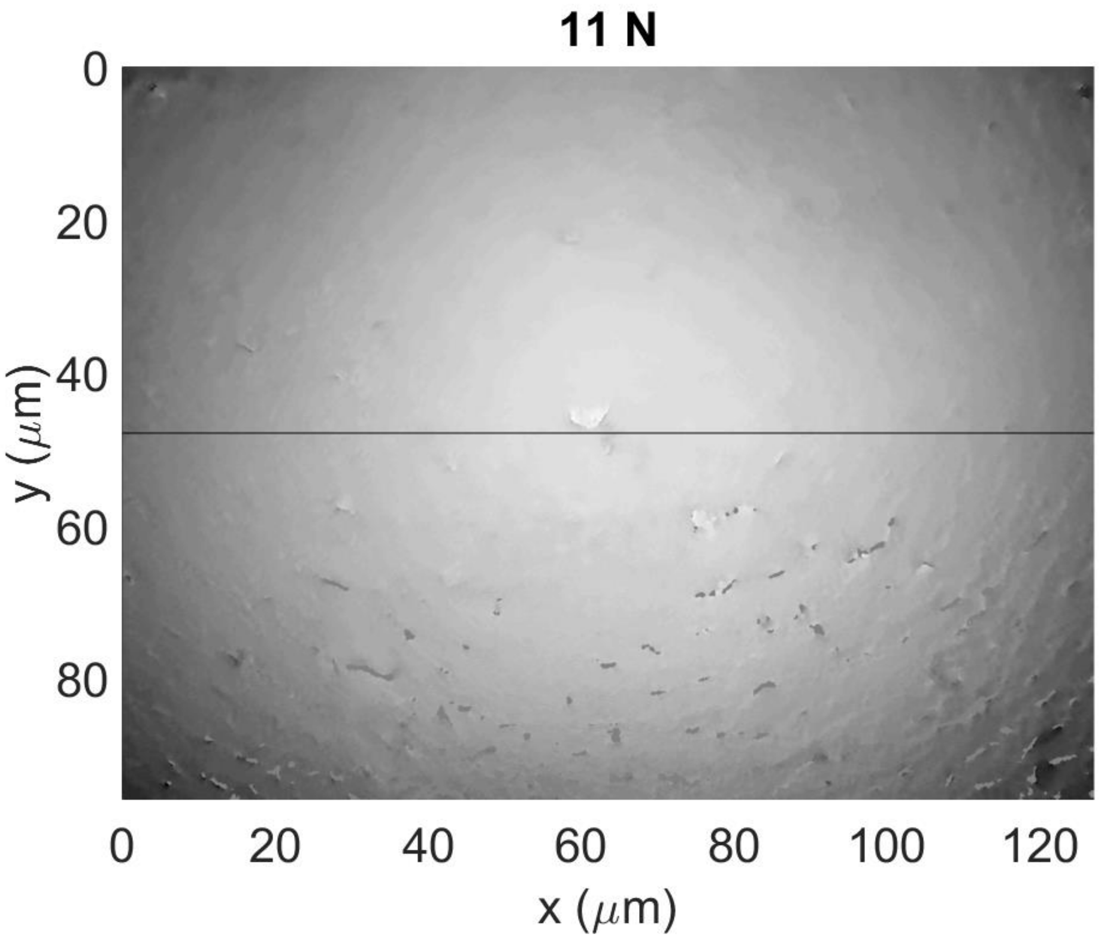

Cavarretta et al. (2016)

Rough surface effects

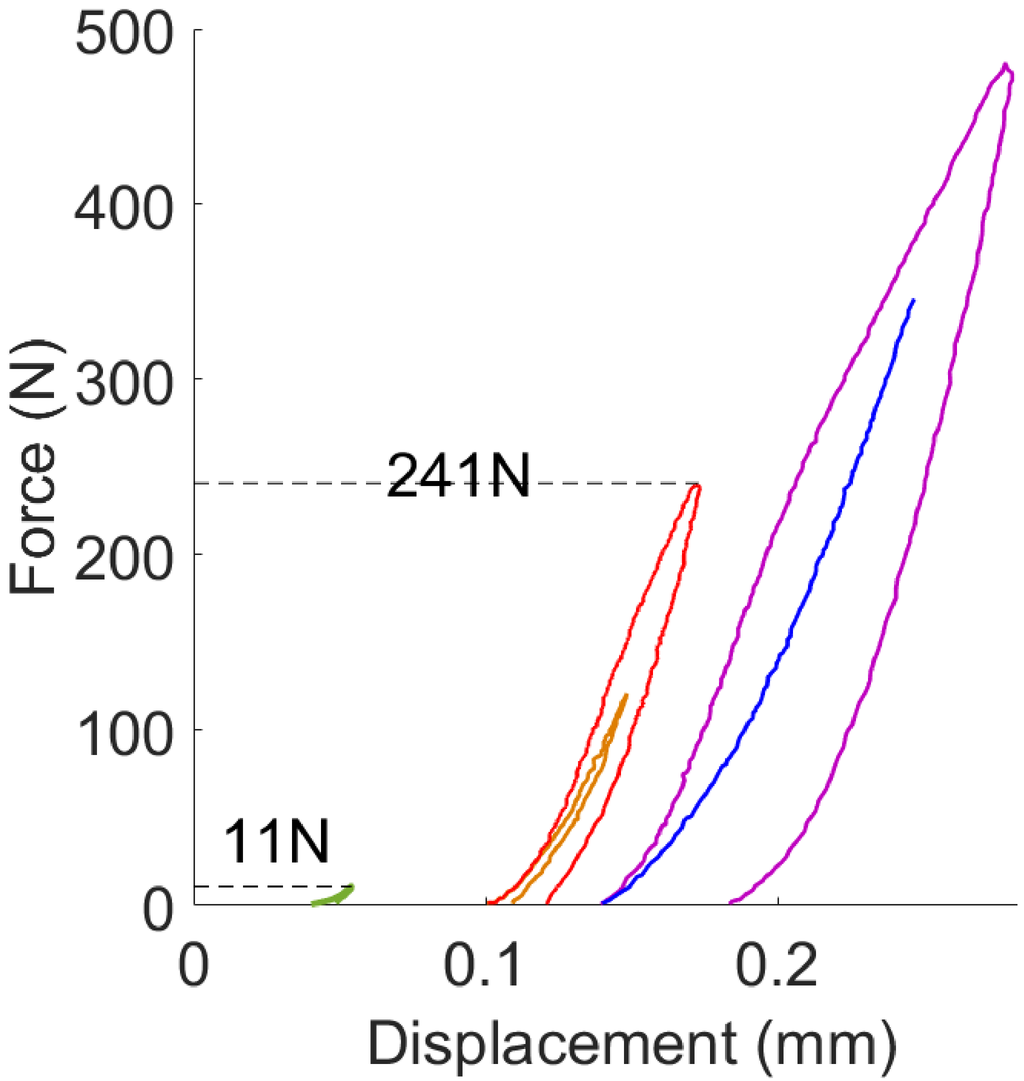

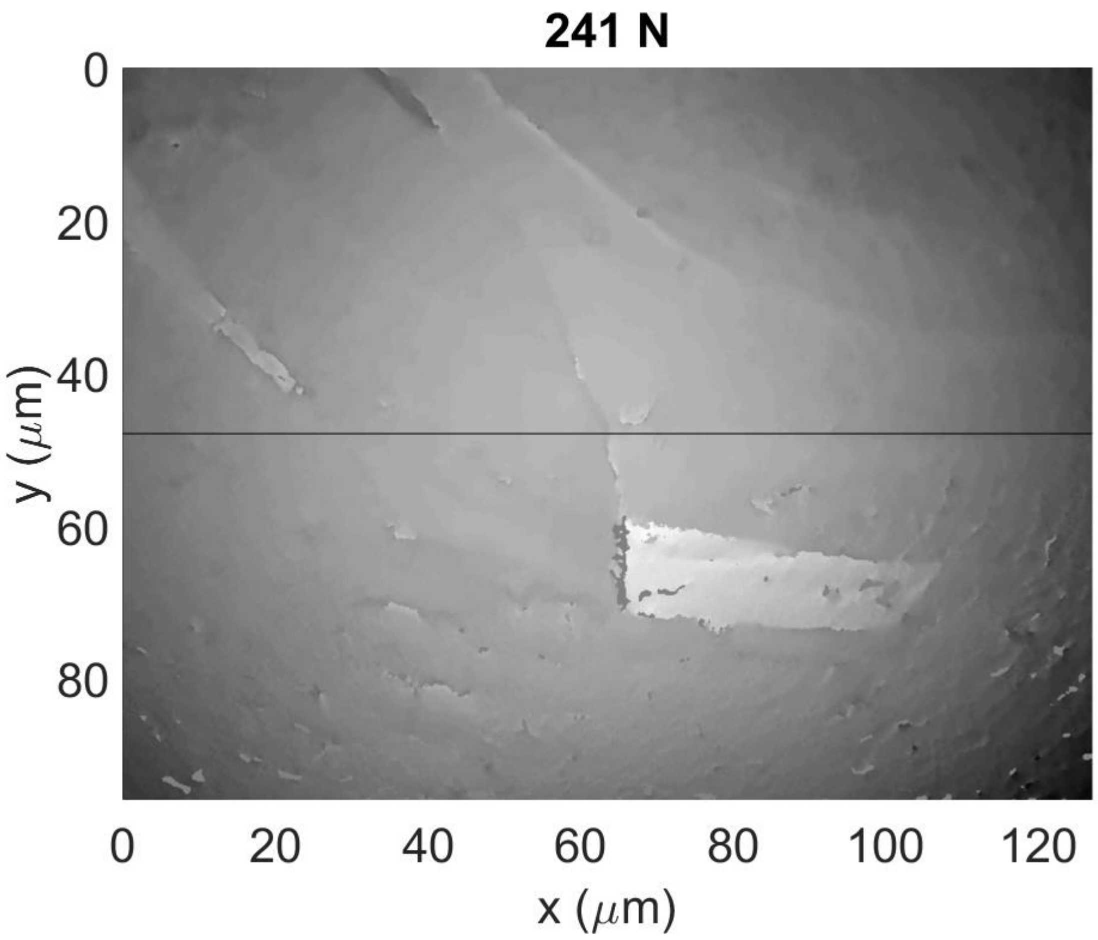

Cavarretta et al. (2016)

Rough surface effects

Rough surface model

N_{T1} and N_{T2} depend on S_q

S_q=root mean square of surface roughness

Smooth case S_q=0.0

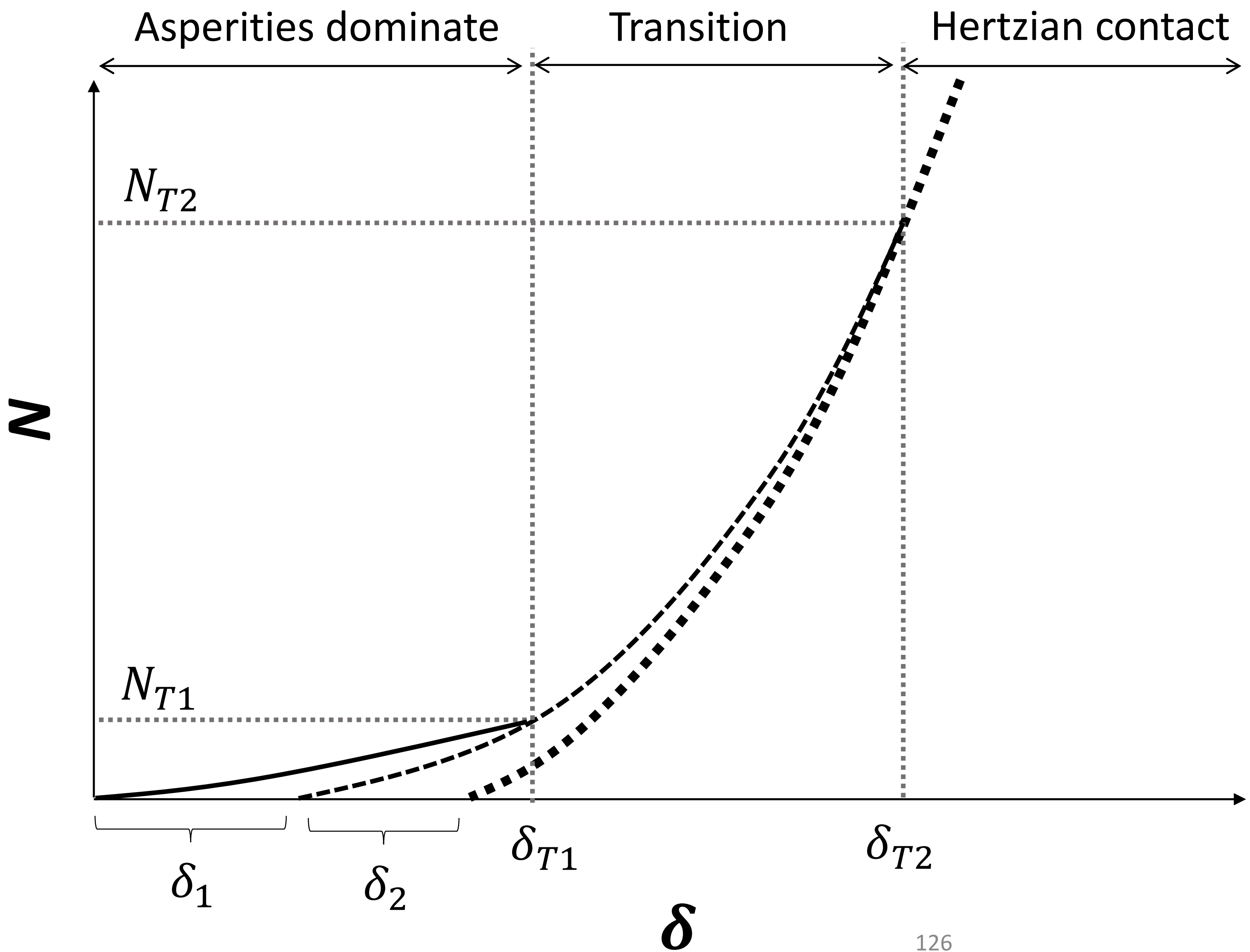

Otsubo et al. (2016)

Rough surface effects

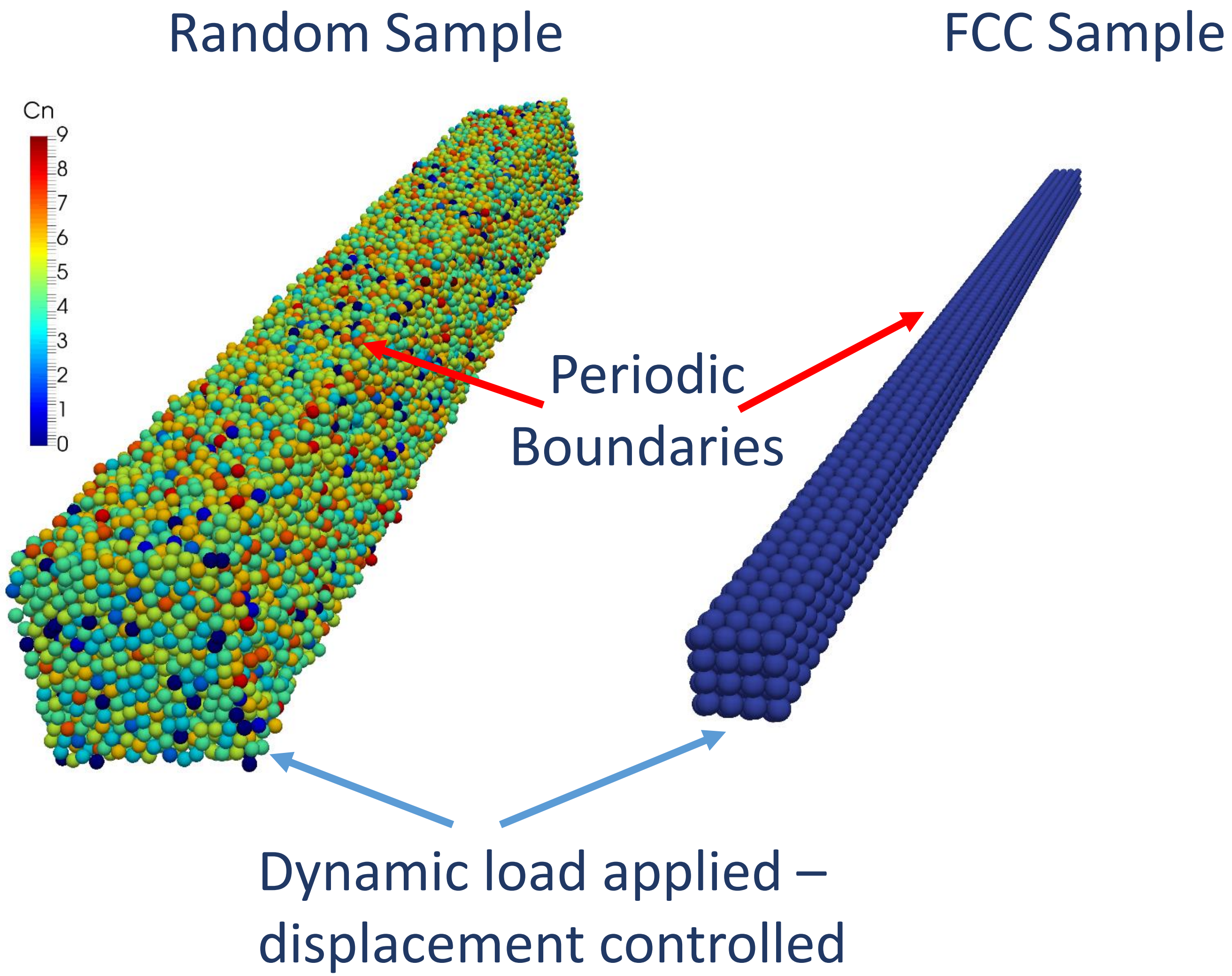

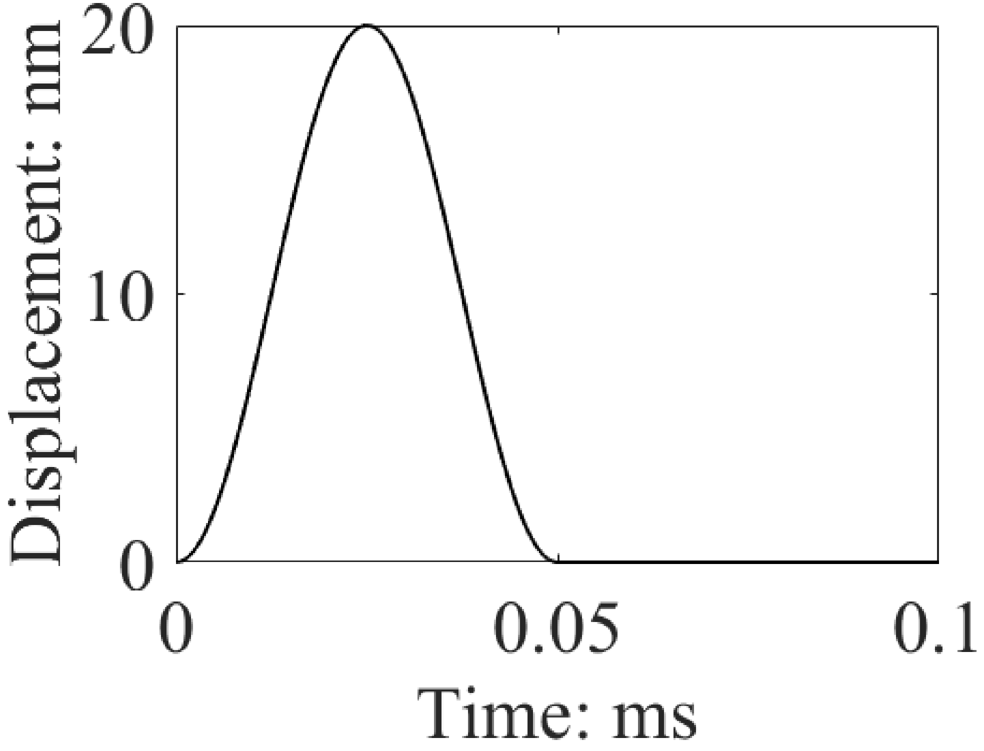

Otsubo et al. (2016)

Rough surface effects

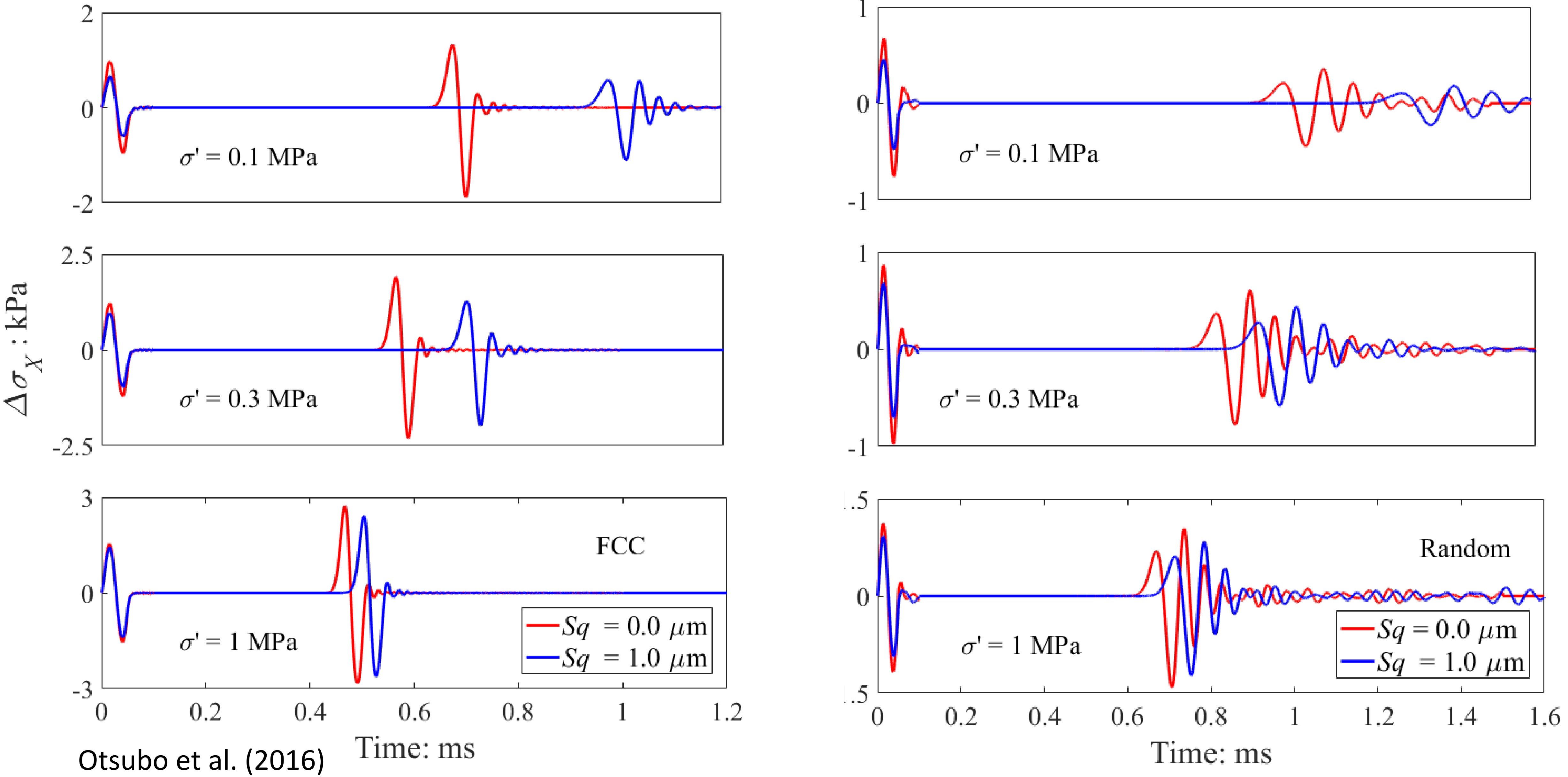

Otsubo et al. (2016)

Rough surface effects

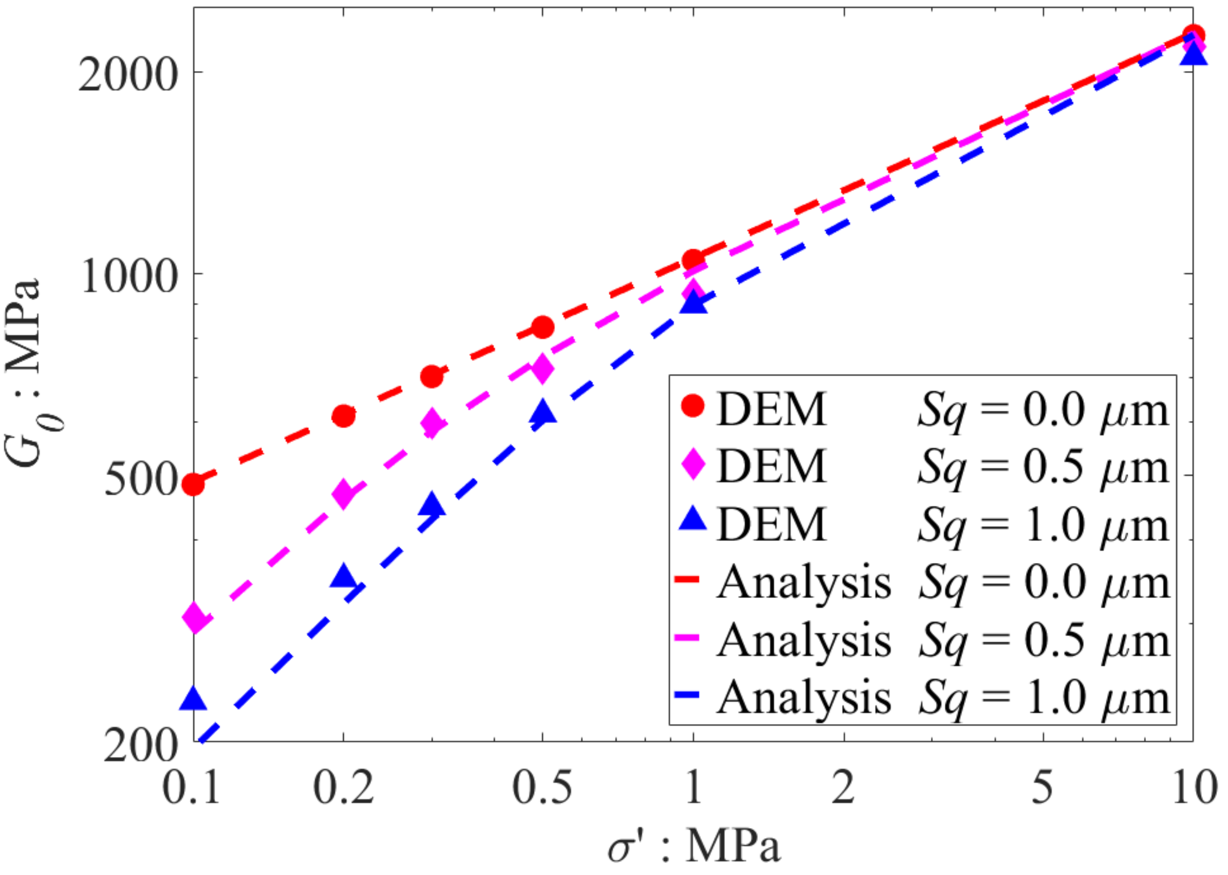

FCC Sample

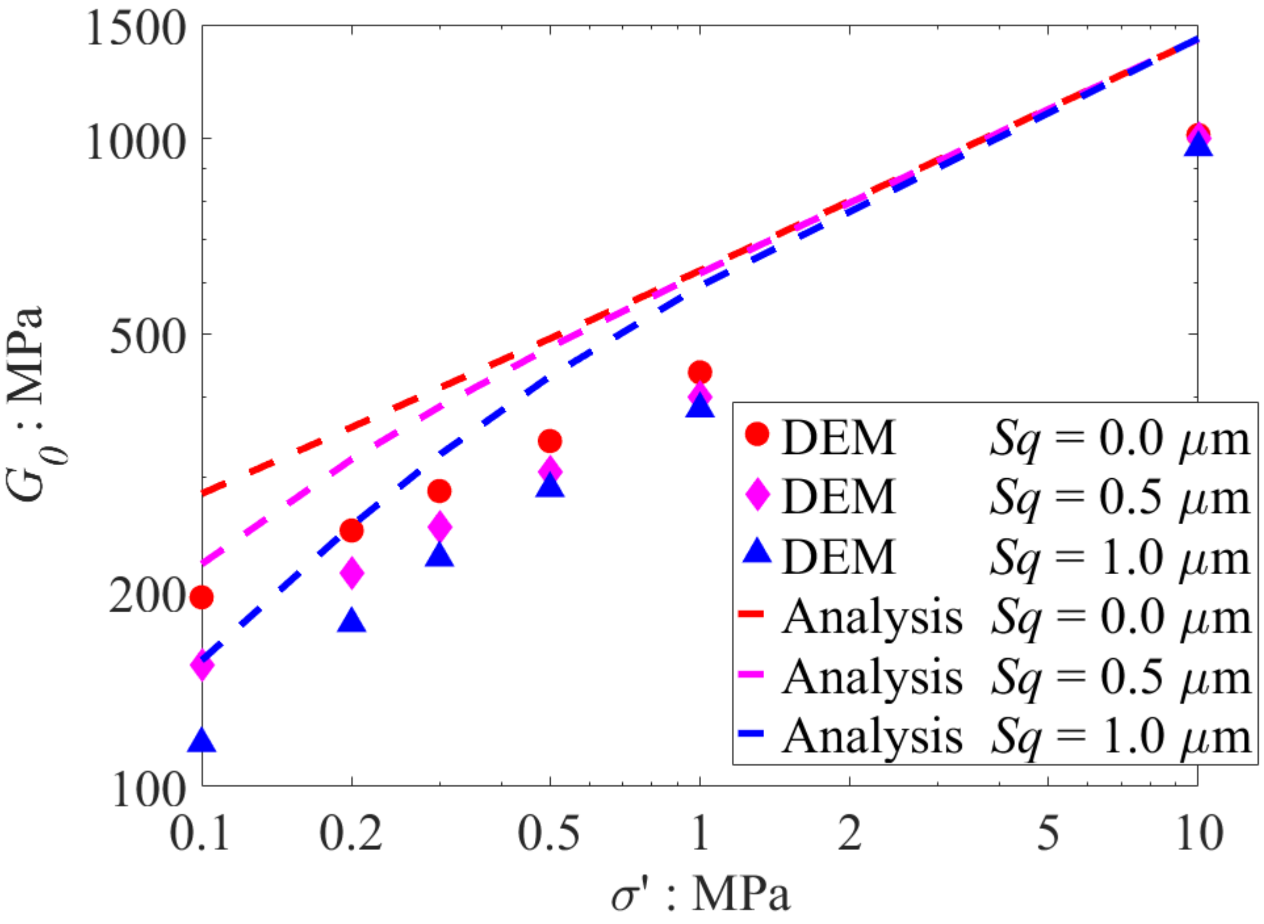

Random Sample

Otsubo et al. (2016)

Conclusions

- Hertz-Mindlin contact model ideal – even for glass ballotini

- Surface roughness - measurable effect on stiffness

- Partial slip – more subtle effect, less significant for regular, lattice packings

Running the simulation

Ensuring quasi-static behaviour

Simple approach – check force balance

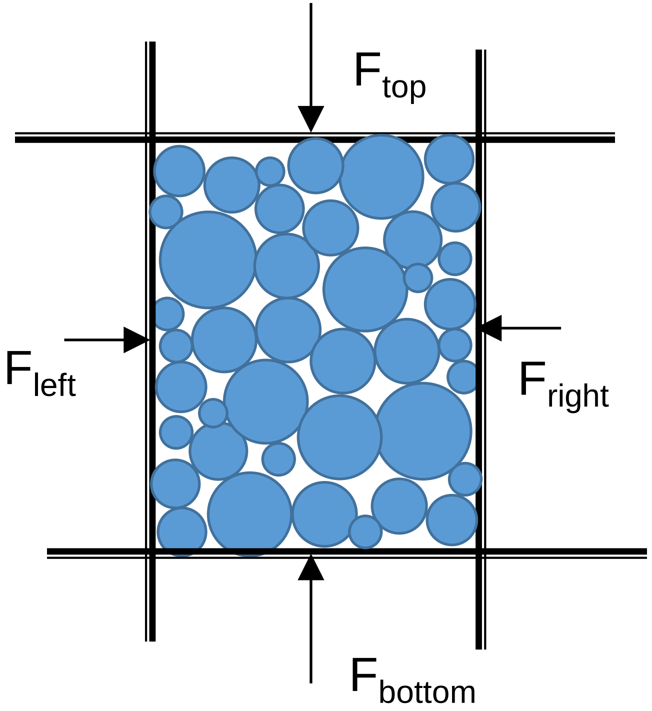

$$\frac{F_{top} - F_{bottom}}{0.5(F_{top} + F_{bottom})} \leq \varepsilon$$

ε = tolerance

Challenges:

How to specify tolerance?
What to do with periodic boundaries?

Intertial number / Inertia number

$$I = \dot{\varepsilon} d \sqrt{\frac{\rho}{p'}}$$

I quantifies the ratio of the inertial forces to the imposed forces

I = inertial number
$\dot{\varepsilon}$ = strain rate
d = mean particle size
ρ = particle density
p' = mean effective stress

da Cruz et al. (2005)

Intertial number / Inertia number

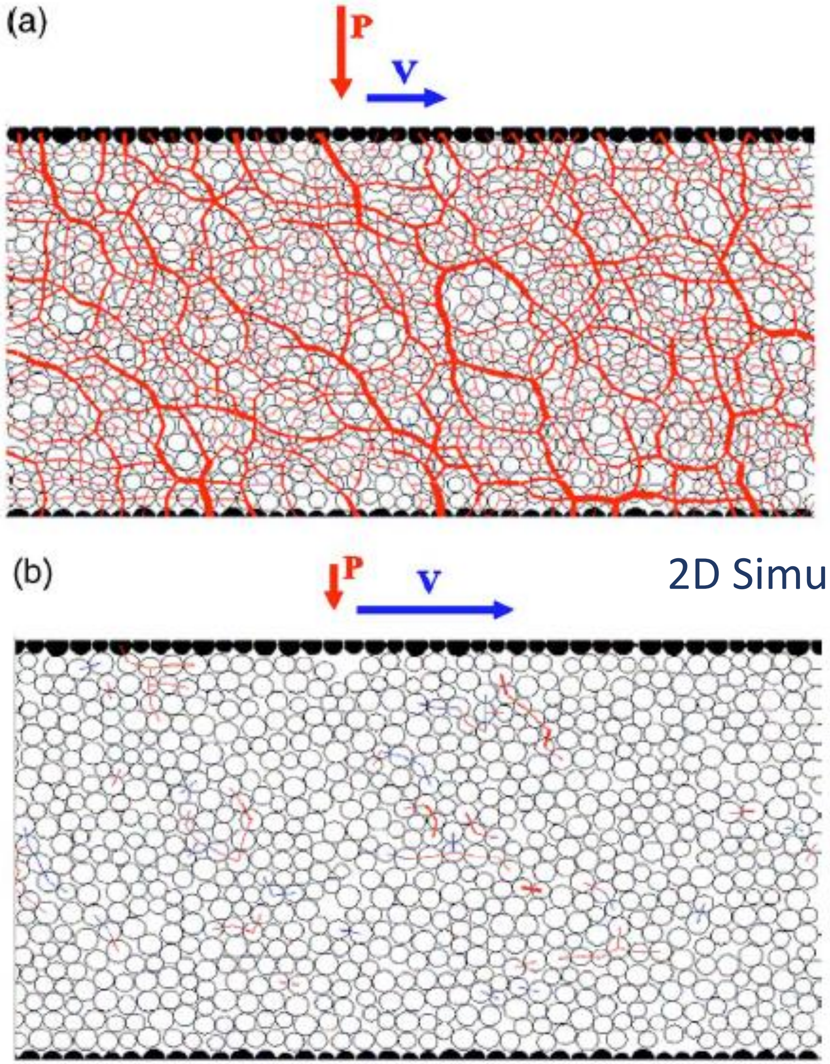

2D Simulations

da Cruz et al. (2005)

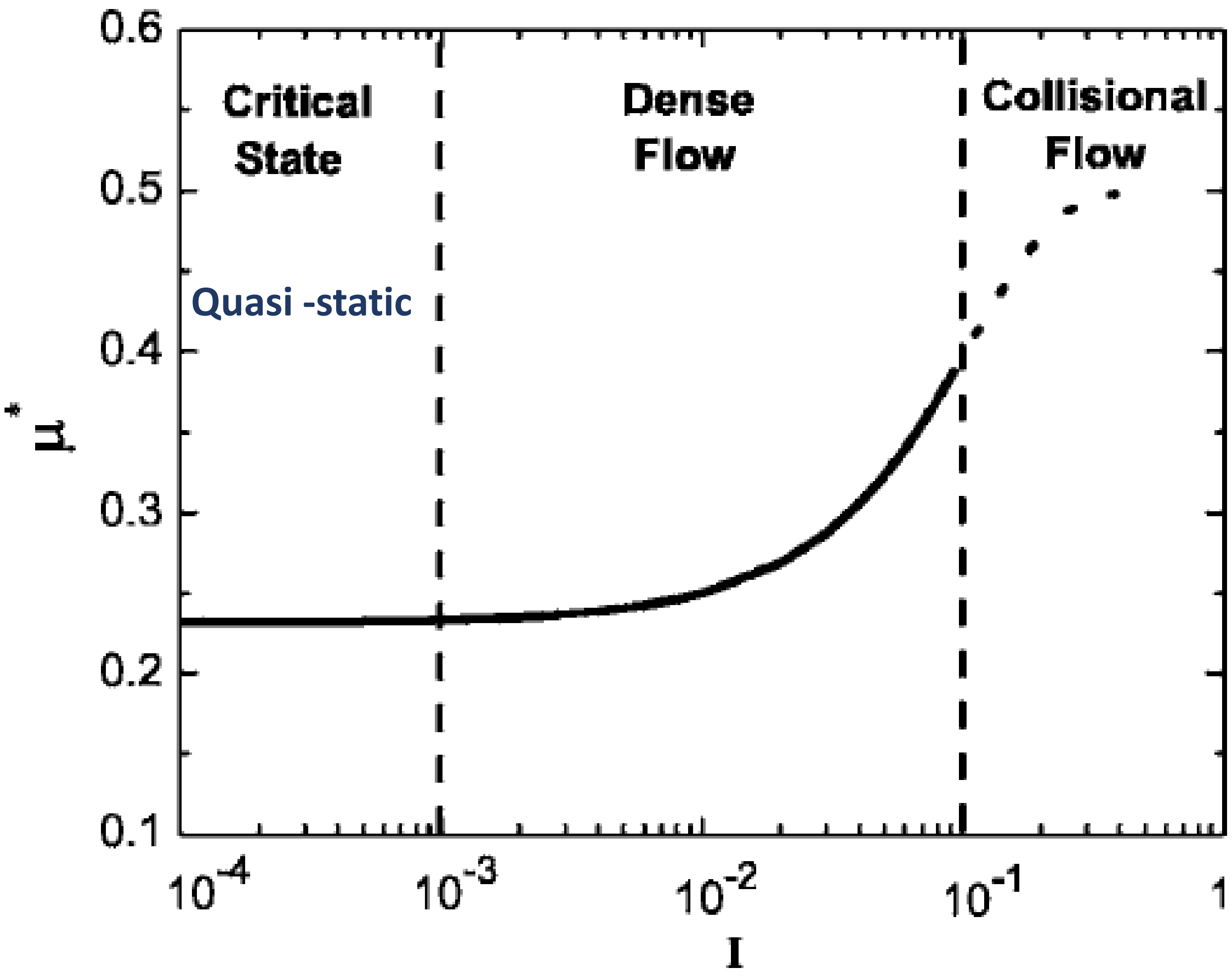

Intertial number / Inertia number

Two key questions

- Can we extrapolate DaCruz findings directly to 3D?
- How does I effect the critical state line?

Lopera Perez et al. (2016)

Influence of I on critical state

Simulation details:

- LAMMPS
- PSD –approximates that of Toyoura sand
- Triaxial compression
- 10,624 particles
- Simplified Hertz-Mindlin contact model (G=29GPa, ν=0.12, ρ=2650 kg/m3)
- μ=0.25

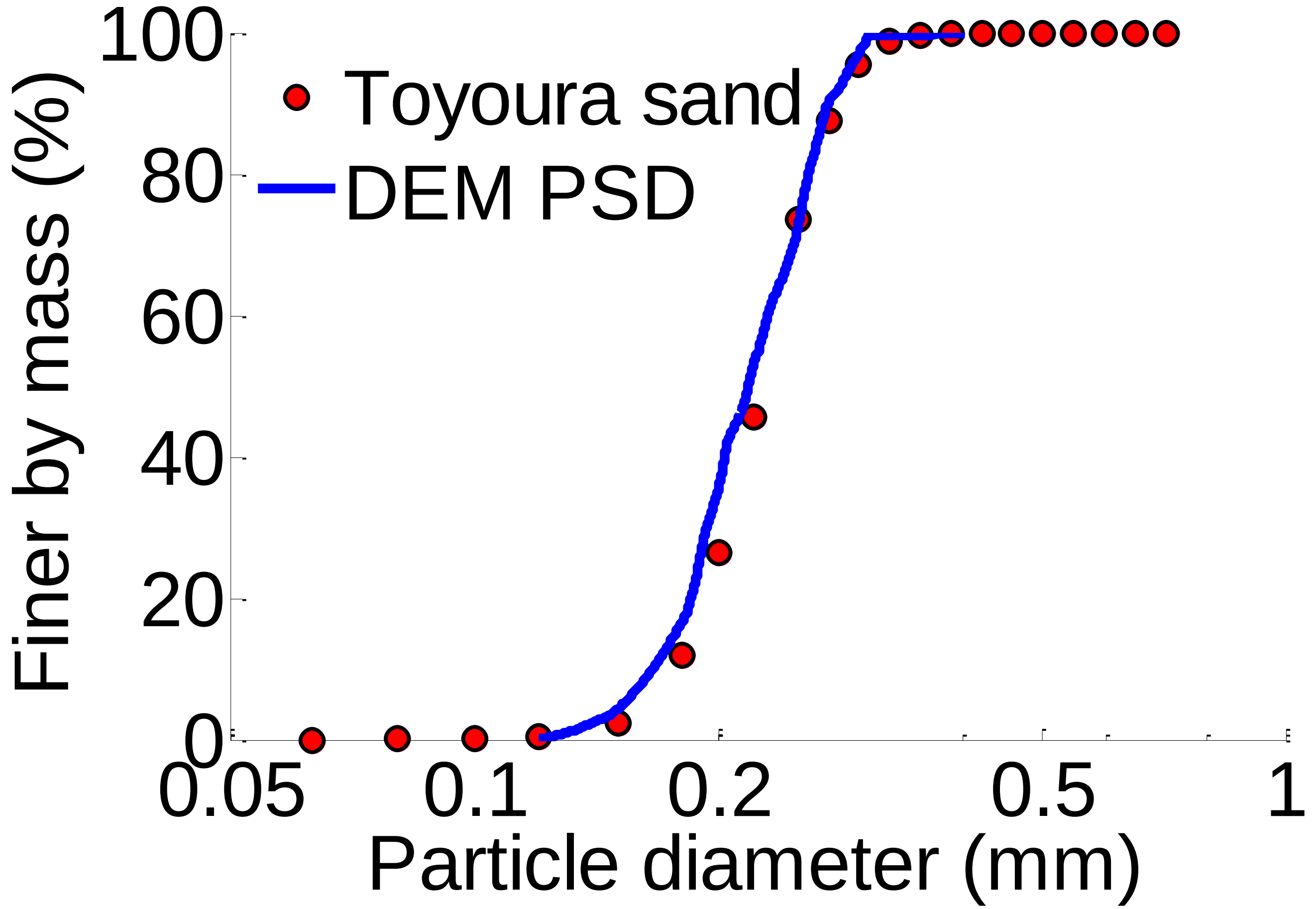

Lopera Perez et al. (2016)

Influence of *I* on critical state

Simulation details:

- Triaxial compression to large strain
- constant p' (mean effective stress)→constant *I*
- 4 confining pressures:
  100kPa ≤p'≤5000 kPa

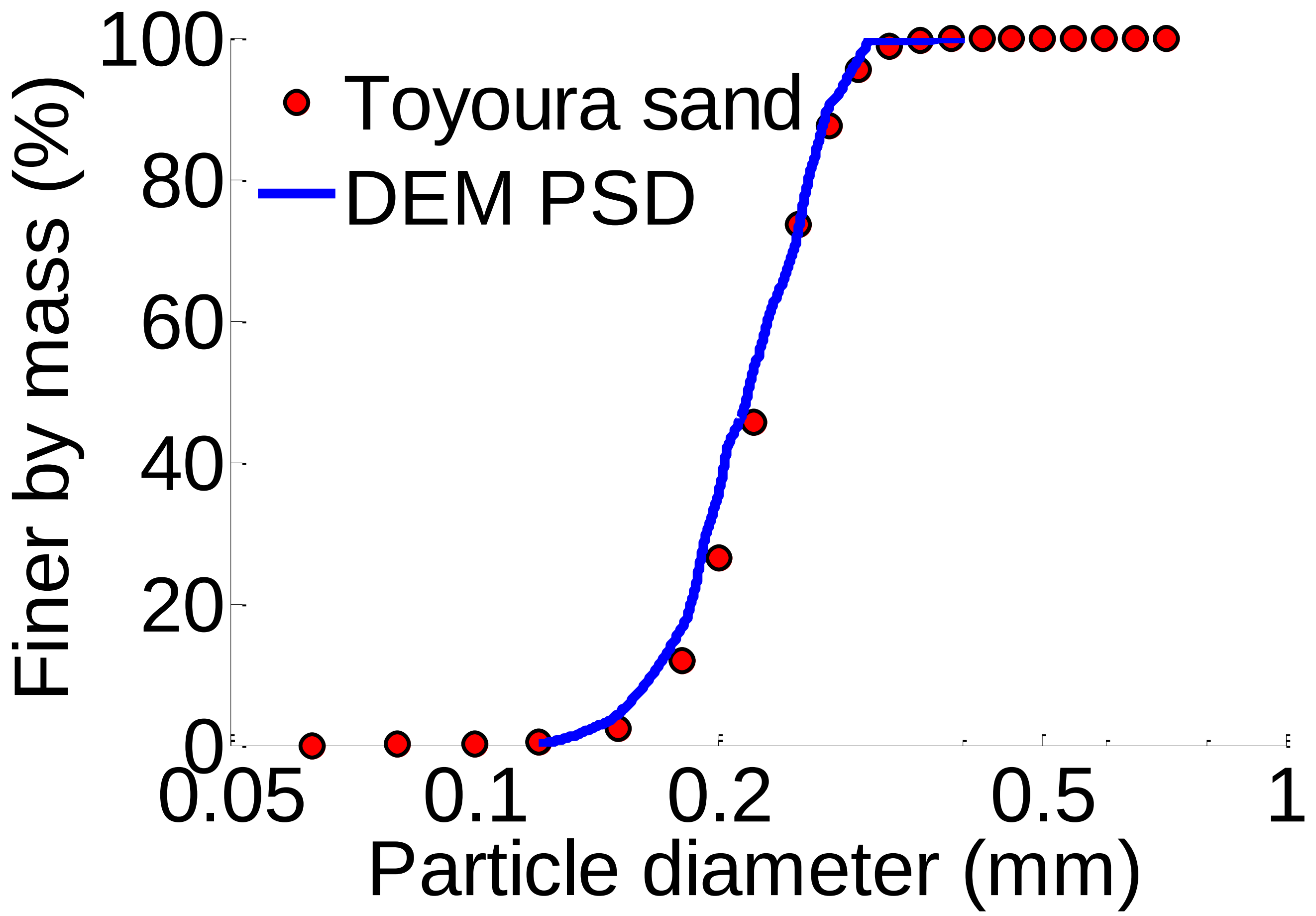

Lopera Perez et al. (2016)

Influence of *I* on critical state

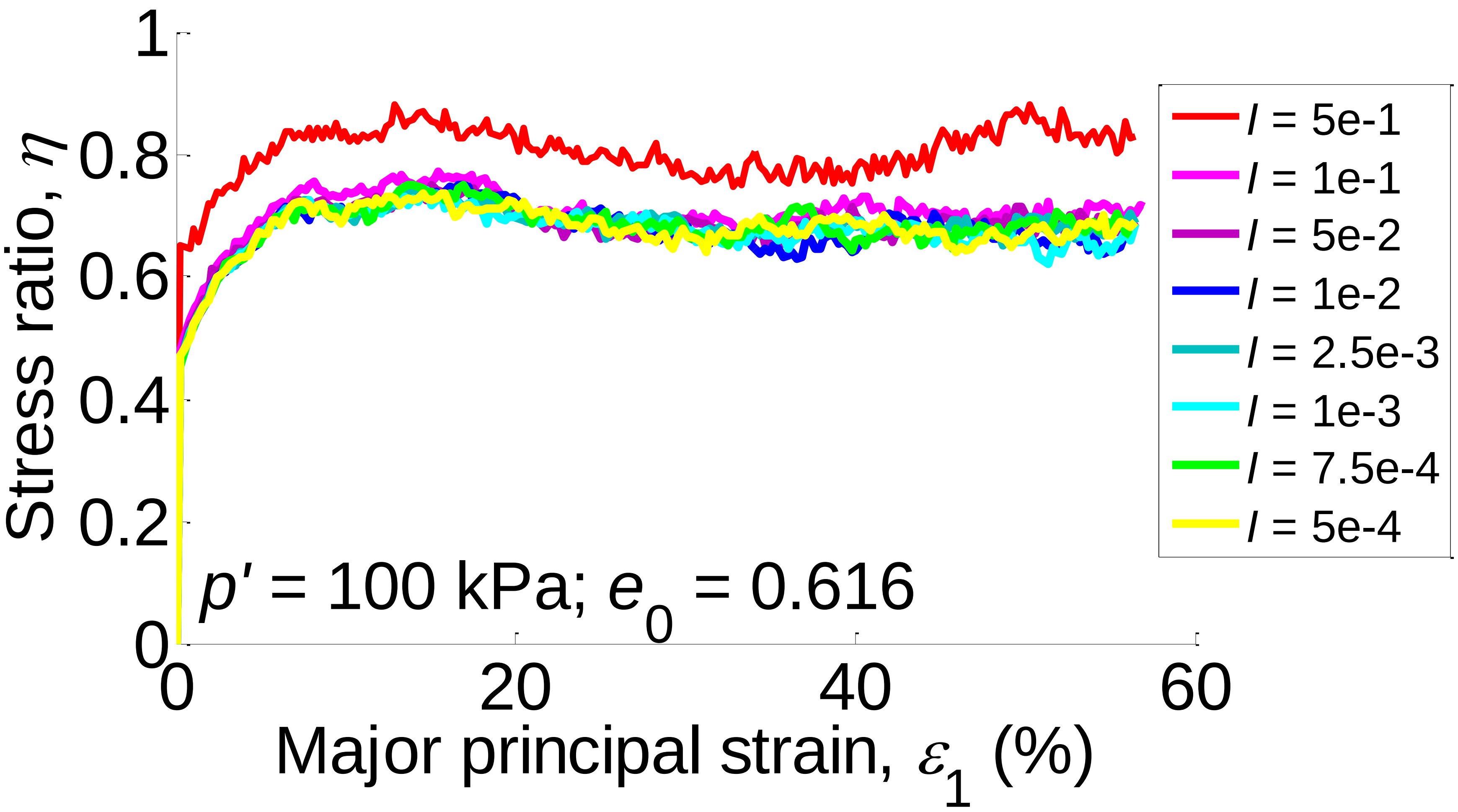

Lopera Perez et al. (2016)

Influence of *I* on critical state

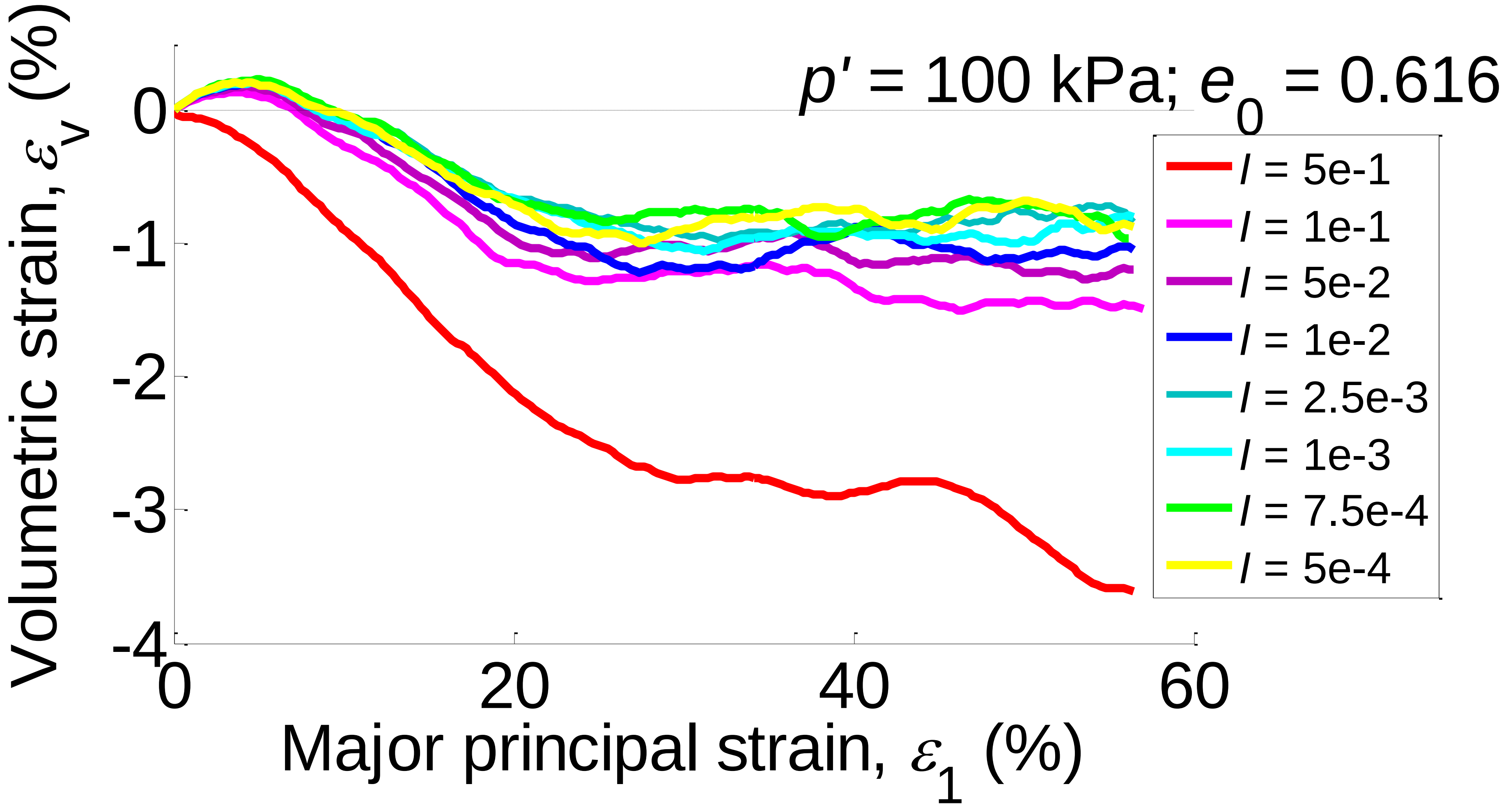

Lopera Perez et al. (2016)

Influence of I on critical state

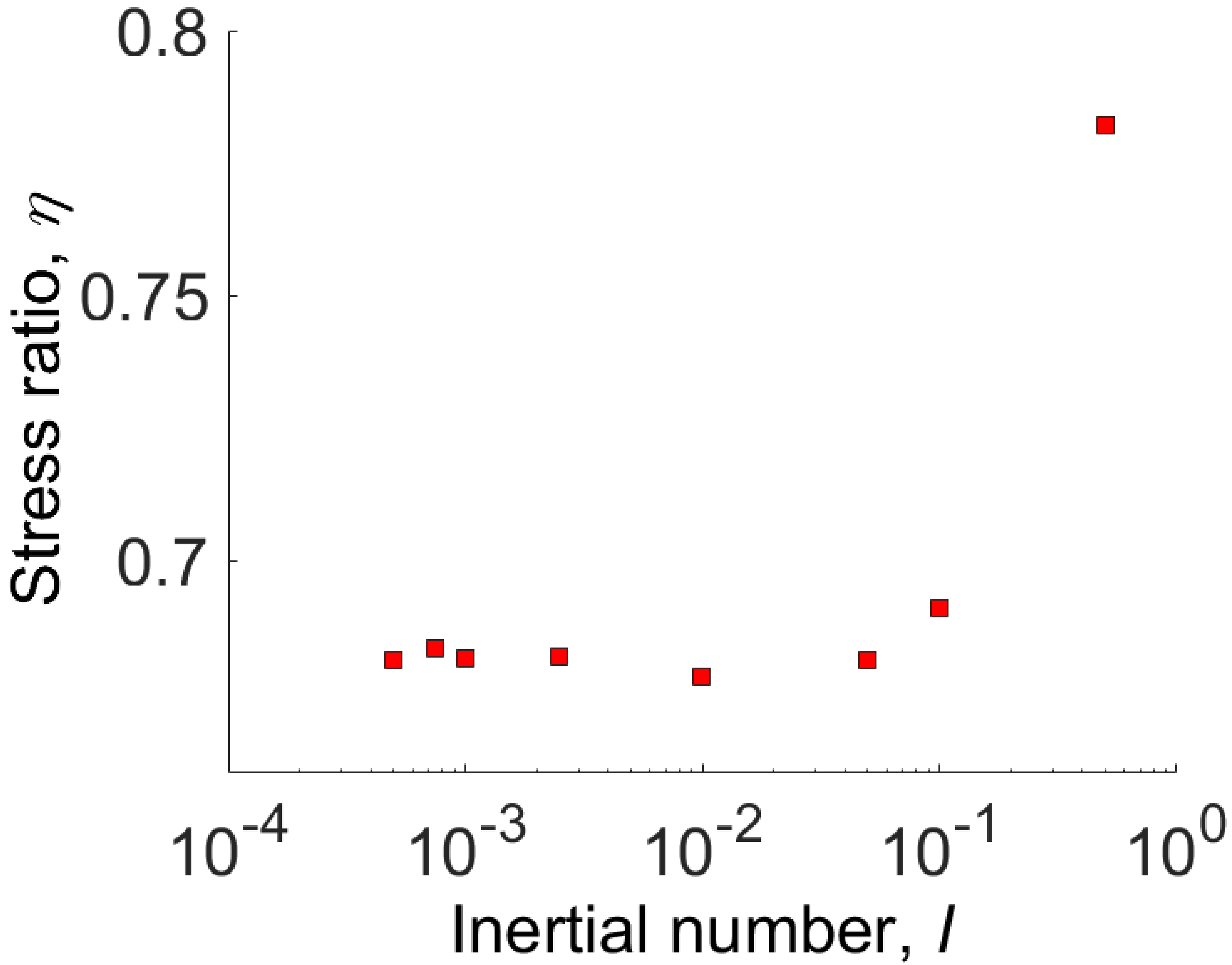

η = stress ratio at critical state = q/p'

$q = \sigma'_1 - \sigma'_3$

$p' = ⅓(\sigma'_1 + 2\sigma'_3)$

Influence of I on critical state

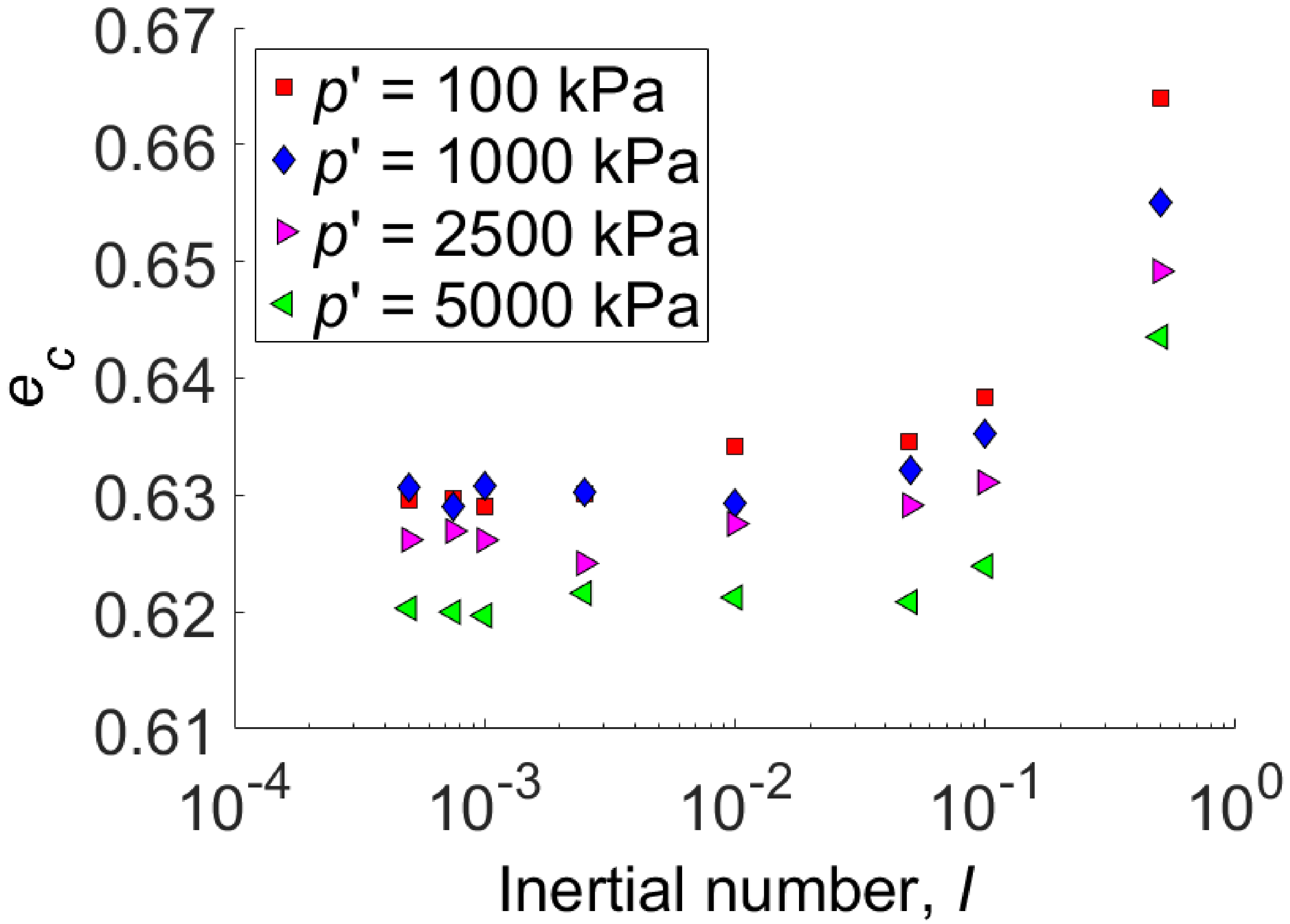

e_c = void ratio at critical state

Influence of I on critical state

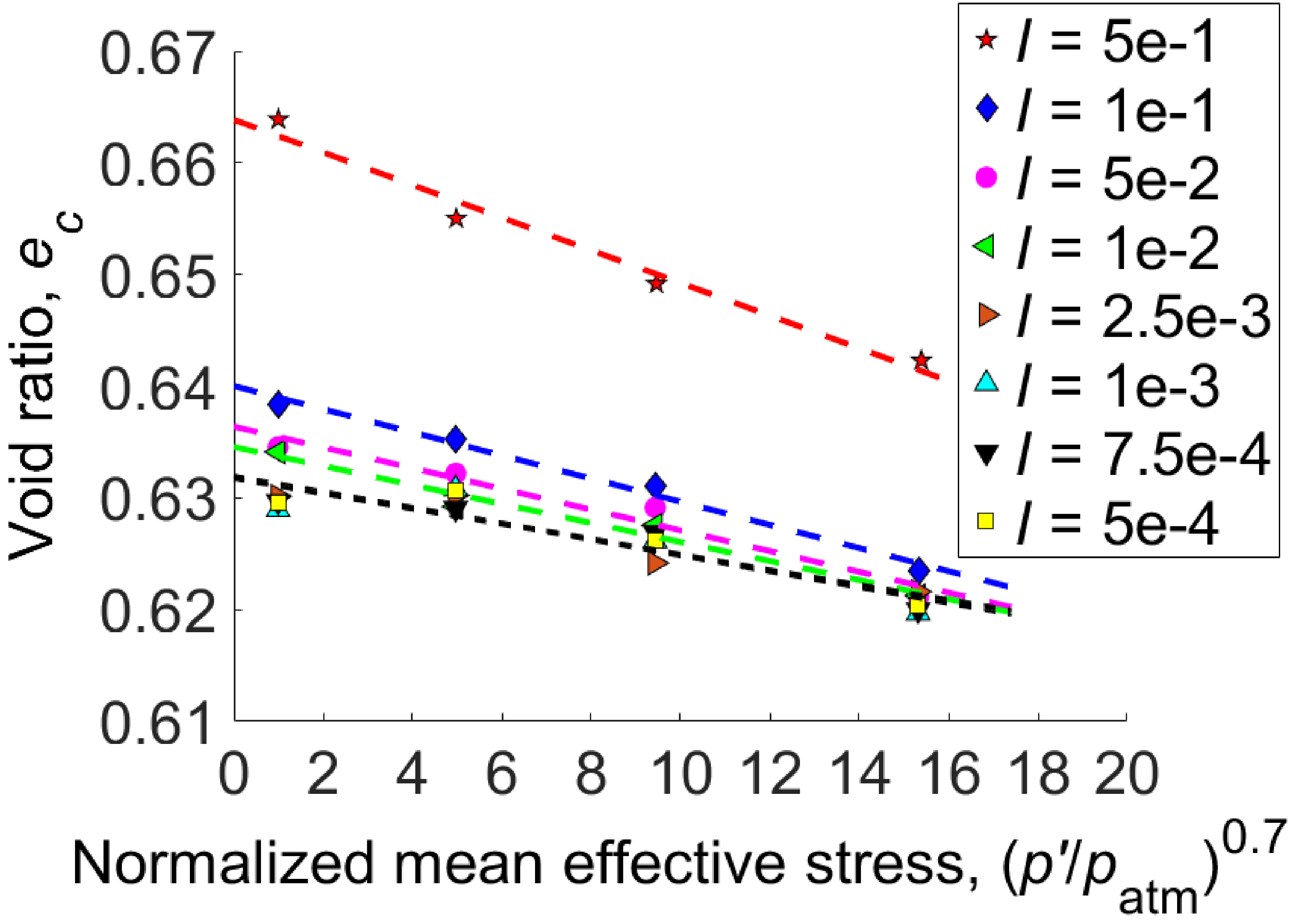

e_c = void ratio at critical state

Influence of I on critical state

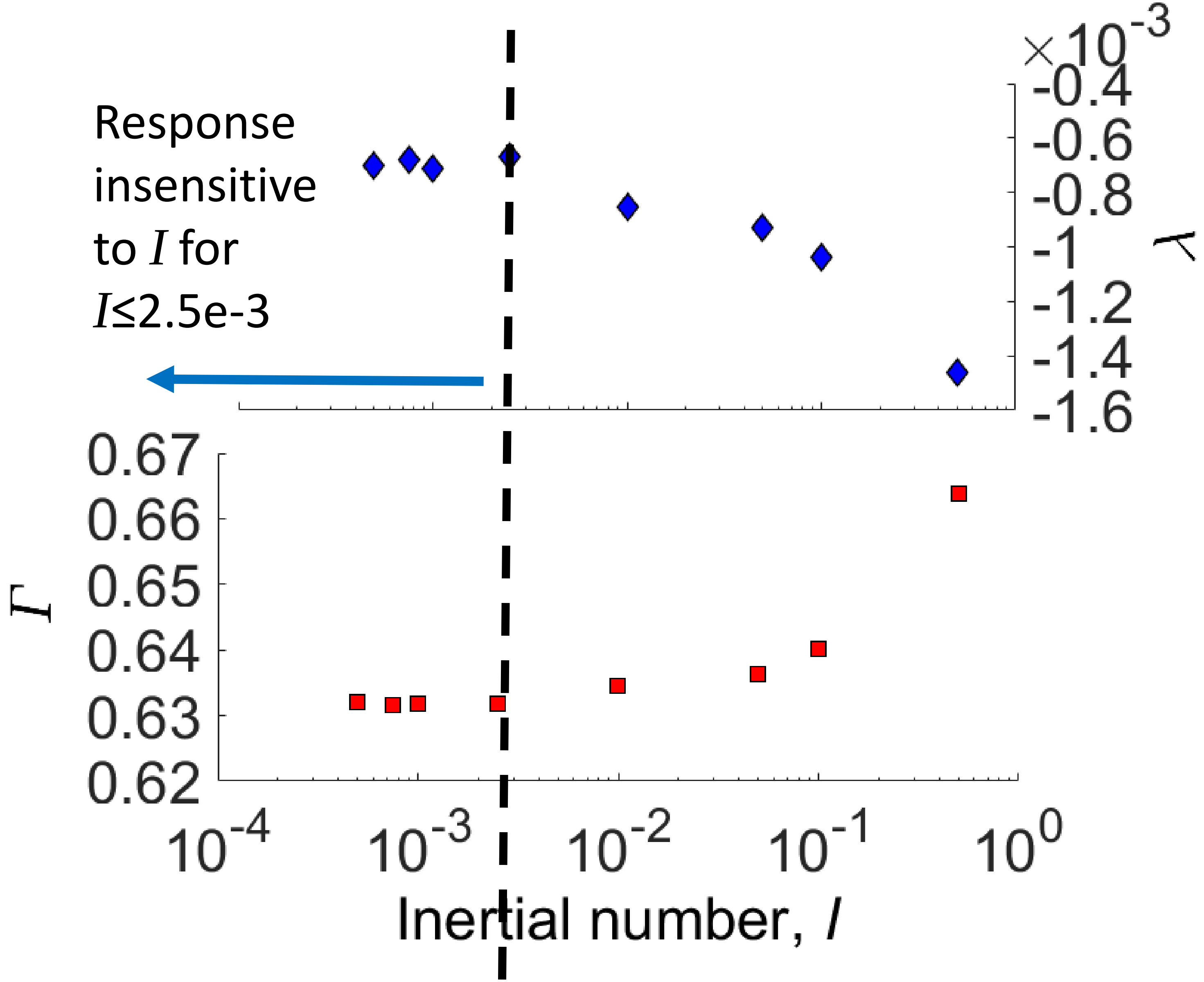

λ = slope of critical state line in e-p' space

Γ = intercept with $(p'/p_a)^{0.7}=0$

Conclusions

- Inertia number effects position of critical state line
- For quasi-static simulations keep $I \leq 2.5e\text{-}3$

Post processing /data interpretation/checks

Direct Shear Test – Coupling Physical Tests and DEM Simulations

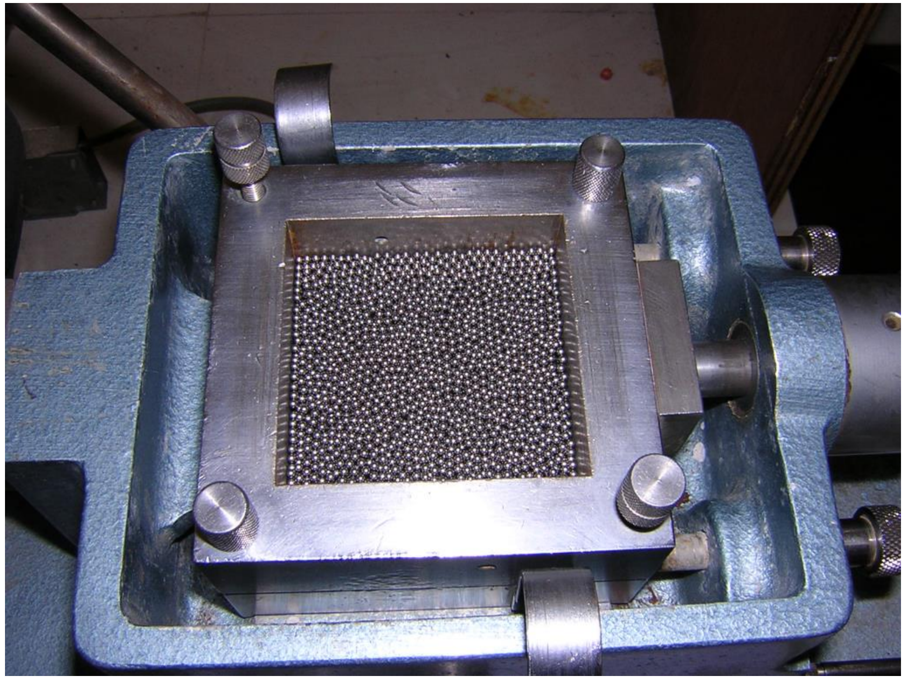

11700 Spheres

Grade 25 steel

Checks

- Over-penetration – if overlap exceeds 5% - violating small overlap assumption in DEM – discard simulation (Hanley et al., 2014)

- Quasi static? – Up until recently always checked force - now focus on inertial number (I)

- Moving towards energy tracing in simulations

- Always look at coordination number, mechanical coordination number, 2nd order fabric tensor, rose diagrams of contact orientations.

Deformed Specimen – DEM Simulation

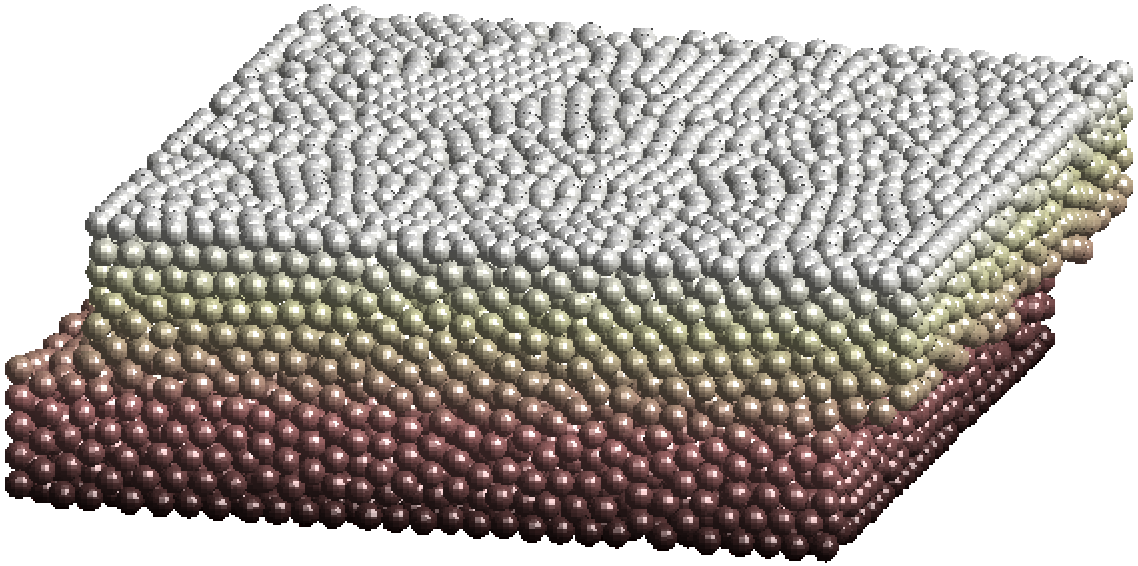

Deformed Specimen

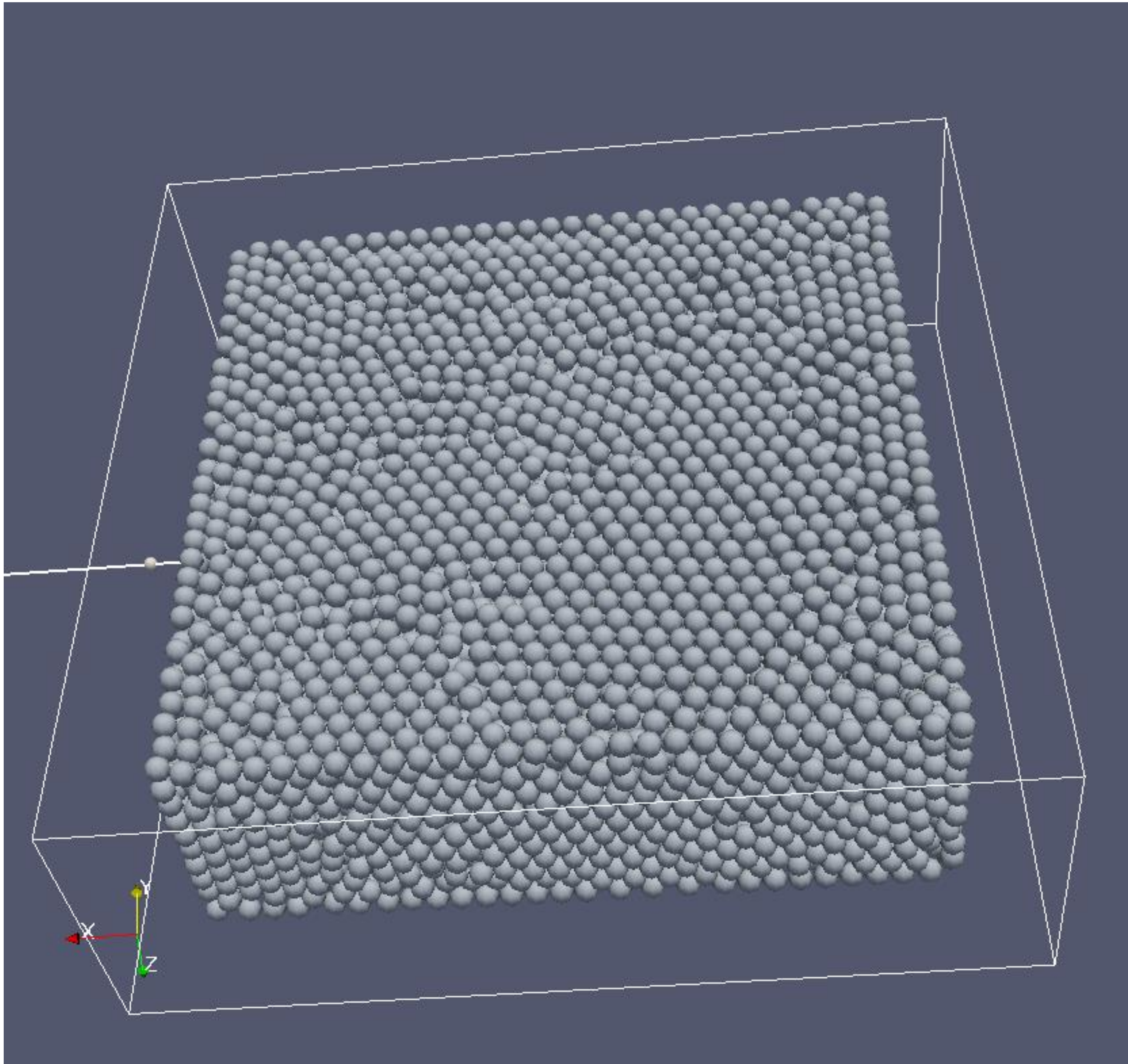

Deformed Specimen

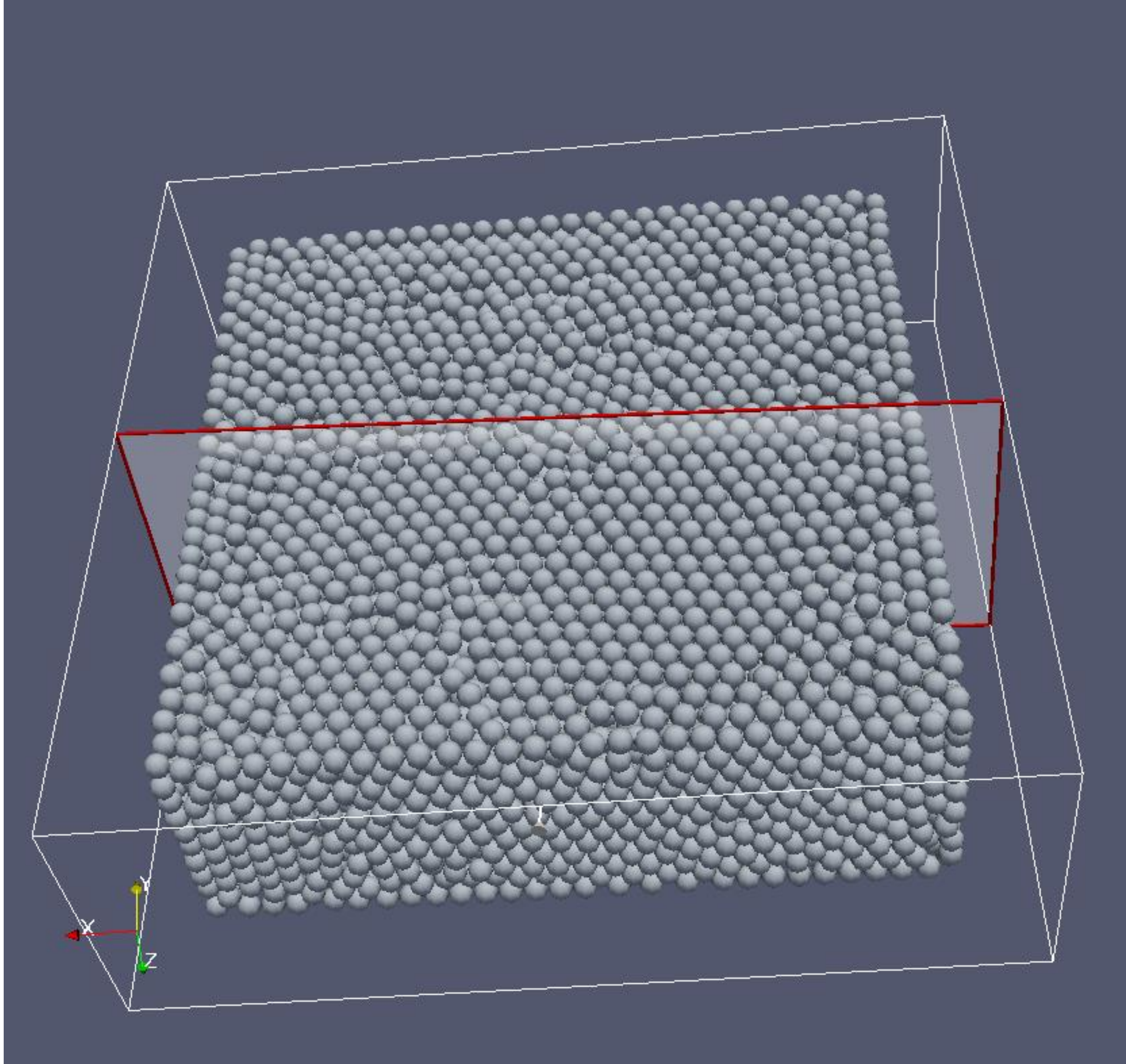

Deformed Specimen

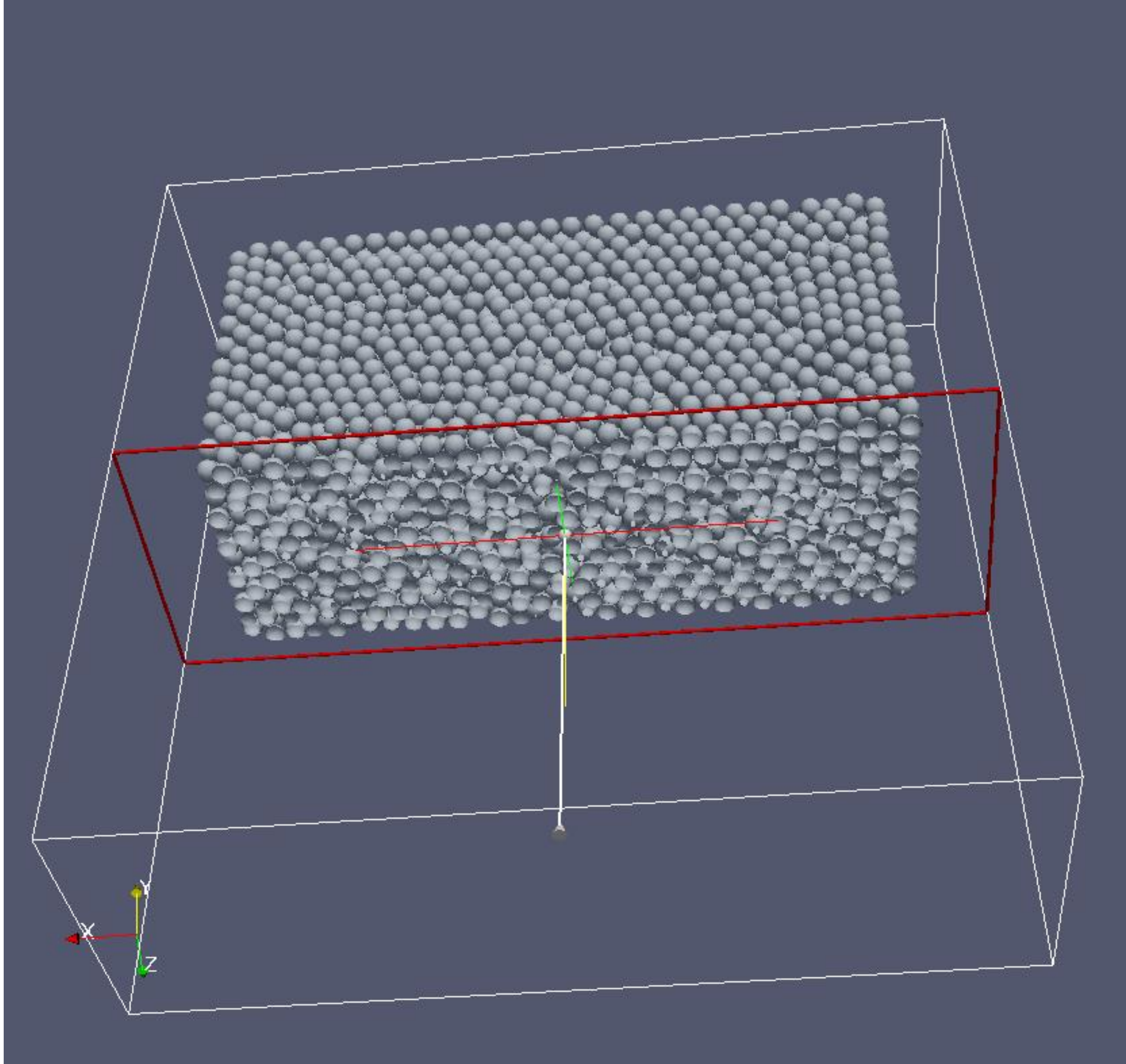

Deformed Specimen

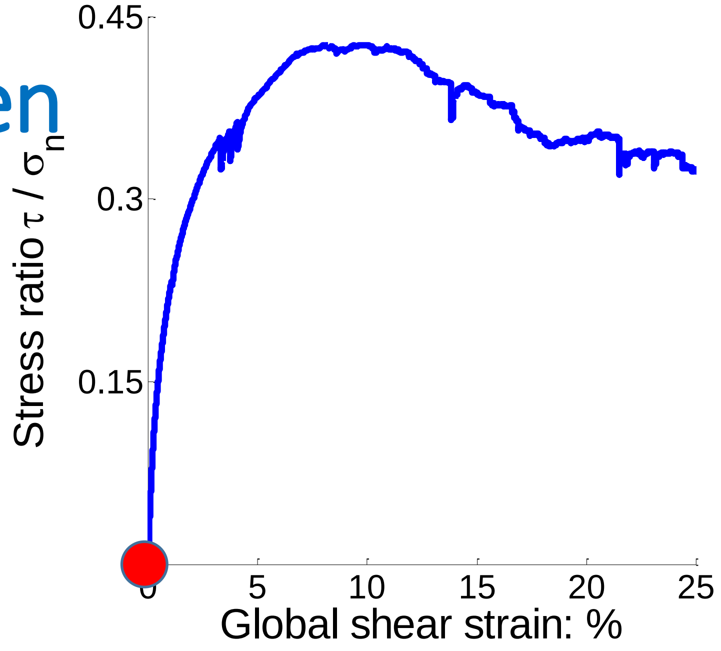

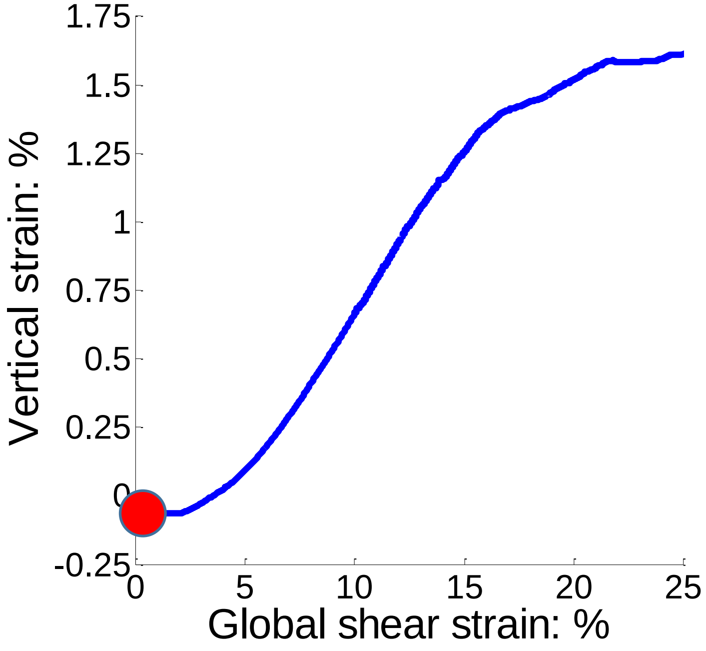

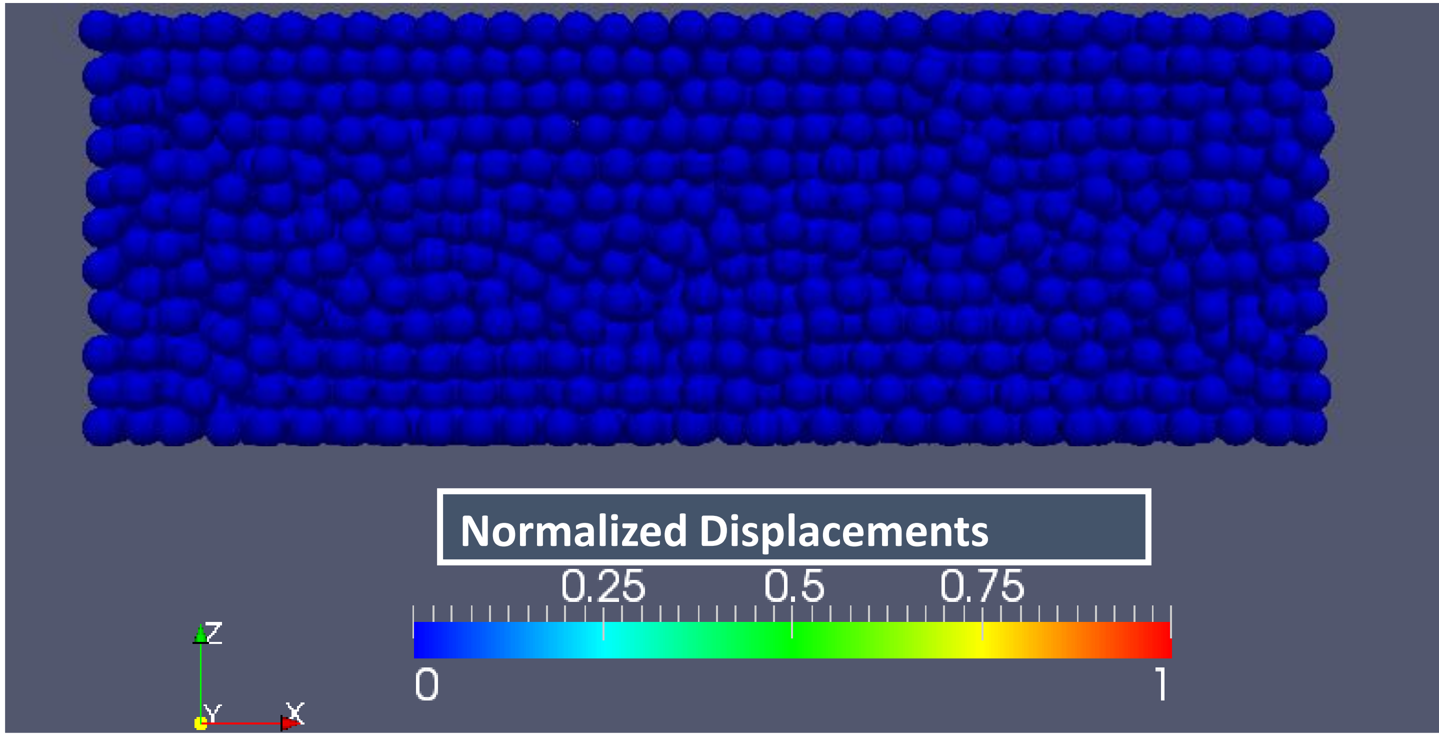

Deformed Specimen

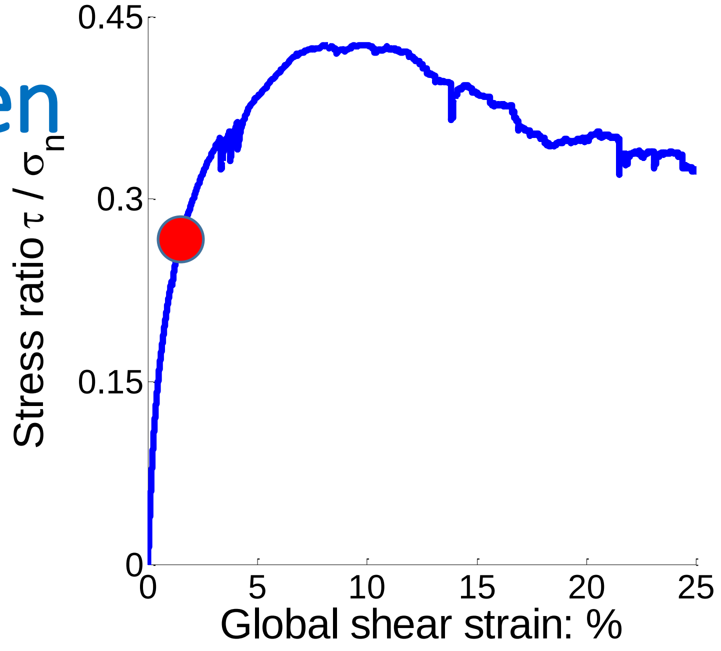

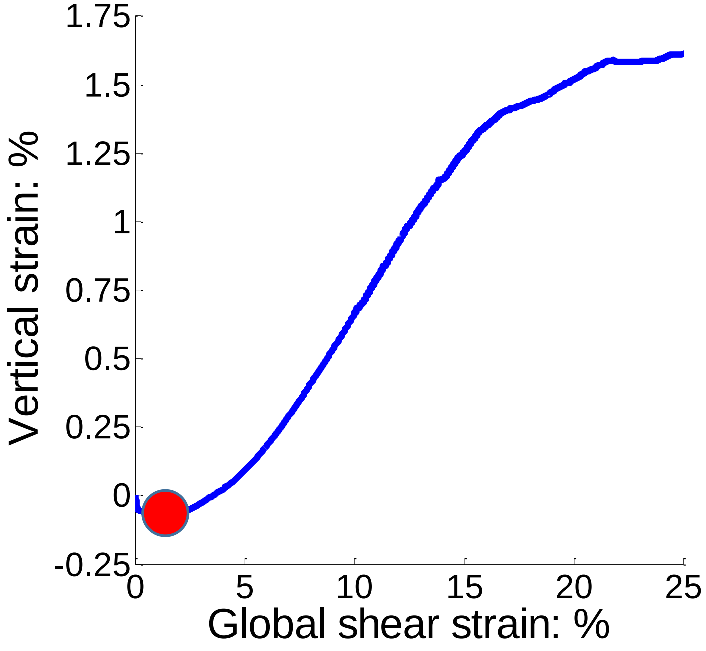

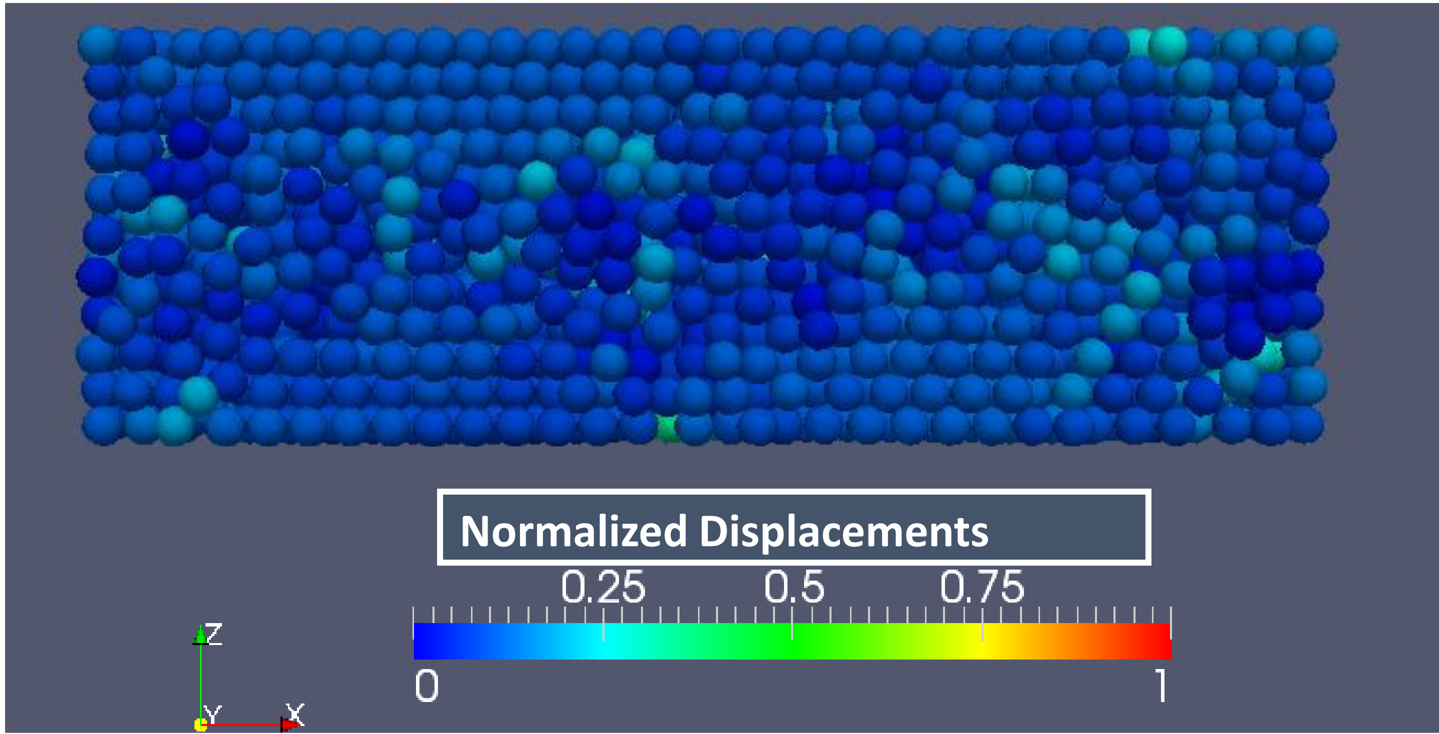

Deformed Specimen

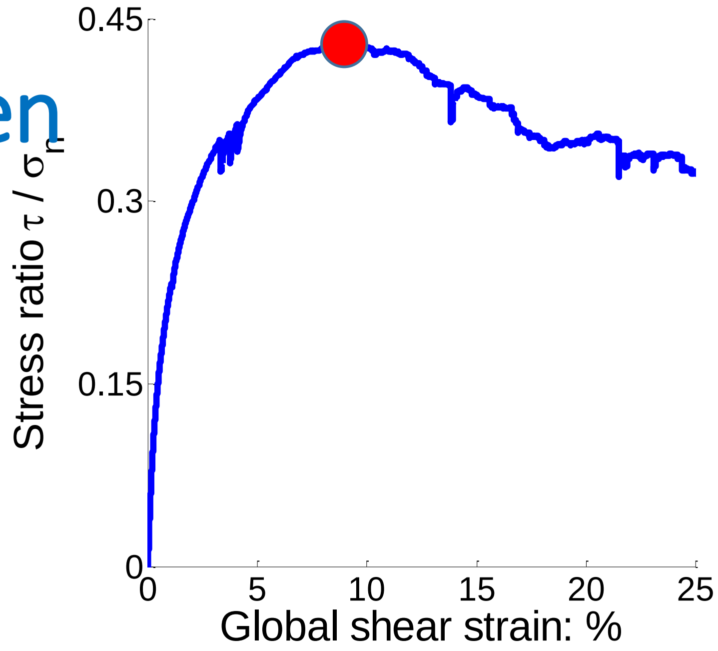

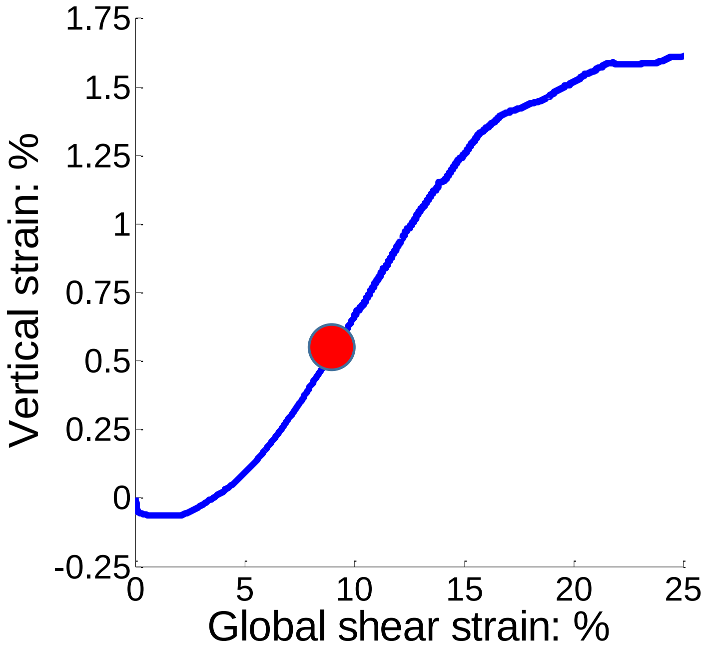

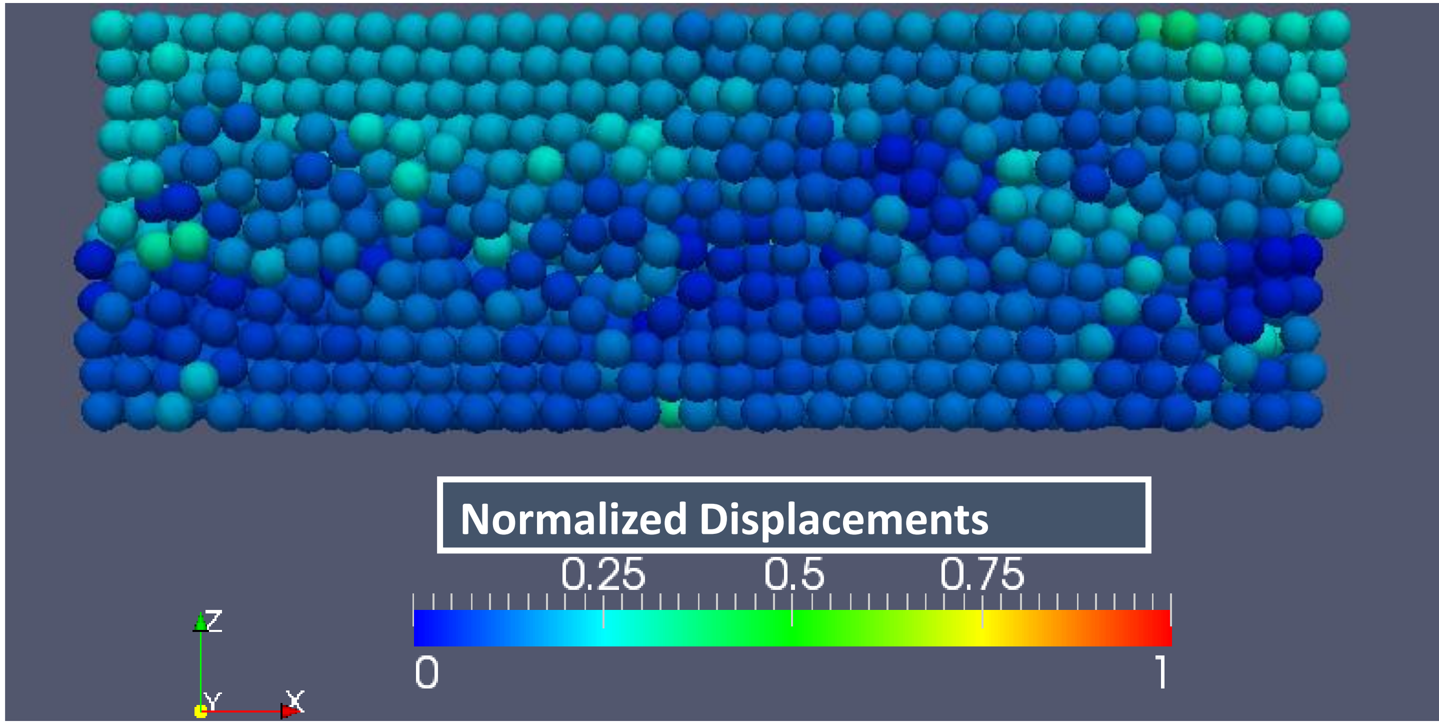

Deformed Specimen

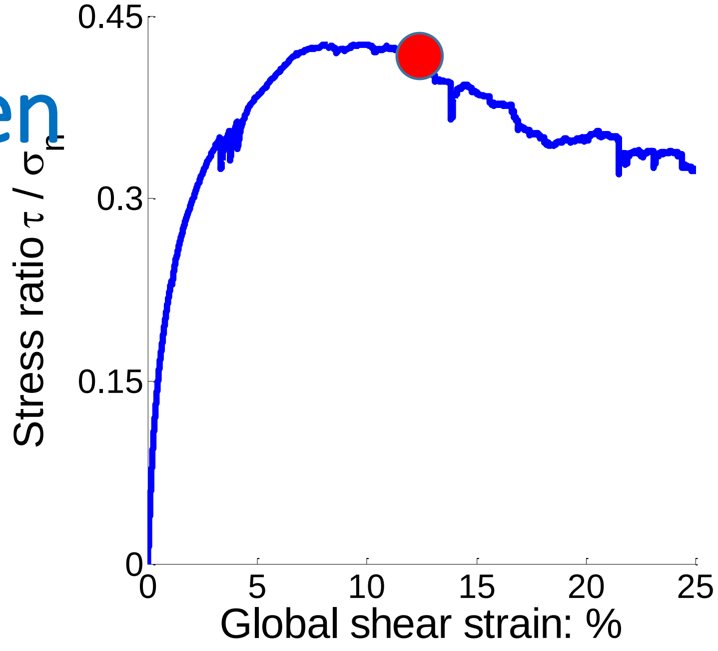

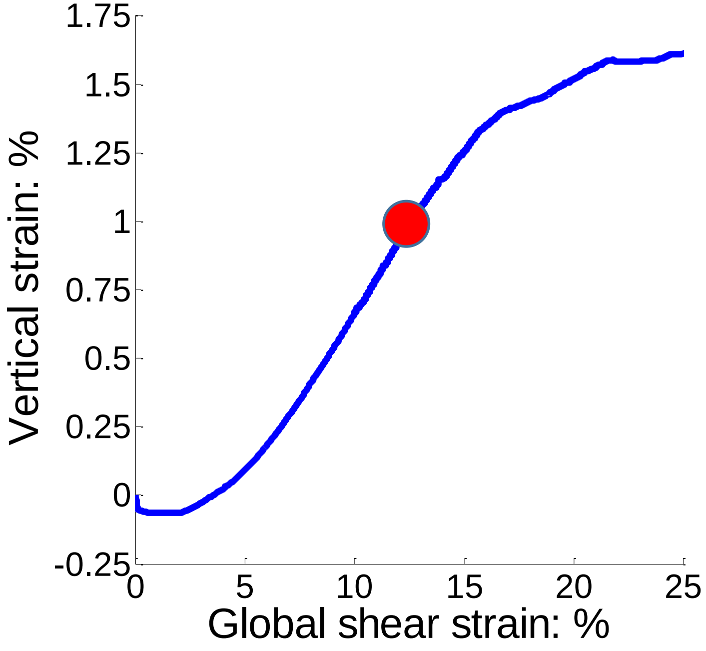

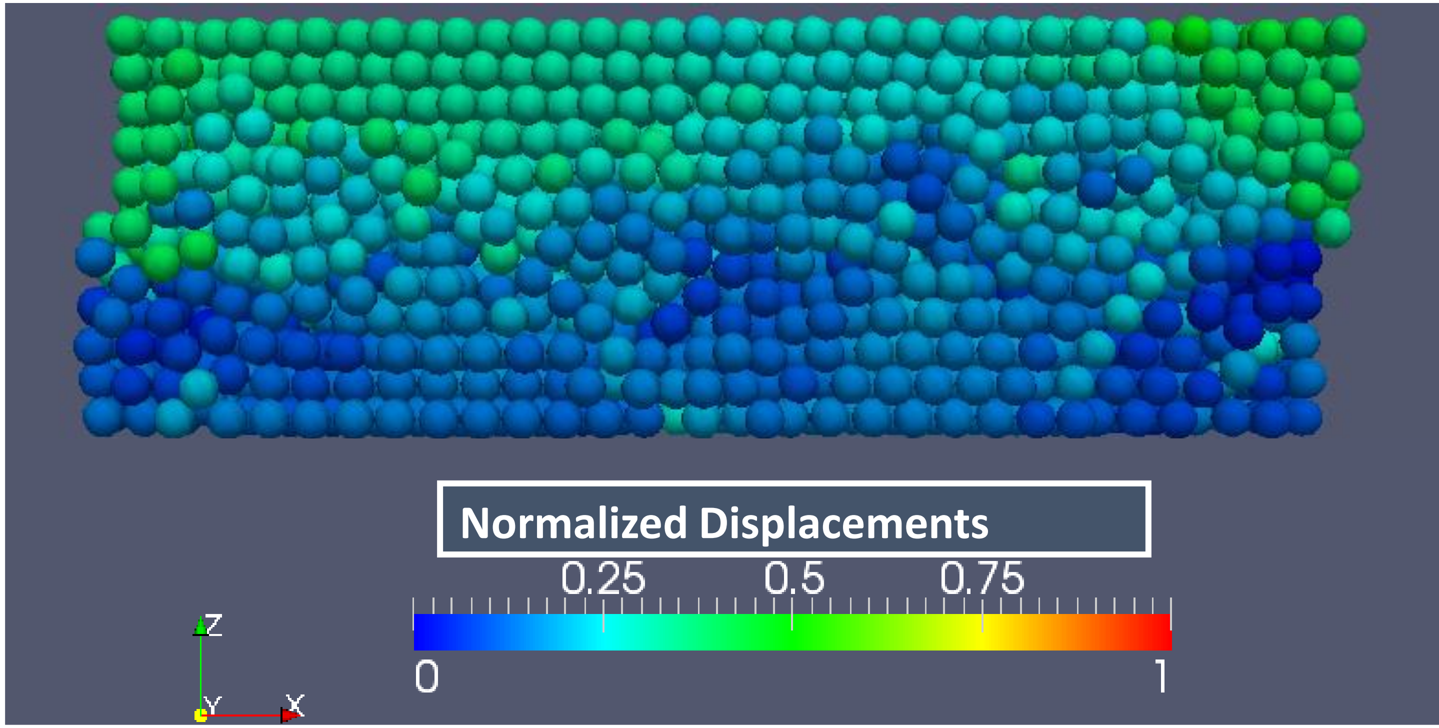

Deformed Specimen

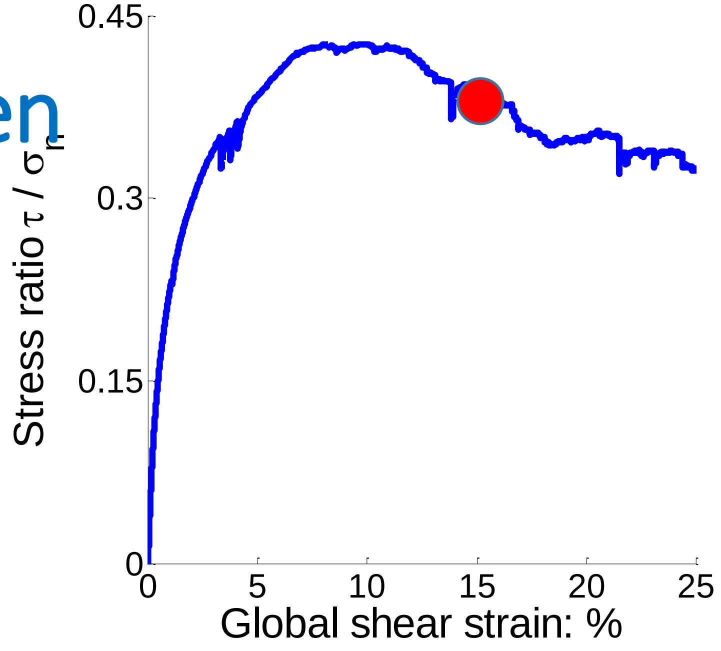

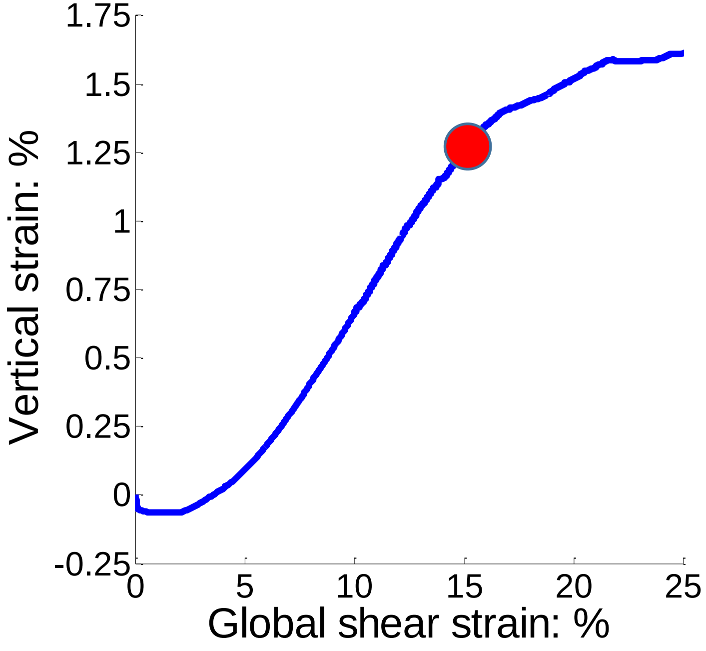

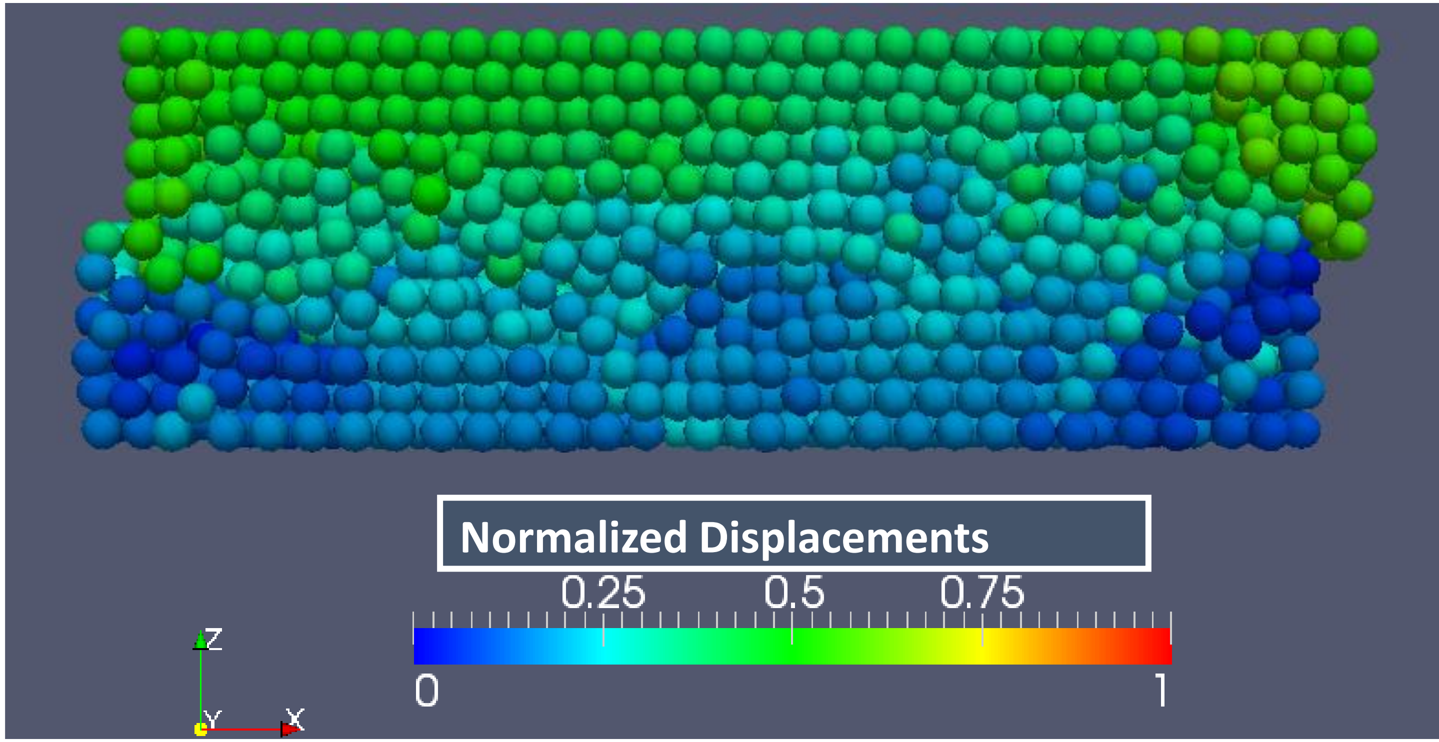

Deformed Specimen

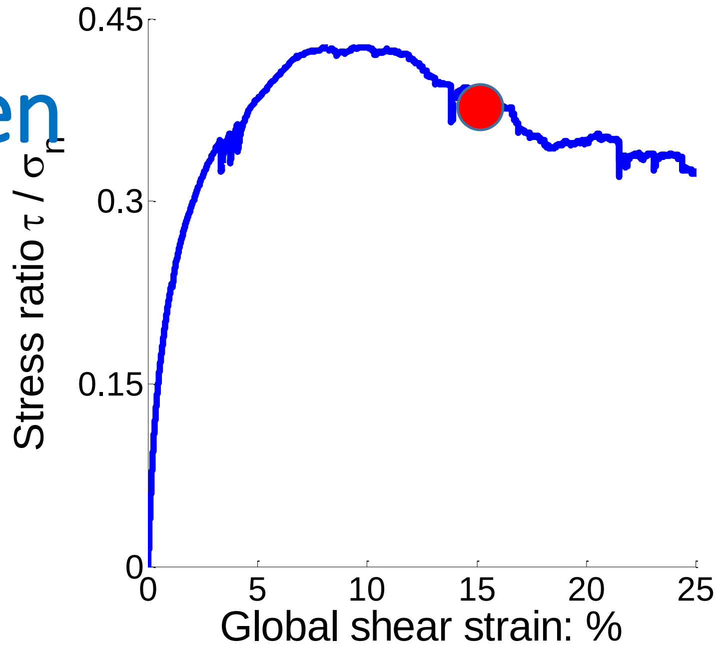

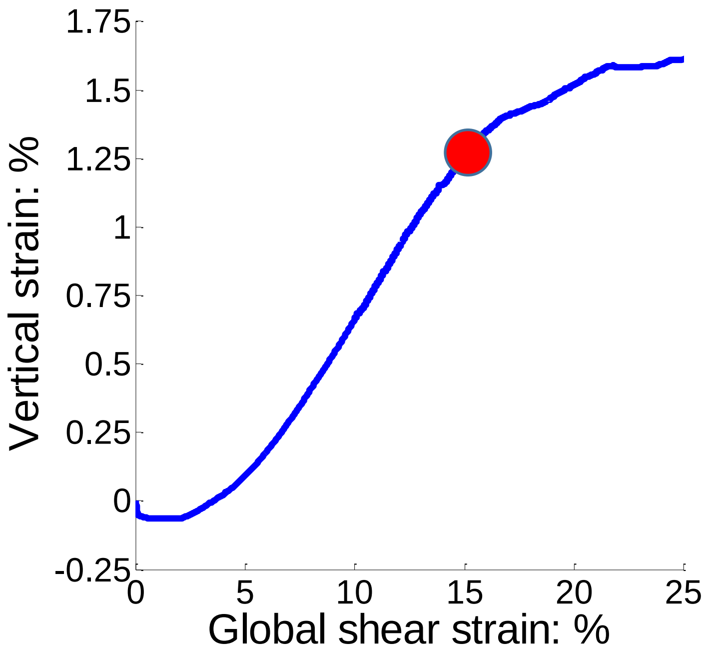

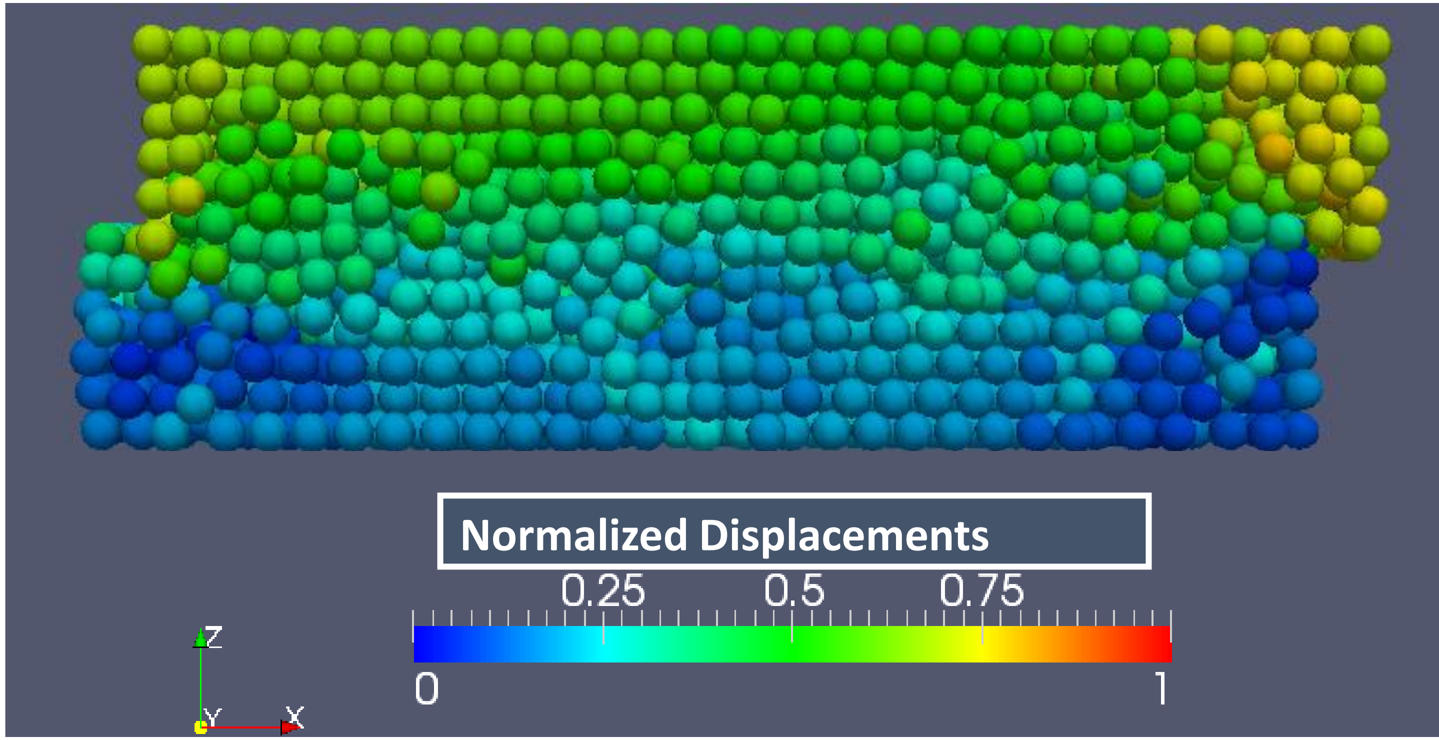

Deformed Specimen

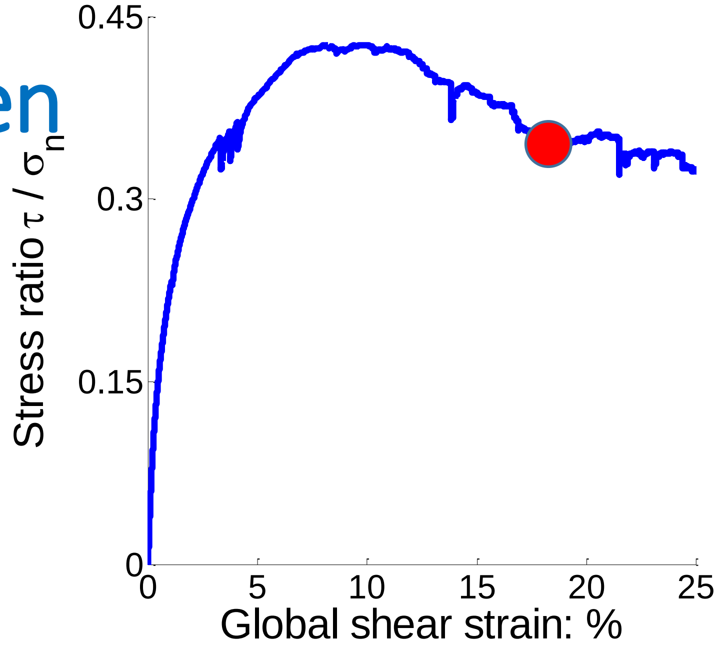

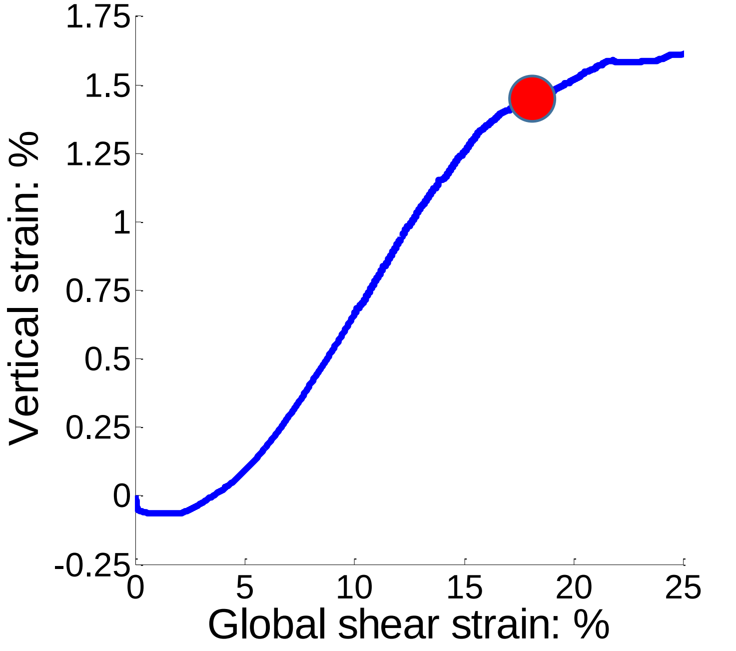

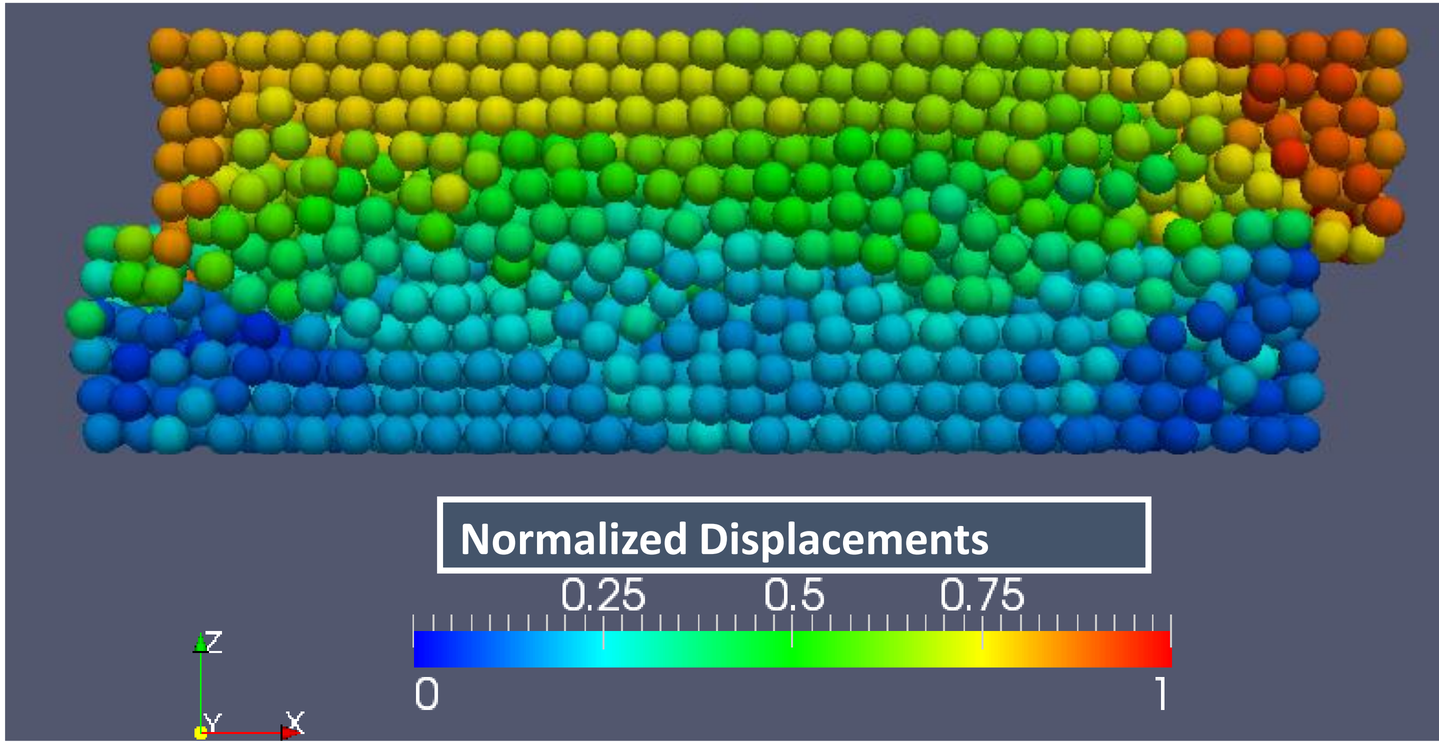

Deformed Specimen

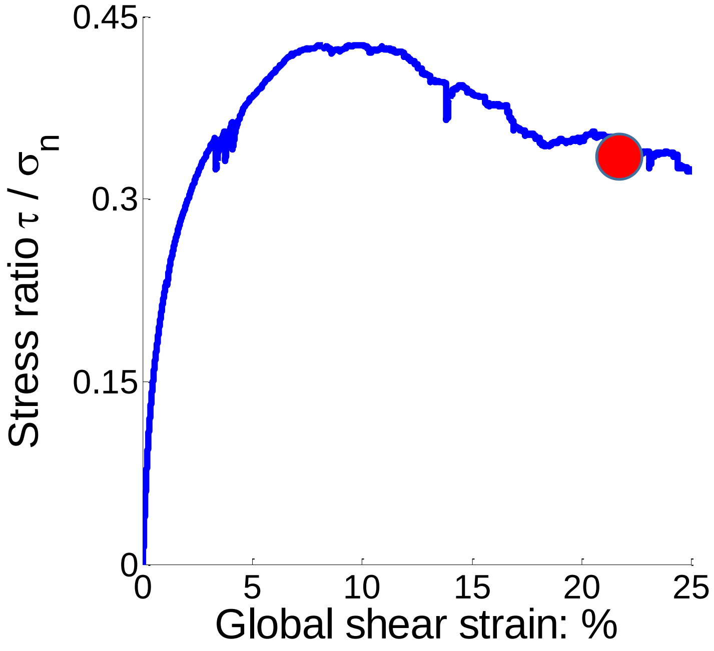

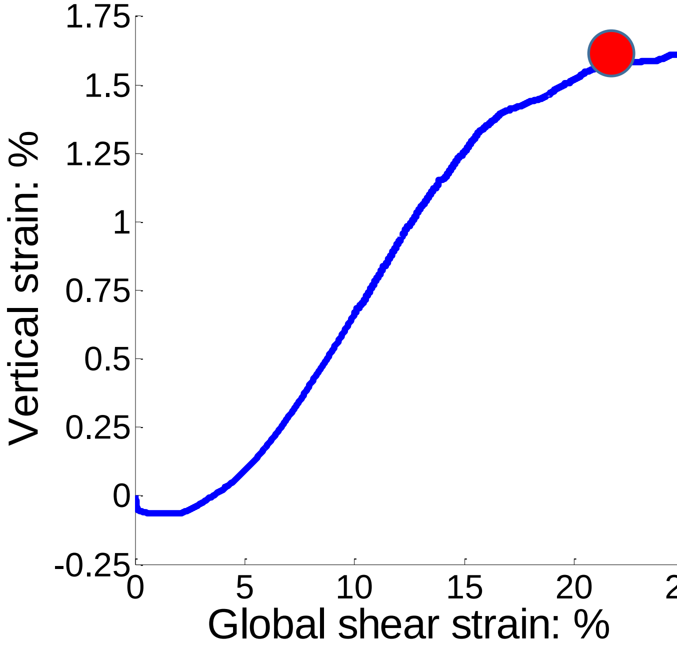

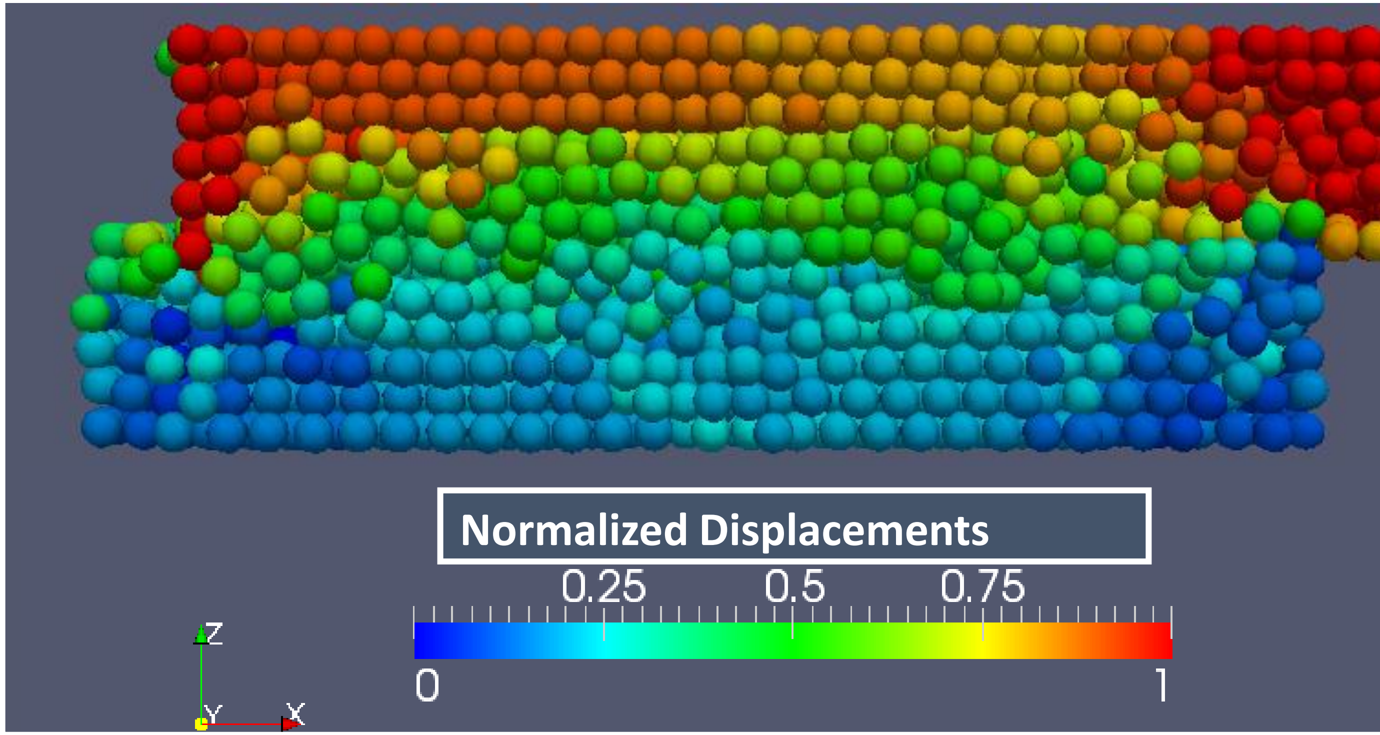

Deformed Specimen

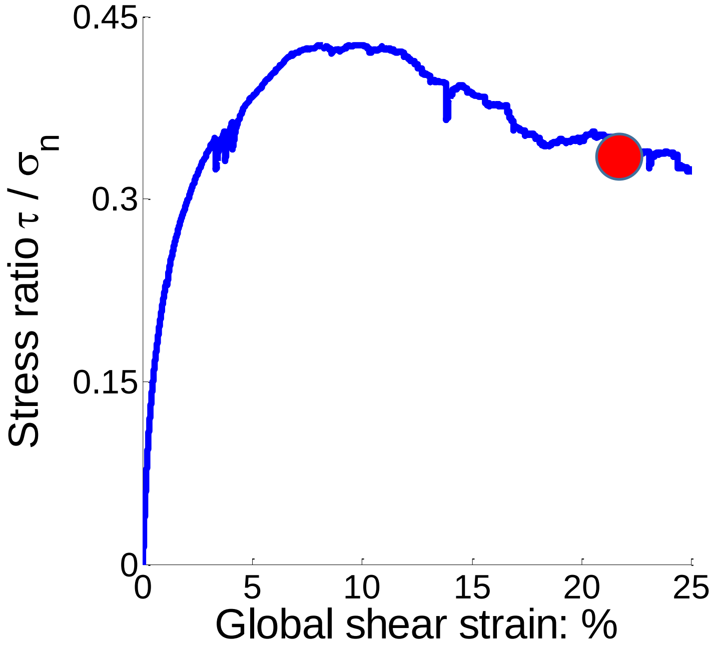

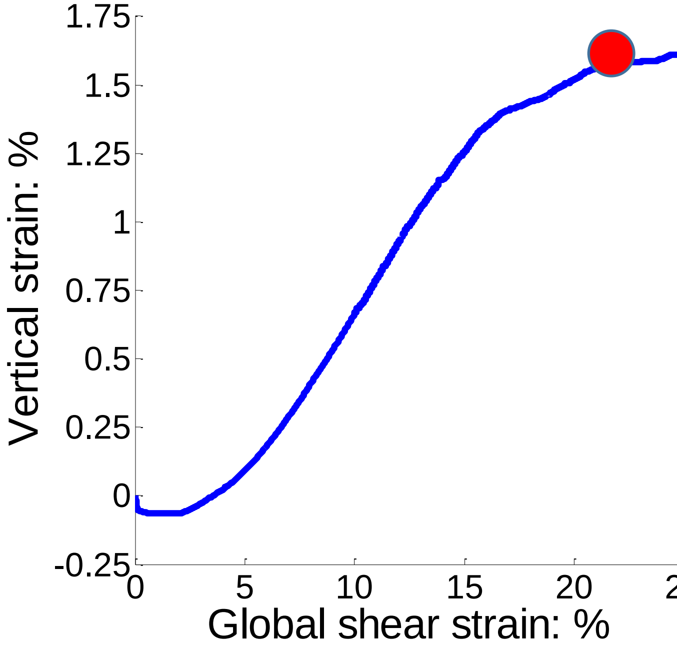

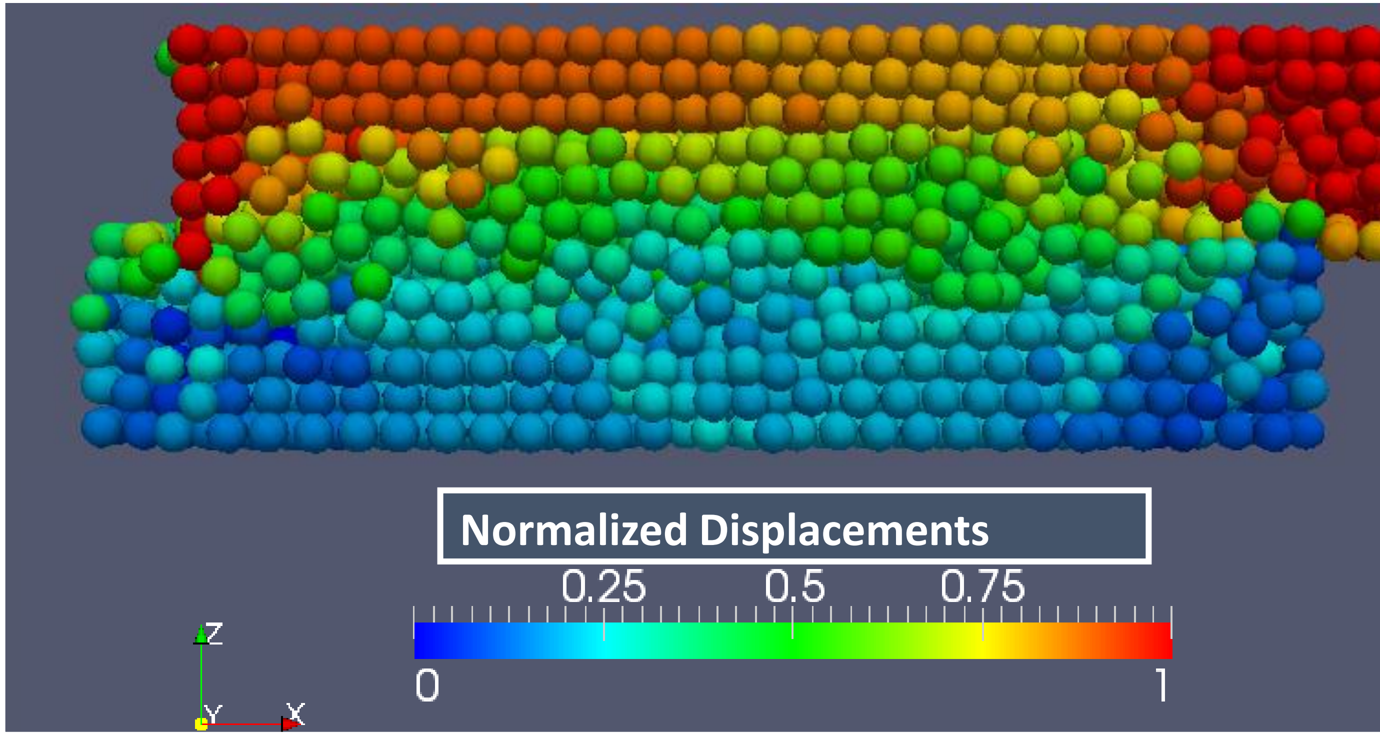

Contact force distribution in x-z plane

γ=1.4%

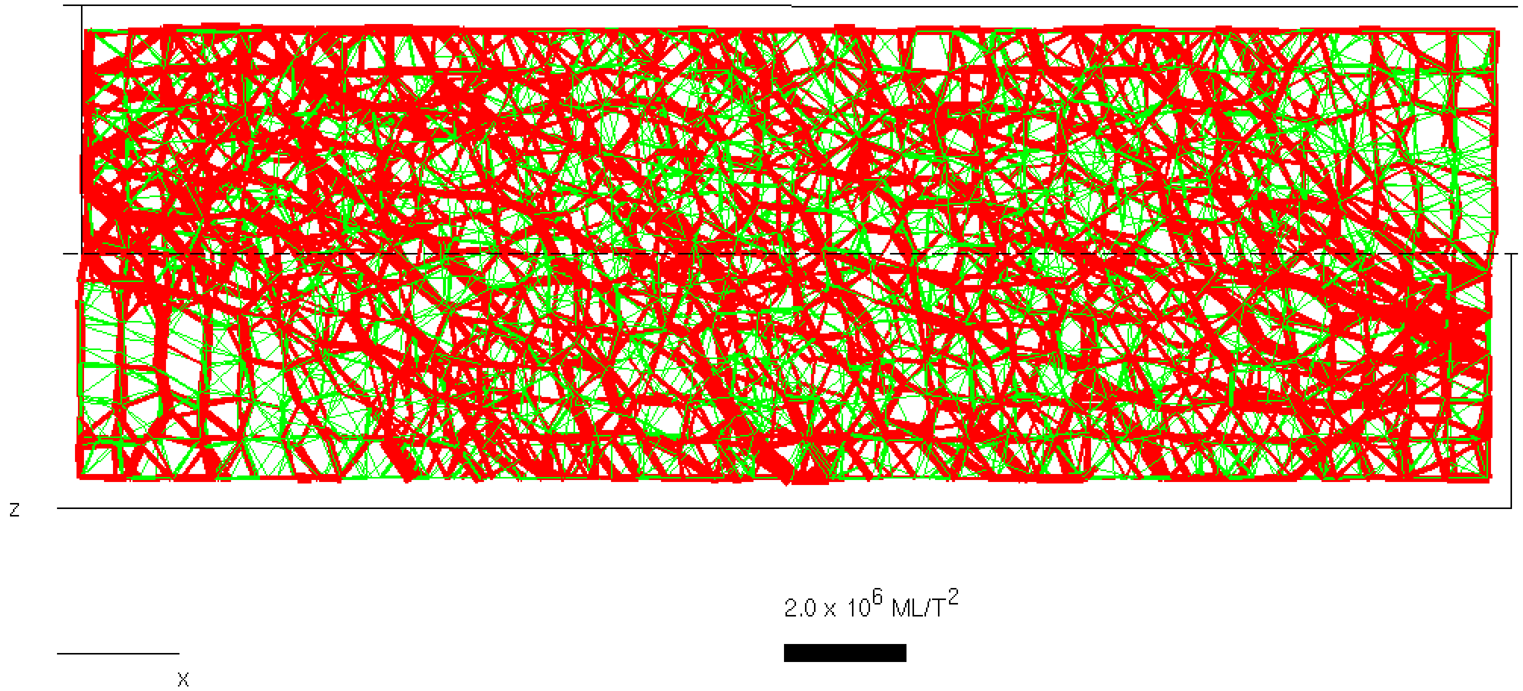

24 L < y <36 L

Contact force distribution in x-z plane
γ=4.9%

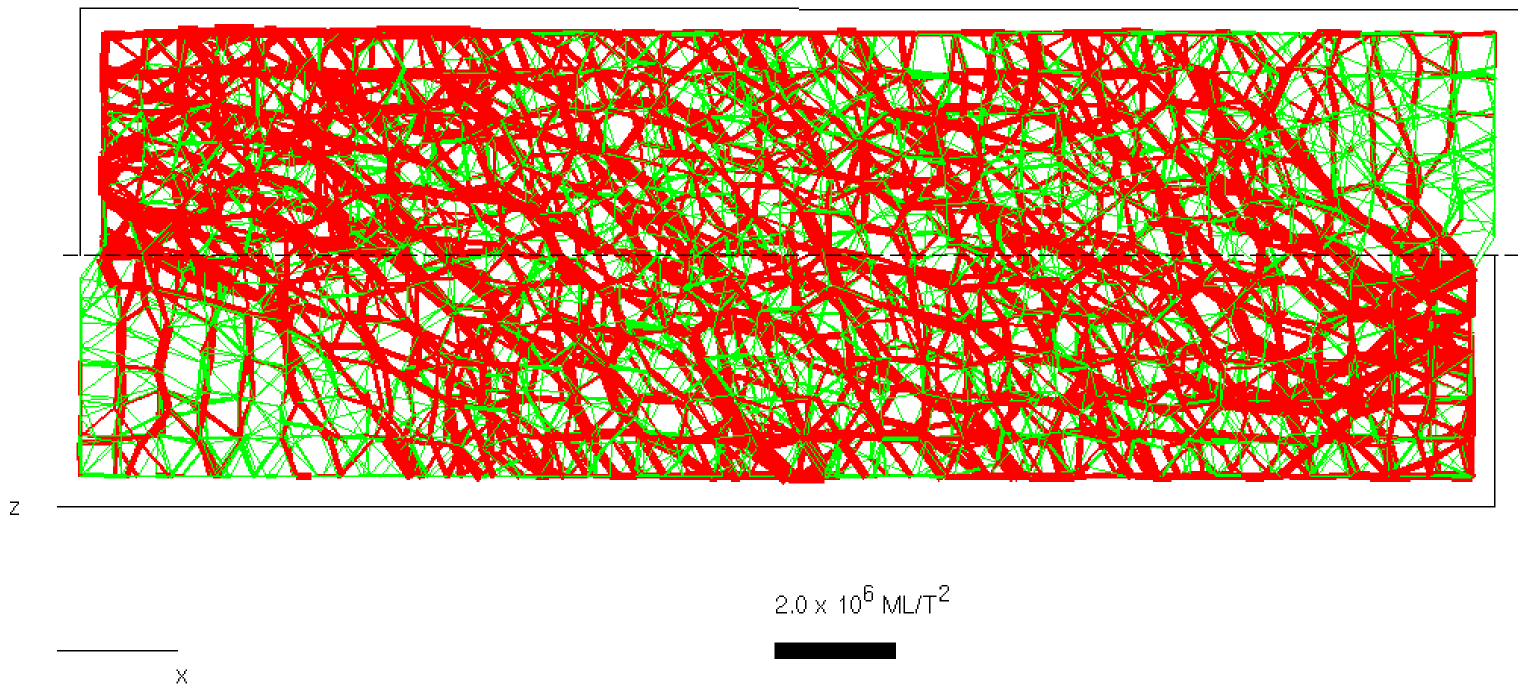

24 L < y <36 L

Contact force distribution in x-z plane
γ=11.8%

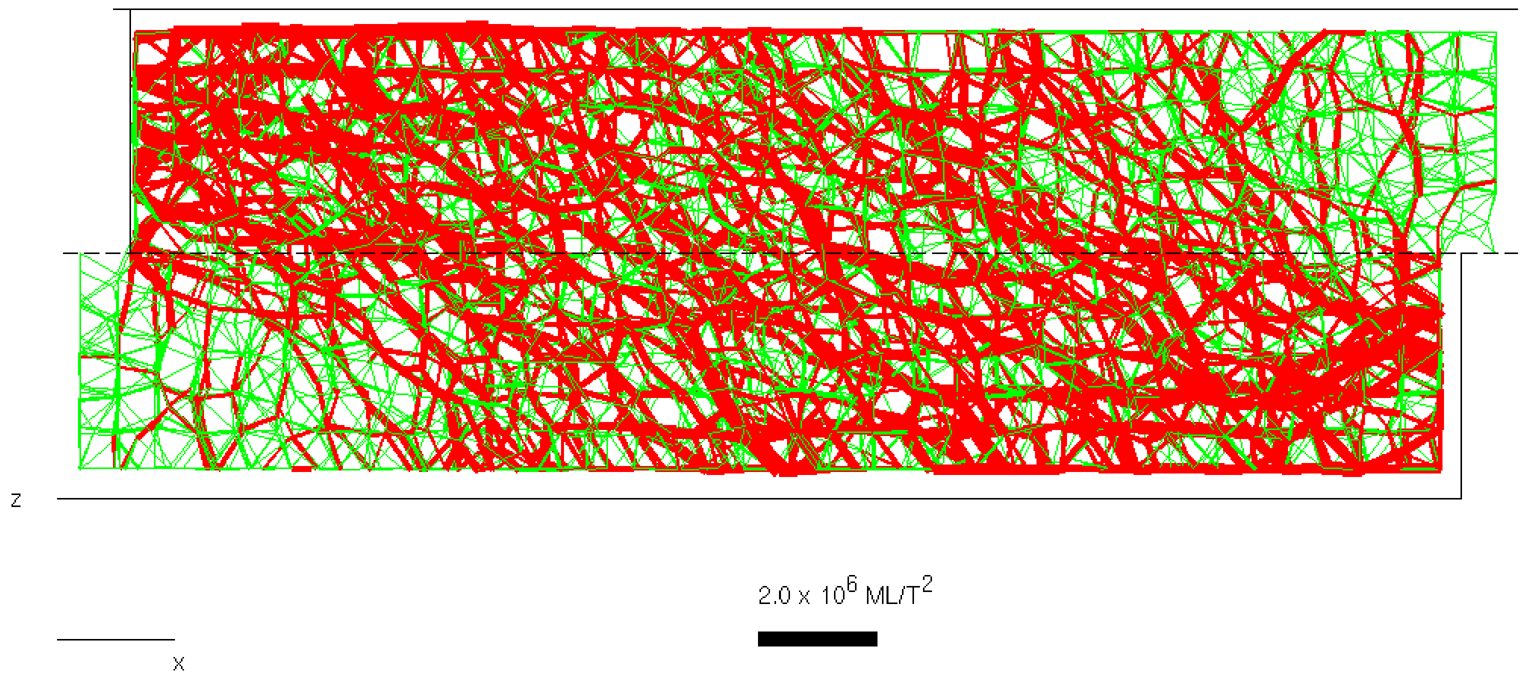

24 L < y <36 L

Contact force distribution in x-z plane
γ=15.3%

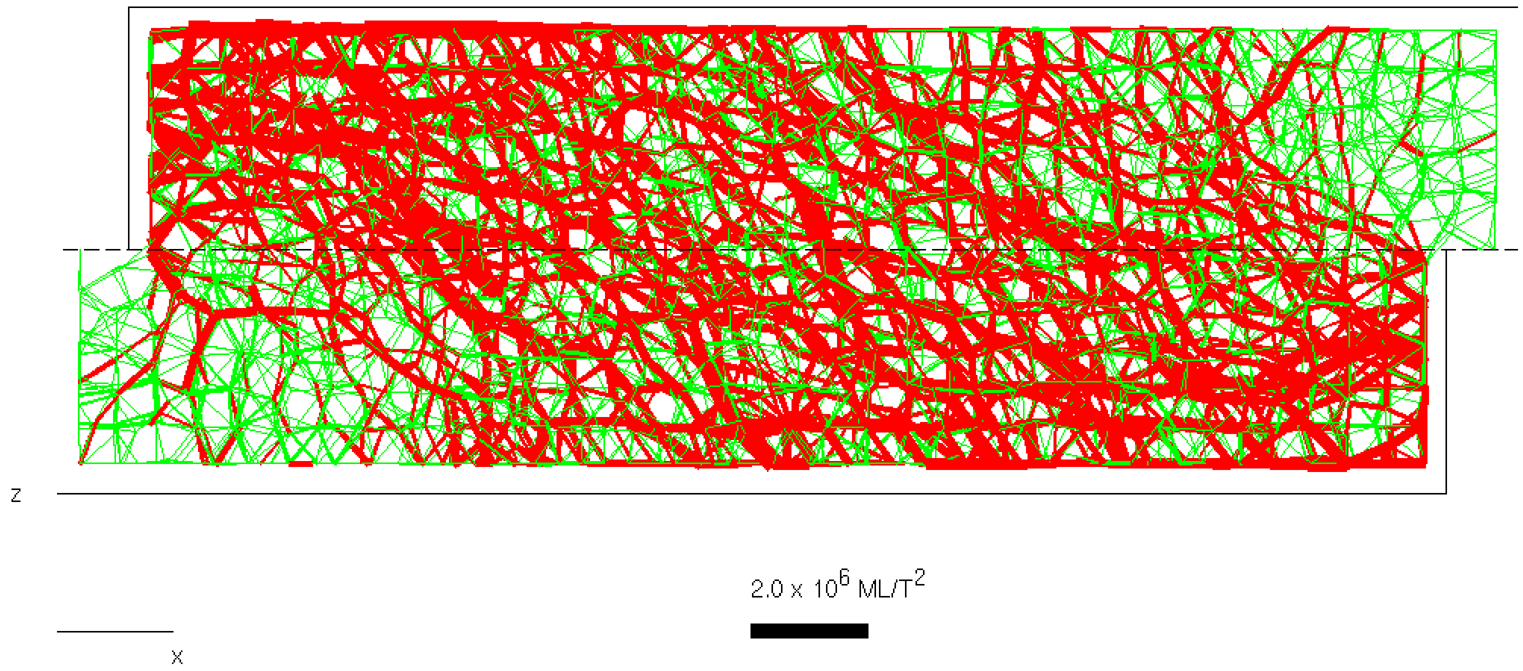

24 L < y <36 L

Contact force distribution in x-z plane

γ=8.4%

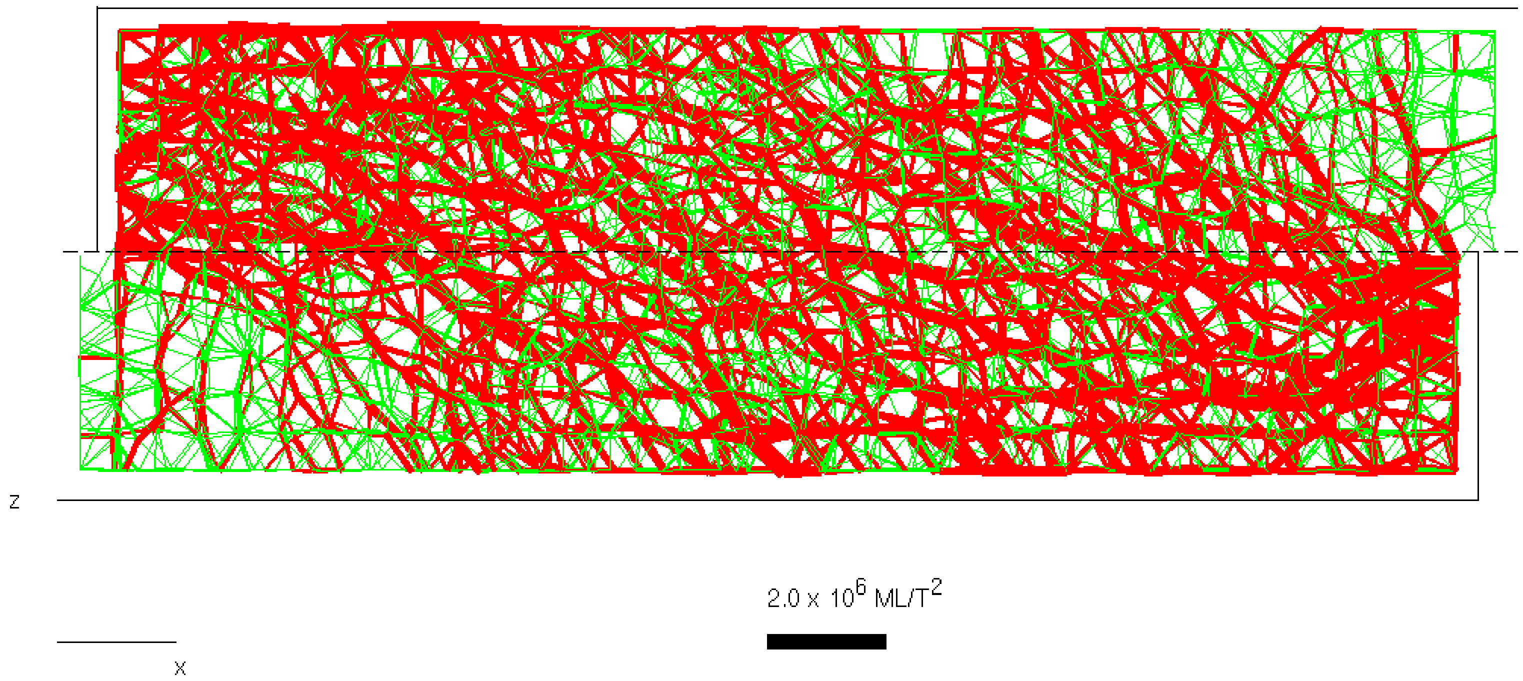

24 L < y <36 L

Contact Network

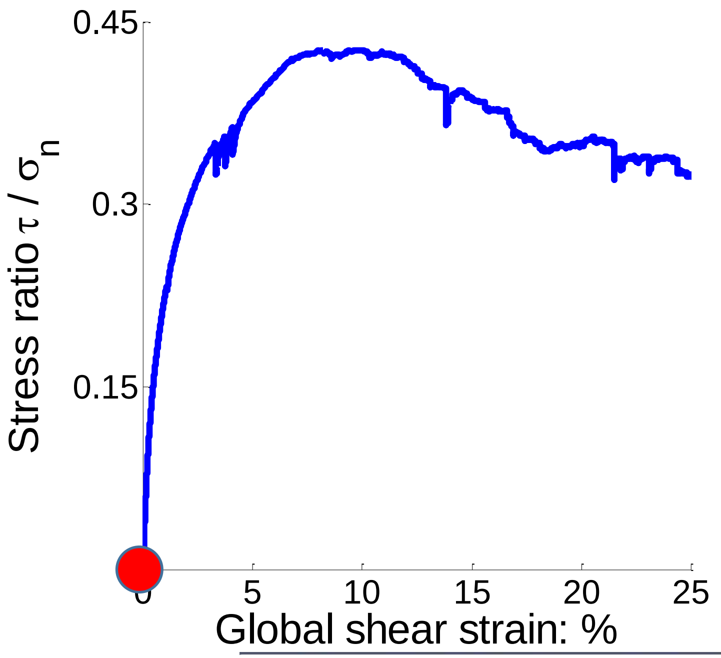

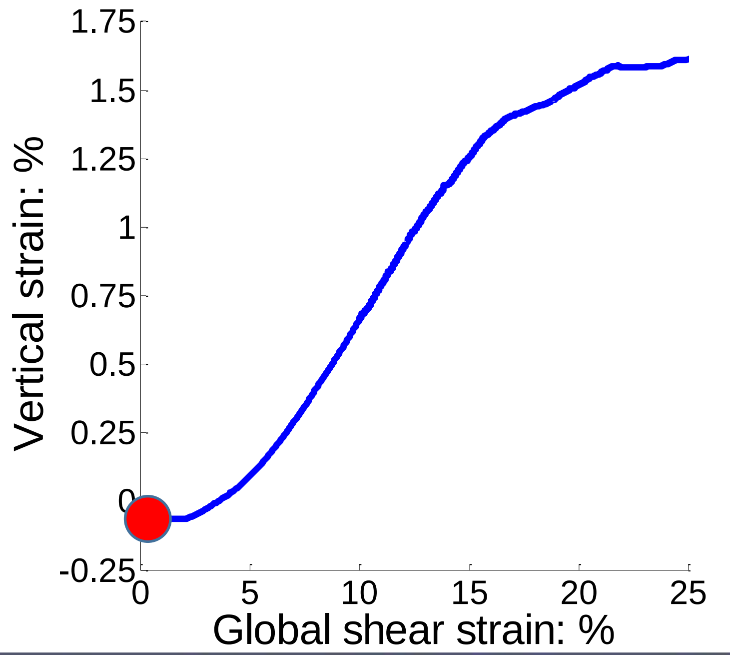

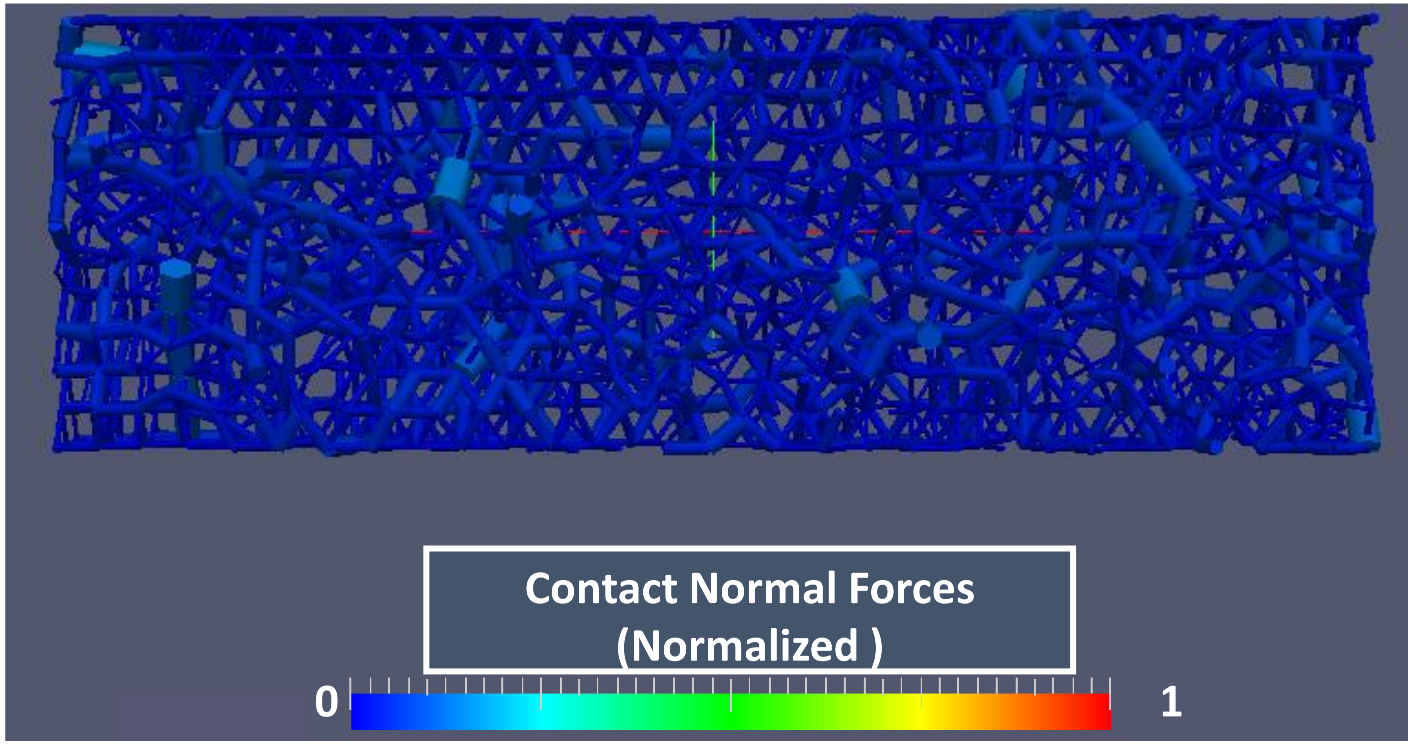

Contact Network

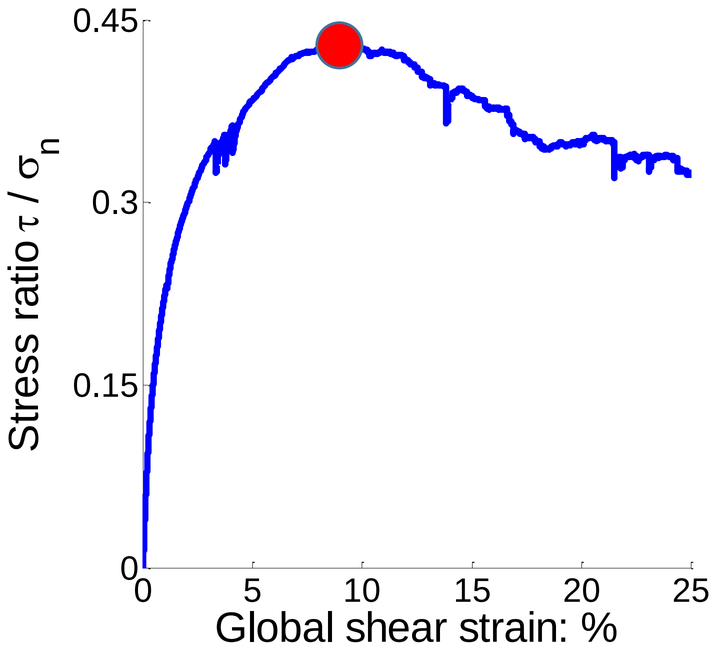

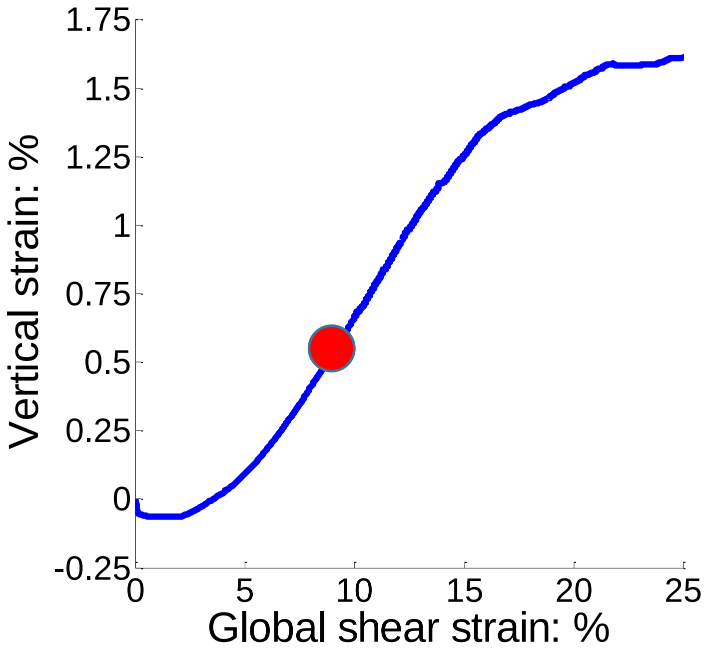

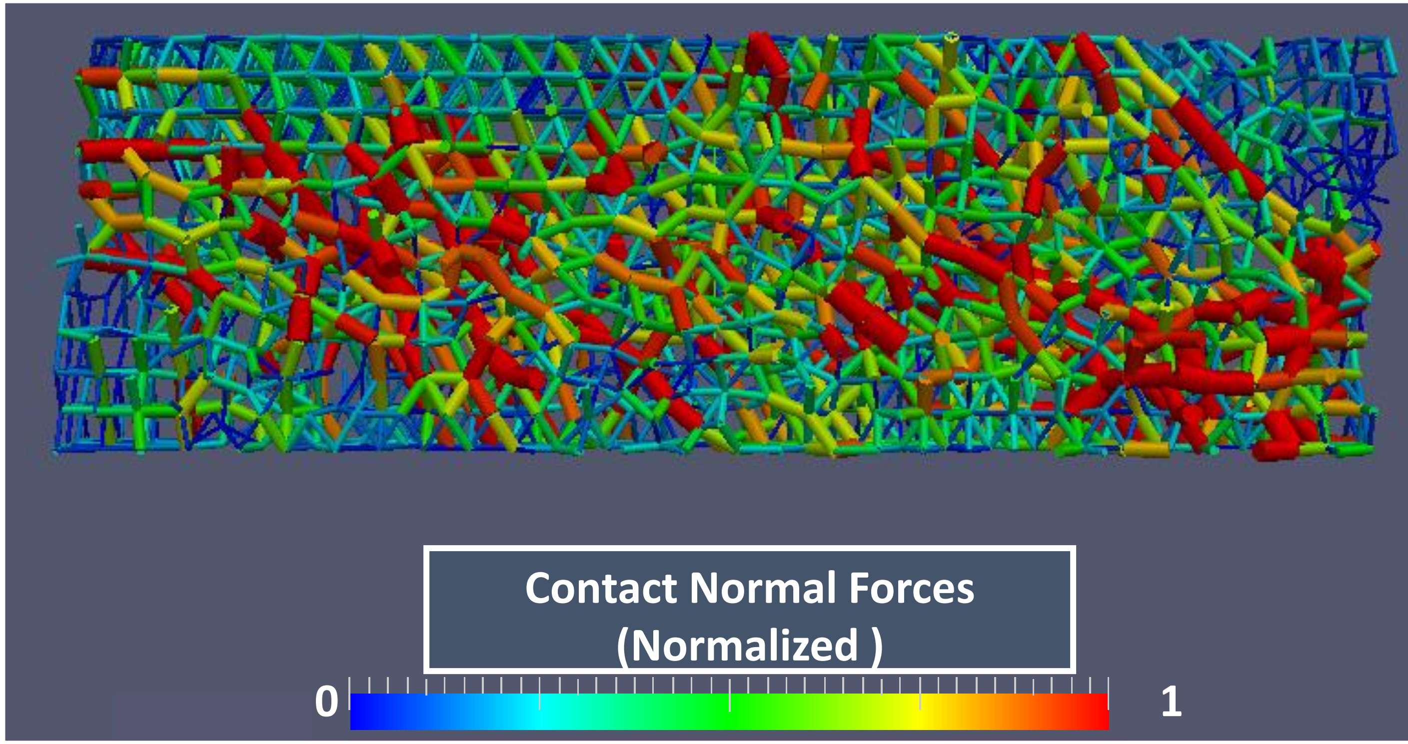

Contact Network

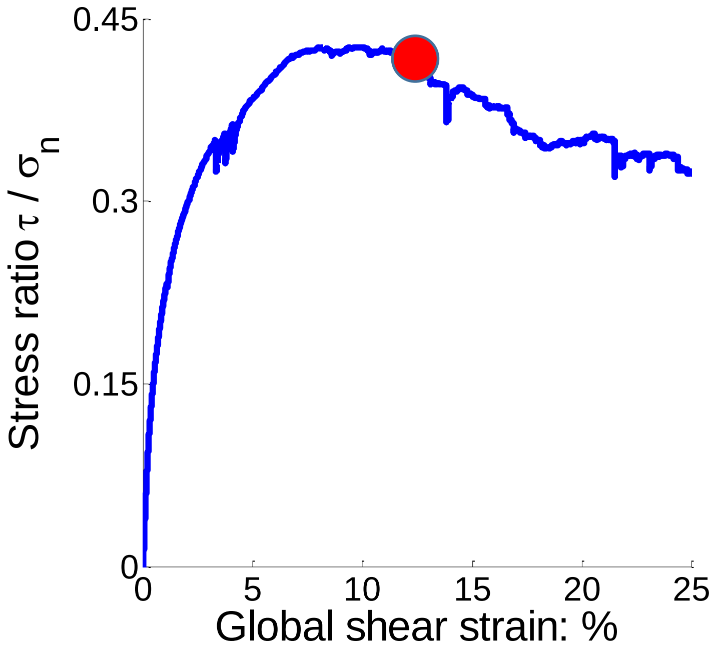

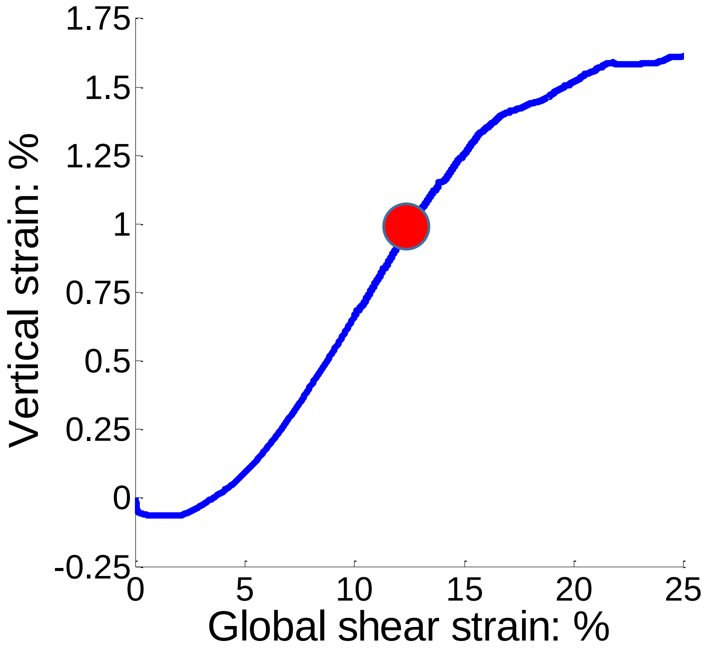

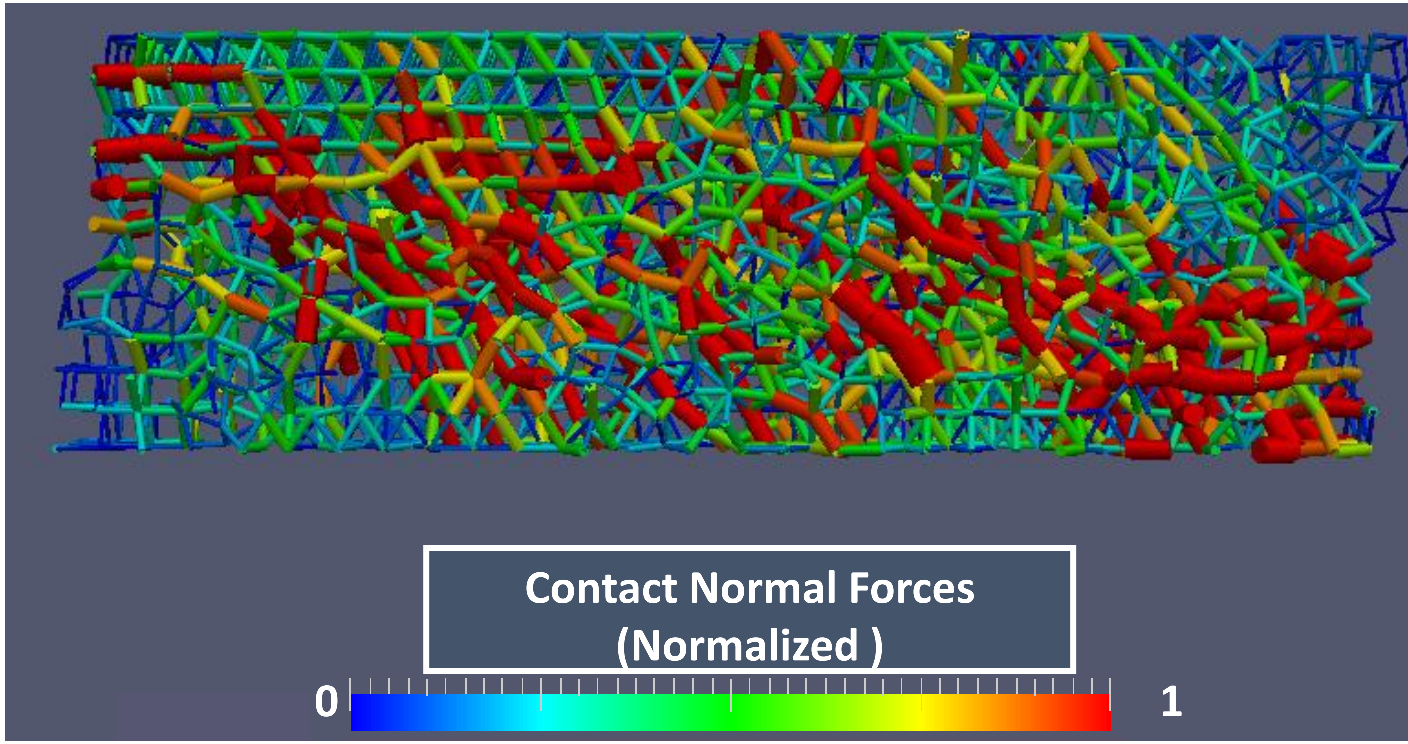

Contact Network

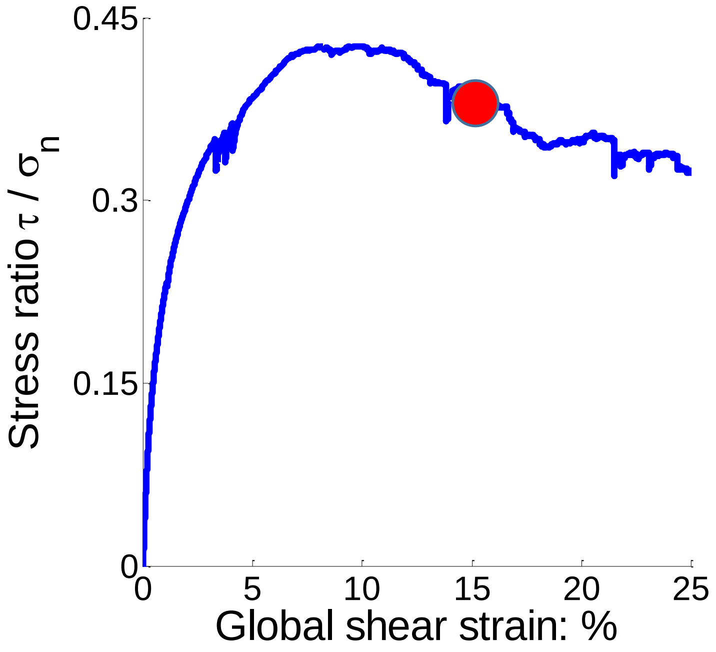

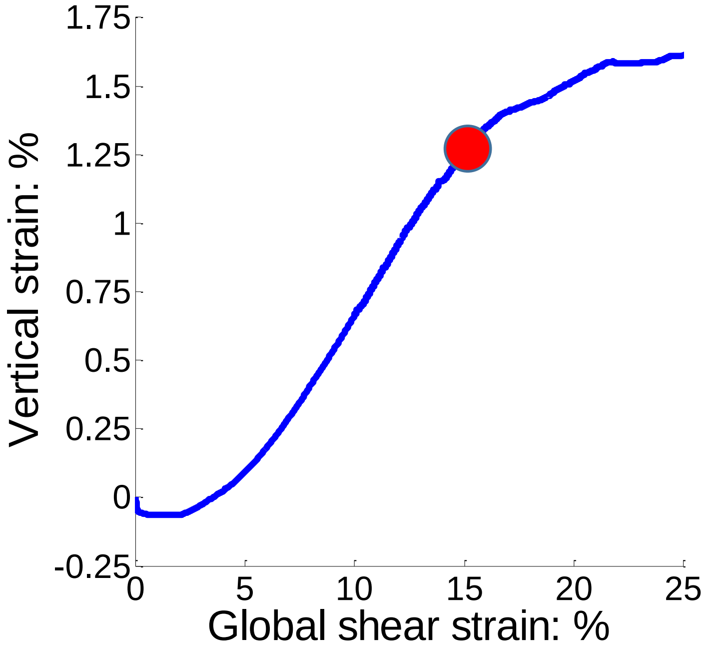

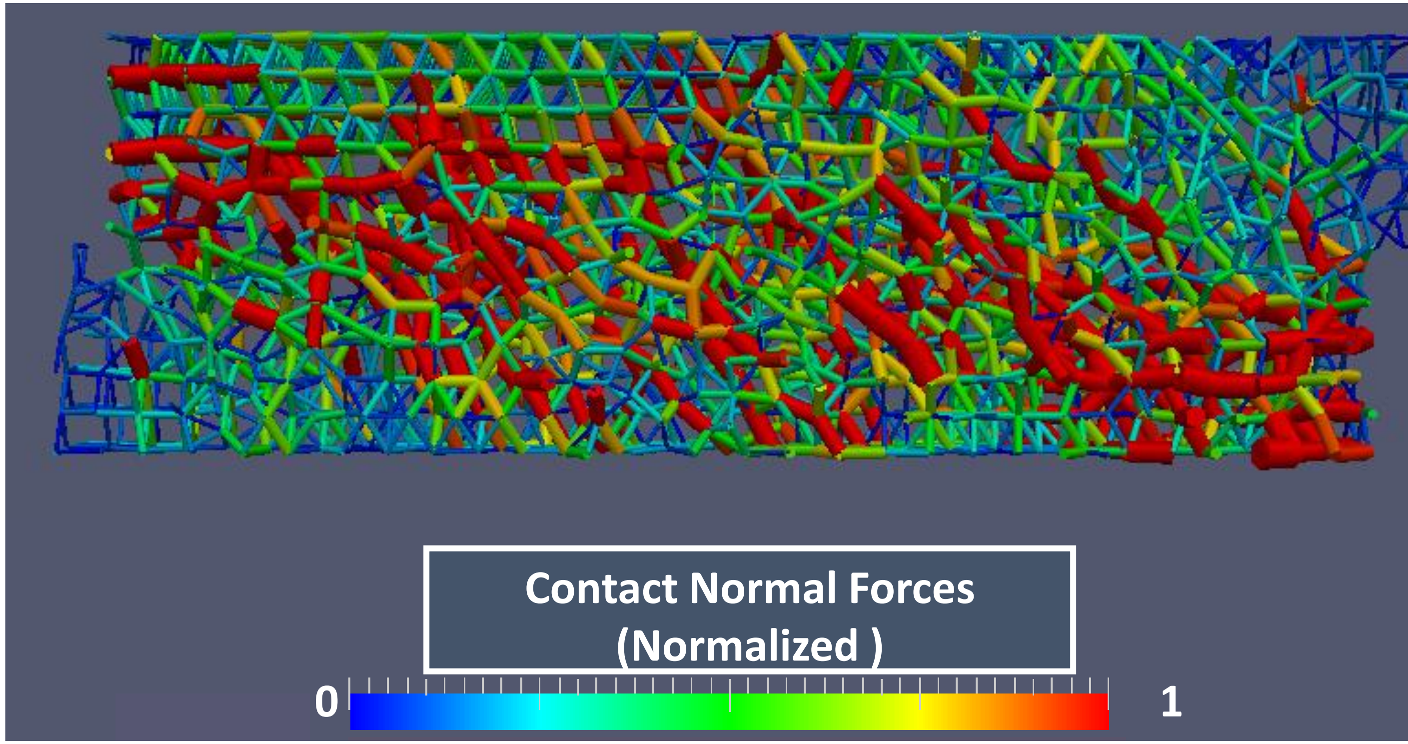

Contact Network

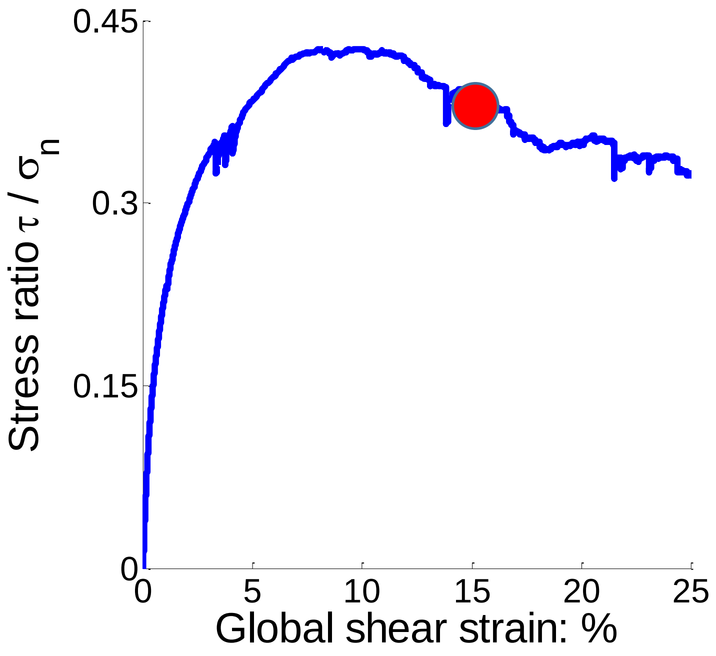

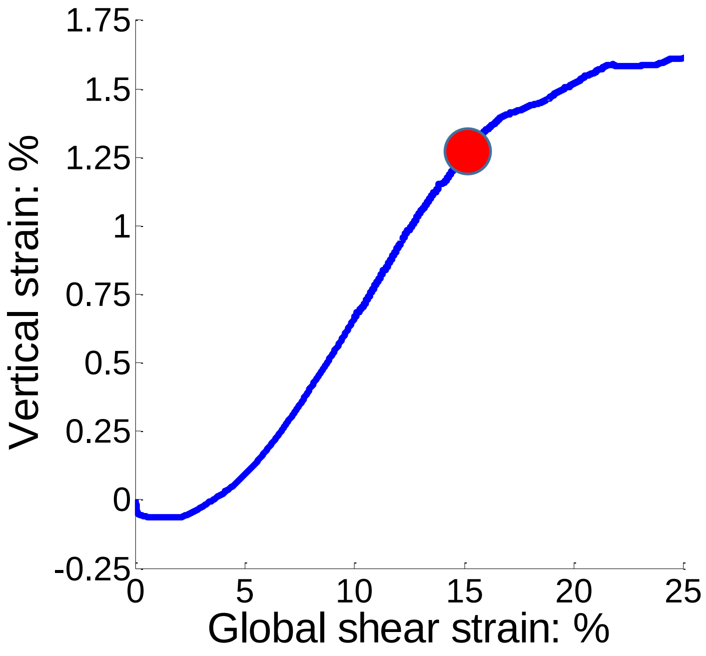

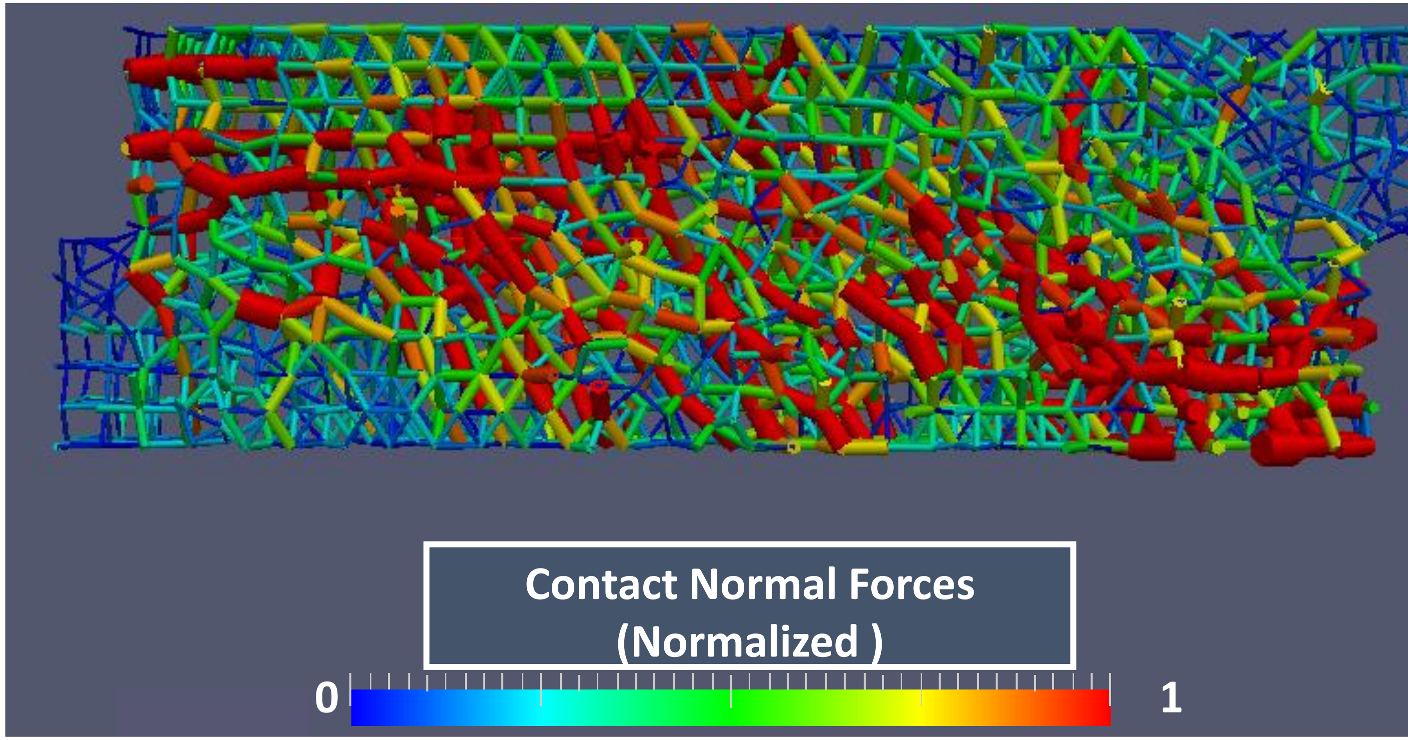

Contact Network

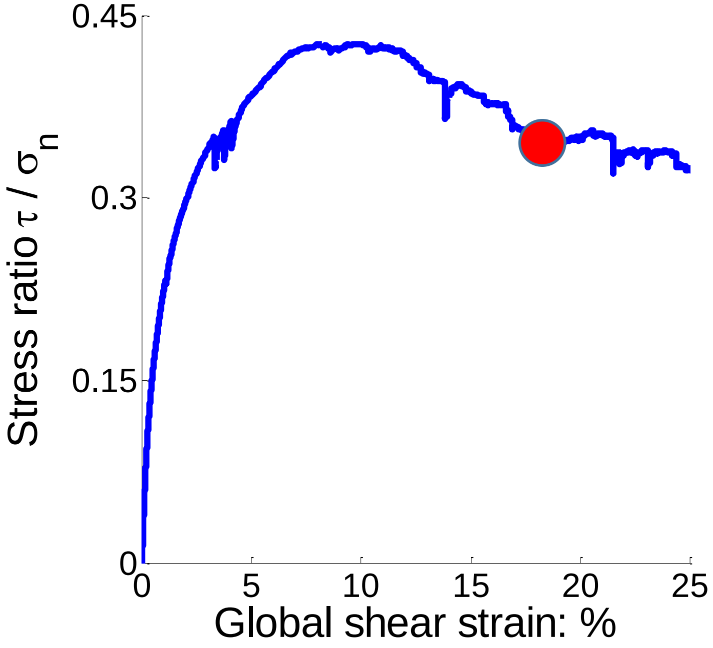

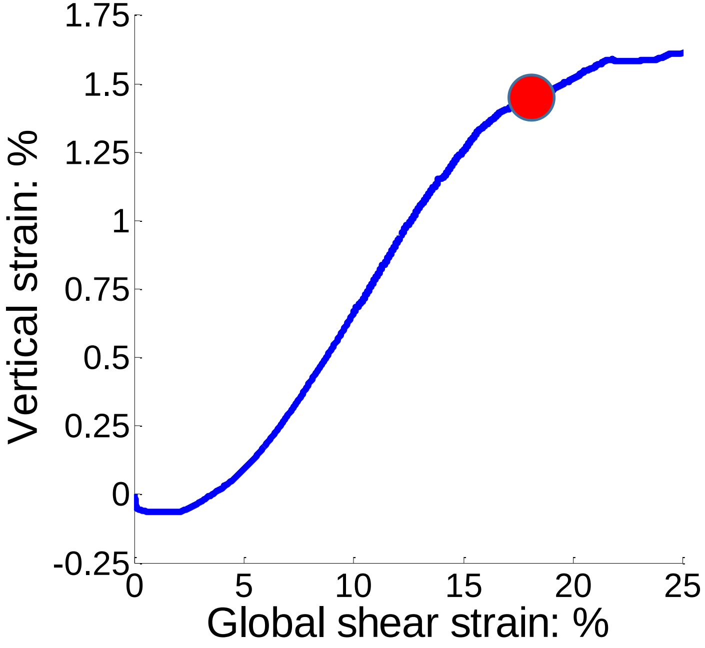

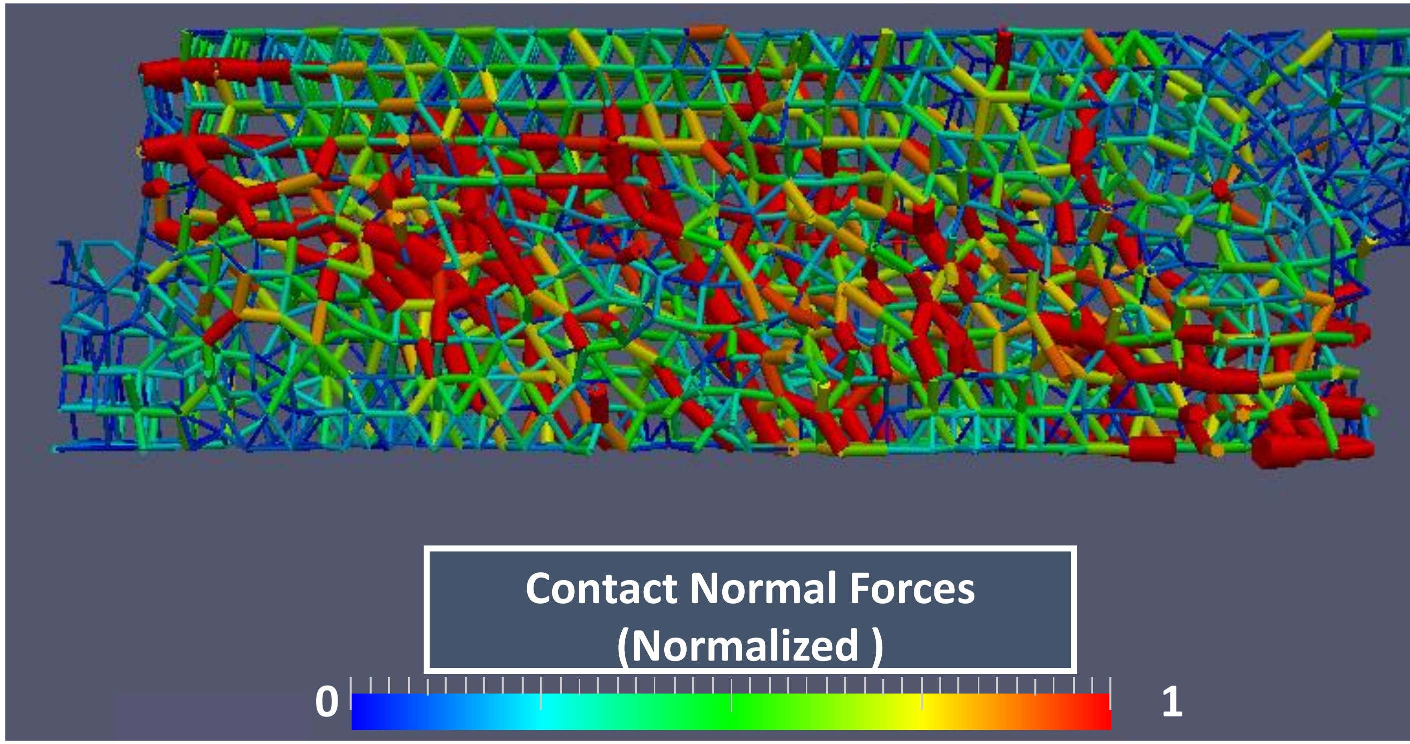

Contact Network

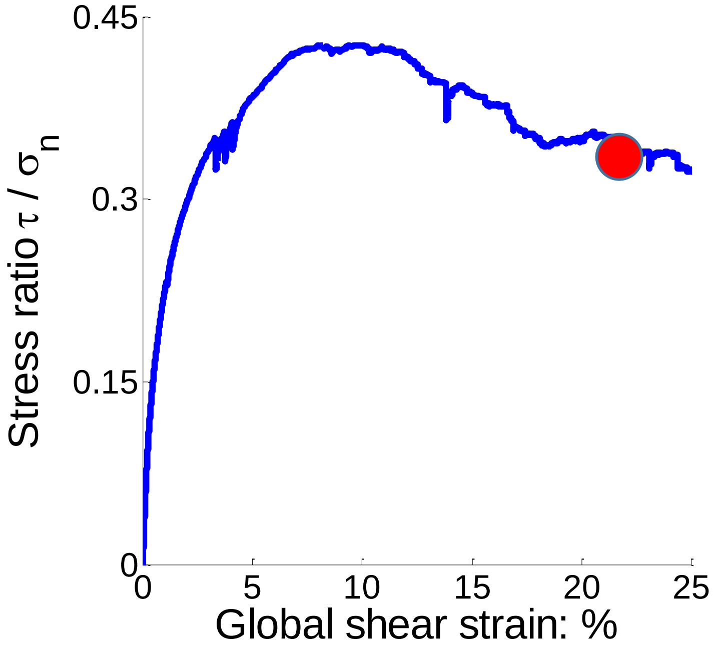

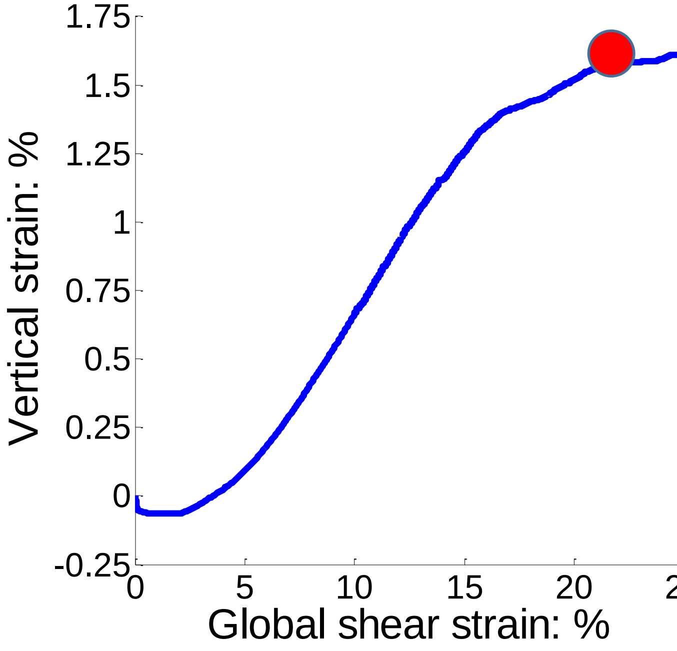

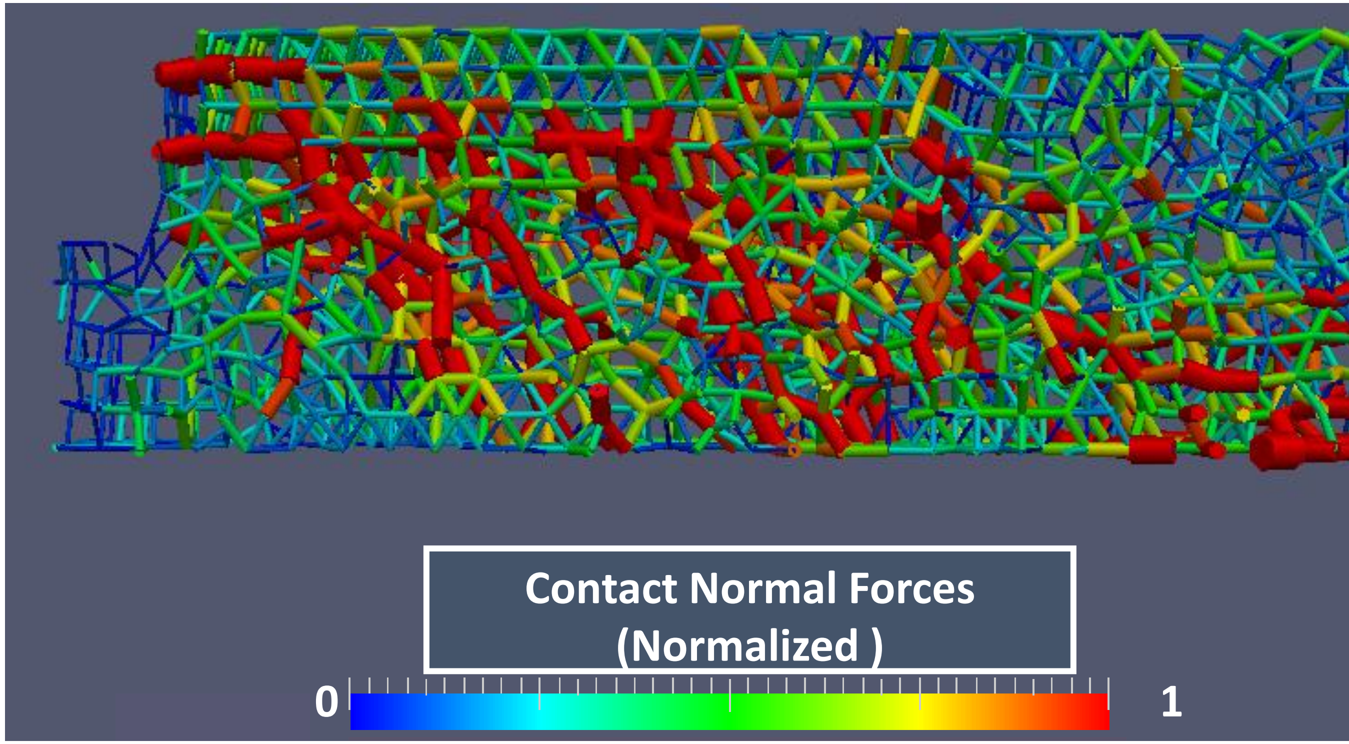

Conclusions

Visualization is essential as a quality check – Paraview is very useful

Conclusions

Choice of code

- PFC is the most popular DEM code based on review of DEM studies published in geomechanics / geotechnical /soil mechanics journals

- Now a good few DEM codes available open source

- Tendency to exploit parallelism.

- YADE / PFC Version 5 – shared memory

- LIGGGHTS / LAMMPS – distributed memory

Validation

- Experimental validation is useful, but not straightforward
- Analytical approaches using regular packing v important
- Benchmarking on random systems is helpful

Time step

- Conditionally stable method

- Essential to be within stability limit, but should not be over conservative

From eigenvalue approach:

- Critical time step depends on contact stiffness (which depends on confining pressure for Hertz-Mindlin model), particle mass and packing density (coordination number)

- Method based on Rayleigh wave speed not always conservative

Boundary Conditions

- Largely three types of boundaries: rigid wall, force, periodic
- Servo control can be used to capture complex conditions
- Use of computationally expensive force / membrane boundaries may not always be justifiable (small strain)
- Post-peak may be more sensitive

Sample size

- V important to establish you have an REV (representative element volume)
- Critical state line position can be affected by boundary conditions – v significant implications for understanding behaviour
- Plots of local void ratio helpful to understand extent of boundary effects
- Periodic cell very useful, but you still need to check an REV is achieved

Specimen generation

- You can achieve a range of densities by varying particle friction during preparation

- May detrimentally effect small strain response

Input parameters

- Using a high coefficient of friction (>0.5) with freely rotating spheres gives a response that is not representative of soil

- Explanation seems to be a transition from sliding to rolling at the contact points

- Use of two codes enhanced our confidence in observations

- Supplemental abstract analyses of small elements of the system were very useful

Contact model

- Hertz-Mindlin contact model ideal – even for glass ballotini
- Surface roughness - measurable effect on stiffness
- Partial slip – more subtle effect, less significant for regular, lattice packings

Running the simulation

- Inertia number effects position of critical state line
- For quasi-static simulations keep $I \leq 2.5e\text{-}3$

Acknowledgements

Collaborators:

Dr. Daniel Barreto, Edinburgh Napier
Prof. Michelle Bernhardt, Univ. Arkansas
Dr. Giovanna Biscontin, Cambridge University
Prof. John Bray, UC Berkeley
Dr. Geraldine Cheung, ARUP
Dr. Liang Cui, University of Surrey
Dr. Ignazio Cavarretta, University of Surrey
Dr. K. Hanley, University of Edinburgh
Dr. X. Huang, Tongji University
Dr. Erdin Ibraim, University of Bristol
Mr. Kenichi Kawano, Kajima
Dr. Fiona Kwok, University of Hong Kong
Dr. Juan Lopera Perez, University of Hong Kong
Dr. George Marketos, Utrecht University
Prof. David Muir Wood, Dundee Unviersity
Dr. John O'Donovan, Gavin & Doherty Geosolutions
Mr. Masahide Otsubo, Imperial College
Mr. Hoang, Nguyen, Imperial College
Dr. Tom Shire, Imperial College
Dr. Way Way Sim, Imperial College

Sponsors:

ARUP
EPSRC
IRCSET (Ireland)
Kajima
O'Reilly Foundation
Royal Commission for the Exhibition of 1851

References: Code validation

- Hoang N., Otsubo, M. and O'Sullivan, C. (2017) An appraisal of the influence of material fabric and stress anisotropy on small-strain stiffness Submitted *to Proc. Powders and Grains* (2017)
- Huang, X., Hanley, K. J., and O'Sullivan, C. Kwok, C.Y. Wadee, M. A. (2014) "Influence of inter-particle friction on critical state behaviour: a numerical investigation" *International Journal of Numerical and Analytical Methods in Geomechanics*, DOI: 10.1002/nag.2259
- Kawano, K. (2016) *Numerical Evaluation of Internal Erosion due to Seepage Flow* MPhil Thesis Imperial College London
- J. O'Donovan, E. Ibraim, C. O'Sullivan, S. Hamlin, D. Muir-Wood, G. Marketos (2016) Micromechanics of seismic wave propagation in granular materials *Granular Matter*, 18: 56. doi:10.1007/s10035-015-0599-4
- C. O'Sullivan and J.D. Bray (2003) "A Modified Shear Spring Formulation for Discontinuous Deformation Analysis of Particulate Media" *ASCE Journal of Engineering Mechanics* Vol 129, No. 7. 830-834
- C. O'Sullivan, J.D. Bray, and M.F. Riemer, (2002) "The Influence of Particle Shape and Surface Friction Variability on Macroscopic Frictional Strength of Rod-Shaped Particulate Media" *ASCE Journal of Engineering Mechanics*, Vol 128, No. 11. p 1182-1192
- O'Sullivan, C. (2014) "Advancing Geomechanics Using DEM" Proceedings *IS-Cambridge 2014*
- Rowe, P. W. (1962) ''The stress-dilatancy relation for static equilibrium of an assembly of particles in contact.'' Proc. R. Soc. London Ser. A, 269(1339), 500–527.
- Thornton, C. (1979) The conditions for failure of a face-centered cubic array of uniform rigid spheres. Géotechnique. 29 (4), 441–459.

References: Timestep

- Hart R, Cundall PA, Lemos J (1988) Formulation of a three-dimensional distinct element model—Part II. Mechanical calculations for motion and interaction of a system composed of many polyhedral blocks. Int J Rock Mech Min Sci Geomech Abstr 25:117–125.
- Itasca Consulting Group (2014) Mechanical Timestep Determination. PFC 5.0 Doc.
- Kremmer M, Favier JF (2001) A method for representing boundaries in discrete element modelling—part II: Kinematics. Int J Numer Methods Eng 51:1423–1436.
- Li Y, Xu Y, Thornton C (2005) A comparison of discrete element simulations and experiments for “sandpiles” composed of spherical particles. Powder Technol 160:219–228.
- O'Sullivan, C and Bray, JD (2004) Selecting a suitable time step for discrete element simulations that use the central difference time integration scheme Engineering Computations 21 (2/3/4), 278-303
- Otsubo, M., O’Sullivan, C., Shire, T. (2016) Empirical assessment of the critical time increment in explicit particulate discrete element method simulations submitted to Computers and Geotechnics, August 2016
- Tsuji Y, Kawaguchi T, Tanaka T (1993) Discrete particle simulation of a two-dimensional fluidized bed. Powder Tech 77:79
- Tu X, Andrade JE (2008) Criteria for static equilibrium in particulate mechanics computations. Int J Numer Methods Eng 75:1581–1606.

References: Boundary conditions

- Bernhardt, ML, Biscontin, G., O'Sullivan, C. (2016) Experimental validation study of 3D direct simple shear DEM simulations *Soils and Foundations* 56(3) J, Pages 336–347
- Cheung, G. and O'Sullivan, C. (2008) "Effective simulation of flexible lateral boundaries in two and three dimensional DEM simulations" *Particuology*, Vol: 6, Pages: 483 – 500.
- Huang, X., O'Sullivan, C., Hanley, K. J., Kwok, C.Y. (2014) "DEM Analysis of the State Parameter", *Géotechnique* 64(12) 954-965 DOI 10.1680/geot./14-P-013
- O'Donovan, J, *Micromechanics of Wave Propagation through Granular Material, PhD thesis.*, Imperial College London, 2013.
- Thornton, C. (2000). Numerical simulations of deviatoric shear deformation of granular media. *Géotechnique 50*(1), 43–53.

References: Sample size

- Barretto, D. and O'Sullivan, C. (2012) "The influence of inter-particle friction and the intermediate stress ratio on soil response under generalised stress conditions" *Granular Matter,* Vol:14, Pages:505-52
- Huang, X, Hanley K. J. , O'Sullivan, C. and Kwok, F.C.Y.(2014) "Effect of sample size on the response of DEM samples with a realistic grading" *Particuology* 15, 107-115
- O'Sullivan, C. (2014) "Advancing Geomechanics Using DEM" Proceedings *IS-Cambridge 2014*
- Shire, T.; O'Sullivan, C. ; Fannin, R.J.; Hanley, K. (2014) "Fabric and effective stress distribution in internally unstable soils" *ASCE Journal of Geotechnical and Geoenvironmental Engineering*, 140(12) DOI 10.1061/(ASCE)GT.1943-5606.0001184
- Shire, T. (2013) *Micro-mechanical analysis of granular filters.* (PhD), Imperial College London.

References: Specimen generation

- Bernhardt, ML, Biscontin, G., O’Sullivan, C. (2016) Experimental validation study of 3D direct simple shear DEM simulations *Soils and Foundations* 56(3) J, Pages 336–347

References: Input parameters

- Been, K. & Jefferies, M. G. (1985). A state parameter for sands. *Géotechnique* 35, No. 2, 99–112
- Huang, X., Hanley, K J, O'Sullivan, C., Kwok, C. Y. (2014) Exploring the influence of interparticle friction on critical state behaviour using DEM *International Journal for Numerical and Analytical Methods in Geomechanics* 38(12) pp 1276-1297
- Verdugo, R. (1992) The critical state of sands-discussion *Géotechnique*. 42 (4), 655–663

References: Contact Model

- Cavarretta, I., Coop, M., O'Sullivan, C. (2010) "The Influence of Particle Characteristics on the Behaviour of Coarse Grained Soils" *Géotechnique* Vol:60, Pages:413-423
- Cavarretta, I., O'Sullivan, C. and Coop, M. (2016) The relevance of roundness to the crushing strength of granular materials Accepted by *Géotechnique*. July 2016
- Johnson, K.L., 1985. *Contact mechanics*, Cambridge University Press.
- Otsubo, M., O'Sullivan, C., Hanley, K.J. and Sim, W. W. (2016) The influence of particle surface characteristics on elastic stiffness and dynamic response Accepted by *Géotechnique* Oct 2016, DOI: 10.1680/geot./16-P-050
- Otsubo, M. (2016) *Particle scale analysis of soil stiffness and elastic wave propagation* PhD Thesis Imperial College London – to be submitted Autumn 2016
- Thornton, C. & Yin, K., 1991. Impact of elastic spheres with and without adhesion. Powder technology, 65, pp.153–166.

References: Running the simulation

- da Cruz F., Emam S., Prochnow M., J. N. Roux and F. Chevoir (2005) Rheophysics of dense granular materials: Discrete simulation of plane shear flows. *Phys. Rev.* E72, 021309.
- Lopera Perez, J. C; Kwok, C. Y.; O'Sullivan, C.; Huang, X.; Hanley, K. J. (2016) Assessing the quasi-static conditions for shearing in granular media within the critical state soil mechanics framework *Soils and Foundations*, Vol. 56, No. 1, 19.02.2016, p. 152–159.

References: Running the simulation

- Hanley, K.J., O'Sullivan, C. ,and Huang, X.(2014) "Particle-scale mechanics of sand crushing in compression and shearing using DEM" Soils and Foundations, 55(5), pp 1100–1112, doi:10.1016/j.sandf.2015.09.011

References: Post-processing

- http://www.paraview.org/